Characterization of Trp-Cage and Its Circular Permutation

Katherine Graham

A dissertation

submitted in partial fulfillment of the

requirements for the degree of

Doctor of Philosophy

University of Washington

2018

Reading Committee:

Niels H. Andersen, Chair

Champak Chatterjee

Stefan Stoll

Program Authorized to Offer Degree:

Department of Chemistry

University of Washington

Abstract

Characterization of Trp-Cage and Its Circular Permutation

Katherine Graham

Chair of the Supervisory Committee:
Niels H. Andersen
Department of Chemistry

The relationship between sequence, the folded structure, and the folding pathway by which that structure is reached presents a topic of tremendous importance in the understanding of proteins. However, the study of most proteins is difficult due to their size and inherent complexity. Smaller protein-like systems may offer a simpler alternative, making them useful model systems for their larger counterparts. At approximately 20 residues in length and with a folding time on the low-microsecond timescale, the Trp-cage miniprotein is an ideal system for characterizing the interactions that stabilize protein folding and exploring folding pathways. Since the development of the original sequence TC5b, the Trp-cage has been optimized through a series of stabilizing mutations. More recently, cyclized and circularly permuted versions of Trp-cage

have been developed. These alternate versions of the miniprotein have been shown to adopt the same characteristic fold as the standard topology.

The work described in this study seeks to characterize the stabilizing interactions and folding pathways of Trp-cage. The first part uses a series of point mutations to reverse the typical stability profile of Trp-cage under acidic conditions. The second part characterizes the stabilizing effect of key folded state interactions in the circularly permuted motif. Finally, dynamics studies explore the folding pathways of both the standard topology and circularly permuted series. Comparisons of the standard Trp-cage to its circularly permuted counterpart offer insights into how contact order influences the stabilizing effects of individual interactions as well as the order of those interactions in the folding pathway.

TABLE OF CONTENTS

LIST OF FIGURES

LIST OF TABLES

ACKNOWLEDGEMENTS

I would like to thank my adviser, Prof. Niels H. Andersen, for giving me the opportunity to join his research group. Throughout my time in the graduate program, he has always been available to offer his perspective on my project or to help me gain a deeper understanding of the science involved. His feedback and guidance have been invaluable to my growth as a researcher.

I would also like to express my gratitude to the other members of the Andersen group. Dr. Brandon Kier acted as an informal mentor and adviser on my project. Jordan Anderson and Kalkena Sivanesam taught me many of our standard lab procedures and were always available to answer questions on the ins and outs of our instruments. Brice Jurban demonstrated a truly touching willingness to talk me through challenging topics. Talented undergraduate researcher Alex Shcherbakov had a talent for offering simple break downs of complicated concepts. Finally, my undergraduate research assistants Ruth Son and Michael Mason have contributed their time and energy to this work and frequently acted as my sounding boards.

My family has offered their unflagging support over the past five years. In particular, I would like to thank my parents, John and Polly Graham, for their love and frequent messages of encouragement. My sister, Heather Straub, is a source of inspiration. I have been proud to see her pursue her degree while starting a family. Finally, thank you to my grandmother, Dorothy Rachford, who makes no secret that she is proud of all her grandchildren.

DEDICATION

To my parents, John and Polly Graham, for their support and encouragement over the years.

And to my wonderful grandmother, Dorothy Rachford.

Chapter 1. INTRODUCTION

1.1 PROTEIN FUNCTION AND STRUCTURE

Serving in structural, signaling, transport and catalysis roles, proteins are a diverse class of biological macromolecules necessary for the countless cellular processes which make life possible. Proteins are encoded in the DNA as a specific series of amino acid residues joined together in a polypeptide chain. Through the process of protein folding, the polypeptide chain then goes on to assume a well-defined conformation referred to as the folded or native state. The thermodynamic properties and structural features of this native state are determined by the amino acid sequence. The relationships between the sequence, the folded state, and folding process are therefore fundamental to the study of protein folding (Dill & MacCallum, 2012).

The structure of proteins is described in terms of four levels of complexity. At the most basic, the primary structure is the sequence of amino acids that make up the polypeptide chain. Local interactions between nearby residues give rise to the secondary structure. Common features of proteins such as α-helices, β-strands and β-turns are all examples of secondary structure. These secondary structural units then fit together in the tertiary structure, which is characterized by long-range interactions between residues distant to one another in the primary sequence. For proteins that are comprised of more than one domain, quaternary structure is the final level in the structural hierarchy.

For most proteins, reaching the fully folded state is necessary to fulfill their biological function. Moreover, the misfolding and aggregation of proteins can lead to diseases such as Alzheimer's (Lambert et al., 1998). Understanding how sequence determines native state could open the door to predicting the structure and biological role of proteins from genome data. Better

structure prediction models could facilitate the study of proteins which are difficult to analyze by current experimental methods. It could suggest treatments for diseases involving protein misfolding. Significantly, structure prediction can identify targets for emerging gene editing methods (Cong et al., 2013). Given the tremendous potential, it is no surprise that de novo structure prediction has been referred to as a "Holy Grail" of protein science despite its inherent challenges (Berendsen, 1998).

1.2 Folding Pathways

In the early 1960's, research by Anfinsen showed that proteins could regain their enzymatic activity after undergoing denaturation. This indicated that the ability to reach the folded conformation was inherent to the polypeptide chain itself, and that the folded conformation must be the thermodynamic minimum for the system (Anfinsen, 1973). By the end of the decade, Levinthal had illustrated that proteins possess too many potential conformations to reach their native state through a purely random sampling of conformational space (Levinthal, 1968). The observation that proteins fold on timescales that should be impossible has been called Levinthal's Paradox (Bai, 2003; Dill & Chan, 1997).

The solution to this apparent paradox was that proteins reach their folded conformation by following a "folding pathway" (Dill & Chan, 1997). The folding pathway was pictured as a set sequence of discrete folding steps which guided the polypeptide to its native state. Such a pathway would narrow the conformational space available to the protein, allowing it to reach its native state in a biologically relevant timeframe. Like the features of the folded conformation, the folding pathway would also be determined by the primary sequence.

However, evidence for this model of folding was mixed. A folding process of well-defined sequential steps would be expected to result in the presence of partially folded intermediates. Some

proteins are in fact seen to exhibit signs of detectable intermediates (Kim, 1990). Others do not. Notably, small proteins of less than 100 amino acids tend to be two-state: they are observed to be fully folded or in an unfolded random coil state.

Two additional models for protein folding are the framework model and hydrophobic collapse. In the framework model, secondary structure forms early, driven by interactions between nearby residues. Once formed, these structures collide, and tertiary contacts occur (Baldwin, 1995; Baldwin & Rose, 1999a, 1999b; Fersht, 1995; Kim, 1990; Kim & Baldwin, 1982; Neira et al., 1996) This is a hierarchical model of folding, with the formation of hydrogen bonds at the initial stages of the folding process, and progressively higher orders of structuring emerging in following steps.

Conversely, in the hydrophobic collapse model, folding is initiated when the polypeptide chain collapses under the hydrophobic effect. Within the confines of the compacted polypeptide, conformational freedom is limited, allowing secondary and tertiary structures to form (Dill, 1990; Dill, Alonso, & Hutchinson, 1989). The existence of molten globules could be seen as evidence for this model (Akiyama, Takahashi, Ishimori, & Morishima, 2000; Jennings & Wright, 1993; Ptitsyn, Pain, Semisotnov, Zerovnik, & Razgulyaev, 1990). Molten globules are compact folding intermediates that contain some of the secondary structure of the folded state but lack definable tertiary contacts.

The nucleation-condensation model works as a hybrid of these two folding models. Rather than a two-stage process, secondary and tertiary structure form together, with the tertiary structure stabilizing secondary structures (Daggett & Fersht, 2003; Fersht, 1997; Onuchic & Wolynes, 2004). Experimental evidence supports the cooperative formation of secondary and tertiary structure. In a study of 41 globular proteins by Uversky and Fink, good correlation was observed

between compact volume and an increase in secondary structure content. Significantly, in no examples was one feature observed without the other (Uversky & Fink, 2002). Coupled secondary and tertiary structure formation is also consistent with the observation of two state proteins, which exhibit no folding intermediate.

The concept of the classic folding pathway assumes a single set (or limited number of sets) of sequential steps by which the polypeptide reaches its fully folded conformation. A more accurate depiction of protein folding is the energy landscape and the folding funnel (Dill & Chan, 1997; Onuchic, Luthey-Schulten, & Wolynes, 1997; Onuchic & Wolynes, 2004; Wolynes, Luthey-Schulten, & Onuchic, 1996; Wolynes, Onuchic, & Thirumalai, 1995). The energy landscape represents the vast number of possible conformations the protein can assume and the corresponding energy for each. In this conceptualization, the folding process is likened to falling down a funnel. At the top, the funnel is wide, representing the large number of possible conformations that are available to an unfolded protein. As initial structural elements form, conformational space is limited, focusing the conformational search and allowing the protein to reach progressively more ordered states through multiple pathways (Dobson & Karplus, 1999; Pande, Grosberg, Tanaka, & Rokhsar, 1998). As the protein travels down the funnel, the available conformational space continues to narrow as the protein reaches the limited number of conformations of the folded ensemble. The folded ensemble occupies the lowest-energy point in the landscape, indicating that the protein has reached its most stable state. Along the way, peaks and hollows represent energetically unfavorable conformations and kinetic traps, respectively. The primary sequence codes for the local interactions that begin the folding process, satisfying Levinthal's Paradox while still allowing multiple pathways to the native state.

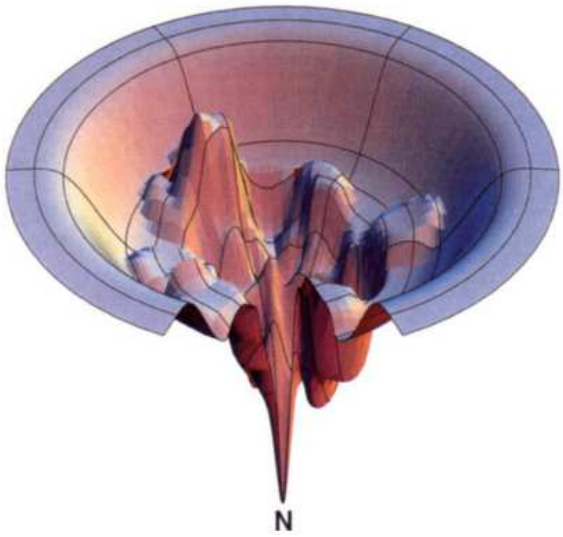

Figure 1.1. A depiction of a folding funnel. A rugged energy landscape with kinetic traps and energy barriers (Dill & Chan, 1997).

1.3 Investigating Relationships Between Primary and Tertiary Structure

1.3.1 *Peptides as Model Systems*

Studying the links between sequence, structure and the folding pathways requires understanding the role of individual residues on conformational stability and folding. However, describing the role of any one residue can be complicated due to the wide array of interactions that take place within a given protein. One way of reducing the complexity is to study fragments of the polypeptide chain rather than the whole. Examining the secondary structures of peptide segments can demonstrate the relationship between primary sequence and local structuring. For instance, peptide fragments can be used to investigate local structuring tendencies that shape the earliest stages of folding (Wright, Dyson, & Lerner, 1988). These local preferences would be difficult to observe in the context of the larger protein.

However, it is difficult to gain insight into the larger protein using peptide fragments. Not only does biological function often depend on the whole protein, the folded structure of a given segment may require the context of the larger protein to properly fold. More significantly, the long-range interactions that mark tertiary structures are typically absent in polypeptide chains of less than 50 amino acids.

For practical reasons, any miniprotein to be used as a model system should be below 40 residues. This is the approximate limit for producing pure peptide samples using solid-phase synthesis. Assuming such a miniprotein was well folded and had long-range contacts, it would have several advantages over regular proteins as a model system. First, it could be produced relatively quickly on a peptide synthesizer rather than grown in E. coli. In addition to speed, a synthesizer has the advantage of easy incorporation of mutations or unnatural amino acids. Smaller sequences can be characterized by CD and ^{1}H NMR, forgoing the need for ^{13}C or ^{15}N enriched amino acids. Finally, small size and presumably quick folding make small systems well suited to computational studies.

1.3.2 *A Priori Proteins and Molecular Dynamics*

Another approach to studying the relationship between primary sequence and folded conformation is through the *a priori* design of proteins. By designing an amino acid sequence to adopt a given fold, it is possible to probe the forces behind protein folding. Over the years, there have been a number of studies devoted to protein design and the determination of requirements for structure formation (Beasley & Hecht, 1997; Dill, Ozkan, Shell, & Weikl, 2008; Head-Gordon & Brown, 2003; Plaxco, Simons, & Baker, 1998).

In addition to the empirical characterization of proteins, computational studies provide another method of studying proteins (Azia & Levy, 2009; Gnanakaran, Nymeyer, Portman, Sanbonmatsu,

& García, 2003; Hellinga, 1997; Kuhlman & Baker, 2004; Naganathan, 2012; Nauli, Kuhlman, & Baker, 2001; Tripathi, Makhatadze, & Garcia, 2013). Not only are computational studies capable of investigating the role of individual amino acids on structure and stability, they can examine folding pathways in more detail than other available methods.

1.4 THE TRP-CAGE

1.4.1 *Development of the Trp-cage*

Exendin-4 is a 39-residue peptide found in the saliva of Gila monster. While insoluble in water, exendin-4 was observed to be largely helical, and in aqueous fluoroalcohol media, its NMR showed long-range NOEs in residues 21 through 38. This fold, defined by a hydrophobic core clustering around a central tryptophan, was termed the 'Trp cage' (Andersen, Fesinmeyer, Neidigh, & Barua, 2001; Neidigh, Fesinmeyer, & Andersen, 2002)

Given the notable degree of folding present in such a short sequence, a study was undertaken to create a small, stable miniprotein based on exendin-4 that would be soluble in aqueous solution. The first modifications to the sequence involved shortening and capping the N-terminal α-helix to bring the miniprotein to 20 residues. A salt bridge was created by the inclusion of aspartic acid and arginine residues at two sites that were close enough to allow Coulombic interactions between the sidechains. A glutamic acid in the helix was replaced with glutamine to avoid charge-repulsion with the sidechain of the newly inserted aspartic acid. Finally, a phenylalanine was mutated to tyrosine to provide greater packing within the core. The result was the Trp-cage miniprotein TC5b (NLYIQWLKDGGPSSGRPPPS) which was >95% folded in water with a melting temperature of 42^{o} C. The defining structural feature was still the burial of a central tryptophan sidechain in a hydrophobic core, particularly by the close association of a glycine and three prolines residues.

Other well-defined structural features included the N-terminal α-helix, a short 3_{10}-helix, and a C-terminal polyProII helix (Neidigh et al., 2002).

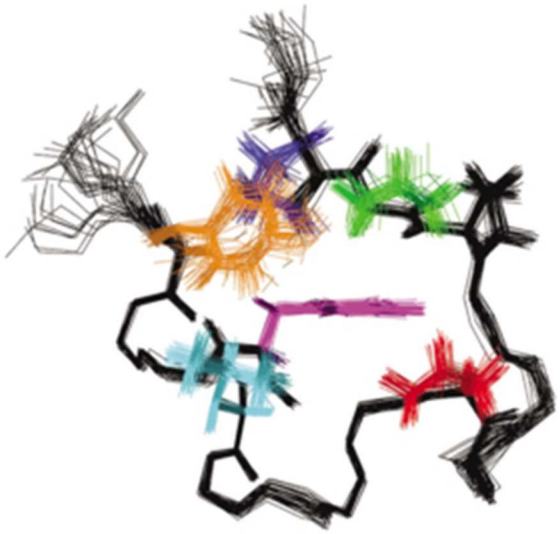

Figure 1.2. NMR generated structure ensemble for Trp-cage TC5b. Key residues are highlighted: tyrosine 3 (orange), tryptophan 6 (purple), leucine 7 (cyan), proline 12 (red), proline 18 (green), and proline 19 (blue) (Neidigh et al., 2002).

Since the publication of the original TC5b sequence, additional mutations have been explored to improve the stability of Trp-cage. Work by the Gai group predicted that a second tryptophan residue at position 12 further stabilizes the folded state (Bunagan, Yang, Saven, & Gai, 2006), and P12W mutations have subsequently been incorporated into Trp-cage variations produced in the Andersen lab (Byrne, 2013; Byrne, Kier, Williams, Scian, & Andersen, 2013). The stability of the N-terminal α-helix was increased through replacing the N-terminal asparagine residue with an aspartic acid, as well as the inclusion of more alanine residues (Barua et al., 2008). Glycine residues at positions 10 and 15, both in loop regions of the structure, were mutated to D-alanine to preserve the dihedral angles of the folded state while decreasing the entropic costs of folding (Williams, Barua, & Andersen, 2008). Mutations to the residues of the salt-bridge were explored,

although it was ultimately concluded that the original Asp/Arg pairing created optimal Coulombic interactions (Williams, Byrne, Stewart, & Andersen, 2011).

Given that the termini of Trp-cage are held within close spatial proximity based on the NMR structures, it was possible to connect them with a short linker sequence. Indeed, a Trp-cage with a -GG- linker was successfully cyclized, giving a hyper-stable construct with a T_M of 95°C by CD (Scian et al., 2012). The cyclic form provided an x-ray crystallographic study that confirmed the structural features that had been found in NMR structures. The success of cyclized Trp-cage led in turn to circular permutation, in which the C-terminal polyPro$_{II}$ helix was moved to the N-terminus and connected to the α-helix by way of a short loop sequence. While the secondary structural elements of the miniprotein were re-ordered, NMR structures revealed that the structure and defining interactions were preserved (Byrne et al., 2013). Comparison of standard sequences and their circularly permuted counterparts is particularly relevant as an avenue of probing the connections between primary sequence, folded structure and folding pathways.

The presence of long-range contacts in Trp-cage are notable given its size and make it an appropriate system for more modeling larger proteins. Initial measures of the folding time of a Trp-cage placed it in the low microseconds range (Andersen et al., 2001; Qiu, Pabit, Roitberg, & Hagen, 2002). Between its small size and fast folding times, it presented an excellent subject for molecular dynamics studies, and it was featured in several such studies once the structure was published (Simmerling, Strockbine, & Roitberg, 2002; Snow, Zagrovic, & Pande, 2002). Additional studies have underscored its usefulness as a protein model (Chowdhury, Lee, & Duan, 2004; Chowdhury, Lee, Xiong, & Duan, 2003; Cote, Maisuradze, Delarue, Scheraga, & Senet, 2015; Day, Paschek, & Garcia, 2010; Ding, Buldyrev, & Dokholyan, 2005; Hu, Tang, Wang, Zhang, & Lei, 2008; Juraszek & Bolhuis, 2006; C. Y. Zhou, Jiang, & Wu, 2015).

1.4.2 *The Trp-cage Folding Mechanism*

While the Trp-cage miniprotein has been thoroughly studied, both experimentally and through molecular dynamics simulations, disagreement remains as to its likely folding mechanism. Given its small size, it might be expected to follow two-state folding, and in fact, early laser temperature jump spectroscopy (Qiu et al., 2002) supported 2-state behavior. However, the original publication of TC5b showed evidence of associations between Gly^{11} with Trp^{6} even in the unfolded state (Neidigh et al., 2002). Other experiments point to long-range contacts between Trp^{6} and Arg^{16} in the unfolded state (Hałabis et al., 2012; Mok et al., 2007). Ahmed et al. showed data suggesting a molten globule state intermediate (Ahmed, Beta, Mikhonin, & Asher, 2005). Culik et al. suggested the early formation of the α-helix followed by the emergence of long-range contacts that do not affect the overall rate of folding but instead stabilize the folded state (Culik, Annavarapu, Nanda, & Gai, 2013).

Of the molecular dynamics studies, some indicated the presence of residual α-helix in the absence of other folded structure (Kannan & Zacharias, 2009). Formation of the α-helix was also proposed as an initial step in the folding pathway (Chowdhury et al., 2004, 2003; Ding et al., 2005). Again in computational studies, the salt bridge was shown to act as a potential kinetic trap early in the folding process, preventing folding from proceeding until it could be broken and then reformed later as a fold stabilizing feature (Ding et al., 2005; R. Zhou, 2003).

Interpretation of experimental values of both fold stability and folding rates depends heavily on the structural features used to measure folded structure mole fraction. Barua et al. proposed the existence of a "half-cage" structure, in which the α-helix and 3_{10} helix have formed, but the C-terminal $polyPro_{II}$ tail has not docked above the central tryptophan residue (Barua et al., 2008). Evidence of half-cage structure exists in standard as well as circularly permuted Trp-cage

sequences (Barua et al., 2008; Byrne et al., 2014, 2013; Neidigh et al., 2002). Some specific data from three Trp-cage sequences reported herein which show diminished folding at C-terminal sites appears in Fig. 1.3. The sequence for (P12W)-TC15b (DAYAQWALDAGWASGRPPPS) is part of the standard topology while (P19W)-cpTC4e (RPPPSDAALYAQWLADaGWAS) and Ac-(P12W)-cpTC4e (Ac-RPPPSDAALYAQWLADaGWAS) are circularly permuted counterparts.

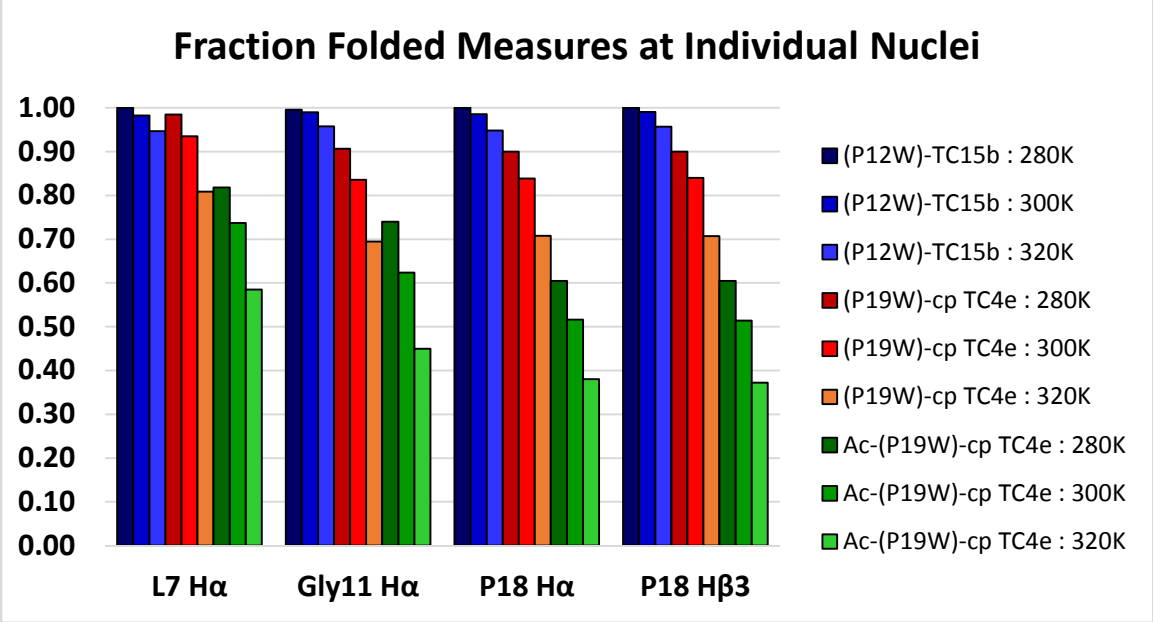

Figure 1.3. Fraction folded as determined by the chemical shift deviations for individual diagnostic nuclei at 280K, 300K, and 320K in standard topology (blue) and circularly permuted Trp-cage (red and green). Well folded Trp-cage peptides such as (P12W)-TC15b are observed to follow two-state folding. Less folded species such as Ac-(P19W)-cp TC4e exhibit residual helicity in less-folded states.

In cases where this intermediate structure is significantly populated, fraction folded values derived from Pro^{18} data will be lower than those derived from Gly^{11} data or measures of helicity. Half-cage contributions to the folding equilibrium are seen to be less significant for well-folded species, which appear to adhere to two-state folding. Assuming a half-cage is part of the on-pathway folding mechanism, its existence becomes evidence for the early formation of the α-helix and 3_{10} helix, followed by the docking of the $polyPro_{II}$ helix. Reliable dynamics data therefore

calls for measures of polyPro$_{II}$ docking rather than helicity or Gly[11] data, which do not necessarily reflect full cage formation. Indeed, folding rate data obtained from NMR measurements of Gly[11] produces values that are well in line with those obtained from measurements of the helix formation. Meanwhile, rate data obtained from residues in the C-terminal region show significantly slower folding rates, suggesting the tail is docking later in the folding process (Byrne et al., 2014).

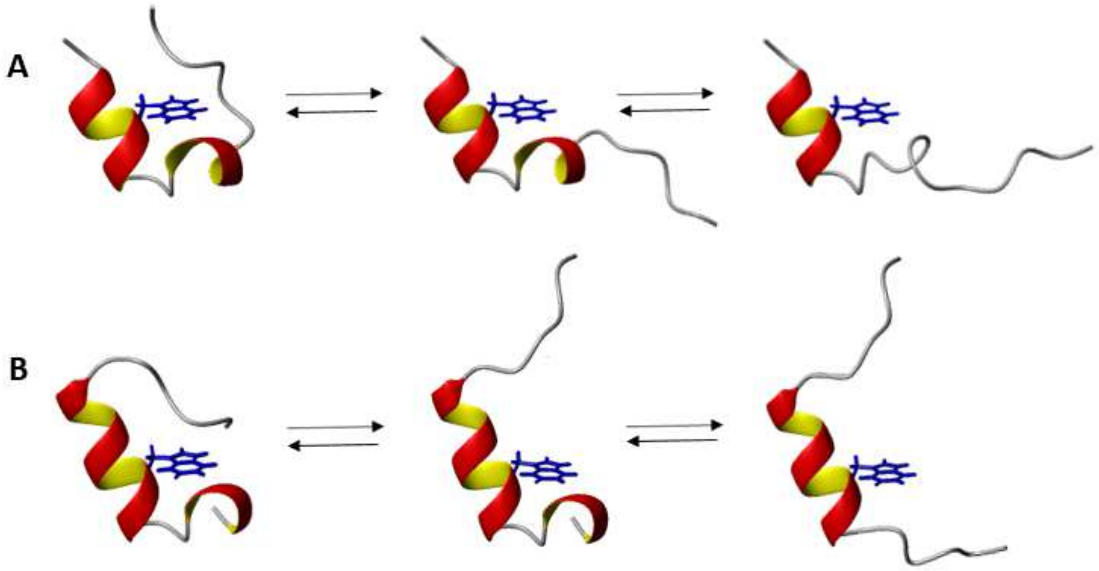

Figure 1.4. Full cage, half cage and residual helix models of Trp-cages: A) standard topology Trp-cage. B) circularly permuted Trp-Cage. The C-terminal and 3_{10} helices are shown in red/yellow while the central Trp[6] (Trp[13] in circularly permuted topology) is in blue.

1.5 Spectroscopic Techniques Employed for Studying Polypeptides

1.5.1 *Circular Dichroism*

Circular Dichroism (CD) measures the differential absorption of left- and right-handed circularly polarized components of plane-polarized light (Kelly & Price, 1997). Absorption in the far-UV

region (260-180 nm) arises from n → π and π → π* transitions of the backbone amides and aromatic sidechains.

Chromophores can demonstrate some form of chirality, either due to their structure, an asymmetric environment, or being covalently linked to a chiral center. In the case of proteins, this chirality is commonly caused by the presence of secondary structural elements such as α-helices or β-sheets. These elements have characteristic molecular ellipticity as a function of wavelength, owing to the orientation of the interacting transition dipoles. The α-helix has minima at 208 and 222 nm and a maximum at 190 nm. β-sheets have a minimum at 218 and a maximum at 195 nm. Random coil structures have a minimum at 200 nm. CD spectra appear as a weighted average of the ellipticity of all the secondary structural elements present, so monitoring the presence of a specific feature requires deconvoluting the spectra.

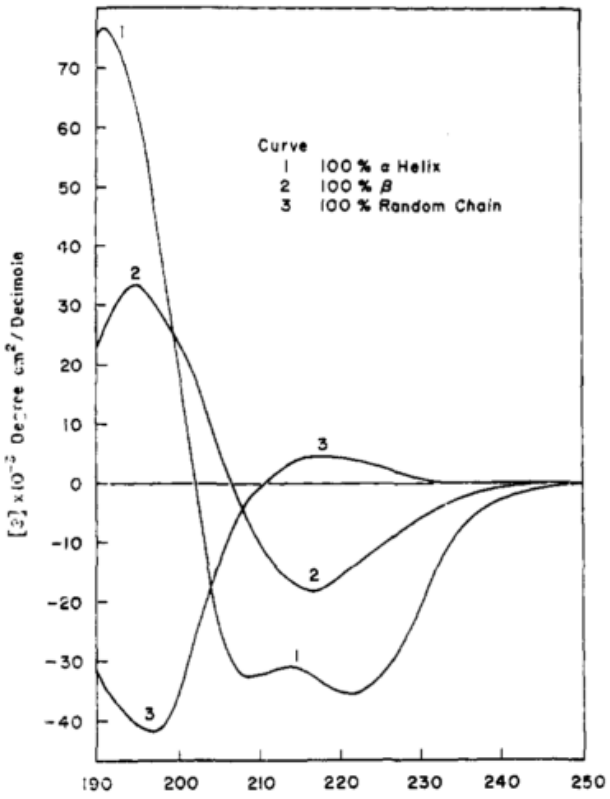

Figure 1.5. Circular dichroism of common protein secondary structures helix, β, and random coil (Greenfield & Fasman, 1969).

CD has the advantage of requiring very small concentrations (typically 20-30 μM), which is useful in cases where sample is in short supply or likely to aggregate at higher concentrations. It can also be monitored over a temperature range from 5° C to 95° C, allowing it to capture the melting of peptides that are stable within the typical temperature range of NMR. However, it is a method that only detects the structuring of the sample as a whole; a spectrum showing half the sample as α-helix could indicate that half the molecules present are completely helical, or that all molecules present are half helical. It cannot offer information about the degree of secondary structure present at the position of a given residue.

In the case of Trp-cage, the primary contributor to the CD spectrum is the N-terminal α-helix. The relative contributions of this feature can be best monitored at its minimum near 222 nm, as opposed to the minimum near 208, which is complicated by the presence of random coil.

1.5.2 *Nuclear Magnetic Resonance*

Nuclear Magnetic Resonance (NMR) is capable of monitoring the chemical environment of individual nuclei. Acquisition of NMR spectra is typically longer than that for CD, and within a narrower range of temperatures (280K – 340K). A practical consequence is that fewer spectra are typically taken for a given sample. NMR also requires samples in the 1-2 mM range for rapid acquisition, which can be problematic for proteins that are prone to aggregation. Despite these considerations, it is superior to CD for monitoring the folding at the level of individual residues and determining whether a protein undergoes two-state folding or if folding intermediates are present.

1.5.3 *Chemical Shift Deviation*

The chemical shift (δ) is the resonant frequency of a nucleus relative to a standard, typically 4,4-dimethyl-4-silapentane-1-sulfonic acid (DSS) for solutions NMR. The chemical shift of the nucleus is dependent on the electron density of its immediate surroundings, which is determined in turn by the surrounding structure. The most significant factor influencing electron density is the electronegativity of nearby substituents and mobile electronic distributions. Nearby electron donating groups tend to increase electron density and decrease chemical shift, while electron withdrawing groups have the opposite effect. Other relevant factors are Coulombic interactions, hydrogen bonding and diamagnetic anisotropy. The most common source of diamagnetic

anisotropy in peptides is the ring-current effect created by the π-electron of aromatic rings. Ring current effects can create quite dramatic differences in chemical shifts for nearby nuclei.

1.5.4 *Population Analysis from Chemical Shifts*

Random coil is defined as the lack of coordinated structure in a peptide. Under given experimental conditions, the chemical shifts for a nucleus in the random coil state, with segmental motion present, depend only on the specific amino acid itself, and the amino acids directly flanking it. If the sequence of the peptide is known, the expected chemical shift for a given nucleus can be calculated.

Within a given residue, the same nucleus will experience different chemical environments depending on the populated conformations of the protein. However, these different states are resolved only when the inter-conversion time scale is approximately two times slower than the shift difference in Hertz ($\tau > \sqrt{2} / \pi \cdot \Delta\nu = 2.22 \cdot \Delta\nu$). Generally, for peptides and very small folded domains, interconversion between conformations is much faster, and so the observed signal for a structured peptide will be the population-weighted average of the folded and random coil chemical shifts. The difference between the observed chemical shift and the random coil shift is termed the chemical shift deviation (CSD), and it is directly proportional to the fraction of proteins in the folded conformation.

1.5.5 *Nuclear Overhauser Effects (NOEs)*

Nuclear Overhauser effects are caused by dipolar interactions happening between two nuclei in close spatial proximity. NOEs are measured as the magnitude of magnetization transferred between nuclei, and the strength of these interactions are proportional to $1/r^6$, where r is the internuclear distance. NOESY 2D NMR is the most commonly used experiment to examine these

through-space interactions. NOESY spectra give cross peaks with intensity dependent on the distance between two nuclei.

The NOEs of a well-folded protein can be used to generate distance constraints. With enough constraints, a three-dimensional structure of the protein can be generated. One consideration is that the protein should be over 70% folded. Otherwise non-native conformations, even the coil state, can result in NOE contributions that lead to inaccurate distance constraints.

1.5.6 *Line Shape Analysis*

The peaks of 1D NMR spectra are observed to broaden due to factors which include exchange between the folded and unfolded states. The relationship between the rates of folding and unfolding with the exchange broadening factor are given by the following equations:

$$k_F = 4\pi \cdot \chi_U \cdot (\chi_F)^2 \cdot (\Delta\nu)^2 \cdot (\Delta^{ex})^{-1} \quad (1.1)$$

$$k_U = 4\pi \cdot \chi_F \cdot (\chi_U)^2 \cdot (\Delta\nu)^2 \cdot (\Delta^{ex})^{-1} \quad (1.2)$$

Here, the values of χ_F and χ_U are calculated from CSD data, and $\Delta\nu$ is the CSD of 100% folded peptide (Piette & Anderson, 1959).

Comparison of the Arrhenius plots of the folding and unfolding rates of various Trp-cage mutants to the wild type indicates whether the mutations change the stability of the folded state through differences in the rate of folding or the rate of unfolding. Moreover, changes to the rate of folding are only seen in cases where the residue participates in interactions that occur before or at the rate limiting step of the folding pathway. By using mutations to eliminate or modify interactions in Trp-cage folding pathway, these interactions can be categorized as occurring either before or after the rate determining step of folding.

1.5.7 *ϕ-Value Analysis*

For simple folding mechanisms, the energy diagram can be represented as an unfolded state at one end and a folded state at the other, separated by an energy maximum. This maximum corresponds to the transition state of folding. ϕ-value analysis is a technique for characterizing the structure of the folding transition state, and through it the folding mechanism itself (Dalby, Oliveberg, & Fersht, 1998; Fersht, 2000; Fersht & Sato, 2004). For a given mutation, the ϕ-value corresponds to the ratio of the change in the energy of the transition state $\Delta\Delta G^{\ddagger},_{U}$ (where $\Delta\Delta G^{\ddagger},_{U} = \Delta\Delta G^{\ddagger},_{U,\ wt} - \Delta\Delta G^{\ddagger},_{U,\ mutant}$) and the change in the energy of the folded protein $\Delta\Delta G_U$ (where $\Delta\Delta G_U = \Delta\Delta G_{U,\ wt} - \Delta\Delta G_{U,\ mutant}$):

$$\Phi = \Delta\Delta G^{\ddagger},_{U} / \Delta\Delta G_U \qquad (1.3)$$

Both $\Delta\Delta G^{\dagger},_{U}$ and $\Delta\Delta G_U$ can be readily obtained from line shape analysis and measures of the folded populations, respectively. A ϕ-value of 1 indicates that the site of the mutation is as structured at the transition state as it is in the final folded state for both the mutant and the wild type protein. A ϕ-value of 0 meanwhile indicates that the site of the mutation lacks structure to the same extent at the transition state as in the unfolded state for both the mutant and the wild type. Values between 1 and 0 indicate structure is partially formed by the transition state. Values outside of the 0 to 1.0 range suggest non-native structuring at the transition state. By evaluating the ϕ-values for mutations that correspond to specific interactions within the folded protein, it is possible to determine which interactions have formed by the rate-limiting step of folding and which occur after.

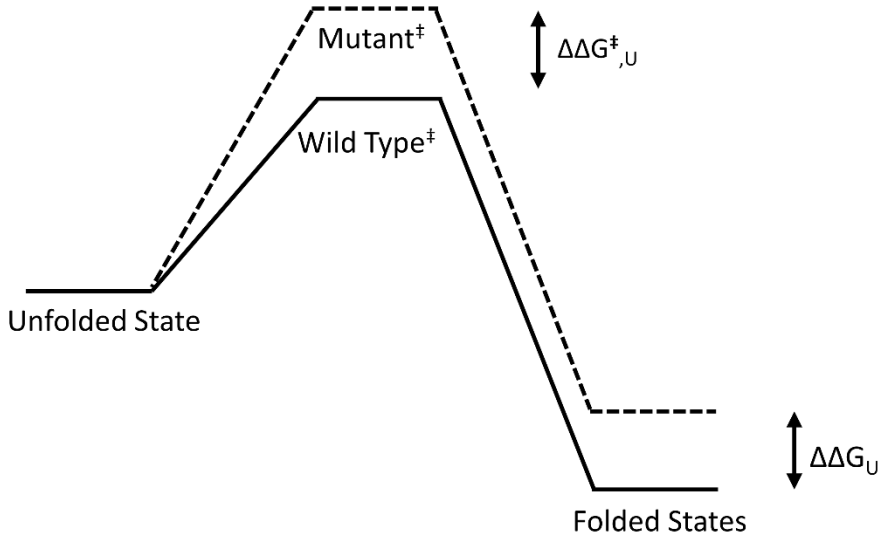

Figure 1.6. Free-energy coordinate of a two-state folding pathway.

Meaningful ϕ-values can be obtained only for mutations which satisfy the following 1) The folding mechanism of the mutant is the same as that of the wild type; 2) The structure of the folded state of the mutant is the same as that of the wild type; 3) The energy of the unfolded state of the mutant is the same as that of the wild type; 4) The mutant does not experience any interactions that were not present in the wild type. For this reason, conservative mutations should be used.

1.6 Research Overview

The focus of this research project is on the Trp-cage miniprotein and relationship between its primary sequence and final folded structure. Mutations were used to disrupt key interactions to characterize their thermodynamic contribution to the folded state. The first stage of this project was the characterization of the pH-dependent interactions through removal of the charged residues of the salt-bridge, as well as the aspartic acids flanking the N-terminal α-helix.

The second stage was the characterization of a circularly permuted version of the Trp-cage. The circular permutation of this protein, first realized by Byrne et al., moves the C-terminal

polyPro$_{II}$ helix to the N-terminal. It has previously been established that the circularly permuted Trp-cage possesses the same contacts as its non-permuted counterparts (Byrne et al., 2013). This study examined if the proximity of residues in the primary sequence affected their relative contributions to Trp-cage folded state stability. Changes in the energy of folding in the circular permutants were compared to those of standard Trp-cage systems.

Finally, line shape broadening was used to probe the folding pathways of both circularly permuted and non-permuted Trp-cage. By observing which mutations caused changes in the rate of folding or unfolding, individual interactions could be placed as occurring before or after the rate determining step of folding.

Chapter 2. MATERIALS AND METHODS

2.1 PEPTIDE SYNTHESIS AND PURIFICATION

Peptides were synthesized using Fmoc solid-phase chemistry on a CEM Liberty Blue peptide synthesizer. For sequences with a C-terminal amide, the synthesis was performed using a Rink amide resin. All other sequences were synthesized using Wang resin preloaded with the appropriate C-terminal residue. Where necessary, acetylation was accomplished by placing the peptide, still attached to the resin, in a solution of 3 mL N,N-dimethylformamide (DMF), 140 μL of triethylamine, and 95 μL acetic anhydride. This solution was shaken for 1 hour and then drained before proceeding to cleavage.

Peptides were cleaved from the resin in a solution of 95% trifluoroacetic acid (TFA), with 2.5% triisopropylsilane (TIPS), and 2.5% nanopure water as scavengers. The solution was shaken for approximately 1.5 hours. After shaking, a vacuum with a dry ice cold-finger was used for 20 minutes to evaporate excess TFA. The remaining solution was then diluted with approximately 30 mL of cold diethyl ether and centrifuged at 3000 rpm for 5 minutes to precipitate the crude peptide. The diethyl ether was decanted, and the wash was repeated once more. The resulting pellet was air-dried overnight or under a low stream of nitrogen gas for approximately 20 minutes.

Once dried of residual diethyl ether, the crude was dissolved in approximately 5-10 mL of nanopure water. A mixture of 50% water, 50% acetonitrile was used to dissolve excess foam. When needed, a few milliliters of 1 M NaOH or 1 M HCl solution was used to solubilize the peptide. The solution was then passed through a syringe filter tip to remove any large particles or aggregates prior to HPLC.

Crude peptide solution was purified using reverse-phase HPLC on an Agilent or Chromolith C18 column with a gradient of water (0.1% TFA) and acetonitrile (0.85% TFA). The

eluent was monitored using UV detection at 215 and 280 nm. The identity and purity of collected fractions was confirmed by the presence of $(M+2H)^{2+}$ and $(M+3H)^{3+}$ ions using mass spectrometry on a Bruker Esquire Ion Trap mass spectrometer. Pure peptide solutions were rotovapped down to 5-10 mL, frozen and lyophilized.

2.2 Trp-cage Cyclization

A cyclized Trp-cage was produced through the folding-mediated cyclization of ALYAQWLADaGWASGRPPPSDA. A solution of 100 μM of peptide in 25 mM MOPS buffer at pH 6.5 was placed in an ice bath. 150 μM of sulfo-NHS sodium salt and 1 mM EDC·HCl were added to the cyclization mixture. The solution was allowed to come to room temperature and react overnight. An equivalent amount of sulfo-NHS and EDC·HCl were added each subsequent day. HPLC was used to separate and isolate the cyclized and uncyclized peptides. The solution of the purified cyclized peptide was rotovapped and lyophilized. Uncyclized peptide was recovered and reacted again.

2.3 Nuclear Magnetic Resonance (NMR) Spectroscopy

1-2 mM samples were prepared by dissolving the appropriate amount of dried peptide powder in 540 μL of 50 mM potassium phosphate buffer of pH 6.5 or pH 2.5, and 60 μL of DSS in D_2O. DSS was used as an internal chemical shift reference. Measurements were taken on Bruker spectrometers of either 700 or 800 MHz.

Peptides were assigned with a combination of TOCSY and NOESY 2D NMR taken over a range of 280K to 320K. For all experiments, water suppression was achieved through excitation sculpting (Hwang & Shaka, 1995). For TOCSY experiments, the DIPSI2 sequence spinlock was used, and mixing time was 60 ms. For NOESY experiments, mixing time was 120 ms.

2.3.1 *Chemical Shift Deviation*

In peptides, the chemical shift deviation (CSD) is defined as the difference between the observed chemical shift of a nucleus and the chemical shift of the same nucleus in the random coil state. CSD is given by the following equation:

$$CSD = \delta_{observed} - \delta_{random\ coil} \quad (2.1)$$

Chemical shifts and in turn CSDs are dependent on the local electronic environment of the nucleus. The CSDs of the folded state are therefore expected to depend on the differing degrees of hydrogen bonding, restricted dihedral angles and ring current effects present. In Trp-cage, the central indole ring of Trp^6 provides a source of ring current effect that causes marked CSDs. For well-folded Trp-cage sequences such as TC16b at 280K and pH 7.0, the CSDs values for diagnostic nuclei are Leu^7 Hα (-0.94 ppm), Gly^{11} Hα2 (-3.63), Pro^{18} Hα (-2.38), Pro^{18} Hβ3 (-2.17) (Scian et al., 2012). These nuclei can serve as probes for the extent of Trp-cage folding and stability.

2.3.2 *Calculating Fold Populations from CSDs*

Because the folding of Trp-cage is fast on the NMR timescale, chemical shifts will appear as the population weighted averages of the folded and unfolded states. CSD values can therefore be used to calculate the fraction folded using the following equation:

$$\chi_F = \frac{CSDobs}{CSD_{100}\%} \quad (2.2)$$

In this case, $CSD_{100\%}$ is the CSD for a fully folded Trp-cage. This value can be approximated using very well folded species. Specifically, cyclized Trp-cages have been observed to have pronounced and characteristic CSD values for the specific nuclei. These CSD values

change very little over the temperature range from 280K – 320K, suggesting that unfolding is minimal.

2.3.3 *Dynamics Studies*

1D NMR samples were prepared from dried peptide powder dissolved to 1-2 mM concentrations in 540 µL of 50 mM K phosphate buffer of pH 6.5 or pH 2.5 and 60 µL of DSS in D_2O. Once dissolved, samples were frozen and placed on the lyophilizer to remove H_2O. Lyophilized samples were then re-dissolved with 99.96% D_2O to minimize the water line in the 1D spectra. Measurements were taken on an 800 MHz Bruker spectrometer. Typically, 256 scans were used.

Lineshape analysis was conducted using P18Hβ3 nuclei. Coupling constants for P18Hβ3 in a given sample were derived for the most well resolved spectrum. Typically, these coupling constants were on the order of 12, 12, 11 and 9 Hz.

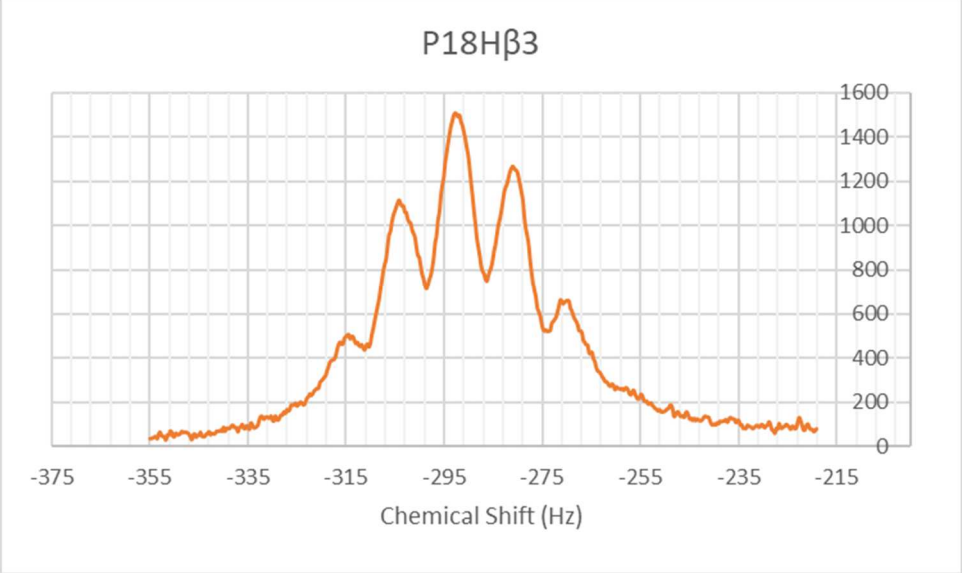

Figure 2.1. Signal for diagnostic P18Hβ3 nuclei. This example was taken from (P12W)-trTC15b at 300K and pH 6.5.

Exchange broadening factors were extracted from 1D spectra by finding the line broadening values of the peaks of interest and subtracting the line broadening values for a reference peak. Reference peaks were typically in the aromatic range and were chosen because they were clearly visible at all relevant temperatures and did not demonstrate significant changes in chemical shift due unfolding over the range of 280K to 320K.

More specifically, the excess broadening observed for the probes is equated with Δ^{ex} and eqn. 2.3; Olsen 2005; Scian 2013) is used to calculated the value of k_F at each temperature.

$$k_F = 4\pi \cdot \chi_U \cdot (\chi_F)^2 \, (\Delta\nu)^2 \, (\Delta^{ex})^{-1} \qquad (2.3)$$

The values of χ_F and χ_U (= 1 - χ_F) are obtained from the CSD of the probe χ_F (Eqn. 2.2). The $\Delta\nu$ in eqn 2.3 is given as the $CSD^{100\%}$ value and has a small, defined temperature dependence; k_U value at each temperature is calculated as $k_U = k_F \bullet (1 - \chi_F) \bullet (\chi_F)^{-1}$.

The sources of error in k_F-values can be traced, in part, to the errors in χ_F and thus back to chemical shift measurement and CSD determination errors. Referring to Eqn. 3, the error in $CSD^{100\%}$ is typically 2% (0.05 ppm for P18Hβ3) while the error in CSD^{obs} is 0.02 ppm reflecting uncertainty in the random coil values – chemical shift measurement errors (< 0.002 ppm) are not a significant factor. The 2% error also applies to $\Delta\nu$ in Eqn. 2 which is identical to $CSD^{100\%}$. The remaining consideration is the error in line shape fitting which provides Δ^{ex}.

In a typical experiment, values for Δ^{ex} are measured for Pro18Hβ3 by modeling the line shape with a custom-built Excel spreadsheet using the P18Hβ3 coupling constants measured at the lowest temperature and varying the line width (Δ^{sim}) until the observed half height width and the %-dip, see Olsen et al. (2005) for the definition, are reproduced (Olsen, Fesinmeyer, Stewart, & Andersen, 2005). Typically, there is a small range of values that provide equally good fits to the

experimental lineshape; this is another source of error in rate calculations. The line width at half height is measured at each temperature for an aromatic signal that does not experience significant changes (Δ^{o}) in its CSD from 280K-320K. The Δ^{ex} values are derived as $\Delta^{sim} - \Delta^{o}$, with Δ^{o} as the average intrinsic broadening of the reference signals. The typical errors in Δ^{ex} were 10% or 1 Hz, whichever is the larger.

Arrhenius plots of kinetic data obtained in this way were then used to compare the effects of different mutations and infer if they occurred before or after the transition state of the folding pathway.

2.3.4 *Mutational ΔΔG and Φ_F Values.*

Changes in fold stability associated with single-site mutations (or acidification to pH 2.5) are given in kJ/mol with the sign convention such that fold stabilization by mutation or acidification affords negative numbers ($\Delta\Delta G_U$). When possible, due to multiple determination, the error is also given. Some examples of ΔΔG values for standard topology systems that have been previously measured (Byrne et al., 2014) in this laboratory are: ΔpH = 3.13 ± 0.61 kJ/mol (over 10 observed cases), Δ(S14A) = 5.55 ± 0.43 (n= 3), Δ(R16Nva) = 5.5 ± 1.6 kJ/mol (n = 4), and

Δ(P17A) = 2.37 ± 0.46 kJ/mol (n = 3) – all at 300K. The P12W mutation has also been measured a number of times in slightly different systems with quite variable results: -1.7 ± 2.9 kJ/mol.

The mutational (or acidification) Φ_F values are calculated at 300−305 K as

$$\Phi_F = 2.5 \cdot [\ \ln (k_F^{mut} / k_F^{ref})\ ] \cdot (\ \Delta\Delta G_U^{mut}\ )^{-1} \qquad (2.4)$$

The rate of folding of the reference sequence and the mutant are designated as k_F^{ref} and k_F^{mut}, respectively. The calculation is repeated using the high and low estimates of the folding rates

and with both the consensus $\Delta\Delta G_U$ value and the specific one for the system under study if the latter was available. This defines the range of values allowed for Φ_F.

2.4 CIRCULAR DICHROISM SPECTROSCOPY

2.4.1 *Obtaining CD Spectra*

Circular dichroism (CD) measures the difference in absorption of the circular component of left- and right-handed plane-polarized light by a chiral sample. CD spectra will be a composite of the different chiral structural elements present in the sample. For a Trp-cage, these elements will be helical and random coil structures as well as an aromatic exciton couplet in some cases. By monitoring the transition from helical to random coil signal, it is possible to monitor the degree of folding under different conditions or over a range of temperatures. The temperature at which the protein is observed to be 50% folded is the melting temperature (T_M), and this measurement gives a simple comparison of the relative stability of Trp-cage species containing different mutations or under different conditions.

CD samples were prepared using small amounts of peptide in 20 mM K phosphate buffer of pH 6.5 or pH 2.5. The concentration of the initial solution was measured using UV absorption at 280 nm. Molar absorptivity values of $\varepsilon = 5690\ M^{-1}\ cm^{-1}$ and $\varepsilon = 1280\ M^{-1}\ cm^{-1}$ were used for each tryptophan and tyrosine residue present. Additional buffer or peptide were then added until the solution reached a calculated concentration of approximately 30 μM.

Spectra were recorded on a Jasco J-720 spectrapolarimeter with a Peltier temperature controller and calibrated to D-10-camphosulfonic acid $[\Theta]_{192.5}$=15,600. CD samples were measured using 0.10 cm path length quartz cells. Measurements were taken in 5°C increments from 5°C to 95°C with a five minute period of equilibration at each temperature. The scan rate

was 100 nm/min with a 0.2 step resolution from 190-270 nm. Typically, 12 scans were taken at each temperature and averaged.

CD spectra were processed by Jasco spectra analysis software. The raw CD signal was first corrected by subtracting a blank of only buffer taken at 5°C. The resulting spectra were then smoothed using a reverse Fourier transform procedure. The raw ellipticity was then converted into mean residue molar ellipticity units $(deg \cdot cm^2)/(residue \cdot dmol)$.

2.4.2 *Analysis of Melting Data*

The CD melting temperature (T_M) of a peptide/protein fold is defined as the temperature at which the CD signal coincides with the average of the fully folded and fully unfolded baselines.

The CD spectrum of the unfolded state is expected to be less sequence dependent and has previously been determined for several classes of Trp-cage constructs including those containing D-Ala (Williams et al., 2008) and Trp[2] species: $[\theta]_U$ = -660 - 24•T(°C) and $[\theta]_U$ = -2600 - 24•T(°C), respectively. For the studies detailed here, a structure-invariant slope of -24° per degree centigrade of warming was assumed. As needed, adjustments were made to the y-intercept so that the unfolded baseline coincided with the observed CD signal observed at high temperatures for the less stable analogs of each series.

The present study entailed an experimental approach to ascertaining the folded baseline, assuming that NMR CSDs can be used to calibrate the CD at 300 and 320K.

At a given temperature, the relationship between the fraction folded and the CD signal can be described by the following equation:

$$\chi_F = \frac{([\theta]_U - [\theta]_{obs})}{([\theta]_U - [\theta]_F)} \qquad (2.5)$$

Here $[\theta]_U$ and $[\theta]_F$ represent the unfolded and folded baselines and χ_F and $[\theta]_{obs}$ are the fraction folded and raw molar ellipticity, respectively. Equation 3 can be rearranged to give the folded baseline in terms of the unfolded baseline, the observed CD signal, and the fraction folded**:**

$$[\theta]_F = [\theta]_U + \frac{[\theta]_{obs} - [\theta]_U}{\chi_F} \quad (2.6)$$

A complete set of $[\theta]_F$–values at intermediate temperatures can be filled in by assuming two-state folding: a sigmoidal relationship such as: $(1 - \chi_F) = 1 / (1 + \exp(-k(a + (T - T_M))))$ with T in degree centigrade and assuming that $\chi_F < 0.01$ at $(T_M + 70)$.

Helicity accounts for nearly all of the observed CD signal for the folded state of Trp-cage. Given the existence of half-cage and residual α-helix in the unfolded state, this helicity can be present without proper placement of the terminal Pro residues. Therefore, χ_F values for the average of the diagnostic L7Hα and G11Hα2 nuclei were used to calibrate the CD spectra.

In previous CD studies of Trp-cage species, folded baselines derived from the melts corresponded to a 0.30 – 0.34% loss of helix signal per °C: at 217 – 222 nm, $[\theta]_F = [\theta]_{F,0°C} - 0.0032 \bullet [\theta]_{F,0°C} \bullet T(°C)$ (Barua et al., 2008; Williams et al., 2011). This relationship was confirmed by pre-melting slopes for hyperstable constructs that displayed, based on NMR shifts, less than 5 % melting up to 320 K. Some prior folded baselines that have been used (Scian et al., 2012) include: for a cyclic Trp-cage $[\theta]_F = [1 - 0.0030 \bullet T(°C)] \bullet -20{,}730$ deg• cm^2/dmol• res; for a species (TC13a) rather similar to TC15 and TC16 reported herein, $[\theta]_F = [1 - 0.0032 \bullet T(°C)] \bullet -18{,}615$ deg• cm^2/dmol• res. For species with the P12W mutation (designated as Trp^2, T^2C species), the treatment of CD data is complicated by the appearance of an indole/indole exciton couplet (CD maximum at 228 nm and a minimum at 215-217 nm) (Anderson et al., 2017; Kier &

Andersen, 2008; Kier, Shu, Eidenschink, & Andersen, 2010) which changes the magnitude and location of the Trp-cage CD minimum, typically from 222 to 218 nm.

Chapter 3. REVERSING PH STABILITY

3.1 CONTEXT

The Trp-cage (Neidigh et al., 2002) has remained an important system for both computer simulation of folding (Chowdhury et al., 2004; Cote et al., 2015; Day et al., 2010; Ding et al., 2005; Hu et al., 2008; Juraszek & Bolhuis, 2006; Mok et al., 2007; Simmerling et al., 2002; Snow et al., 2002; R. Zhou, 2003) and experimental work aiming to measure the $\Delta G_{folding}$ contributions (Barua et al., 2008; Byrne et al., 2014; Mok et al., 2007; Williams et al., 2008) of specific tertiary interactions and secondary structure stabilization methods. As it turns out, several stabilizing interactions in the Trp-cage folded state have a strong pH dependence; and all prior Trp-cage mutants have been destabilized under carboxylate-protonating conditions. Notable among the pH dependent stabilizing interactions within the Trp-cage are: 1) an Asp as the helix N-cap, 2) an H-bonded Asp9/Arg16 salt bridge, 3) an interaction between the chain termini which are in close spatial proximity, and 4) additional sidechain interactions with Asp9.

In the initial optimization of the Trp-cage fold (Neidigh et al., 2002), the introduction of the H-bonded salt bridge between Arg16 and Asp9 was one of the key steps that lead to fold stabilization and solubilization. This salt bridge (with D/R versus E/R versus D/K variants examined) has been the subject of a number of studies (Barua et al., 2008; Byrne et al., 2014; Rovó et al., 2011; Williams et al., 2011). The fold enhancing effect of this "salt bridge" is clearly pH dependent (Barua et al., 2008; Byrne et al., 2014, 2013; Williams et al., 2011). There is also another aspartate in most optimized Trp-cages; Asp is a superior replacement for the N-terminal Asn in the initial Trp-cage sequence (Barua et al., 2008). Both Asn and Asp are known helix N-caps. N-capping has been incorporated into Lifson-Roig (Lifson & Roig, 1961) helix formation theory

(Andersen & Tong, 1997; Doig, Chakrabartty, Klingler, & Baldwin, 1994; Shalongo & Stellwagen, 1995). While early measures (Andersen & Tong, 1997; Doig & Baldwin, 1995; Rohl, Chakrabartty, & Baldwin, 1996) of the N-capping constants of aspartate and asparagine placed them as nearly equally good caps, later studies (Barua et al., 2008; Song, Stewart, Fesinmeyer, Andersen, & Simmerling, 2008; Stewart, 2009; Stewart, Lin, & Andersen, 2008; Williams et al., 2011) revealed a greater capping proficiency for aspartate. In both the early studies and the later series, the Asp N-capping value was found to be highly pH dependent, corresponding to $\Delta\Delta G_F$ = +2.4±0.3 kJ/mol for the protonation effect on helicity in peptide models such as **X**-$(AAAAK)_3$-GY-NH_2 and Ac-YGG**X**-$(KAAAA)_3$-K-NH_2 (where **X** is a variable N-cap) (Stewart, 2009; Stewart et al., 2008). This value also finds support in Table 3.1: the $\Delta\Delta G_F$ for pH adjustment drops by 2.5 kJ/mol when Asp1 is replaced by an acetyl group (TC16b versus trTC16b).

Key stages in the optimization of Trp-cage structures are collected in Table 3.1. At each optimization stage listed, fold stability is significantly greater at pH 6.5-7 than at pH 2.5. Typically, this difference is approximately 4 kJ/mol, with the one lower value corresponding to a species lacking the N-terminal Asp.

Table 3.1. Serial Improvement of the Trp-Cage: Circular Dichroic Spectral Melting Temperatures and the Fold Destabilizing Effect of Protonation[a]. (Barua et al., 2008; Neidigh et al., 2002; Stewart, 2009; Stewart et al., 2008; Williams et al., 2008)

	Sequence	CD T_M (°C) at pH 6.5-7 (T_M at pH 2.5)	$\Delta\Delta G_F^{280}$ (kJ/mol) for protonation at 280 K
TC5b	NLYIQWLKDGGPSSGRPPPS	42	4.0
TC9b	NAYAQWLKDGGPSSGRPPPS	51	3.3
TC10b	**D**AYAQWLKDGGPSSGRPPPS	56	3.7
TC13b	DAYAQWL**A**DGGP**A**SGRPPPS	68 (49.5)	4.2
TC15b	DAYAQWLAD**a**GPASGRPPPS	74 (69)	3.7
T^2C15b	DAYAQWLAD**a**G**W**ASGRPPPS	81 (74)	≈ 4.4
TC16b	DAYAQWLAD**a**GPAS**a**RPPPS	83 (74)	4.5
trTC16b	**Ac-**AYAQWLAD**a**GPAS**a**RPPPS-**NH_2**	par67	2.0

[a] D-Ala mutations are indicated as **a**. All ΔΔG values reported herein are defined such that a negative value corresponds to a mutation that stabilizes the fold, or an increase in stability upon acidification.

Although all the mutations appearing in the entries for TC15b and T^2C15b have been reported previously, the present work is the first including these specific sequences. One deserves some comment: the Gly to D-Ala mutations (Anil, Song, Tang, & Raleigh, 2004; Byrne et al., 2013; Williams et al., 2008); D-Ala is indicated as **a** in sequences.

The significant change in the helix N-capping effect of $Asp^{\mathbf{1}}$ upon protonation has complicated the evaluation of the Coulombic component of stabilization associated with the H-bonded D9/R16 salt bridge. There are additional pH-dependent interaction in these Trp-cages besides the N-capping Asp and the salt bridge: the helix-stabilizing QXXXD interaction is also pH dependent (Huyghues-Despointes, Klingler, & Baldwin, 1995; Huyghues□Despointes, Scholtz, & Baldwin, 1993; Stapley & Doig, 1997), it gets weaker upon Asp protonation, and an effect related to protonation at the extreme C-terminus could also be expected since there could be a Coulombic interaction with the relatively nearby N-terminus.

The most complete prior examination of the origin of pH-induced stability changes is due to Barua et al. (Barua et al., 2008). That effort employed a series of single and multiple site mutants of TC9b, with Asn[1] as the N-cap, to reduce the pH dependence of the N-capping effect.

Table 3.2. Asparagine-terminated Constructs: Mutational and pH Effects on Stability[a]

Sequence	pH 7		pH 2.5		$\Delta\Delta G_F$ mutation (kJ/mol) (at pH 7)	$\Delta\Delta G_F$ (ΔpH) (kJ/mol)
	χ_F [b] at 300 K	CD T_M (^oC)	χ_F [b] at 300 K	CD T_M (^oC)		
NAYAQWLKDGGPSSGRPPPS	0.86	51	0.62	34.5	**ref**	3.3
NAYA**A**WLKDGGPSSGRPPPS	0.72	41	0.50	27	2.2	2.4
NAYAQWLK**N**GGPSSGRPPPS	0.65	38	0.47	25	3.0	1.8
NAYAQWLKDGGPSSG**Nva**PPPS	0.56	32	0.59	33	3.9	-0.3
NAYAQWLK**N**GGPSSGRPPPS-$\mathbf{NH_2}$	0.55	30	0.45	22	4.0	1.0

[a] Reported in Barua et al. (Barua et al., 2008). Nva stands for nor-valine, the des-guanidino analog of Arg.

[b] The mole fraction of the fully-formed cage (χ_F) for each analog was determined from NMR structuring shifts as described in the Methods section.

With the exception of the last entry, which combines D9N with C-terminal amidation, this study only examined single–site mutations. Depending on how it's measured, eliminating the C-terminal negative charge (by protonation or amidation) appeared to be a 1 – 1.8 kJ/mol effect. The data suggested, but did not prove, that the QXXXD-stabilization of the helix could be as large as 2-3 kJ with Asp ionized. But a firm quantitation of the Coulombic component of the salt bridge remained unattainable. The study also provided the first instance of a Trp-cage analog, the R16Nva entry in Table 3.2, which was not significantly stabilized by carboxylic acid deprotonation.

The results obtained from the latest in depth exploration of salt-bridge optimization (Williams et al., 2011) provided some clarification. While it appeared, based on its melting temperature, that

(D9E)-TC10b was as stable as TC10b itself (Barua et al., 2008; Hudáky et al., 2008; Williams et al., 2008), it is now clear that this is due more to an intrinsic helicity increase rather than an improvement in the salt bridge. The study established that a D9E mutation is fold stabilizing in the absence of R16. Interactions of sidechain charges with the helix macrodipole are the basis for these effects and the prior confusion concerning the relative stabilizing effects of the E9/R16 versus D9/R16 salt bridges (Williams et al., 2008).

It has been known for some time that carboxylate sidechains can influence helix stability and that the effect is position dependent (Andersen & Tong, 1997; Doig & Baldwin, 1995). As previously noted, Asp^- is the most effective helix N-cap while Asp^0 is less effective than Asn. In like manner, based on the helix macrodipole model, the presence of aspart**ate** at or near the C-terminus of a helix should be notably destabilizing. D9 of the Trp-cage is so located. This raises a question, does the salt-bridge offset or mitigate the unfavorable effect of the negative sidechain of Asp at the C-terminus of an α-helix? Studies by J. Stewart (Stewart, 2009) have provided a direct measure of the helix stabilization associated with the protonation of a C-capping aspartate, see Figure 3 of Williams *et al.* (Williams et al., 2011). The model helix system in that study was Ac-$(KAAAA)_3$-**X**GY-NH_2 where **X** is in the C-cap position. The following stability series, ΔΔG in kJ/mol, was observed, **X** (ΔG_U): **R** (-0.4) > **A** (the reference) > **N** (0.2) > $\mathbf{E}^-$ (1.0) > $\mathbf{D}^-$ (1.7). Assuming Asn is a model for protonated Asp, the ionization effect at the helix C-terminus (helix destabilization) is nearly as large as the helix-favoring effect at the N-terminus.

Examination of the pH-sensitive interactions herein is intended to answer the remaining questions regarding the pH/stability relationships for Trp-cage species and to provide Trp-cages that are distinctly more stable under acidic conditions for structural studies. Previous work by Byrne focused on the highly stable TC16b and trTC16b series (Byrne, 2013). Current studies

detailed here involve TC15b and the corresponding trTC15b series. In addition to the characterization of additional mutations, the trTC15b series is more analogous to the circularly permuted Trp-cage series discussed in Chapter 4.

3.2 Prior Studies of pH Sensitive Interactions

To design a Trp-cage that was more stable at low pH, it was clear that D9 should, at the higher pH, only be involved in a helix-destabilizing interaction to achieve systems which would be more stable when carboxylates are protonated; *i.e.* there should be no salt bridge interaction and that other pH dependent effects should be minimized. The first series of mutations undertaken by Byrne to achieve this goal, pH stability reversal for a Trp-cage, was based on TC16b and is shown immediately below in Table 3.3 (Byrne, 2013). This series of mutants was also intended to provide measures of several individual ionization effects.

Table 3.3. A Set of Mutants Based on TC16b Designed to Probe Specific pH Dependent Interactions Which Can Influence Fold Stability (Byrne, 2013)[a].

Peptide	**Sequence**
TC16b	DAYAQWLADaGPASaRPPPS
trTC16b	**Ac**-AYAQWLADaGPASaRPPPS-**NH_2**
(Q5A)-trTC16b	**Ac**-AYA**A**WLADaGPASaRPPPS-**NH_2**
(D9N)-trTC16b	**Ac**-AYAQWLA**N**aGPASaRPPPS-**NH_2**
(Q5A,D9N)-trTC16b	**Ac**-AYA**A**WLA**N**aGPASaRPPPS-**NH_2**
(Q5A,R16Nva)-trTC16b	**Ac**-AYA**A**WLADaGPASa**Nva**PPPS-**NH_2**
(Q5A,D9N,R16Nva)-trTC16b	**Ac**-AYA**A**WLA**N**aGPASa**Nva**PPPS-**NH_2**
(R16Nva)-trTC16b	**Ac**-AYAQWLADaGPASa**Nva**PPPS-**NH_2**
(R16Cit)-trTC16b	**Ac**-AYAQWLADaGPASa**Cit**PPPS-**NH_2**

[a] Nva stands for norvaline, the des-guanidino version of Arg. Cit stands for citrulline.

In all cases, the constructs lack Asp[1] and were both acetylated and amidated. Acetyl is the second best N-cap (after aspartate) and is significantly more helix-promoting than aspartic acid or Asn (Barua et al., 2008; Stewart, 2009; Stewart et al., 2008; Xia, Zhang, Huang, Zhou, & Sun, 2008). The presence of the acetyl and amide at the termini also served to eliminate any Coulombic effects between the termini, which are close in space in the Trp-cage fold. An alanine inserted at the 5 position removed the potential helix stabilizing QXXXD interaction. Both the D9N and R16Nva mutations eliminated the salt bridge. The likely stabilizing interaction of the Arg sidechain with the buried indole ring was considered. An arginine to norvalene mutation was selected to provide enough sidechain length at position 16 to wrap around the central Trp; facilitating its burial. The alternative mutation of arginine to citrulline was examined since it might allow for H-bonding between it and both the Asp9 and Gln5 but would be lacking any electrostatic interactions. The observed mutational and pH effects on stability are collected in Table 3.4. Two measures of relative fold stability were used in the study: NMR chemical shift deviations (CSDs)

and how they change from 280 to 300 K and the melting temperature as measured by circular dichroism (CD).

Table 3.4. Fold Populations at 300 K and CD T_M's of trTC16b Analogs at Both pH 7 and pH 2.5[a].

Peptide	CD T_M (°C)	χ_F at 300 K	ΔG_U at 300K	$\Delta\Delta G_F$ mut	CD T_M (°C)	χ_F at 300 K	ΔG_U at 300K	$\Delta\Delta G_F$ mut	$\Delta\Delta G_F$ ΔpH
	pH 7				pH 2.5				
trTC16b	67.7	0.958	7.80	**ref**	67.9	0.909	5.74	**ref**	2.06
R16Nva	49.5	0.784	3.22	4.58	**65.2**	0.847	4.27	1.47	**-1.05**
R16Cit	49.7	0.841	4.15	3.65	**67.4**	0.888	5.16	0.58	**-1.01**
D9N	57.9	0.841	4.15	3.65	59.1	0.840	4.14	1.60	0.01
Q5A	63.7	0.946	7.14	0.66	64.4	0.916	5.96	-0.22	1.18
Q5A,D9N	62.7	0.845	4.23	3.57	59.9	0.843	4.19	1.55	0.04
Q5A,R16Nva	41.9	0.756	2.82	4.98	**63.3**	0.854	4.41	1.33	**-1.59**
Q5A,D9N,R16Nva	61.9	0.845	4.23	3.57	60.4	0.845	4.23	1.51	0.00

[a] Data by Byrne (Byrne, 2013). Mutational and pH-induced changes in fold stability. In this case, the $\Delta\Delta G_U$ values are based on the Σ CSD measures at the following sites: G11Hα2, P18Hα/Hβ3 and P19Hδ2/δ3. ΔΔG(pH) is the effect of ionization; positive values indicate fold destabilization. Instances of fold stabilization are shown in **red**. In two ***cases***, a small increase in apparent thermal stability observed by CD at pH 2.5 appears even when there is a decrease in fold stability at 280K and 300K (based on NMR measures); this has not been fully rationalized. It may represent an error in the derivation of CD baselines for pH 2.5. It could also reflect greater residual helicity in the unfolded state at the lower pH and higher ionic strength.

At pH 7, R16Nva was the most destabilizing single-site mutation: 4.6 kJ/mol, which is nearly 1 kJ more than observed for the D9N and R16Cit mutations under the same conditions. At pH 2.5, the destabilization associated with the R16Nva mutation dropped to 1.5 kJ/mol. Replacing R16 with the closest neutral analog, citrulline, resulted in a somewhat smaller destabilization than R16Nva at both pHs. The greater fold stability for R16Cit versus R16Nva could reflect, rather than residual H-bonding effects, the surface placement of the residue-16 sidechain. Even if all the variants of the residue 16 sidechain examined wrap around the edge of the Trp indole ring, one

side of the sidechain is fully surface exposed. The apolar norvaline would be less favorable in a surface exposed position.

These analogs, which eliminate the salt bridge while maintaining the Asp^9 – (R16Cit)-trTC16b and (R16Nva)-trTC16b, as well as (Q5A, R16Nva)-trTC16b – also displayed a significant increase (1 – 1.6 kJ/mol) in fold stability upon acidification. The increase in structuring CSDs was observed to be uniform throughout the sequence (Byrne, 2013).

The D9N mutation was also destabilizing at pH 7, but not to as great an extent as the R16Nva mutation (3.6 versus 4.6 kJ/mol). The difference can be rationalized as a consequence of a 1 – 1.4 kJ favorable arginine-sidechain / indole-ring interaction. As expected, all constructs containing a D9N mutation, displayed no pH dependence in fold stability (Byrne, 2013). The free-energy change corresponding to the D9N mutation can be attributed, primarily, to the loss of the D9/R16 salt-bridge.

3.3 Mutational Studies for Deconvoluting pH Effects on the Trp-cage and Stability Optimization at pH 2.5.

Table 3.4 contains the first instances of the Arg to citrulline mutation in the Trp-cage, and this result raised a number of questions. When D9 was present, the R16Cit mutant displays a slightly higher fold population than the R16Nva mutant at both pHs; suggesting that some favorable polar interactions are still present with the Cit sidechain. It should be noted that these might even include the Q5 sidechain. Even at pH 2.5 markedly different $\Delta\Delta G_F$ values were observed for mutations which alter the D9/R16 interaction: R16Nva (1.5 kJ/mol), R16Cit (0.6 kJ/mol), and D9N (1.6 kJ/mol). An alternative rationale could be based on differences in the penalties for surface exposure of these residues.

In the present study, NMR chemical shift deviations (CSDs) and how they change from 280 to 300 K and the melting temperature as measured by circular dichroism (CD) are presented. Only the chemical shift measures at sites that reflect a fully formed Trp-cage were employed to derive ΔG_U and $\Delta\Delta G$ of folding values for protonation and mutations. Table 3.5 contains our efforts to determine the generality of the R16Nva versus R16Cit results in Table 3.4 and to ascertain with certainty, which of these mutations should be present in a Trp-cage analog used for a detailed structure elucidation at pH 2.5. Also included was a D9Abu mutation which removes all polar character from the residue-9 sidechain. Likewise, the R16A mutation eliminates any polar or H-bonding interactions with Asp^9 while also providing a sidechain too short to effectively bury the indole ring of Trp^6.

Table 3.5. D9/R16 Mutations in the Ac-AYAQWLADaGPASGRPPPS-NH_2 Sequence With (trT^2C15b) and Without (trTC15b) a Fold-Stabilizing P12W Mutation.[a]

Peptide	CD T_M (^oC)	χ_F at 320 K	ΔG_U at 300K	$\Delta\Delta G_F$ mut	CD T_M (^oC)	χ_F at 320 K	ΔG_U at 300K	$\Delta\Delta G_F$ mut	$\Delta\Delta G_F$ ΔpH
	pH 7				pH 2.5				
trT^2C15b	67	0.863	8.50	**ref**	70	0.836	6.36	**ref**	2.14
R16Nva	55	0.612	3.76	4.74	64	0.722	4.41	1.95	-0.65
R16Cit	53	0.584	4.08	4.42	65	0.753	5.07	1.29	-0.99
trTC15b	65	0.787	7.09	**ref**	62	0.673	4.35	**ref**	2.74
R16Nva	48	0.467	2.33	4.76	62	0.617	3.27	1.08	-0.94
R16Cit	49	0.458	2.67	4.42	63	0.640	3.82	0.53	-1.15
R16A	34	0.258	-0.01	7.10	49	0.406	1.18	3.17	-1.19
D9Abu	49	0.458	2.67	4.42	54	0.508	2.54	1.81	0.13
D9Abu, R16Nva	50	0.443	1.79	5.30	55	0.521	2.43	1.92	-0.64
D9Abu, R16Cit	52	0.456	2.11	4.98	54	0.505	2.26	2.09	-0.15

[a] Mutational and pH-induced changes in fold stability. To retain the standard residue numbering, the N-terminal acetyl is considered to be residue #1. The ΔG_U values are based exclusively on the CSDs observed at P18Hα/Hβ3. These measures are, in all cases, within 0.03 population mole fraction units of the value derived from G11Hα2. $\Delta\Delta G_F(\Delta pH)$ is the effect of ionization; negative values indicate fold stabilization upon protonation.

Table 3.5 includes additional cases in which a 0.7 - 1.2 kJ/mol fold stabilizations result upon D9 sidechain protonation. In this series of comparisons, an advantage of R16Cit over R16Nva for fold preservation appears only at pH 2.5 and all the differences in mutational $\Delta\Delta$G-values are much smaller. While the $\Delta\Delta$G–values for these mutations were similar to D9N and D9Abu mutational values at pH 6.5, some structural stability loss was observed for R16 mutations *even at pH 2.5*. The R16Nva and R16Cit, as expected, were lacking in effect at both pH 7 and 2.5 in the presence of the D9Abu mutations. With D9 still present, there is still a destabilizing effect (0.53 – 1.95 kJ/mol) for R16Nva and R16Cit mutations at pH 2.5. Clearly some questions remained concerning the functions of the residue 16, particularly at pH 2.5.

The increased stability associated with these R16X mutations at pH 2.5 is greater as the temperature is increased. This readily seen in the pH-induced change in the CD melt, Figure 3.1. The increase in stability at pH 2.5 is presumably due almost exclusively to protonation of the carboxylate of D9 at the lower pH. The carboxylate anion of aspartic acid at pH 7 interacts with the C-terminal negative charge of the helix macrodipole in an unfavorable manner; thus, the protonation of the Asp side chain carboxylate at pH 2.5 has a stabilizing effect.

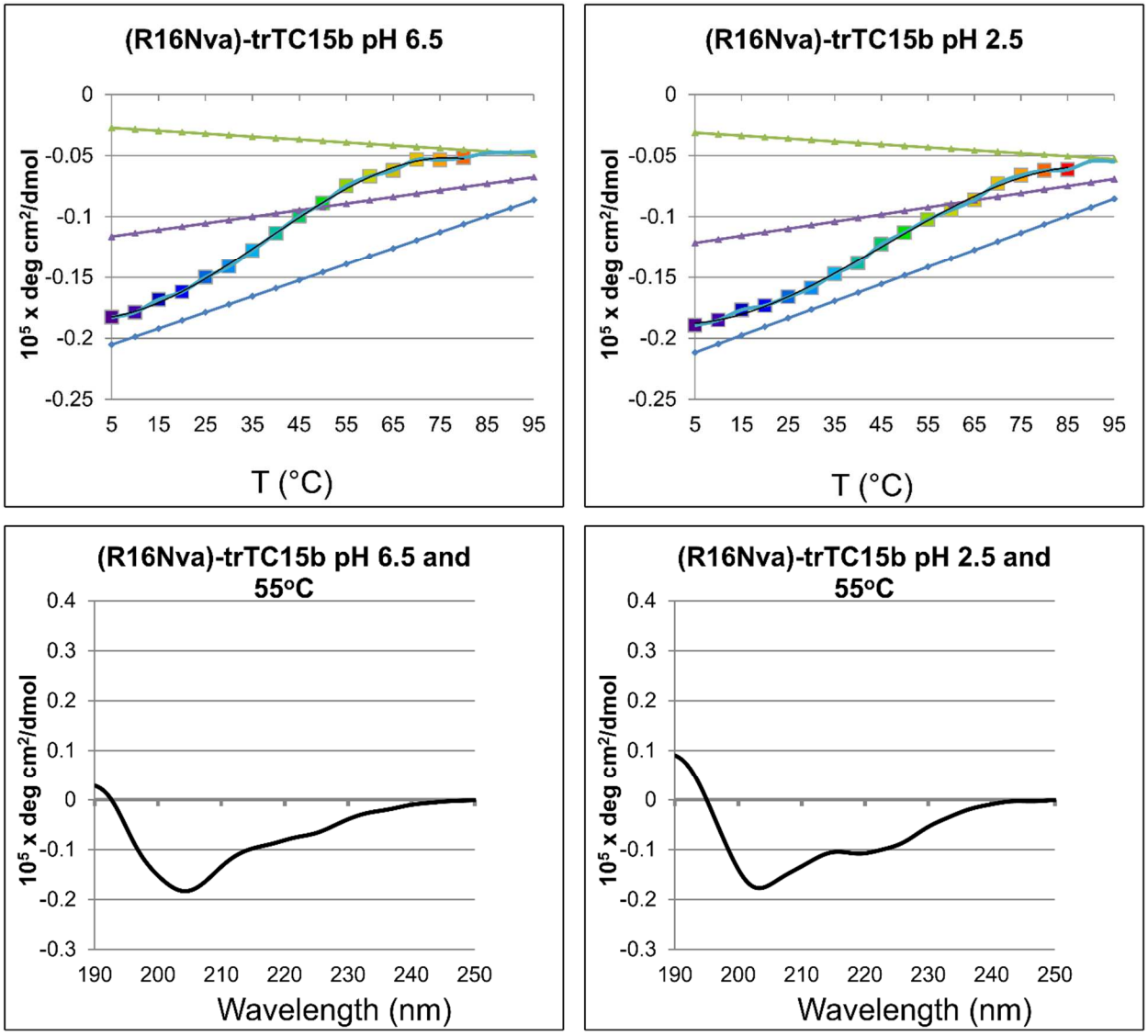

Figure 3.1. CD melts for trTC15b 16Nva at pH 6.5 and pH 2.5(top) and the corresponding raw CD signal at 55°C (bottom). The more pronounced helix signal at pH 2.5 is reflected in a higher T_M.

The R16A mutation included in Table 3.5 addresses a question unrelated to pH effects: an 'encagement effect', an interaction with the Trp indole has been attributed to the aliphatic portion of the Arg sidechain. Both the R16A and R16Nva mutants should have no Coulombic interactions with the indole. The R16Nva versus R16A corresponds to a $\Delta\Delta G_U$ of -2.22 ± 0.13 kJ/mol for a

Nva → Ala mutation independent of pH. The much shorter Ala fails to provide complete indole encagement.

3.4 THE TRP-CAGE MOTIF AT PH 2.5

An important question regarding the pH-dependence of the Trp-cage motif was examined in earlier work by Byrne. Given the significant mutations required to generate a Trp-cage with enhanced stability at pH 2.5 and the resulting changes in both local and more remote interactions that might result, it was possible that a change in Trp-cage structure might occur upon acidification. An NMR structure at pH 2.5 was required. (R16Nva)-trTC16b was chosen due to its lack of polar long-range interactions associated with the salt bridge. Conservative treatment of the CSD data for (R16Nva)-trTC16b suggests that the fraction folded is equal to or greater than 0.90 at 280K; a fold population high enough to guarantee that the observed NOEs are an accurate reflection of folded-state geometry (Byrne, 2013).

Higher precision NOESY data, with an 80-millisecond mixing time, was collected for the calculation of an NMR structure ensemble. Over the accepted structures in the resulting ensemble (31 structures from 40 random starting points), the pairwise RMSD for residues 3–19 (full-length Trp-cage numbering, the acetyl in this truncated species is viewed as residue 1) was 0.13 ± 0.05 Å for the backbone atoms and 0.54 ± 0.14 Å for all heavy atoms (Byrne, 2013). The accepted ensemble appears in Figure 3.2.

All of the ensemble members place the 16-norvaline sidechain in a position that implies a role in Trp burial. A slight majority of the ensemble members place the N-terminal acetyl function in position to provide a stabilizing H-bonding interaction in the N-terminal turn of the helix. In contrast, the C-terminus, past P19, was disordered (Byrne, 2013).

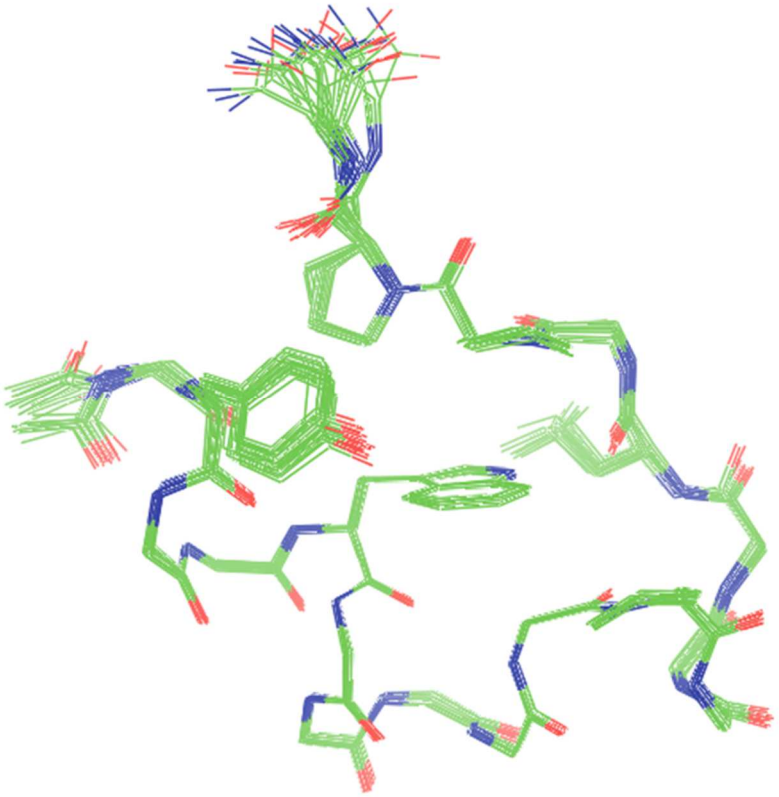

Figure 3.2. The NMR structure ensemble for (R16Nva)-trTC16b at pH 2.5. The only sidechains that are included in this structure depiction are those of Y3, W6, Nva16 and P19 (Byrne, 2013).

An overlay of a representative member of the (R16Nva)-trTC16b ensemble and a typical member of the TC16b ensemble (Williams et al., 2008) gave an RMSD of 0.90 Å for the backbone atoms over residues 3-19 (Figure 3.3) (Byrne, 2013). To ascertain whether the R16Nva mutation or end-capping, had any more subtle effects on the cage geometry we compared this ensemble to previously structures (both by NMR at pH 6.5 – 7 and by X-ray) obtained for the Trp-cage, Table 3.6 (Barua et al., 2008; Hudáky et al., 2008; Neidigh et al., 2002; Scian et al., 2012; Williams et al., 2008, 2011).

The only significant deviation between the structures is in the 3_{10} helix segment; the S14 sidechain does not penetrate into the core to as great an extent when arginine has been replaced

with norvaline. When arginine is present, the serine hydroxyl can H-bond to the ε-NH of the arginine sidechain.

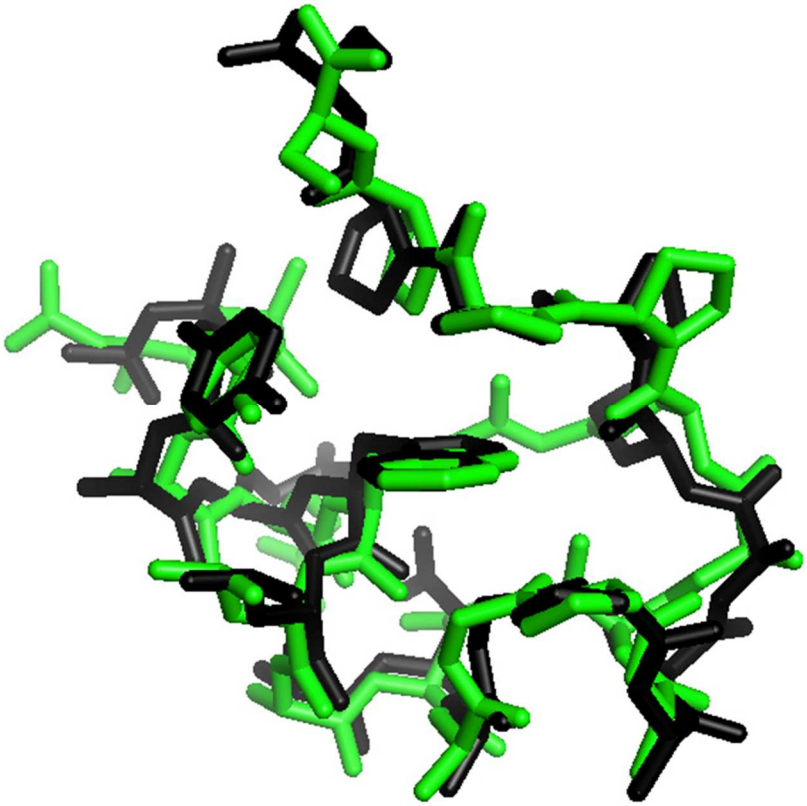

Figure 3.3. Structure overlay, (R16Nva)-trTC16b (black) with TC16b (green) (Byrne, 2013).

3.5 DISCUSSION

The detailed NMR structure for a Trp-cage lacking the D9/R16 salt bridge was obtained under acidic conditions that preclude other Coulombic interactions as well, including those between the chain termini. Comparing this structure to prior NMR structures obtained from pH 6.5-7 data in which the salt bridge is intact, the structures are observed to match to within a 0.9 Å backbone RMSD. It is then clear that the detailed geometry of the Trp-cage is not determined by the salt bridge or any other Coulombic interactions. These interactions do, however, influence fold stability. The specific ΔG_U contributions of these interactions can be derived from the mutational and pH induced fold stability changes reported in Tables 3.1, 3.2, 3.4 and 3.5.

The largest stabilizing factors associated with Asp ionization are: helix N-capping when Asp is present as the N-terminal residue and the Asp9/Arg16 salt-bridge. The increased helix N-capping associated with Asp^- corresponds to a 2.4 ± 0.3 kJ/mol stabilization in other models (Andersen & Tong, 1997; Rohl et al., 1996; Song et al., 2008) and is a major contributor to the 4.0 ± 0.4 kJ/mol stabilization observed for Trp-cage carboxylate deprotonation in Table 3.1. Our best estimate is that the N-cap effect is 2 kJ/mol with an additional 0.5 – 1 kJ associated with a favorable Coulombic interaction between the extreme chain termini which are quite close in folded structure.

At first glance this analysis seems to imply that the salt-bridge effect is much smaller than suggested by early estimates (Barua et al., 2008; Neidigh et al., 2002). This is a reflection of a countervailing destabilization associated with the ionization of Asp^9: an unfavorable interaction between the negative sidechain charge and the C-terminus of the helix macrodipole. This effect, 1.5 kJ/mol in model helices (Andersen & Tong, 1997; Rohl et al., 1996; Stewart, 2009; Williams et al., 2011), became the basis for preparing Trp-cage analogs that are more stable under acidic rather than neutral conditions. The data tabulated herein provides ten distinct measurements of

this effect: a fold stabilization of 0.87 ± 0.72 kJ/mol upon acidification. The actual value could be 0.5 – 0.7 kJ/mol larger since there is a helix destabilization associated with Asp protonation in a QXXXD sequence within a helix. Indeed, the largest ΔpH helix-favoring effect ($\Delta\Delta G_U$ = +1.6 kJ/mol) was recorded for a Q5A species (Table 3.4). With these considerations the stabilizing effect of the Asp^-/Arg salt bridge can be placed in the 3 – 3.5 kJ/mol range.

The largest stability changes due to single-site mutations in the present study are replacements of R16. The $\Delta\Delta G_F$ values for R16Nva mutations were measured with position 9 being an aspartate (4.78 ± 0.20 kJ/mol, n = 4) and with a D9Abu mutation or with protonated Asp^0 (1.42 ± 0.54 kJ/mol, n = 5), another indication that the salt bridge is worth 3.3 kJ/mol. In more specific comparisons, an R16Nva mutation displays a 0.7 – 1.5 kJ/mol fold destabilization that appears to be unrelated to the salt-bridge. As previously noted, this may be attributed to the less favorable placement of the apolar, norvaline residue at an exposed surface position. Based on the NMR structure, it is clear Nva, just like Arg, wraps around the periphery of the indole ring completing the "encagement" of the Trp indole ring. An even larger destabilization was observed for an R16A mutation: 7.10 kJ/mol at pH 7, 3.17 kJ/mol at pH 2.5 (Table 3.5). An alanine does not provide enough alkyl chain-length to complete the cage with this deficit giving rise to a 2 - 3 kJ/mol destabilization independent of the pH.

Chapter 4. OPTIMIZING THE FOLD STABILITY OF THE CIRCULARLY PERMUTED TRP-CAGE MOTIF

4.1 CONTEXT

Circular permutation is defined as linking the N- and C-termini of a linear polypeptide by an amide bond or short peptide linker and cutting the backbone elsewhere in the sequence. Changing the location of the termini in a sequence could change the resulting fold, but a common topology is observed in many cases. Circular permutation can thus serve for the study of contact order effects on folding rates and pathway selection. The successful circular permutation of a number of small proteins (Kier, Anderson, & Andersen, 2014; Kier, Byrne, Scian, Anderson, & Andersen, 2012) has recently been accomplished in this laboratory, including what is likely the smallest folded domain, the Trp-cage miniprotein (Byrne et al. 2013). Current studies reported here describe the further mutational optimization of the circularly-permuted Trp-cage (cp-TC) fold and also compare and contrast the effects of individual single-site mutations in circularly permuted versus standard topology analogs.

Since the N- and C- termini of folded Trp-Cages are held in close spatial proximity, cyclisation, and also circular permutation can be accomplished using quite short linkers. The cyclisation of a Trp-cage ($G^{(-1)}$DAYAQWLADGGPSSGRPPPSG, T_M = 58 °C; T_M = 68 °C without the added terminal glycines) was reported by Scian et al. (Scian et al., 2012). This corresponds to the standard Trp-cage with a Gly at each terminus. Cyclization, resulting in a simple Gly-Gly linkage of the ends of the standard Trp-cage, resulted in a hyperstable construct (T_M = 95 °C). High resolution X-ray crystallographic data indicated that the structure of the cyclic construct was essentially identical to prior solution-state NMR structures generated for acyclic Trp-cage species.

The only successful circular permutation to date, corresponds to deletion of G15 in the cyclic version of the sequence above. This produced the circularly-permuted Trp-cage sequence, RPPP-SGGDA-YAQWLADGGPSS (cpTC1). Peptide cpTC1 did fold into a Trp-cage fold but the stability was significantly reduced: T_M = 1 °C, fraction folded (χ_F) = 0.43 at 280K. In the first series of optimization attempts (Byrne et al., 2013) stability was improved significantly (to ΔG_U^{300} = +6 kJ/mol), and one of the most stable constructs afforded an NMR structure ensemble that confirmed the geometry of cage formation was the same as in the standard topology Trp-cage. It was also established that the Asp/Arg salt bridge was still a feature of the structure even with its permutation from a D9/R16 to R1/D16 interaction. Current studies described here are aimed at providing information about the cp-TC fold and more stable examples of it. Reported here are the further mutational optimization of the cp-TC fold and rationalize the observed stability trends. Another aim was to prepare analogs that would provide folding pathway insights through dynamics studies which are detailed in the following chapter.

4.2 Some Prior, But Unpublished, Studies of Circular Permutants.

The previously reported circular permutants all corresponded to deletion of Gly15 from the previously reported (Scian et al., 2012) cyclic form of the Trp-cage. Gly15 is the connecting unit between the short 3_{10} helix and Arg16 which is the N-terminus of a short $polyPro_{II}$ unit. The first thing we examine here are alternative cut points in a cyclo-Trp-cage to confirm that the initial choice, deletion of G15 was, indeed, optimal. Two alternative cut sites were examined: between the alpha helix and 3_{10} helix (a G10/G11 or G11/P12 cut in the standard Trp-cage numbering) - all other points would be within secondary structure elements. The resulting circular permutants are too destabilized for CD measures of fold melting. NMR probes with large structuring shifts that

reflect cage formation indicate very low populations of the cage state (Table 4.1). Inserting the equivalent of a P12W mutation which is strongly fold stabilizing in both the standard Trp-cage and the prior cp-TC series as well as addition of a helix formation favoring co-solvent, did little to rescue stability.

Table 4.1. Comparison of the Stability of Trp-Cage Circular Permutants With Different Cut Sites[a]

	χ_F (280K)	χ_F (300K)	χ_F (320K)
Cut 1 (G10/G11)	0.12	n.d.	0.05
Cut 2 (G11/P12)	0.24	n.d.	0.10
Cut 2 (with 30 vol-% TFE)	0.33	n.d.	n.d.
Cut 2 (with P19W mutation)	n.d.	0.17	n.d.

[a] Based on unpublished data by Byrne et al (Byrne et al., 2013). Sequences are based on DAYAQWLADGGPSSGRPPPS cyclized using a GG linker. No data is indicated by n.d.

Returning to the use of D-Ala substitutions, since earlier studies (Williams et al., 2008) of G10**a** and G15**a** mutations in the Trp-cage, other groups have examined D-amino acid substitutions at position 10. In one case, Rodriguez-Granillo (Rodriguez-Granillo, Annavarapu, Zhang, Koder, & Nanda, 2011) hypothesized that polar D-amino acids could stabilize the carboxy termini of the alpha helix through sidechain to backbone hydrogen bonds; in the event, these authors observed that the presence of D-Gln at the 10 position of the TC5b variant of Trp-cage yielded an NMR structure showing the presence of capping interactions in the form of a D-Gln hydrogen bond with the backbone carbonyl of Lys8, leading to a more stable structure. The authors reported that the D-Gln substitution raised the CD melting temperature by 23 °C, compared to just 20 °C for the D-Ala. Substitution. When D-Gln was incorporated into the cpTC2b series with the STADA-loop, at the corresponding G17 position, the fold stability improvement was not significant (Table 4.2).

Table 4.2. The Effects of Alternative D-Amino Acids[a]

	χ_F (280K)	χ_F (320K)	NMR T_M (°C)	ΔG_U^{300K} (kJ/mol)
cpTC2b	0.55	0.24	15	−1.08
(G17**q**)-	0.565	0.29	16	−0.87
cpTC2d2 (SGUDA)	0.695	0.31	34	+0.37
(G17**r**)-	0.71	0.36	36	+0.65

[a] Based on unpublished data by Byrne (Byrne, 2013).

A D-Arg mutation at the same site was also explored. A DeGrado study (Schneider & DeGrado, 1998) showed that a D-Arg at the C-capping site of a helix stabilized the helix by approximately 1.2 kcal/mol (5.0 kJ/mol). This mutation was incorporated into the SGUDA linker series. Again, the D amino acid substitution offered minimal increased stability at 280K, although the melting of the structure was slower than with D-Ala. As neither D-Gln nor D-Arg offered a significant benefit (equal to or less than 0.3 kJ/mol) to stabilization, it was decided to retain D-Ala as the residue at the position corresponding to G10 in standard topology, so that further circular permutants would be as similar to their non-circularly permuted counterparts.

4.3 Determination of Optimal Loop Length and Sequence

Circular-permutant TC2a, which serves as a reference starting point, retains the GG linker of the initial cyclized Trp-cage model. The sequence, RPPP-SGGDA-YAQWLAD **a** GPSS (**a** = D-Ala), is shown in 3 segments: RPPP (no mutations were made in this sequence segment), -SGGDA- (hence forth designated as the 'loop'), and the 12-residue segment which form two helices, with GPSS being a short 3_{10} helix. The number in cpTC# names indicates the core sequence; the cpTC4 series includes a stabilizing S20A mutation in the 3_{10} helix. The final letter in the names indicates

which loop sequence is present; the key to this appears in Table 4.3. The loop region has already been mutated extensively, much of that work being based on the observation that residues GDA adopt helical ϕ/ψ angles in the cyclic Trp-cage (Scian et al., 2012). Some of the key results of the loop mutation studies both from the prior effort and the present are collected in Table 4.3. Based on aiming for helix stabilization, glycine substitutions by Leu, Ala and Aib (U) figured heavily in these studies.

The original choice of a 2-residue connector (GG) for the cyclic forms of the Trp-cage, and thus a 5-residue SGGDA connector between the C-terminal poly-Pro_{II} region and the aryl-bearing portion of the α helix, had not been demonstrated to be optimal. Table 4.3 includes a further exploration of this linker region, entries 1-9 reflect work by Byrne (Byrne, 2013).

Table 4.3. Loop Nomenclature and the Effects of Loop Modifications on Fold Stability[a]

	χ_F (280K)	χ_F (320K)	NMR T_M (°C) (CD T_M)	ΔG_U^{300} (kJ/mol)
1 SGGDA (a)	0.53	0.18	10 (17)	-1.63
2 SDAAA	0.56	0.35	25 (36)	-0.15
3 STADA *(b)*	0.55	0.24	15 (20)	-1.09
4 SDUAA *(c)*	0.64	0.42	34 (48)	+0.40
5 DGUDA *(d)*	0.71	0.32	32 (36.5)	+0.48
5b SGUDA *(d2)*	0.695	0.31	34 (n.d.)	+0.37
5b SGUNA *(d3)*	examples of this loop appear in later Table 4.5			
6 SDAAL *(e)*	0.72	0.40	38 (43.5)	+0.94
7 SGNAA	0.52	0.17	9 (15)	-2.0
8 SGGNAA	0.42	0.12	1 (6)	-2.74
9 SG_4NAA	0.54	0.10	10 (13)	-2.42
10 $(Gly)_8$[c]	0.29	< 0.03	(15)[d]	≈ -5.85 [b]

[a] Unless otherwise specified, the stability data is for the cpTC2 sequence, RPPP-loop-YAQWLADaGPS S (**a** = D-Ala).

[b] At 280 K, the value is -2.16 kJ/mol.

[c] The sequence for this entry was RPPP-loop-YAQWLAD a GPASD, a (D22)-cpTC4 series analog.

[d] Since the full-cage T_M based on NMR data would be less than 0 °C, the higher CD T_M (which is based on helicity loss) indicates significant contributions by a helical half-cage conformation as well as the usual contribution due to partial helicity in the unfolded state.

Entries 7-10 address the question of optimal loop length in the circular permutants. A one-residue increase (entry 8) was demonstrably less favorable than the most analogous 5-residue loop, while a 3-residue increase (entry 9) had little effect except for enhanced melting at 320K. However, much longer flexible chain additions in the loop region of cpTC2 resulted in difficult to interpret NMR spectra suggesting slower folding rates. Interpretable data was obtained for long loop species with additional stabilizing features, see entry 10. Cage formation still occurs with the longer 8-residue loop, but the increased number of glycine residues result in a very dramatic melt-out on warming.

Keeping the loop size the same, the SDUAA loop displayed the greatest stability at 300K and it was, in our prior effort (Byrne et al., 2013), selected for further study examining the inclusion of the equivalent of the "P12W" and "S13A" mutations (P19W/S20A) which afforded the most stable cp-Trp-cage (cpT^{2}C3b, T_M^{CD} = 63°C, ΔG_U^{300} = 3.45 kJ/mol) in our 2013 account. Regarding the loop choice, at T < 310K both the DGUDA and SDAAL loops displayed greater folded-state populations than SDUAA loop species. The present study focused instead on investigations using the –SDAAL–, –SNAAL–, –STADA–, and –SGUDA– loops.

4.4 Examining Coulombic Interactions

As previously noted, the circular permutation produced new termini and mutations at these sites were not examined in the prior study (Byrne et al., 2013). One intriguing feature was the radical contact order change for what had been the D9/R16 salt bridge. Upon circular permutation this becomes R1/D16 requiring the presumably less restrained sidechain of the N-terminal residue to make both favorable H-bonding and Coulombic interactions with a sequence remote carboxylate. As previously reported (Byrne et al., 2013), NMR shift data for the Arg1 sidechain suggested a similar disposition relative to the indole ring of Trp13 as observed between R16/W6 in the standard topology Trp-cages. The ring current shifts for Arg sidechain resonances were of the previously observed sign but somewhat lesser magnitude.

Considering that the N-terminal arginine, in addition to forming the R1/D16 salt-bridge, could interact with the nearby C-terminus, and that either interaction might involve the backbone ammonium ion rather that the guanidinium sidechain, a number of terminal modifications were examined. These include N-terminal acetylation, as well as Arg1 deletions and mutations (typically Arg to norvaline, Nva). A portion of these studies appears in Table 4.4. As another

probe of chain termini interactions, a C-terminal aspartic acid was added to the sequence in hopes of creating additional Coulombic interactions between the terminal residues.

In the case of cpTC2b, the addition of an extra terminal D-aspartic acid resulted in significant fold improvement ($\Delta\Delta G_U$ = 2.08 kJ/mol at 280 K) (Byrne, 2013). A more extensive examination was based on cpTC4e, RPPP-SDAAL-YAQWLAD **a** GPAS, in this case the terminal Asp addition was an L-Asp residue. This increased the fold population from 72% to 87% at 280 K ($\Delta\Delta G_U$ = 2.23 kJ/mol). The T_M also increased by 7 °C at pH 6.5. The structure-favoring effect of the addition of an Asp to the C-terminus is smaller at 300K, with measures ranging from 0.81 – 1.51 kJ/mol and when other fold-favoring features are present. An exception to this stabilizing effect is seen in the context of N-acetyl function, where the D22 addition is seen to slightly favor the unfolded state ($\Delta\Delta G_U$ = -0.34 kJ/mol at 300K).

For the corresponding sequence with the stabilizing P12W mutation, the increment was 2.0 kJ/mol at 280K; this addition of the terminal L-Asp residue afforded the most stable Trp-cage circular permutant produced to date, with a fold population of 96% at 280K, and a T_M to 67°C at pH 6.5. This species appears as the last entry in of Table 4.4. Proton CSD comparisons to a standard topology comparison and two cyclized sequences that represent 100% folding appear as Figure 4.3. This species appears as the last entry in of Table 4.4.

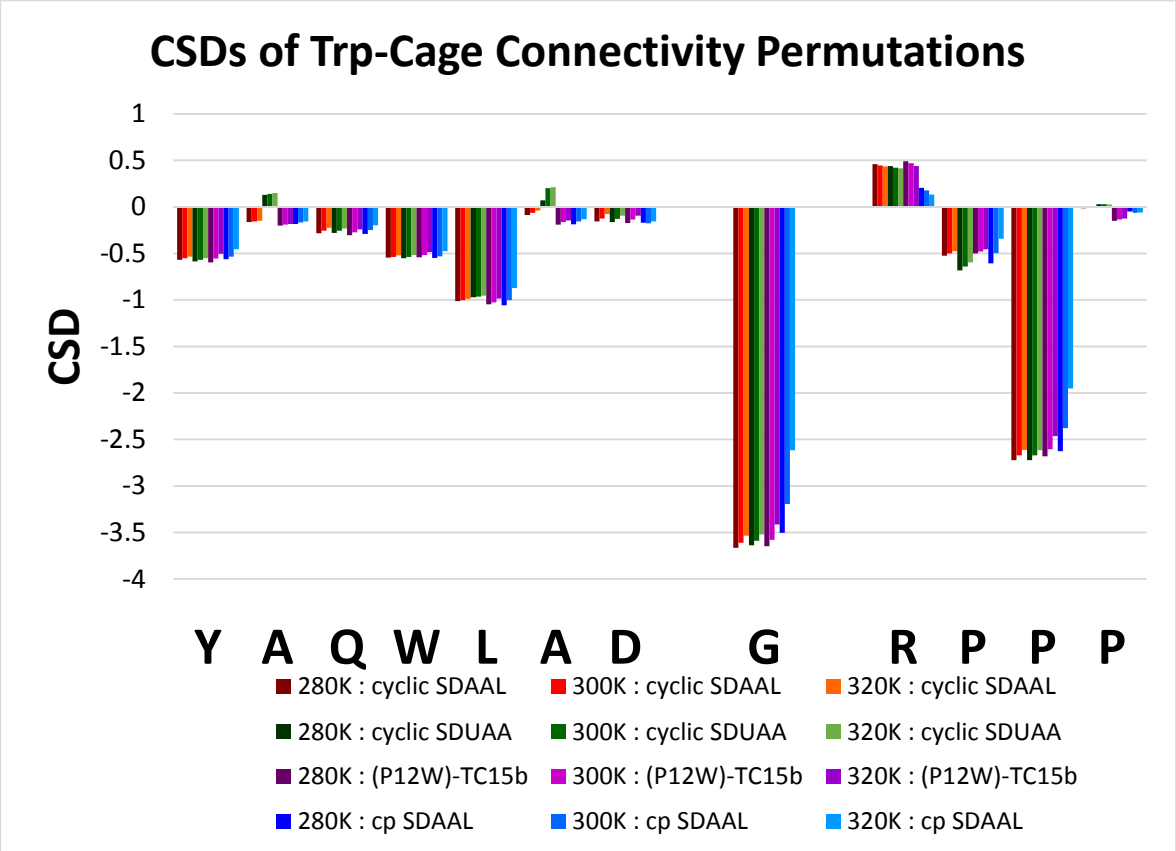

Figure 4.1. The Hα CSD values for cyclized, non-cyclized standard topology, and circularly permuted Trp-cage peptides. CSD values shown are for the C-terminal α-helix, diagnostic Gly11 residue, and N-terminal polyPro$_{II}$ helix. Sequences are for cyclic SDAAL: RPPP-SDAAL-YAQWLADaGWASG, cyclic SDUAA: RPPP-SDUA-AYAQWLADaGWASa (Byrne et al., 2013), (P12W)-TC15b: DAYAQWLADaGWASGRPPPS, cp SDAAL: RPPP-SDAAL-YAQWLADaGWASD.

Quite large destabilization effects upon acidification appear in Table 4.4. Some of these are larger than the 3 – 4 kJ/mol effect observed for standard topology Trp-cages with both the helix N-capping Asp and the D9-R16 salt bridge. Of some interest here, the stabilizing D22 addition in cp-Trp-cages does not appear to increase $\Delta\Delta G_U$ associated with carboxylate protonation.

In the case of cp-Trp-cages, *a priori*, it is not clear to what extent an Asp at different positions in the loop can serve as a helix N-cap or retains the large pH-dependence (Andersen & Tong, 1997; Doig & Baldwin, 1995; Williams et al., 2011) of this capping effect. This has now been

addressed, Table 4.5 (*vide infra*). As it turns out it is still difficult to ascertain the pH dependence of the R1/D16 interaction since there are additional Asp residues and a C-terminal carboxylate that could interact with positively charged sites.

Table 4.4 has numerous instances where the T_M by CD is much higher than the values based on NMR shifts for Pro^3, indicating a significant equilibrium contribution of the half-cage conformation (Byrne et al., 2013) for these species. This is universally the case at pH 2.5; any rationale of pH- and mutation-induced changes in fold stability needs to take this into account. The fully formed cage and half-cage folds of cp-TC sequences differ in a notable way: the C- and N-termini are close in space only in the full-cage conformation. Modifications at the N-terminus, including mutations and deletion of R1, changed cage stability and the value of the $\Delta\Delta G_U$ associated with carboxylate protonation. Based on Tables 4.4 and 4.6 data, complete deletion of R1 was destabilizing by only 2.9±0.3 kJ/mol at pH 6.5, but also lead to enhanced structure loss upon carboxylate protonation at pH 2.5. Guanidino removal (R1Nva, R1A, R1Cit) was only slightly more destabilizing (by 3.5±1.1 kJ/mol) than complete removal of R1.

The effects of N-terminal acetylation were highly informative. In the absence of a C-terminal Asp residue, N-acetylation results in a 2.35-3.88 kJ/mol destabilization at pH 6.5 which is replaced by a 0.57-0.90 kJ/mol stabilization at pH 2.5. We view this as proof that the N-terminal-NH_3^+ interacts with a carboxylate, which one, however, is unclear, with the C-terminus or D16 as the more likely possibilities. An interaction between the N- and C-termini cannot provide a full explanation of the N-acetylation effects. C-terminal amidation (Table 4.4) is much less fold disrupting than N-acetylation, and the C-terminal amide has an even larger structural loss on going from pH 6.5 to 2.5 ($\Delta\Delta G_U$ = 6.41 kJ/mol). We return to this question at the end of the discussion section.

Mutations of Arg in the D9/R16 salt bridge of standard topology Trp-cages have now been examined in detail, see Chapter 3. At pH 6.5 with D9 present throughout, the stability sequence is (from greatest stability to least): Arg [-$(CH_2)_3NHC(NH_2)=NH_2^+$] >> Cit [-$(CH_2)_3NHC(NH_2)=O$] ≥ Nva [-$(CH_2)_2CH_3$] >> Ala (–CH_3). Data for R1 mutations of cp-Trp-cages appear in Table 4.4 and a few more appear in Table 4.6 (*vide infra*). Table 4.6 also includes fold stability effects for the most analogous standard topology Trp-cages: TC15b [DAYAQWLADaGPSSGRPPPS] and trTC15b (Ac-AYAQWLADaGPSSGRPPPS-NH_2). These were chosen for the comparison based on sequence analogy and include both a species with a D1 N-cap and a "truncated" species which lacks the Asp and has no chain terminal charges.

Table 4.4. Effects of Chain Termini Modifications (N-acetylation, R1 Deletion and Mutations, C-terminal Amidation, and C-terminal Asp Additions). All free-energy differences are given in kJ/mol.

	pH 6.5				pH 2.5				$\Delta\Delta G_U$ ΔpH
	χ_F (280K)	ΔG_U (300K)	T_M (°C) CD melt	$\Delta\Delta G_U$	χ_F (280K)	ΔG_U (300K)	T_M (°C) CD melt	$\Delta\Delta G_U$	
cpTC2b [d]	0.55	-1.09	36	**ref**	n.d.				
(d22)	0.71	+0.42	n.d.	+1.51	n.d.				
(ΔR1)	0.27	-2.8	n.d.	-1.71	(-3.2 for ΔR1)		n.d.		
cpTC4e	0.72	+1.10	51	**ref**	0.22	-3.87	43[b]	**ref**	-4.97
(ΔR1)	0.41	-1.51	23 [a]	-2.61	n.d.[c]	-7.00	37[b]	-3.13	-5.49
(R1Nva)	0.42	-1.27	34[a]	-2.37	n.d.[c]	-3.58	n.d.	+0.29	-2.31
(R1A)	n.d.	-1.95	41[a]	-3.05	0.19	-3.65	n.d.	+0.22	-1.70
(D22)	0.87	+1.91	58	+0.81	0.23	-3.67	45[b]	+0.20	-5.58
(N-acetyl)	0.46	-1.25	36[a]	-2.35	n.d.[c]	-2.97	45[b]	+0.90	-1.72
(D22)	0.40	-1.59	36[a]	-2.69	0.24	-3.17	50[b]	+0.70	-1.58
(P19W)-cpTC4e	0.91	+4.37	65	**ref**	n.d.[c]	-2.71	48[b]	**ref**	-7.08
(N-acetyl)	0.64	+0.49	49	-3.88	n.d.[c]	-2.14	48[b]	+0.57	-2.63
(S21-NH_2)	0.83	+2.44	55	-1.93	n.d.[c]	-3.97	46[b]	-1.26	-6.41
(D22)	0.96	+5.20	68	+0.83	n.d.[c]	-3.63	49[b]	-0.92	-8.83

[a] At pH 6.5, P18 CSD values suggest expected T_M values which are significantly lower than T_M values calculated from the CD melt. This indicates that these modifications give rise to significant amount of half-cage formation.

[b] At pH 2.5, all Trp-cage peptides show T_M values calculated by P18 CSD values that are significantly lower than T_M values calculated by CD measurements. This indicates that acidic conditions give rise to significant amounts of half-cage formation.

[c] cp-TC species were observed to be less soluble, particularly at pH 2.5 and low temperatures. As a result, reliable χ_F data could not always be obtained.

[d] cpTC2d sequences were characterized by Byrne (Byrne, 2013)

Returning to the data, in Tables 4.4 (and also Table 4.6) for Arg replacements, the Arg > Cit ≥ Nva > Ala stability series as seen in normal topology Trp-cages was generally observed for the circular permutants, but with a number of differences: 1) the $\Delta\Delta G_U$ values are smaller for the circular permutants, 2) in the standard topology, all three Arg replacements that remove the

guanidino charge eliminate, or even reverse (see Chapter 3), the pH-induced change in fold stability - in the circular permutants, a significant loss of fold stability upon protonation remains after the Arg mutations, and 3) the large additional drop in fold stability (2.34 kJ/mol) for the R16Nva to R16A change is not observed in the circular permutant (0.68 kJ/mol). The third difference suggests that the aliphatic portion of the Arg sidechain does not wrap around the indole ring to complete the Trp encagement.

Clearly there are other factors beyond the peptide chain termini and the salt bridge involved in the acidification-induced fold stability loss. Aspartate mutations presented another route for studying the sources of pH dependent fold stability changes, Table 4.5. Asp16 is the site involved in the putative R/D salt-bridge. In the case of standard topology analogs (Table 4.6), the D9Abu mutation is, at pH 6.5, as destabilizing as the R16Nva mutation. In the case of the trTC15b species that lacks the Asp helix N-cap, a D9Abu mutation nearly eliminates the pH dependence of fold stability. With D9 at a helix C-capping position, protonation is expected to stabilize the helix, see Chapter 3. In the case of circular permutants, we examined both an Asp→Abu and an Asp→Ser mutation. Both should completely eliminate the salt bridge, but the two could have somewhat different effects on the intrinsic stability of the helix and H-bonding effects. At pH 6.5, the fold stability losses for both D16Abu and D16S were modest, 2.65 and 1.91 kJ/mol at 300K, respectively. Both of these are less than the effects of R1Nva mutations in either the cp (or standard topology) series (3.56 ± 1.20 kJ/mol) and the effect of a D9Abu mutation in trTC15b (4.42 kJ/mol). This likely implies that the salt-bridge is 1.5 kJ/mol less favorable in circularly permuted versus standard topology Trp-cages.

Table 4.5. Effects of Loop Modifications

	pH 6.5				pH 2.5				$\Delta\Delta G_U$ ΔpH
	χ_F (280K)	ΔG_U (300K)	T_M (°C) CD melt	$\Delta\Delta G_U$	χ_F (280K)	ΔG_U (300K)	T_M (°C) CD melt	$\Delta\Delta G_U$	
cpTC2d2 SGUDA	0.716	+0.56	37	**ref**	n.d.				
Y10L	0.51	-1.52	19[a,d]	-2.08	0.26	-3.90	<7	**ref**	-2.38
D8N	0.43	-2.48	10[a]	-3.04	0.29	-3.71	<7	+0.19	-1.23
Y10A	0.07	-8.35	<7	-8.91	n.d.				
cpTC4e	0.72	+1.10	41	**ref**	0.22	-3.87	n.d.	**ref**	-4.97
D6N (loop)	0.59	-0.44	43[a]	-1.54	0.13	-4.55	n.d.[c]	-0.68	-4.11
(P19W)-cpTC4e	0.91	+4.37	65	**ref**	n.d.[c]	-2.71	48[b]	**ref**	-7.08
D6N (loop)	0.89	+3.54	59	-0.83	n.d.[c]	-1.06	50[b]	+1.65	-4.60

a At pH 6.5, P18 CSD values indicate T_M values which are significantly lower than T_M values calculated by CD measurements. This indicates that these modifications give rise to significant amount of half-cage formation.

b At pH 2.5, all Trp-cage peptides show T_M values calculated by P18 CSD values that are significantly lower than T_M values calculated by CD measurements. This indicates that acidic conditions give rise to significant amounts of half-cage formation.

c cp-TC species were observed to be less soluble, particularly at pH 2.5 and low temperatures. As a result, reliable χ_F data could not always be obtained.

d the $\Delta\Delta G$ for the D8N mutation is -0.96 kJ/mol.

In the standard topology reference compounds the D9Abu mutation abolishes the pH dependence of fold stability; there is essentially no loss (< 0.8 kJ/mol, see Table 4.6) in ΔG_F upon acidification, which corresponds to protonation of the Ser20-CO_2^- (and in one case, also the D1 sidechain carboxylate). Solubility problems prevented the same measurement for the D16Abu analog in the cp-series, but the data could be obtained for the D16S species: the acidification $\Delta\Delta G_U$ is −5.32 kJ/mol. At least a portion of this has to be attributed to protonation of the loop aspartate (Asp6).

As previously noted, there was no *a priori* basis for estimating the extent to which the Asp in some of the loops used in cp-Trp-cages serves as a powerful N-cap as is the case within the -DAYA- unit of standard topology cages. In the case of -DAYA- terminated Trp-cages, an Asp to Asn mutation results in a 1.2 – 2.0 kJ/mol fold-stability decrease (Barua et al., 2008; Meuzelaar et al., 2013), presumably associated with helix stability contribution to fold stability. Table 4.5 includes data for circular permutants with -DAALYA- and -G-Aib-DAYA- sequences at the helix starting point; in both cases, fold destabilization was observed for the Asp→Asn mutation, 1.54 and 0.96 kJ/mol, respectively. These helix N-capping effects probe the importance of helix formation to full cage stability.

In the past, one other mutation has been used to ascertain the importance of the D1-D9 helix: an A8G mutation. In the (P18A)-TC16b series, the A8G mutation was found to be destabilizing by 4.1 kJ/mol at pH 6.5, 3.5 kJ/mol at pH 2.5. (Byrne et al., 2014) In the present cp-Trp-cage series this is reduced to 1.87 kJ/mol at pH 6.5 (Table 4.6). This and the somewhat reduced effect of N-capping may simply reflect a lesser importance of intrinsic helix stability for full cage formation in the circularly permuted Trp-cage. The A8G effect is reduced further (0.31 kJ/mol) at pH 2.5.

However, some portion of the loss of fold stability upon acidification for a variety of cp-series mutants must be attributed to protonation of the loop aspartate (D6) and that portion greatly exceeds the expectation based on the helix N-capping difference between protonated and ionized aspartate.

4.5 THE HYDROPHOBIC CLUSTER

The Y10 mutations that appear in Table 4.5 serve as an introduction to the next subject, comparisons of the effects of specific single-site mutations in the distinct hydrophobic clusters that are present in standard topology versus circularly-mutated Trp-cages. Y10 in a cp-Trp-cage

corresponds to the tyrosine in the Y3/P19 hydrophobic staple that holds the ends of the standard Trp-cage together (Barua et al., 2008). In the case of cp-Trp-cages, it has been suggested that the added stability associated with the P19W mutation is, at least in part, due to W19/P2-P3,W13 interactions functioning as a hydrophobic staple tying the termini together (Byrne et al., 2013). The staple that holds together the ends of (P19W)-cp-Trp-cages is not purely hydrophobic in nature. There is a wealth of Coulombic interactions possible (with some mutational evidence for each of them): R1-sidechain/D16, R1-NH_3^+/D16, R1-sidechain/Ser21-CO_2^- , and R1-NH_3^+/Ser21-CO_2^-.

Table 4.6. Comparisons of ΔG_U Effects of Single-Site Mutations in Circularly Permuted Trp-cages Versus Analogs of Standard Topology. All ΔG_U–values are based exclusively on CSD data for the far upfield proline signals associated with complete cage formation.

	pH 6.5				pH 2.5				$\Delta\Delta G_U$ ΔpH
	χ_F (280K)	ΔG_U (300K)	T_M (°C) CD melt	$\Delta\Delta G_U$	χ_F (280K)	ΔG_U (300K)	T_M (°C) CD melt	$\Delta\Delta G_U$	
Circularly Permuted Trp-Cage									
(D22)-cpTC4e	0.87	+1.91	58	**ref**	0.23	-3.67	45	**ref**	-4.58
ΔR1	0.48	-1.00	34[a]	-2.91	n.d.[c]	-6.69	38[b]	-3.02	-5.69
Y10L	0.81	+1.66	49	-0.25	n.d				
Y10A	0.43	-3.01	11[a]	-4.92	n.d.				
(P19W)-cpTC4e	0.91	+4.37	65	**ref**	n.d.[c]	-2.71	48[b]	**ref**	-7.08
D16Abu	n.d.	+1.72	54	-2.65	n.d. (solubility issues)				
D16S	0.79	+2.46	67[a]	-1.91	n.d.[c]	-2.86	44[b]	-0.15	-5.32
(P19W, D22)-cpTC4e	0.96	+5.20	67	**ref**	n.d.[c]	-3.63	49[b]	**ref**	-8.83
A8G	0.93	+3.33	49	-1.87	n.d.[c]	-3.94	26[b]	-0.31	-7.27
R1Cit	0.75	+1.51	52	-3.69	n.d.				
R1Nva	0.66	+0.62	50	-4.58	n.d.[c]	-3.38	n.d.	+0.25	-4.01
Y10L	0.92	+4.23	61	-0.97	n.d.				
Y10A	0.78	+0.22	11	-4.98	n.d.				
P4A	0.13	-5.71	34[a]	-10.91	n.d.				
Standard Topology Comparisons									
TC15b	0.98	+6.93	74	**ref**	0.92	+4.76	67	**ref**	-2.17
D9Abu	0.88	+3.74	67	-3.19	0.85	+3.01	59	-1.75	-0.73
R16Nva	0.86	+3.60	63	-3.33	0.86	+3.71	70	-1.05	+0.11
Y3L	0.95	+5.49	71	-1.44	0.85	+2.83	62	-1.93	-2.66
Y3A	0.77	+0.46	36	-6.47	n.d.				
P19A	0.37	-2.34	38[a]	-9.27	n.d.				
(P12W)-TC15b	>0.99	≥ 10.0	81	**ref**	0.95	+6.53	73	**ref**	≤ -3.5
D9S	0.96	+6.71	n.d.	≤-3.3	0.95	+6.20	n.d.	-0.51	-7.22
Y3L	0.97	+7.37	73	≤-2.6	0.95	+5.32	70	-1.21	-2.05
Y3A	0.90	+2.96	48	≤-7.0	n.d.				
P19A	0.37	-1.53	48[a]	≤-11.5	n.d.				
trTC15b	0.99	+7.09	65	**ref**	0.92	+4.35	63	**ref**	-2.74
D9Abu	0.86	+2.67	49	-4.42	0.85	+2.54	54	-1.81	-0.13
R16Nva	0.85	+2.33	48	-4.76	0.86	+3.27	62	-1.08	+0.94
R16A	0.70	-0.01	35	-7.10	0.73	+1.18	50	-3.17	+1.19
Y3L	0.93	+3.82	53	-3.27	0.85	+2.37	55	-1.98	-1.45

Y3V	0.76	+0.27	35	-6.82	0.64	-0.36	n.d.	-4.71	-0.63
Y3Abu	0.75	+0.22	34	-6.87	0.57	-1.34	n.d.	-5.69	-1.56
Y3A	0.61	-1.93	18	-9.02	0.45	-2.79	n.d.	+7.14	-0.86
(P12W)-trTC15b	0.99	+8.50	67	**ref**	0.95	+6.36	70	**ref**	-2.14
R16Nva	0.93	+3.76	55	-4.74	0.89	+4.41	65	-1.95	+0.65

a At pH 6.5, P18 CSD values suggest expected T_M values which are significantly lower than T_M values calculated by CD measurements. This indicates that these modifications give rise to significant amount of half-cage formation.

b At pH 2.5, all Trp-cage peptides show T_M values calculated by P18 CSD values that are significantly lower than T_M values calculated by CD measurements. This indicates that acidic conditions give rise to significant amounts of half-cage formation.

c cp-TC species were observed to be less soluble, particularly at pH 2.5 and low temperatures. As a result, reliable χ_F data could not always be obtained.

In standard topology Trp-cage systems the P12W mutation is stabilizing (Culik et al. 2011) although an exception has been noted, (P18A)-TC16b ($\Delta\Delta G_U$ = -1.3 kJ/mol for the P12W mutation)(Byrne et al., 2014). With that exception excluded, the $\Delta\Delta G_U$ value for prior determinations is -2.3 ± 0.6 kJ/mol. Table 4.7 compares the $\Delta\Delta G_U$ values for P12W mutations in the standard topology Trp-cage and the equivalent P19W mutation in the circularly permuted series reported herein. Over the more closely analogous standard topology systems, the -$\Delta\Delta G_U$ value ranges from 1.4-3 kJ/mol at pH 6.5. The $\Delta\Delta G_U$ for the P12W mutation appears to be pH independent: 1.14 - 2.50 kJ/mol (n = 8). In the case of N-acetylated cp-Trp-cages, we measure a modest 1.74 kJ/mol for the P19W mutational $\Delta\Delta G_U$ at pH 6.5. Of the remaining nine measures of the P19W mutation effect in circular permutants, six range 2.57-3.49 kJ/mol. The exceptions are SDAAL loop species at pH 2.5, $\Delta\Delta G_U$ = 0.60 ± 0.56 kJ/mol). Four values for the P12W mutation at pH 2.5 are available for standard topology systems in Table 4.6 and 4.7 (1.82 ± 0.68 kJ/mol). Yet the analogous P19W mutation results in less net stabilization at pH 2.5 for the otherwise quite stable SDAAL loop cp-species. We will return to rationalizing the pH differences, but for now

conclude that the P/W interactions have a greater fold stabilizing effect when serving as the hydrophobic portion of an end-capping staple rather than an internal structure connected by a smaller loop.

Table 4.7. Comparisons of $\Delta\Delta G_U$ Effects of P12W/P19W Mutations.

	pH 6.5				pH 2.5				$\Delta\Delta G_U$ ΔpH
	χ_F (280K)	ΔG_U (300K)	T_M (°C) CD melt	$\Delta\Delta G_U$	χ_F (280K)	ΔG_U (300K)	T_M (°C) CD melt	$\Delta\Delta G_U$	
Circularly Permuted Trp-Cage									
cpTC4e	0.72	+1.10	51	**ref**	0.22	-3.87	43[b]	**ref**	-4.97
(P19W)	0.91	+4.37	65	+3.27	n.d.[c]	-2.71	48[b]	+1.16	-7.08
(D22)-cpTC4e	0.87	+1.91	58	**ref**	0.23	-3.67	45[b]	**ref**	-5.58
(P19W)	0.96	+5.20	67	+3.29	n.d.[c]	-3.63	49[b]	+0.04	-8.83
(Ac-)-cpTC4e	0.46	-1.25	36[a]	**ref**	n.d.[c]	-2.97	45[b]	**ref**	-1.72
(P19W)	0.64	+0.49	49[a]	+1.74	n.d.[c]	-2.14	48[b]	+0.83	-2.63
(D6N)-cpTC4e	0.59	-0.44	43	**ref**	0.13	-4.55	n.d.	**ref**	-4.11
(P19W)	0.89	+3.54	59	+3.98	n.d.	-1.06	50	+3.49	-4.60
(Y10L,D22)-cpTC4e	0.81	+1.66	49	**ref**	n.d.				
(P19W)	0.92	+4.23	61	+2.57	n.d.				
(Y10A,D22)-cpTC4e	0.43	-3.01	11[a]	**ref**	n.d.				
(P19W)	0.76	+0.22	36	+3.23	n.d.				
Standard Topology Comparisons									
TC15b	0.98	+6.93	74	**ref**	0.92	+4.76	67	**ref**	-2.17
(P12W)	≥0.99	≥ 10.0	81	≥ +3	0.95	+6.53	73	+1.77	≤-3.5
(Y3L)-TC15b	0.95	+5.49	71	**ref**	0.85	+2.83	62	**ref**	-2.66
(P12W)	0.97	+7.37	73	+1.88	0.95	+5.32	70	+2.49	-2.05
(Y3A)-TC15b	0.77	+0.46	36	**ref**	n.d.				
(P12W)	0.90	+2.96	48	+2.50	n.d.				
trTC15b	0.99	+7.09	65	**ref**	0.92	+4.35	63	**ref**	-2.74
(P12W)	0.99	+8.50	67	+1.41	0.95	+6.36	70	+2.01	-2.14
(R16Nva)-trTC15l	0.85	+2.33	48	**ref**	0.86	+3.27	62	**ref**	+0.94
(P12W)	0.90	+3.76	55	+1.43	0.89	+4.41	65	+1.14	+0.65

a At pH 6.5, P18 CSD values suggest expected T_M values which are significantly lower than T_M values calculated by CD measurements. This indicates that these modifications give rise to significant amount of half-cage formation.

b At pH 2.5, all Trp-cage peptides show T_M values calculated by P18 CSD values that are significantly lower than T_M values calculated by CD measurements. This indicates that acidic conditions give rise to significant amounts of half-cage formation.

c cp-TC species were observed to be less soluble, particularly at pH 2.5 and low temperatures. As a result, reliable χ_F data could not always be obtained.

Turning to the Y3/P19 staple (P4/Y10 in the circular permutants), prior data (Barua et al., 2008; Byrne et al., 2013) indicated the following destabilization measures for mutations: Y3L (3.4 – 4.4 kJ/mol), Y3A (10 – 12 kJ/mol), and P19A (> 12 kJ/mol). Rather similar, but somewhat smaller, values were obtained for the specific standard topology comparisons in Table 4.6: Y3L (2.36 ± 0.92 kJ/mol), Y3V (6.82 kJ/mol), Y3A (7.75 ± 1.28 kJ/mol), and P19A (10.39 ± 1.12 kJ/mol). For the circular permutants examined (Tables 4.5 & 4.6), a significant drop in the destabilization effect was observed for Y10L (0.61 ± 0.36 kJ/mol) and Y10A (4.95 ± 0.03 kJ/mol), but not for the P4A mutation (10.91 kJ/mol). It should be noted that the P4A mutation affects both the hydrophobic interaction and the conformational stability in the N-terminal 5-residue unit (RPPPX *versus* RPPAX): the reduced rigidity of the polyPro$_{II}$ structure herein upon insertion of the alanine could also reduce the favorable Coulombic interactions at the N-terminus. The reduced $\Delta\Delta G_U$-values for the Y10A mutation, and to a lesser extent Y10L, likely reflect the reduced loop length connecting the staple components: P4/Y10 no longer staples the extreme 'ends' of the peptide chain together. Of interest, the shorter valine sidechain is, in a standard topology model, essentially as effective as alanine and much less effective than leucine.

4.6 DISCUSSION

Although it is evident that the circularly permuted Trp-cages share the same folding motif as the original sequence; there are a number of clear distinctions. For one, we have not been able to achieve very high levels of fold stability ($\chi_F^{280K} \geq 0.98$, $\Delta\Delta G_U > 8$ kJ/mol at 300K) in the cp-series; such stabilities were observed for the standard topology after helix optimization when either (or both) of two key glycines were replaced by D amino acid residues. This can be attributed to the

fact that these two sites, G10 and G15, represent single-residue kinks between secondary structure elements in the standard sequence. In the cp-species, 'G15' was deleted as the cut point and there is, instead, an inherently more fluxional 4 – 5 residue linker between the α-helix and the polyPro$_{II}$ unit. Fold stability is, indeed, greatly influenced by the sequence of this linking region. As it turned out, the new -SDAAL- loop sequence developed herein is more stabilizing only when its aspartate residue is ionized. The D6N mutation is more destabilizing at pH 6.5 than at pH 2.5 (Table 4.5). As a result, the pH dependence of the stability of the full-cage conformation is more dramatic for the circularly permuted species. The resulting pH-dependent stability appears to represent both a loop conformational preference change and a larger α-helix N-capping effect in the ionized state (Andersen & Tong, 1997; Doig & Baldwin, 1995).

The loop sequence also has a dramatic influence on the effect of the P19W mutation. The P19W mutation establishes the W19/P2-P3,W13 hydrophobic staple. With the SDAAL loop sequence present, the P19W mutation is significantly less fold stabilizing at pH 2.5 even though our comparisons with standard topology models clearly show that this hydrophobic staple has a greater fold stabilizing effect when it is a part of the interactions that hold the extreme termini in close proximity. However, the P19W mutation retains its fold favoring effect at pH 2.5 in circularly permuted Trp-cage using an -SNAAL- loop sequence. Unlike aspartate, asparagine does not undergo a change in protonation state at pH 2.5. It seems likely that it is protonation of the SDAAL aspartate that causes conformational changes in the circularly permuted peptides that eliminate the favorable interactions in the hydrophobic staple.

As previously noted, there are two long-range Coulombic interactions that utilize the deprotonated Ser21 carboxylate: with the R1-sidechain and with R1-NH_3^+. Alternative interactions would place these R1 sites near D16. As a result, I posit that carboxylate protonation

reduces the end-capping effect which allows a pH-induced (D6 protonation) loop conformational change that increases the end-to-end distance such that a W19/P2-3 hydrophobic interaction is no longer available.

It appears that the full set of potential Coulombic interactions can contribute to fold stability but not in a fully additive fashion; mutations that eliminate some of them can result in a greater importance for the unaltered ones. The best guide to ranking their relative importance comes from the effects of 'deleting mutations' at pH 6.5 and the remaining pH-induced fold stability changes after such mutations. These are collected in Table 4.8. The notable differences relative to the standard topology comparisons are that ΔΔG for mutations at both the R and D of the salt bridge are 1-3 kJ/mol less fold disruptive in the cp-series and that, in the standard topology, both types of mutations remove or even reverse the pH-induced ΔΔG. In the cp-series, the pH-induced fold stability change can be as large as 5 kJ/mol after mutational elimination of the salt bridge.

Table 4.8. A Summary of ΔΔG-values Associated with Coulombic Effects.

Mutation	$-\Delta\Delta G_U$ at pH 6.5	pH-induced $\Delta\Delta G_U$
N-acetylation	2.35 - 3.88	1.72 – 2.63
R1 sidechain mutation	2.37 – 4.58	1.70 – 4.01
Complete R1 deletion	2.61 – 3.20	4.97 – 5.69
D16Abu	2.65	n.d.
S21-NH2	1.93	6.41
D16S	1.91	5.32
D6N	0.83 – 1.54	4.11 – 4.60

Ranking of fold loss at pH 6.5: D6N < D16S = S21-NH_2 < D16Abu ≤ ΔR1 < N-Ac ≤ R1-sc
Remaining acidification ΔΔG: S21-NH_2 > D16S > ΔR1 > D6N > R1-sc ≥ N-Ac

The dramatic stability loss at pH 6.5 for N-acetylation is not matched by a comparable change associated with C-terminal amidation. This implies that R1-NH_3^+ has fold-stabilizing interactions with another carboxylate, presumably that on the D16 sidechain. The difference in the remaining fold-stability loss associated with carboxylate protonation for the D16S mutant and the C-terminal amide suggest that the fold stabilizing Coulombic interactions with the D16 sidechain carboxylate are about 1 kJ/mol greater than those for the C-terminal carboxylate.

While a number of attempts to employ the $\Delta\Delta G_U$ values above indicate a significant degree of either non-additivity or unexpected correlations, there is one notable agreement – the sum of the $\Delta\Delta G_U$ values for D16-CO_2^- and S21-CO_2^- deletions (a loss of 4 – 4.6 kJ/mol) matches the remaining pH-induced change for the D6N mutant (which would retain these two carboxylates). However, these values are well shy of the ≥ 7 kJ/mol pH-dependence observe for species with no mutations at charged sites. This implies that an acidification-induced change at or near D6 (in the SDAAL loop) destabilizes the cage fold by more than the $\Delta\Delta G_U$ = 0.6 – 1.6 kJ/mol at pH 6.5 observed for the D6N mutant. It appears that Asn is not an acceptable model for "protonated Asp".

The latter brings me back to the pH-dependence of the P12W(P19W) effect in standard topology versus cp-Trp-cages. In the standard topology examples, the P12W is equally stabilizing at pH 2.5 and 6.5. Turning to the cp-series, for the D6N mutant, the difference in the $\Delta\Delta G$ for P19W is 3.48 - 3.98 kJ/mol, with the greater effect at pH 6.5. In the analogous -SDAAL- loop species, the value is 3.27 kJ/mol. In light of the complete data set, this likely indicates an increased propensity for a loop conformation that place the N- and C-termini far

apart at pH 2.5 rather than positing a specific favorable loop conformation for SDAAL sequence when the aspartate is ionized.

Extending mutational studies of Trp-cage fold stability to circularly permuted species as well as analogs that include the stabilizing 'G17**a**' mutation and lacking chain terminal charges has uncovered some additional stabilizing and destabilizing interactions. As it turns out these are not fully comparable in the standard versus circularly-permuted topologies. End effects appear to be more important for the cp-series while the Y10/P4 interaction in the cp-series is not as significant a stabilizing feature as Y3/P19 in the standard topology series. A quite distinct folding mechanism may apply. Studies of mutational effects on folding dynamics (Chapter 5) were intended to provide a resolution of this question.

Chapter 5. EXPLORING THE FOLDING MECHANISM OF CIRCULARLY PERMUTED TRP-CAGES VERSUS STANDARD TOPOLOGY SYSTEMS

5.1 CONTEXT

Since the initial publication of its sequence (Neidigh et al., 2002), the Trp-cage has been an invaluable model system for the study of protein folding. At approximately 20 residues and with a folding time measured in the low microsecond range, it is well suited as the subject of molecular dynamics (MD) simulations. A series of studies have optimized the stability of its folded state (Barua et al., 2008; Bunagan et al., 2006; Williams et al., 2008, 2011), and more recently, cyclized and circularly permuted versions have been successfully produced (Byrne et al., 2013; Scian et al., 2012). While the Trp-cage fold is still observed after these changes to the primary sequence, it is not clear whether it follows the same folding mechanism as the standard topology. Dynamics studies comparing the standard topology to its circularly permuted counterparts can explore how the events in the folding mechanism are affected by contact order.

Although Trp-cages have been extensively characterized through both experimental and computational methods, conflicting evidence exists as to its exact folding pathway. The first published sequence, TC5b (NLYIQ WLKDG GPSSG RPPPS), was found to have a T_M = 42 ºC. The folding rate was found to be on the low microsecond timescale at (≤ 7 μs at 25-40 °C) based on IR-monitored T-jump and NMR exchange broadening monitoring the G11Hα2 nuclei (Andersen et al., 2001) and 4.1 μs at 23.5 °C based on fluorescence monitored T-jump experiments (Qiu et al., 2002).

The Gai group measured the effect of the Gly10 to D-Ala (G10**a**) mutation on folding rates, found that this mutation increases the rate of folding by a factor of 2 (Culik et al., 2013). In a later

study using similar methodology, they examined the R16K and P19A mutations. The folding rate of the mutants was not seen to change significantly, suggesting that both formation of the salt bridge and docking of the polyPro$_{II}$ helix must occur after the folding transition (Culik et al., 2011). The P12W mutation, which was studied by Bunagan *et al.* (Bunagan et al., 2006), and was observed to give a folding rate of $1/k_F$ of 1 μs at 300K. This represented a 3.5-fold increase in the rate of folding, and the P12W mutation has been incorporated into some Trp-cage sequences produced in our own lab as a means of increasing fold stability (Barua et al., 2008; Byrne et al., 2013).

Our previous dynamics studies have utilized NMR exchange broadening to obtain rate data (Andersen et al., 2001; Byrne et al., 2014). While our initial study used the G11Hα2 nucleus as a probe, a more recent study examined the Hβ signal of an alanine substitution at position 18, which is positioned in the C-terminal polyPro$_{II}$ helix. This position experiences significant chemical shift deviations due to its positioning over the central indole ring in the fully folded cage structure. The results obtained suggested that while the α-helix was already present at the transition state, neither the salt bridge nor the hydrogen bonds between hydroxyl group of Ser14 and the residues within the hydrophobic core had yet formed (Byrne et al., 2014). This probe also provided contradictory data concerning the fold stabilizing effects of a P12W mutation.

Some discrepancies in the evidence for a folding pathway originate from the method used to obtain rate data. The most complete dynamics study from the Andersen group used the NMR exchange broadening of the highly-shifted methyl of P18A mutants. Other laboratories have used T-jump experiments monitoring fluorescence changes or the disappearance of the helical amide I' bands on partial melting. There is experimental evidence suggesting the N-terminal helix is partially formed in the unfolded state (Barua et al., 2008; Williams et al., 2011), and MD

experiments have depicted it as occurring in the earliest stages of the folding pathway (Gelman & Gruebele, 2014; Lindorff-Larsen, Piana, Dror, & Shaw, 2011). Evidence in favor of a partially-folded "half cage" structure that is present in the unfolded ensemble or as an intermediate step in the folding pathway has also been presented (Barua et al., 2008; Mok et al., 2007; Neidigh et al., 2002). In this scenario, it is possible that the α- and 3_{10} helices have fully formed before the docking of the C-terminal polyPro$_{II}$, making these regions unreliable reporters for the formation of the fully folded cage.

Trp-cages with alanine mutations within the polyPro$_{II}$ unit have been informative; A P19A mutation effectively blocks formation of fully folded cage but allows formation of the half-cage structure (Barua et al., 2008). Indeed, T_M values from CD measures of helicity were largely unchanged in the absence of C-terminal docking. The P17A and P18A mutations were well tolerated. Evidence for full cage formation with the P18A mutation includes a 1.16 ppm upfield shift for A18Hβ, with other CSD comparisons indicating that the P18A mutation resulted in only a 1.2 kJ/mol cage-fold destabilization. More significantly, rate data obtained from the Gly11Hα2 probe gave values for rates of folding and unfolding that were within experimental error for those measured by T-jump. However, when NMR exchange broadening was instead measured at Ala18, the rates were much slower than those obtained in IR-monitored T-jump experiments. This evidence supported the model where Gly11α2 reports on formation of the half-cage rather than formation of the fully folded structure, while position 18 gives longer folding and unfolding times as it only exhibits the CSDs of the folded state after the C-terminal tail assumed its folded position above Trp6.

Another consideration in the design of exchange broadening studies is the choice of nuclei to use as the probe and whether mutations cause folding pathway changes. In the previous study by

Byrne, a P18A mutation was used to introduce an easily modeled peak in the form of A18Hβ. However, in the presence of P18A, the P12W mutations, which is typically stabilizing, instead destabilized the fold. A good probe would ideally be a nucleus found in the "wild type" sequence. In this present study, I retain the proline at position 18 to preserve the structure of the polyPro$_{II}$ helix and avoid differential interactions with Trp6, Trp12, and P19. While both the Hα and Hβ3 of Pro18 experience dramatic CSDs due to ring current effects, Hα is in crowded regions of the spectra and is frequently obscured by other signals. However, the Hβ3 signal generally appears in uncrowded regions of the spectra near 0 ppm. While this nucleus gives a complicated quintet rather than the simple doublet of the alanine methyl; in well resolved cases, the coupling constants can be measured to accurately model the peak, see Figure 5.1.

In the case of the dynamics studies herein, the increase in line width for the P18Hβ3 signal affords dynamics data; the chemical shift provides the equilibrium constant at each temperature. The 100% folded values for this signal, taken from the most stable Trp-cage analogues, are -2.748 and -2.174 ppm, respectively, for species with and without a P12W substitution.

In a typical experiment, values for Δ^{ex} are measured for Pro18Hβ3 by modeling the line shape with a custom-built Excel spreadsheet using the P18Hβ3 coupling constants measured at the lowest temperature and varying the line width (Δ^{sim}) until the observed half height width and the %-dip are reproduced (Olsen et al., 2005; Scian, Shu, Olsen, Hassam, & Andersen, 2013). Similarly, the line width at half height is measured for an aromatic signal that does not experience significant changes (Δ^{o}) in its CSD from 280K-320K. The Δ^{ex} values are derived as $\Delta^{sim} - \Delta^{o}$, with Δ^{o} as the average intrinsic broadening of the reference signals.

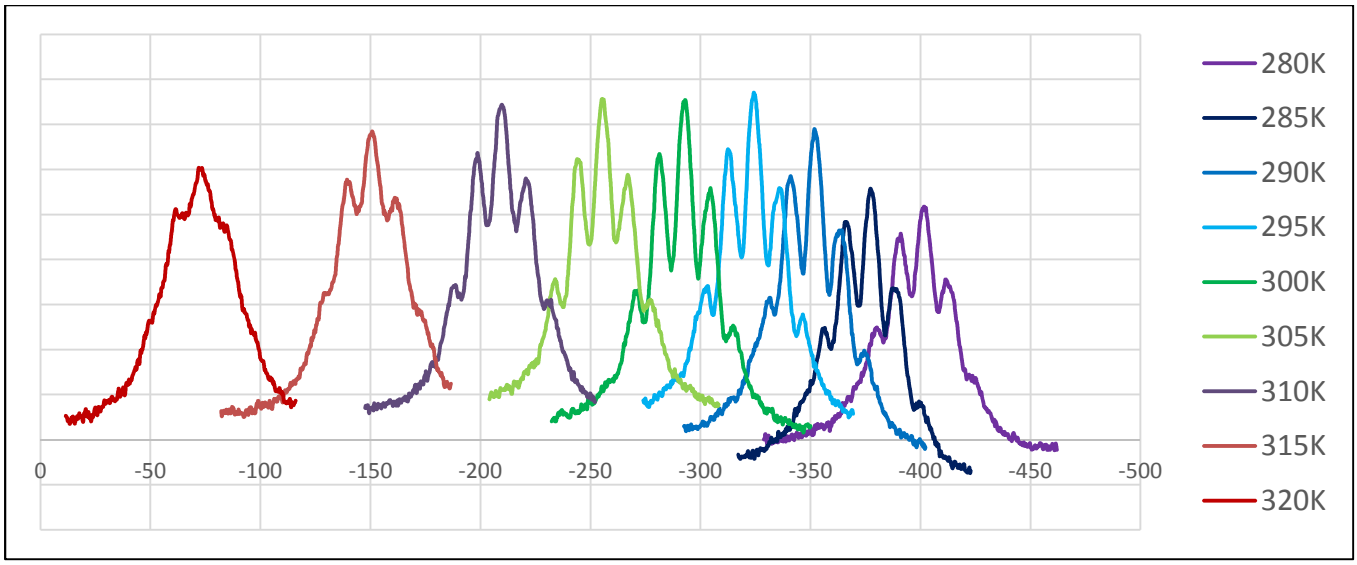

Figure 5.1. ^{1}H NMR Signal for P18Hβ3 of (P12W)-trTC15b and pH 6.5. Line shape fitting of a peak in the aromatic region of the spectrum, which shifts less than 0.03 ppm over the 40° range, provides the intrinsic line width parameter (Δ^{o}) for the experiment. The line width increments due to exchange broadening results in a wider P18Hβ3 peak with less separation, %-dip (Olsen 2005; Scian 2013), between the lines of the peak.

The excess broadening observed for the probes is equated with Δ^{ex} and Equation 5.1(Olsen et al., 2005; Piette & Anderson, 1959; Scian et al., 2013) is used to calculated the value of k_F at each temperature.

$$k_F = 4\pi \cdot \chi_U \cdot (\chi_F)^2 \cdot (\Delta\nu)^2 \cdot (\Delta^{ex})^{-1} \qquad (5.1)$$

The values of χ_F and χ_U (= 1-χ_F) are obtained from the CSD of the probe: χ_F = $CSD^{obs}/CSD^{100\%}$. The $\Delta\nu$ in eq 1 is given as the $CSD^{100\%}$ and has a small temperature dependence. The k_U value at each temperature is calculated as $k_U = k_F \cdot (1- \chi_F) \cdot (\chi_F)^{-1}$.

A list of the Trp-cage species used in this dynamics study appears as Table 5.1. This also provides, again, the T_M and ΔG_U^{300K} appearing in earlier chapters.

Table 5.1. Structure Designations[a], Sequences, and Fold Stability Data[b] for Trp-Cage Variants and Their Single Site Residue Mutants Appearing in this Study.

Designation	Sequence	T_M (CD)	ΔG_U^{300K} (kJ/mol)
TC15b	DAYAQWLADaGPASGRPPPS	74	6.9
(Y3A)		36	0.5
(Y3A, P12W)		48	3.0
(Y3L)		71	5.5
(Y3L, P12W)		73	7.4
trTC15b	Ac-AYAQWLADaGPASGRPPPS-NH_2	65	7.1
pH 2.5		63	4.4
(P12W, R16Cit)		53	4.1
(R16Cit)		49	2.7
(R16Nva)		48	2.3
cp TC4e	RPPPSDAALYAQWLADaGWAS	51	1.1
(D16Abu, P19W)		54	1.7
(D16S, P19W)		67	2.5
(P19W)		65	4.4
(D22)-cpTC4e	RPPPSDAALYAQWLADaGPASD	58	1.9
(A15G, P19W)		49	3.3
(P19W)		67	5.2
(R1Nva, P19W)		50	0.6
(Y10L)		49	1.7
(Y10L, P19W)		61	4.2

[a]The structure designations are given here. ΔG_U values are calculated from 2D NMR data. Unless otherwise noted, the ΔG_U values are calculated at 300K and pH 6.5.

[b]The ΔG_U values are calculated using the average of χ_F values from P18Hα and P18Hβ3 nuclei to represent "complete cage formation." ΔG_U values are listed in kJ/mol and given to the nearest 0.1 kJ. ΔG_U values greater than 8 kJ/mol are uncertain in as they represent $\chi_F \geq 0.96$ observations. ΔG_U values in the 5.5-8.5 kJ/mol range are accurate to ±0.6; values less than 4.5 kJ/mol are given a ±0.3 kJ/mol error.

The data appearing in Table 5.1 provide multiple determinations for a number of single-site mutations and for acidification (pH 2.5 stabilities versus those at pH 6.5). Acidification effect is

designated as ΔpH. The effect of circular permutation is examined first. Single-site mutations examined include P12W (P19W in the circularly permuted series); D9X and R16X (D16X and R1X in the circularly permuted series) for studying the effects of the salt bridge; Y3X (Y10X in the circularly permuted series) for studying the effects of the hydrophobic staple. All values are based on data at 300K.

The mutational (or acidification) Φ_F values are calculated at 300K as:

$$\Phi_F = 2.5[\ln(k_F^{mut}/k_F^{ref})](\Delta\Delta G_U^{mut})^{-1} \quad (5.2)$$

The calculation was performed with both the consensus $\Delta\Delta G_U$ value and the specific one for the system under study if the latter was available. This defines the range of values allowed for Φ_F.

5.2 Effects of Circular Permutation on Folding Rate

One of the aims of this study has been the examination of how circular permutation affects folding pathways and rates. When the circular permutant of Trp-Cage was first characterized by Byrne, one characteristic of the "cp" series was a decrease in stability (Byrne et al., 2013). Unfortunately, the circularly permuted version of TC15b was too unfolded to obtain exchange broadening factors at more than two temperatures. A stabilizing P19W mutation increased the stability of the circular permutant to where the P18Hβ3 resonance could still be observed at the higher temperatures; however, the stability of the non-permuted (P12W)-TC15b counterpart was too high for reliable rate calculations. An additional D→S mutation was employed to eliminate the salt bridge, lowering the fraction folded values of both circular permutant and the corresponding standard Trp-cage into the appropriate range for lineshape analysis.

Figure 5.2 shows the rate comparison of (D9S, P12W)-TC15b and (D16S, P19W)-cp TC4e. There is little difference in the rates of folding. Instead, loss in stability observed for the circular permutant results from a much greater rate of unfolding.

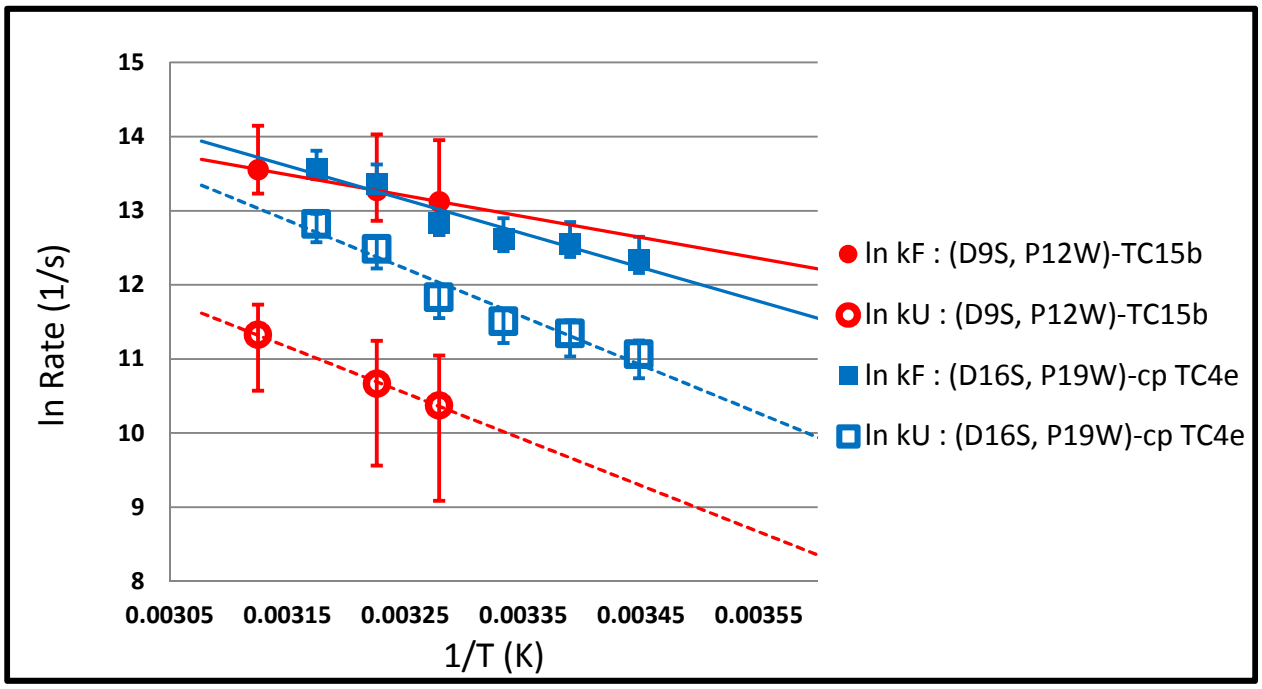

Figure 5.2. Folding/unfolding Arrhenius plots for (D9S, P12W)-TC15b and (D16S, P19W)-cp TC4e at pH 6.5.

To increase stability of the circularly permuted series, an aspartic acid residue was added to the C-terminus of the sequence as described in Chapter 4. This D22 addition is seen to increase stability by 0.9 kJ/mol for cp TC4e and 0.8 kJ/mol for (P12W)-cp TC4e. Significantly, in sequences with N-terminal acetylation, no increase in stability is observed upon D22 addition, indicating that this carboxylate sidechain interacts with the N-terminal ammonium ion. While the presence of D22 introduces an interaction not seen in the standard topology references, it succeeds at increasing the number of temperatures at which exchange broadening can be measured. As shown in Figure 5.2, D22 addition is fold stabilizing but folding rate retarding. This could indicate

that D22 is participating in a kinetic trap early in the folding pathway of the circularly permuted Trp-cage. One potential candidate is the positively charged side chain of Arg1.

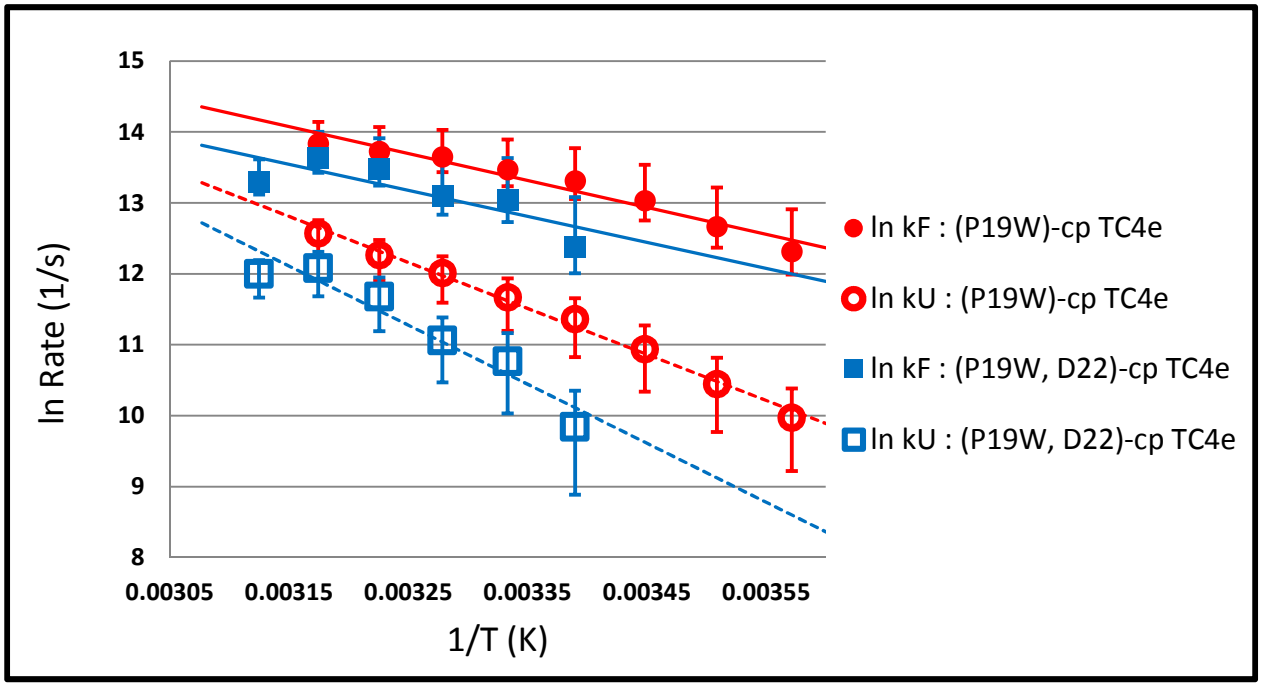

Figure 5.3. Folding/unfolding Arrhenius plots for (P19W)-cp TC4e and (P19W, D22)-cp TC4e at pH 6.5.

5.3 Examining the P12W Effect

In addition to circular permutation, a number of single-site mutations were included in this study to examine the role of specific interactions in folding and how these might change upon circular permutation. Perhaps the most significant of these is P12W (P19W in the cp-series), which was originally suggested by Bunagan (Bunagan et al., 2006). In the case of the TC15b and closely related trTC15b series, the addition of P12W was seen to increase stability of the folded state by 2.2 ± 0.8 kJ/mol at 300K and pH 6.5. In the circularly permuted cp TC4e series, this increase is 2.9 ± 1.2 kJ/mol, see Chapter 4. An exception to this stabilizing effect occurs in the standard topology in the presence of a P18A mutation. As P18A was used in our 2014 dynamics study in

order to incorporate a signal with easily modeled exchange broadening, the resulting rate data does not necessarily reflect the role of Trp^{12} in more typical Trp-cage constructs (Byrne et al., 2014). With the use of Pro18 Hβ3 as the probe, a re-evaluation is now possible.

In the standard topology Trp-cage, the inclusion of P12W pushes the fraction folded above the $\chi_F = 0.940$ cutoff for accurate rate determination. To achieve a more modest χ_F value, Y3L and Y3A mutants were employed. These mutations, which were originally reported by Barua et al. (Barua et al., 2008), decrease the contact in the hydrophobic staple that exists between Y3/P19 (Y10/P4 in the circular permutant). In the TC15b series, the inclusion of Y3L leads to a 1.4 kJ/mol loss of fold stability. The Y3A mutation leads to a more dramatic loss of 6.5 kJ/mol. No NMR structure exists for these mutants, but MD simulations give them the same overall fold as the wild-type cage (C. Y. Zhou et al., 2015).

The original study of P12W indicated that it conferred about a 3.5-fold acceleration in the rate of folding (Bunagan et al., 2006). Here, the effects of P12W on folding appear to be highly contextual. For (Y3L)-TC15b, the P12W mutation increases folding through a faster rate of folding, but in this case the improvement is more modest: a factor less than 2-fold. Conversely, in the presence of Y3A, the P12W mutation carries no change in the folding rate but rather stabilizes through a decrease in the unfolding rate. Taken together, it appears the interactions of the second tryptophan residue occur before the transition state when the hydrophobic staple interaction is part of the folding pathway, and after the transition state when the hydrophobic staple is absent. This suggests that the interactions involving the Trp6/Trp12 aryl-aryl cluster are occurring before those involving Y3, and that the latter is involved in the transition state.

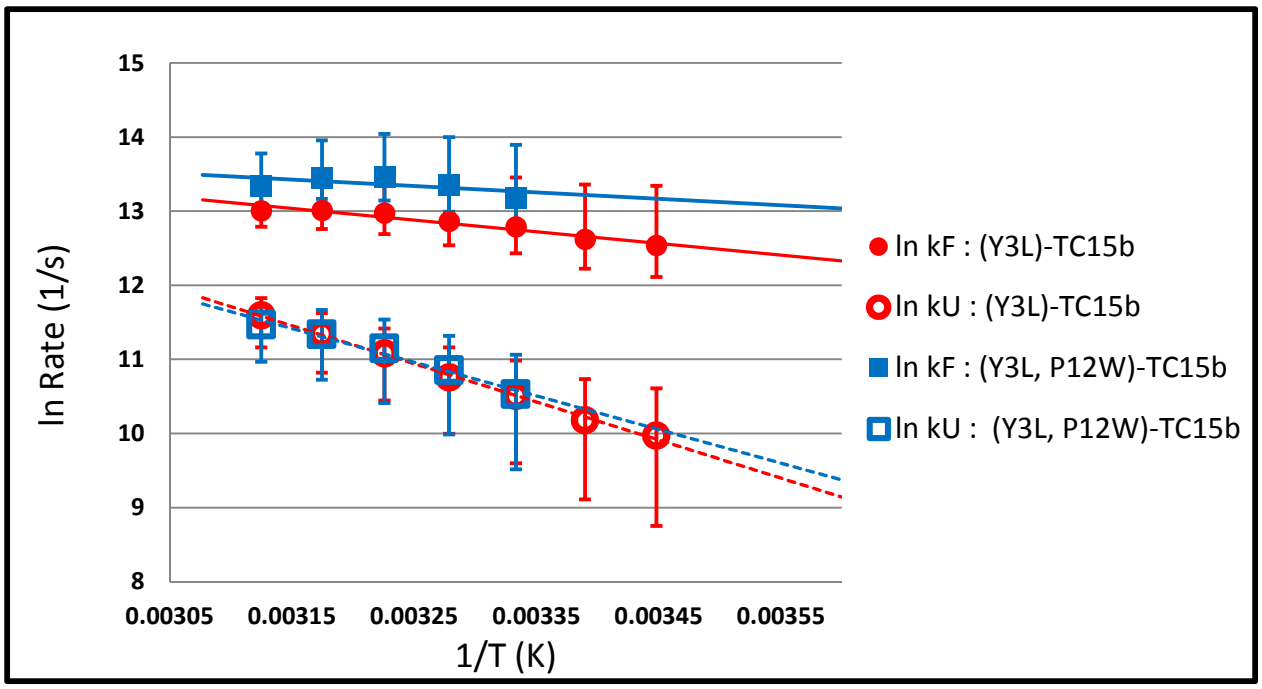

Figure 5.4. Folding/unfolding Arrhenius plots for (Y3L)-TC15b and (Y3L, P12W)-TC15b at pH 6.5.

However, we have also observed cases in which the P12W mutations in TC15b and trTC15b species, while still notably fold stabilizing, have little or no effect of the folding rate. Two examples appear in Figure 5.5. and 5.6.

It is not just the presence of the hydrophobic staple that influences the effects of P12W. In the absence of the salt bridge between Asp9/Arg16, the increase in folding rates is not seen for P12W. This can be accomplished by either changing the pH to from 6.5 to 2.5 or by incorporation of R16Cit or R16Nva mutations. This observation is more difficult to rationalize. In each case, P12W is still stabilizing through a decrease in the rate of unfolding.

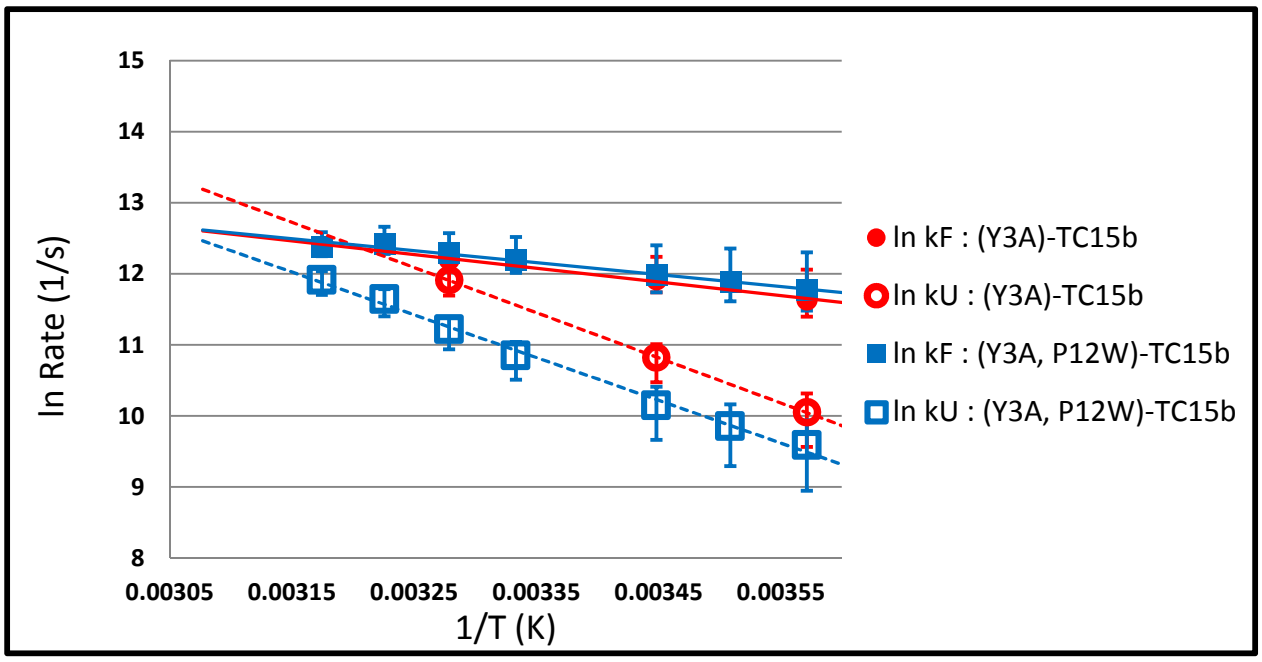

Figure 5.5. Folding/unfolding Arrhenius plots for (Y3A)-TC15b and (Y3A, P12W)-TC15b at pH 6.5.

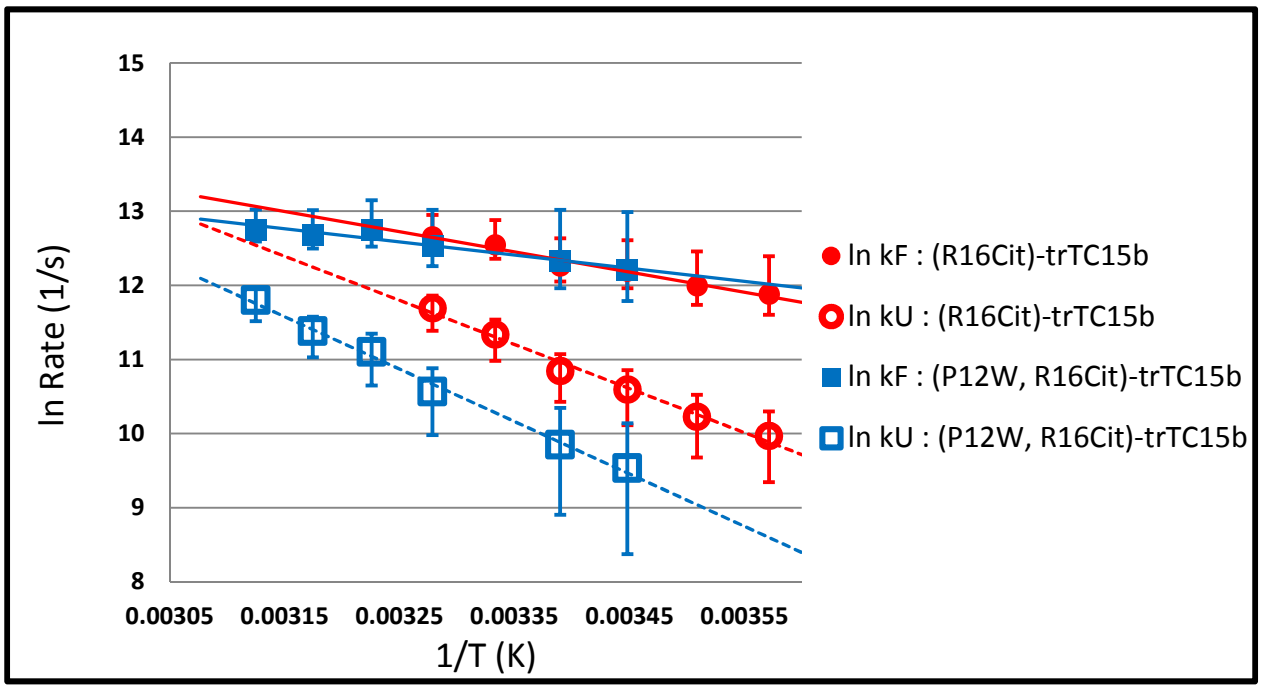

Figure 5.6. Folding/unfolding Arrhenius plots for (R16Cit)-trTC15b and (P12W, R16Cit)-trTC15b at pH 6.5.

The absence of folding rate increases is also seen in the circularly permuted Trp-Cage [D22]-cpTC4e, where $\Phi = 0.14$. While the value of $\Delta\Delta G_U$ of P12W is comparable in the circular permutation, it appears that the most important stabilizing interactions are formed after the transition state. It is possible that the change in contact order has shifted the sequence of steps in the folding pathway.

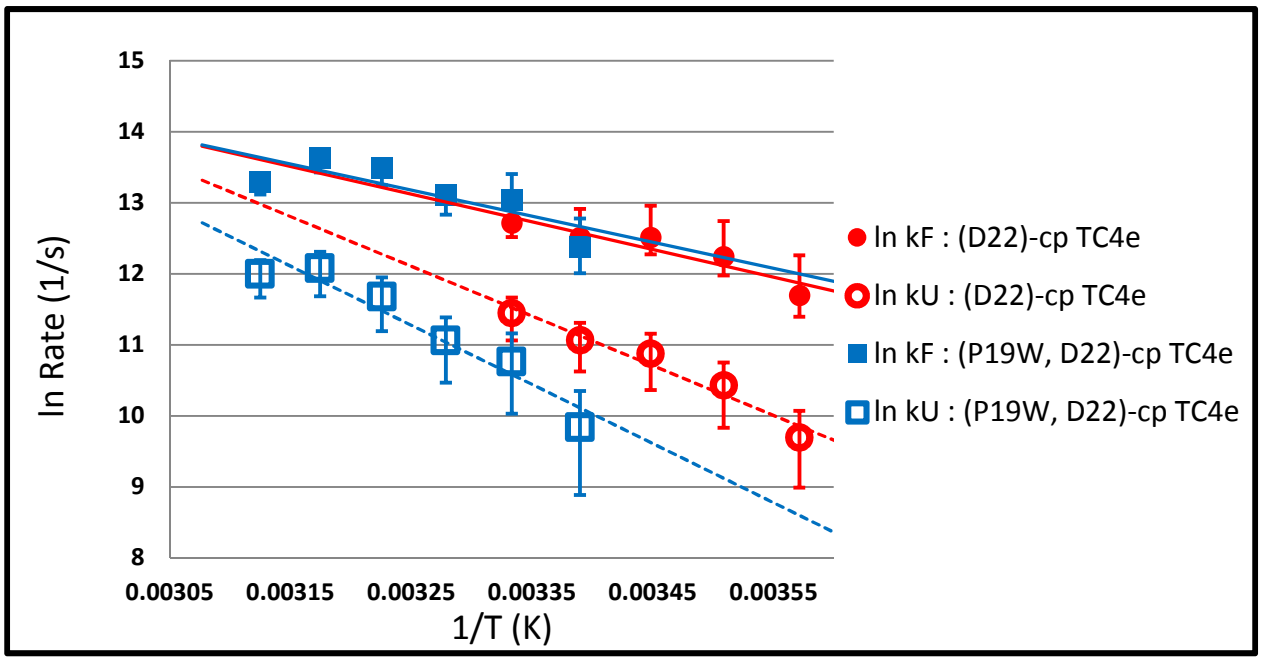

Figure 5.7. Folding/unfolding Arrhenius plots for (D22)-cpTC4e and (P19W, D22)-cpTC4e at pH 6.5.

5.4 The Salt Bridge

In our 2014 study, acidic conditions were used to examine the role of the Asp9/Arg16 salt bridge (Byrne et al., 2014). The rate data for (A8G, P18A)-TC16b indicated that the rate of folding was the same at pH 7 and pH 2.5. If anything folding was slightly faster at pH 2.5 even though the folded structure is destabilized by carboxylate protonation. An examination of the closely related

TC15b series at pH 6.5 and pH 2.5 showed the same trends in rate data. This data would be consistent with a scenario in which the salt bridge folds after the transition state of folding. However, the Coulombic interactions between Asp9 and Arg16 are not the only pH sensitive features of the sequence. At pH 6.5, the aspartate residues at Asp1 and Asp9 will interact with the helix macrodipole, offering stabilizing and destabilizing interactions, respectively. The charged N- and C-termini are capable of a second salt bridge interaction. Finally, hydrogen bonding between Gln5/Asp9 serves to stabilize the α-helix. Changes in pH introduce several changes in stability that may or may not be reflected in the rate of folding.

A more specific probe of the formation of the salt bridge is achieved through R16Nva or R16Cit mutations, which eliminate the Asp9/Arg16 Coulombic forces without affecting other pH-sensitive elements present. Rather than the TC15b series, we use the closely related truncated series trTC15b. This sequence, as well as being amidated at the C-termini to prevent any possible interactions involving the free carboxylate there, replaces the first aspartic acid residue with an acetyl group to eliminate the pH-sensitivity of the N-cap.

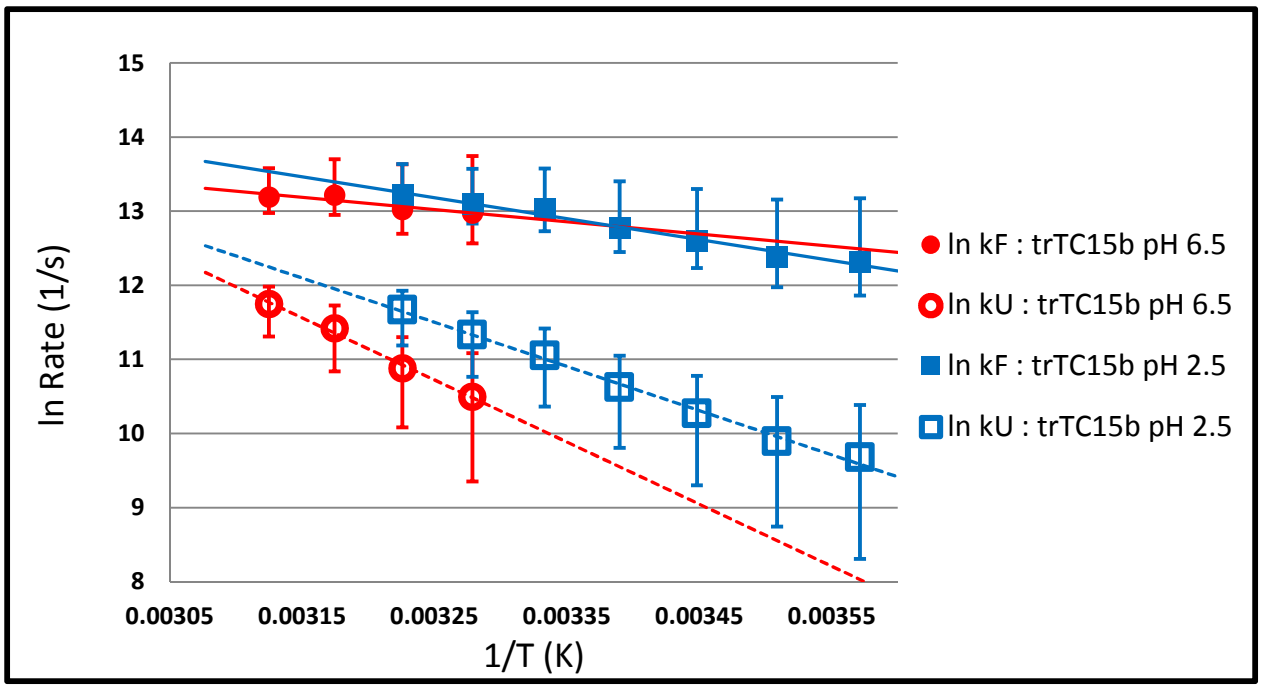

Figure 5.8. Folding/unfolding Arrhenius plots for trTC15b at pH 6.5 and trTC15b pH 2.5 at pH 2.5.

As shown in Figure 5.8, when the salt bridge is eliminated at pH 2.5, the resulting folding rates are markedly similar to those at pH 6.5. While this is in line with the work of Byrne, it is also possible that the loss of the Coulombic interactions is offset by the increase in stability that comes from eliminating the negatively charged carboxylate group at the C-terminus of the helix. Alternatively, when mutations R16Cit and R16Nva were used to eliminate the salt bridge, the rate of folding decreased for the former and increased for the latter, Figure 5.9. An increase in folding rate could be consistent with the elimination of a kinetic trap, and in fact such a trap has been proposed for Asp9/Arg16 (Ding et al., 2005; R. Zhou, 2003) However, the introduction of an R16Cit mutation leads to a decrease in the folding rate. It would appear the R16Nva folding rate increase is due to the norvaline sidechain itself for reasons that are not clear rather than the elimination of the salt bridge. Based on R16Cit data, it would appear the salt bridge can form

before the transition state, contrary to the conclusions of previous studies (Byrne et al., 2014; Culik et al., 2011); however, it provides little folding acceleration.

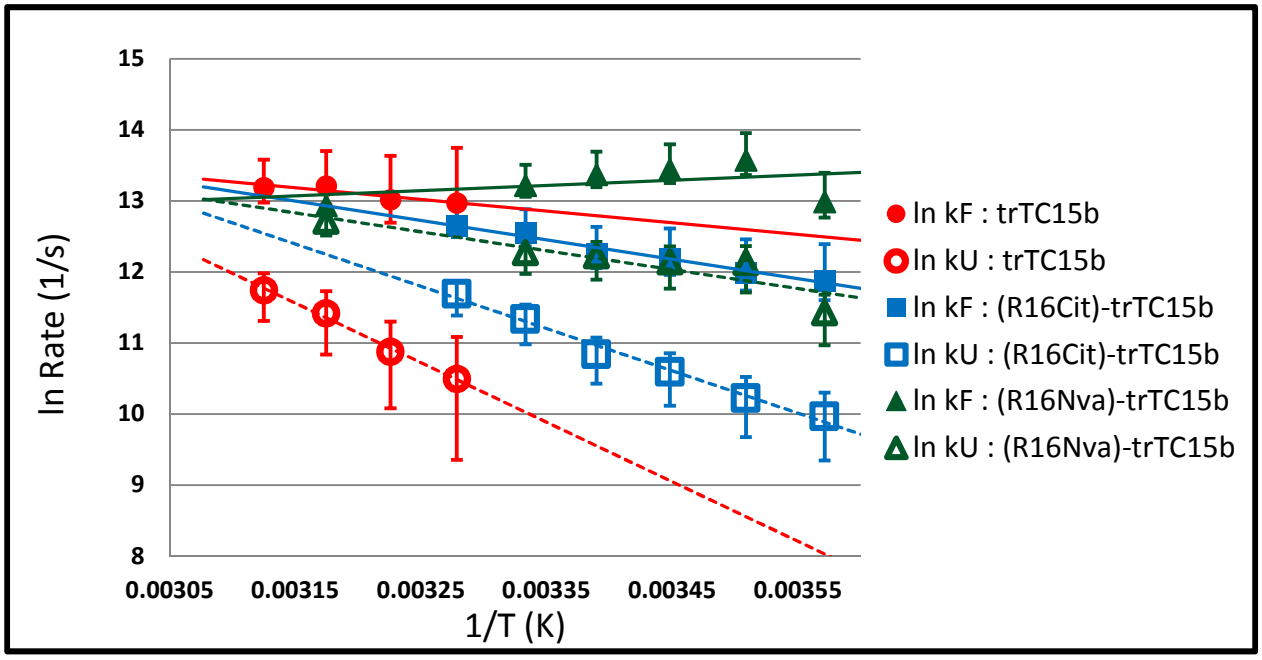

Figure 5.9. Folding/unfolding Arrhenius plots for trTC15b, (R16Cit)-trTC15b and (R16Nva)-trTC15b at pH 6.5.

Turning to the circular permutant**,** R1Nva once again leads to a loss of stability but an increase in the rate of folding – $1/k_F$ = 1.6 μs versus 2.3 μs for the [P19W, D22]-cpTC4e reference. An R1Cit mutant was also produced but the P18 Hβ3 peaks were too poorly resolved to determine exchange broadening factors. Instead, D16S and D16Abu mutations were used to eliminate the salt bridge from the other side (figures 5.11 and 5.12). Replacing the ionized Asp at the C-terminus of an α-helix is expected to stabilize the helix. However, the net change is a decrease in the folding rate, indicating that in the folding pathway for the circular permutant, the salt bridge is again formed before (or at) the transition state. At 300K, the phi value 0.57 based on Figure 5.11, 1.45 based on Figure 5.12.

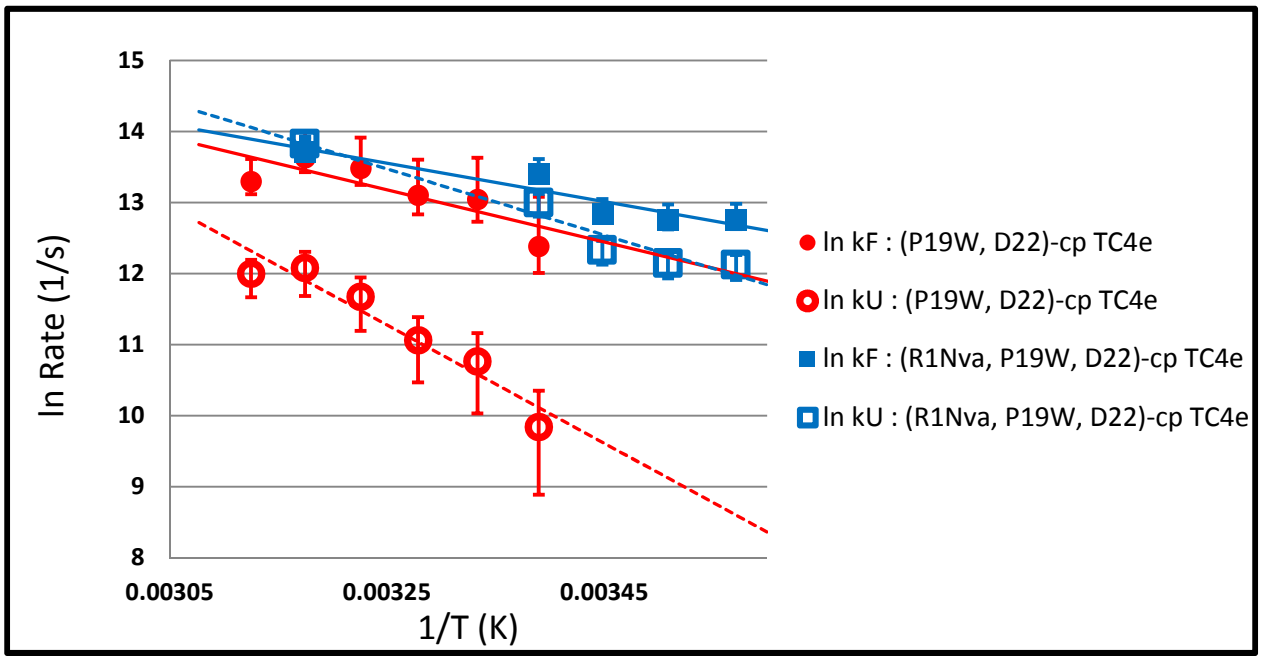

Figure 5.10. Folding/unfolding Arrhenius plots for (P19W, D22)-cp TC4e, (R1Nva, P19W, D22)-cp TC4e at pH 6.5.

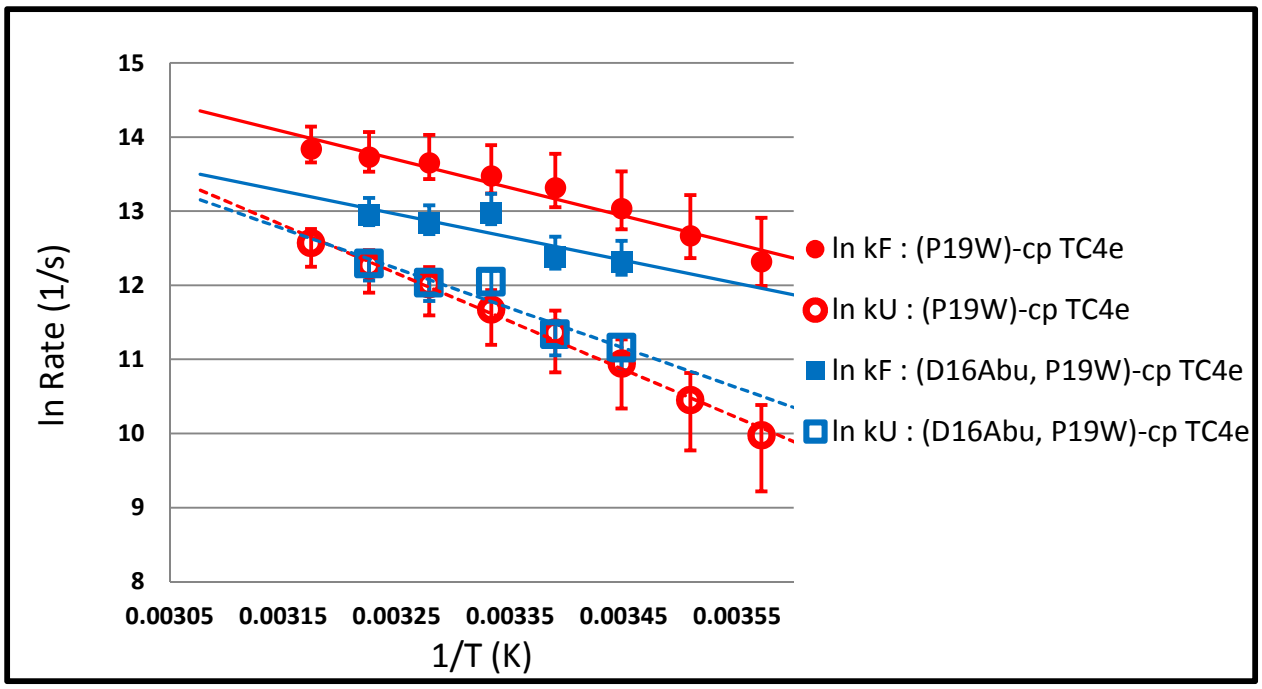

Figure 5.11. Folding/unfolding Arrhenius plots for (P19W)-cp TC4e, (D16Abu, P19W)-cp TC4e at pH 6.5.

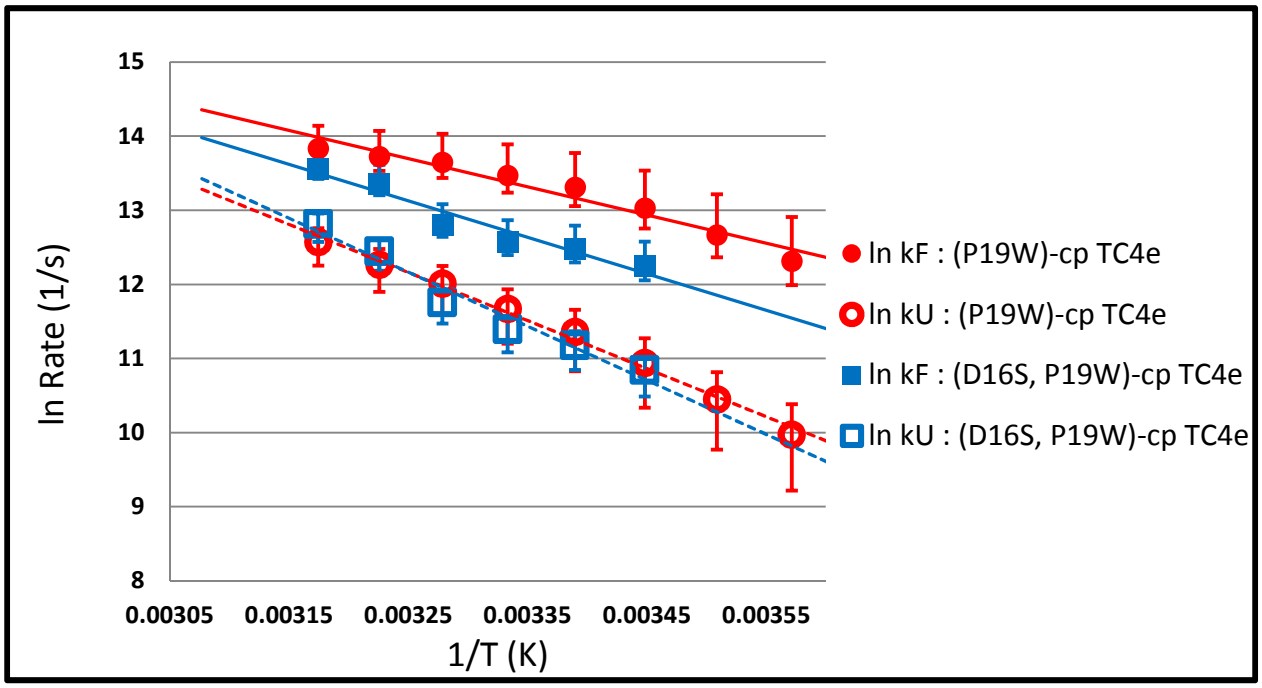

Figure 5.12. Folding/unfolding Arrhenius plots for (P19W)-cp TC4e, (D16S, P19W)-cp TC4e at pH 6.5.

5.5 THE HYDROPHOBIC STAPLE

As is the case for the salt-bridge, circular permutation changes the distance in the primary sequence between the residues of the hydrophobic staple. In the standard topology, the hydrophobic staple is a Y3/P19 contact and has been shown to be highly stabilizing, with P19A mutations leading to losses of 9 kJ/mol in TC15b and 11 kJ/mol (P12W)-TC15b. This mutation is not well suited for this study, as the resulting miniprotein is so destabilized that the P8Hβ3 cannot be observed in unobscured regions of the 1D NMR spectrum. Instead, Y3L and Y3A mutations were used to study the staple. Y3L and Y3A mutations were first reported by Barua et al. (Barua et al., 2008). In TC15b, these mutations lead to stability losses of 1.4 kJ/mol and 6.5 kJ/mol, respectively.

The decrease in folding rates is, however, not in proportion to ΔΔG-values. The Φ_F values from Figure 5.13 calculated at 300K are 0.48 (Y3L) and 0.40 (Y3A), indicative of the presence of some hydrophobic stapling at the cage folding transition state. While (P12W)-TC15b is too well folded to derive accurate rate data, a comparison between (Y3L, P12W)-TC15b and (Y3A, P12W)-TC15b also show the decrease in folding rate (Figure 5.14). Here, the Φ_F value is 0.83. This is consistent with our earlier observations on P12W mutants that suggested the formation of the hydrophobic staple as the rate determining step in the standard topology.

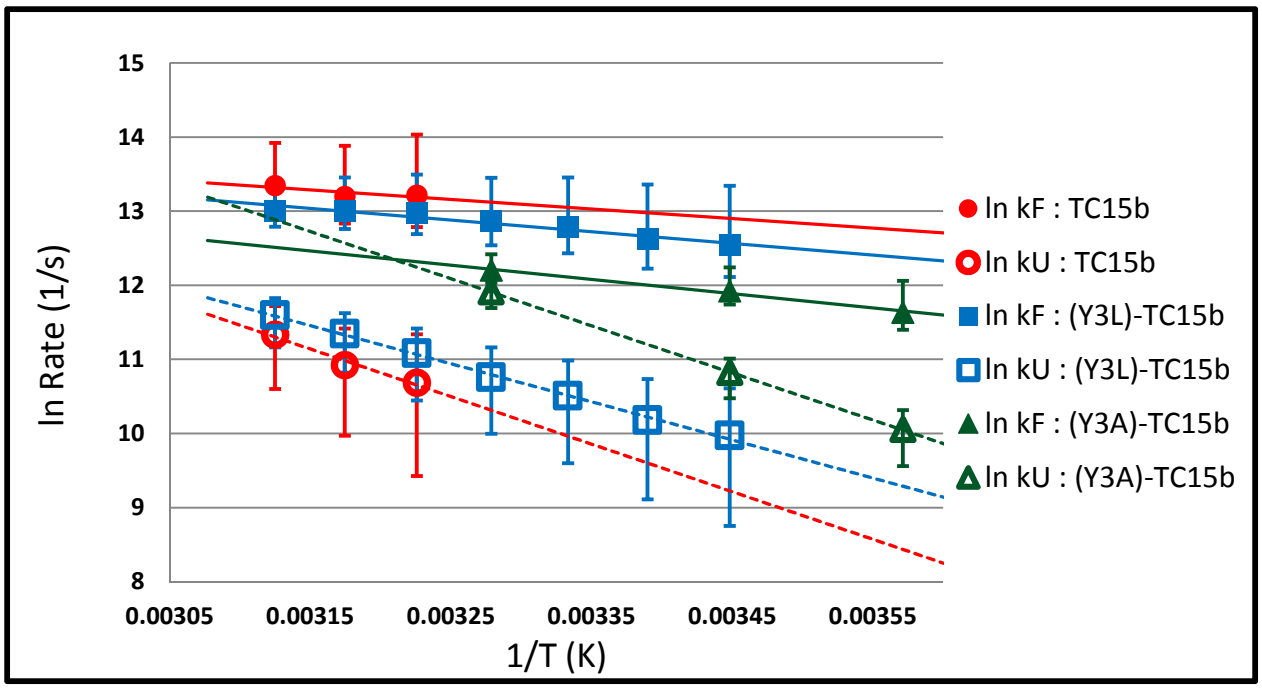

Figure 5.13. Folding/unfolding Arrhenius plots for TC15b, (Y3L)-TC15b and (Y3A)-TC15b at pH 6.5.

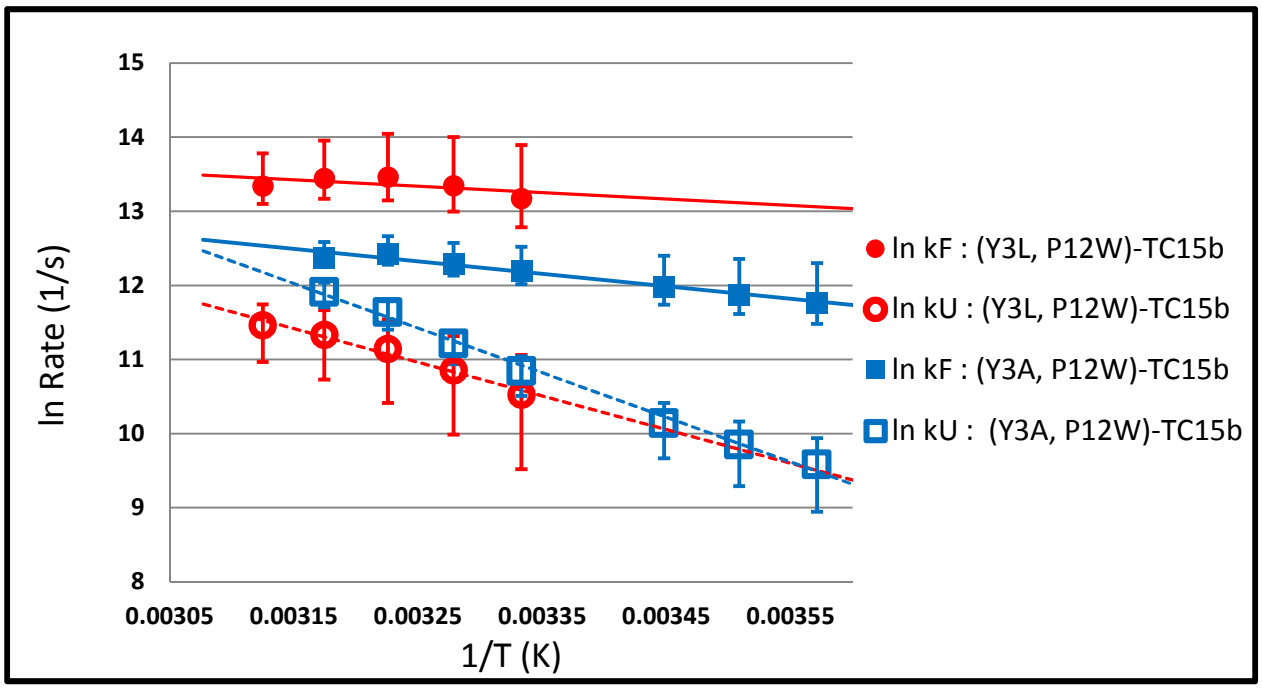

Figure 5.14. Folding/unfolding Arrhenius plots for (Y3L, P12W)-TC15b and (Y3A, P12W)-TC15b at pH 6.5.

In the circularly permuted series, the presence of the equivalent Y10L mutation provides a small folding rate acceleration. It is possible that the smaller, more flexible leucine sidechain is more readily able to make contacts with proline due to a greater number of acceptable orientations between them.

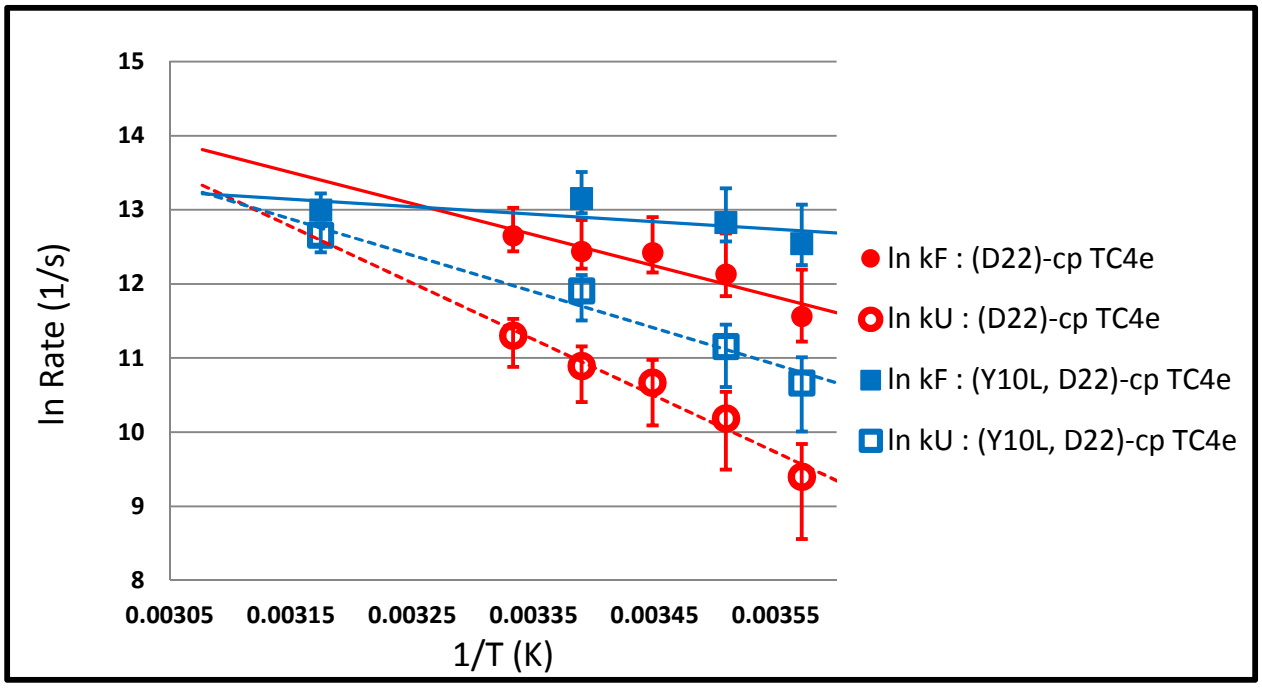

Figure 5.15. Folding/unfolding Arrhenius plots for (D22)-cp TC4e and (Y10L, D22)-cp TC4e at pH 6.5.

With the P19W mutation present (Figure 5.16), again a small folding rate increase results with the Y10L mutation. My error analysis, however, casts doubts on the significance of the rate change. The Y/P hydrophobic staple does not appear to have a key role in the folding of the circularly permuted Trp-cage.

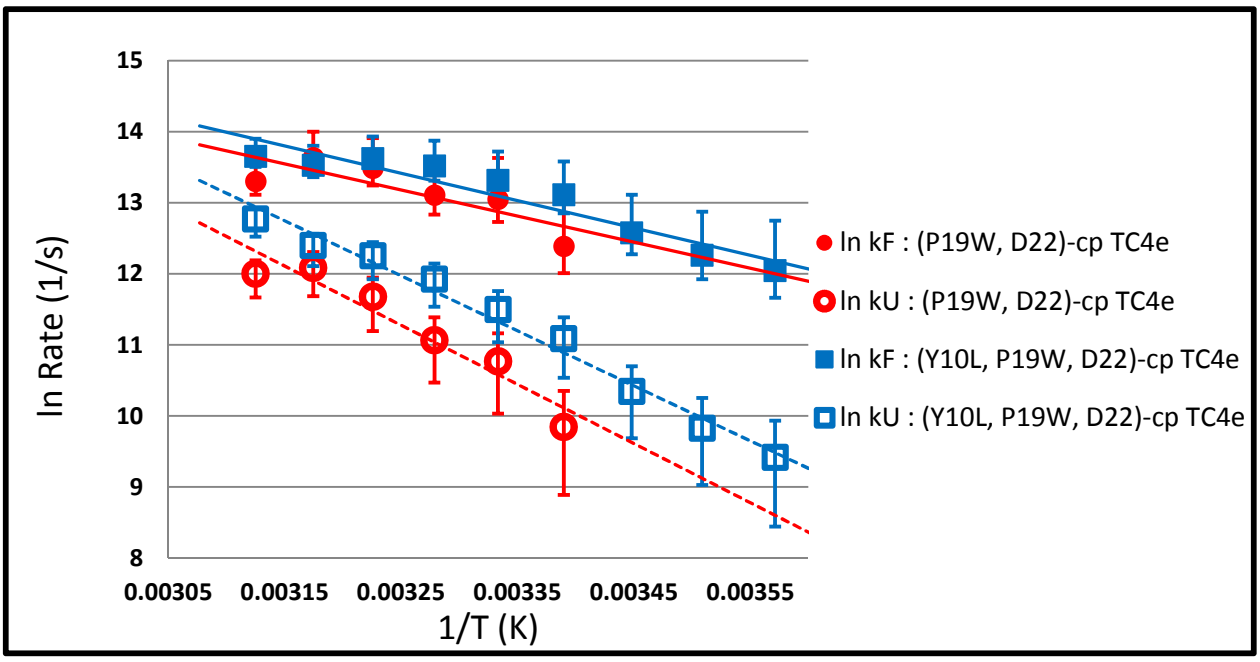

Figure 5.16. Folding/unfolding Arrhenius plots for (P19W, D22)-cp TC4e and (Y10L, P19W, D22)-cp TC4e at pH 6.5.

5.6 Formation of the Alpha-Helix

As a last comparison between standard and circularly permuted topologies, the A8G mutation was examined as a probe of α-helix destabilizing effects on folding dynamics. In the 2014 study, it was determined that the effects on the rate were consistent with helix formation before (or at) the transition state: $\Phi_F =$ 1.19 at 305K for A8G mutations in the TC16b series (Byrne et al., 2014). In the present study, the same mutation was incorporated into the analogous circular permutant (A15G, P19W, D22)-cp TC4e. Early helix formation is indicated here as well; the Φ_F is calculated to be 0.68. Given the presence of "half-cage" and residual helix present in the folding equilibria of circular permutants, the formation of a-helix before the rate-determining step of the folding pathway, was expected (Byrne et al., 2013).

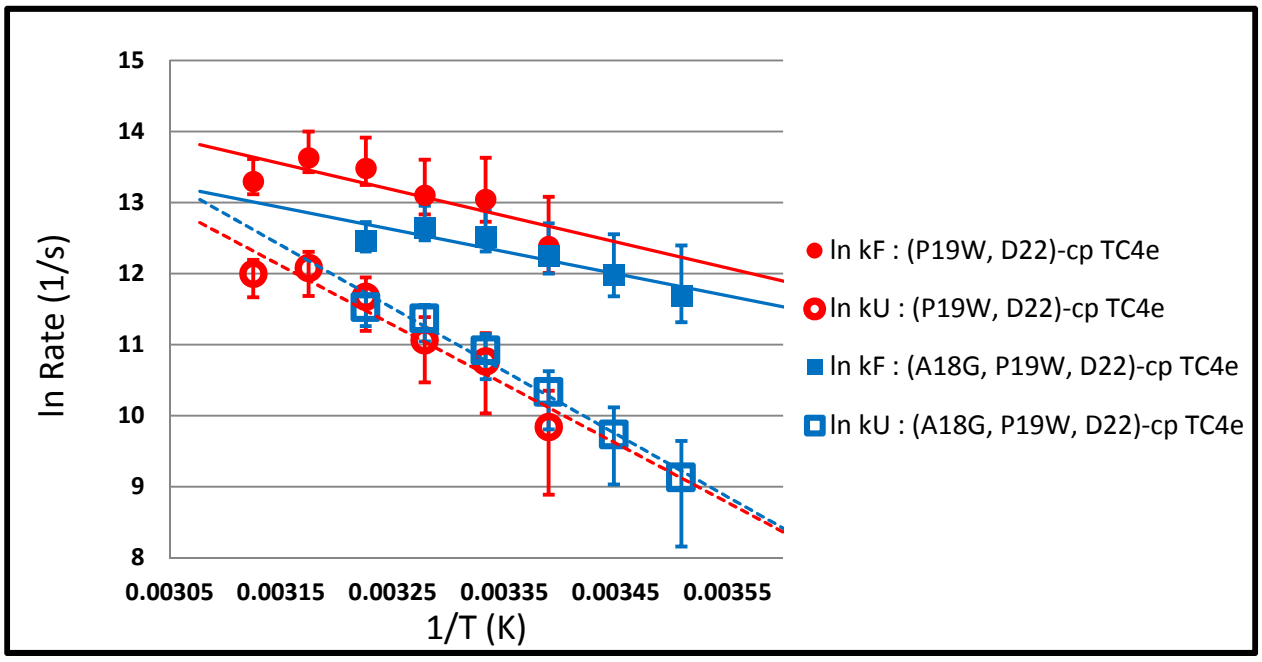

Figure 5.17. Folding/unfolding Arrhenius plots for (P19W, D22)-cp TC4e and (A15G, P19W, D22)-cp TC4e at pH 6.5.

5.7 Discussion

In this study, we report on the thermodynamics stability and rate data for a variety of Trp-cage sequences in the TC15b/trTC15b series and their closest analogs in the circularly permuted series. Using point mutations and changes in pH, a series of interactions characteristic of the folded state were examined and placed relative to one another on the folding pathway. Differences between the standard and circularly permuted topology serve to elucidate the effects of contact order on the folding mechanism.

Exchange broadening was measured using the Hβ3 resonance of Pro18 (Pro3 in the cp-series). This proline, which is located in the polyPro$_{II}$ tail, is an ideal probe. In the folded state, this residue is positioned close to the Trp6 indole sidechain, resulting in dramatic CSDs via a ring current effect. Significantly, these large shifts would not be present until the docking of the polyPro$_{II}$ tail,

making this nucleus a reporter of full cage formation only. This analysis assumes two-state folding, and that χ_U can be defined as all species that are not the fully folded cage as calculated from Pro18 CSDs. In contrast, CSDs that result predominantly from helicity reflect a different collection of conformers. For some sequences, there is partial helicity in the unfolded state, and throughout all series there is essentially the same fractional helicity in any "half-cage" conformation as in the full cage conformation. The results for mutations within the standard topology are in a number of cases different than reported when an Ala18 methylene is used as a dymamics probe, with P12W as a notable example (Byrne et al., 2014).

Gauging the effects of circular permutation on folding rates proved to be problematic. Comparison of the cp-TC4e sequence to the most closely analogous TC15b sequence was not possible because some of the circularly permuted Trp-cage were too unfolded to observe the Hβ3 signal at more than two temperatures. The addition of the stabilizing P12W mutation pushed the circularly permutant into the appropriate folded range but left the corresponding (P12W)-TC15b too folded to obtain reliable rate calculations. A D9S mutation (D16S in the cp-series) was used to ensure that the standard topology was unfolded enough for comparison. The addition of a D22 residue on the C-terminus of cp TC4e improved fold stability enough to analyze folding rates. However, as D22 changes the rate of folding and unfolding, a direct comparison of folding rates of D22 mutants and their TC15b counterparts is not possible. In sum, it appears that circular permutation does not speed up cage formation significantly.

P12W was seen to be stabilizing in all the examples characterized here. However, its effect on folding rates was observed to depend on other interactions present. In general the folding rate effects were quite small, certainly smaller than the effects on $\Delta\Delta G_U$. In the presence of Y3L mutations, P12W conferred an increased folding rate. Y3A, which eliminates the hydrophobic

staple to a greater degree, results in rates of folding that were identical between (Y3A)-TC15b and (Y3A,P12W)-TC15b. The Trp6/Trp12 aryl-aryl interactions appear to be occurring before the transition state when the hydrophobic staple is intact but not in its absence. This in turn suggested that formation of the staple can be a key feature of the transition state of folding under some circumstances. The absence of the Asp9/Arg16 salt bridge is also seen to mitigate the effects of P12W. In circumstances where the salt bridge is disrupted, either by protonation of the Asp at pH 2.5 or R16X mutations, no increase in folded rates are observed for P12W. The equivalent P19W mutation also failed to increase the folding rate in the circular permutation, although it was seen to be stabilizing to a similar extent as the standard topology. This may be evidence to the two series following different folding pathways.

The significance of the Y3/P19 staple was readily ascertained: Y3L or Y3A mutations were seen to decrease the rate of folding at pH 6.5. In the standard topology, the decrease in folding rate was seen in Y3L mutations in both the TC15b and trTC15b series, and at both pH 6.5 and pH 2.5 in the TC15b series. However, in the circular permutation series, Y10L was observed to increase the folding rate. A further reduction in hydrophobic interactions, Y10A rather than Y10L, was distinctly destabilizing and decreased the folding rate significantly. Hydrophobic staple formation is rate-determining in the standard topology Trp-cage.

However, in the circular permutation series, the Y10L mutation was observed to increase the folding rate or have a very small effect. As might be anticipated, with the shorter contact order in the cp-series; this hydrophobic staple is of reduced importance in folding.

Although previous computational studies have suggested an Asp9/Arg16 interaction could act as a kinetic trap, the R16Cit mutation did not provide evidence for this. It is also worth reiterating that in otherwise stabilized (P18A) standard topology systems salt bridge formation was definitely

a post-transition state event. R16Nva did give an increase in the rate of folding, but we interpret this rate increase to be caused by the presence of the apolar sidechain rather than salt bridge elimination. The folding rate decrease created by R16Cit would place salt bridge formation earlier in the folding pathway, before the rate determining step.

To examine the salt bridge in the circularly permuted series without the confounding effects of R1Nva, Asp16Ser and Asp16Abu mutations were used to eliminate the salt bridge instead. These mutations resulted in a decrease in folding rate, indicating that salt bridge formation is definitely occurring before or at the rate determining step in the folding pathway of these circular permutants.

The results of the dynamics measurements for the standard topology and closely related truncated species examined herein have the aryl-aryl cluster and salt bridge forming before the rate determining step of the hydrophobic staple. This model is consistent with the structure of a half-cage in which a fully folded conformation the N-terminal α-helix (and probably the 3_{10}-helix); with the docking of the polyProII tail occurring later. In the case of the circular permutant, the interactions of the hydrophobic staple, involving residues which are no longer holding together the far termini, is not rate determining. Likewise, the aryl-aryl cluster is happening later in the folding pathway. The interactions of the salt bridge, involving residues which are now farther apart in the primary sequence, now occur before or at the rate determining step.

BIBLIOGRAPHY

Ahmed, Z., Beta, I. A., Mikhonin, A. V., & Asher, S. A. (2005). UV-resonance Raman thermal unfolding study of Trp-cage shows that it is not a simple two-state miniprotein. *Journal of the American Chemical Society*, *127*(31), 10943–10950. https://doi.org/10.1021/ja050664e

Akiyama, S., Takahashi, S., Ishimori, K., & Morishima, I. (2000). Stepwise formation of alpha-helices during cytochrome c folding. *Nature Structural Biology*, *7*(6), 514–520. https://doi.org/10.1038/75932

Andersen, N. H., Fesinmeyer, R. M., Neidigh, J. W., & Barua, B. (2001). The Trp-Cage: A Notably Stable Mini-Protein Fold. In *Peptides* (pp. 45–46).

Andersen, N. H., & Tong, H. (1997). Empirical parameterization of a model for predicting peptide helix/coil equilibrium populations. *Protein Science*, *6*(9), 1920–1936. https://doi.org/10.1002/pro.5560060913

Anderson, J. M., Shcherbakov, A. A., Kier, B. L., Kellock, J., Shu, I., Byrne, A. L., … Andersen, N. H. (2017). Optimization of a β-sheet-cap for long loop closure. *Biopolymers*, *107*(3), 1–11. https://doi.org/10.1002/bip.22995

Anfinsen, C. B. (1973). Principles that Govern the Folding of Protein Chains. *Science*, *181*(4096), 223–230. https://doi.org/10.1126/science.181.4096.223

Anil, B., Song, B., Tang, Y., & Raleigh, D. P. (2004). Exploiting the right side of the ramachandran plot: Substitution of glycines by D-alanine can significantly increase protein stability. *Journal of the American Chemical Society*, *126*(41), 13194–13195. https://doi.org/10.1021/ja047119i

Azia, A., & Levy, Y. (2009). Nonnative Electrostatic Interactions Can Modulate Protein Folding: Molecular Dynamics with a Grain of Salt. *Journal of Molecular Biology*, *393*(2), 527–542. https://doi.org/10.1016/j.jmb.2009.08.010

Bai, Y. (2003). Hidden intermediates and levinthal paradox in the folding of small proteins. *Biochemical and Biophysical Research Communications*. https://doi.org/10.1016/S0006-291X(03)00800-3

Baldwin, R. L. (1995). The nature of protein folding pathways: The classical versus the new view. *Journal of Biomolecular NMR*, *5*(2), 103–9. https://doi.org/10.1007/BF00208801

Baldwin, R. L., & Rose, G. D. (1999a). Is protein folding hierarchic? I. Local structure and peptide folding. *Trends in Biochemical Sciences*. https://doi.org/10.1016/S0968-0004(98)01346-2

Baldwin, R. L., & Rose, G. D. (1999b). Is protein folding hierarchic? II. Folding intermediates and transition states. *Trends in Biochemical Sciences*. https://doi.org/10.1016/S0968-0004(98)01345-0

Barua, B., Lin, J. C., Williams, V. D., Kummler, P., Neidigh, J. W., & Andersen, N. H. (2008). The Trp-cage: Optimizing the stability of a globular miniprotein. *Protein Engineering, Design and Selection*, *21*(3), 171–185. https://doi.org/10.1093/protein/gzm082

Beasley, J. R., & Hecht, M. H. (1997). Protein design: The choice of de novo sequences. *Journal of Biological Chemistry*. https://doi.org/10.1074/jbc.272.4.2031

Berendsen, H. J. (1998). A glimpse of the Holy Grail? *Science*, *282*, 642–3. https://doi.org/10.1126/science.282.5389.642

Bunagan, M. R., Yang, X., Saven, J. G., & Gai, F. (2006). Ultrafast folding of a computationally designed trp-cage mutant: Trp 2-cage. *Journal of Physical Chemistry B*, *110*(8), 3759–3763. https://doi.org/10.1021/jp055288z

Byrne, A. (2013). *NMR Studies of Polypeptide Structuring and Aggregation*. University of Washington.

Byrne, A., Kier, B. L., Williams, D. V., Scian, M., & Andersen, N. H. (2013). Circular Permutation of the Trp-cage: Fold Rescue upon Addition of a Hydrophobic Staple. *RSC Advances*, *3*(43), 19824–19829. https://doi.org/10.1039/C3RA43674H

Byrne, A., Williams, D. V., Barua, B., Hagen, S. J., Kier, B. L., & Andersen, N. H. (2014). Folding dynamics and pathways of the trp-cage miniproteins. *Biochemistry*, *53*(38), 6011–6021. https://doi.org/10.1021/bi501021r

Chowdhury, S., Lee, M. C., & Duan, Y. (2004). Characterizing the rate-limiting step of Trp-cage folding by all-atom molecular dynamics simulations. *Journal of Physical Chemistry B*, *108*(36), 13855–13865. https://doi.org/10.1021/jp0478920

Chowdhury, S., Lee, M. C., Xiong, G., & Duan, Y. (2003). Ab initio folding simulation of the Trp-cage mini-protein approaches NMR resolution. *Journal of Molecular Biology*, *327*(3), 711–717. https://doi.org/10.1016/S0022-2836(03)00177-3

Cong, L., Ran, F. A., Cox, D., Lin, S., Barretto, R., Habib, N., … Zhang, F. (2013). Multiplex genome engineering using CRISPR/Cas systems. *Science*. https://doi.org/10.1126/science.1231143

Cote, Y., Maisuradze, G. G., Delarue, P., Scheraga, H. A., & Senet, P. (2015). New Insights into Protein (Un)Folding Dynamics. *The Journal of Physical Chemistry Letters*, *6*, 1082–1086. https://doi.org/10.1021/acs.jpclett.5b00055

Culik, R. M., Annavarapu, S., Nanda, V., & Gai, F. (2013). Using D-amino acids to delineate the mechanism of protein folding: Application to Trp-cage. *Chemical Physics*, *422*, 131–134. https://doi.org/10.1016/j.chemphys.2013.01.021

Culik, R. M., Serrano, A. L., Bunagan, M. R., & Gai, F. (2011). Achieving secondary structural resolution in kinetic measurements of protein folding: A case study of the folding mechanism of Trp-cage. *Angewandte Chemie International Edition*, *50*(46), 10884–10887. https://doi.org/10.1002/anie.201104085

Daggett, V., & Fersht, A. R. (2003). Is there a unifying mechanism for protein folding? *Trends in Biochemical Sciences*. https://doi.org/10.1016/S0968-0004(02)00012-9

Dalby, P. A., Oliveberg, M., & Fersht, A. R. (1998). Folding intermediates of wild-type and mutants of barnase. I. Use of Φ-value analysis and m-values to probe the cooperative nature of the folding pre-equilibrium. *Journal of Molecular Biology*. https://doi.org/10.1006/jmbi.1997.1546

Day, R., Paschek, D., & Garcia, A. E. (2010). Microsecond simulations of the folding/ unfolding thermodynamics of the Trp-cage miniprotein. *Proteins: Structure, Function and Bioinformatics*, *78*(8), 1889–1899. https://doi.org/10.1002/prot.22702

Dill, K. A. (1990). Dominant Forces in Protein Folding. *Biochemistry*, *29*(31), 7133–7155. https://doi.org/10.1021/bi00483a001

Dill, K. A., Alonso, D. O. V., & Hutchinson, K. (1989). Thermal Stabilities of Globular Proteins? *Biochemistry*, *28*, 5439–5449. https://doi.org/10.1021/bi00439a019

Dill, K. A., & Chan, H. S. (1997). From Levinthal to pathways to funnels. *Nature Structural Biology*, *4*, 10–19. https://doi.org/10.1038/nsb0197-10

Dill, K. A., & MacCallum, J. L. (2012). The protein-folding problem, 50 years on. *Science*, *338*(6110), 1042–1046. https://doi.org/10.1126/science.1219021

Dill, K. A., Ozkan, S. B., Shell, M. S., & Weikl, T. R. (2008). The Protein Folding Problem. *Annual Review of Biophysics*, *37*(1), 289–316. https://doi.org/10.1146/annurev.biophys.37.092707.153558

Ding, F., Buldyrev, S. V., & Dokholyan, N. V. (2005). Folding Trp-cage to NMR resolution native structure using a coarse-grained protein model. *Biophysical Journal*, *88*(1), 147–155. https://doi.org/10.1529/biophysj.104.046375

Dobson, C. M., & Karplus, M. (1999). The fundamentals of protein folding: Bringing together theory and experiment. *Current Opinion in Structural Biology*. https://doi.org/10.1016/S0959-440X(99)80012-8

Doig, A. J., & Baldwin, R. L. (1995). N- and C- capping preferences for all 20 amino acids in alpha-helical peptides. *Protein Science*, *4*(7), 1325–1336. https://doi.org/10.1002/pro.5560040708

Doig, A. J., Chakrabartty, A., Klingler, T. M., & Baldwin, R. L. (1994). Determination of Free Energies of N-Capping in α-Helices by Modification of the Lifson-Roig Helix-Coil Theory To Include N- and C-Capping. *Biochemistry*, *33*(11), 3396–3403. https://doi.org/10.1021/bi00177a033

Fersht, A. R. (1995). Optimization of rates of protein folding: the nucleation-condensation mechanism and its implications. *Proceedings of the National Academy of Sciences*, *92*(24), 10869–10873. https://doi.org/10.1073/pnas.92.24.10869

Fersht, A. R. (1997). Nucleation mechanisms in protein folding. *Current Opinion in Structural Biology*, *7*, 3–9. https://doi.org/10.1016/S0959-440X(97)80002-4

Fersht, A. R. (2000). Transition-state structure as a unifying basis in protein-folding mechanisms: Contact order, chain topology, stability, and the extended nucleus mechanism. *Proceedings of the National Academy of Sciences*, *97*(4), 1525–1529. https://doi.org/10.1073/pnas.97.4.1525

Fersht, A. R., & Sato, S. (2004). -Value analysis and the nature of protein-folding transition states. *Proceedings of the National Academy of Sciences*, *101*(21), 7976–7981. https://doi.org/10.1073/pnas.0402684101

Gelman, H., & Gruebele, M. (2014). Fast protein folding kinetics. *Quarterly Reviews of Biophysics*, *47*(2), 95–142. https://doi.org/10.1017/S003358351400002X

Gnanakaran, S., Nymeyer, H., Portman, J., Sanbonmatsu, K. Y., & García, A. E. (2003). Peptide folding simulations. *Current Opinion in Structural Biology*. 2: 168–174. https://doi.org/10.1016/S0959-440X(03)00040-X

Greenfield, N., & Fasman, G. D. (1969). Computed Circular Dichroism Spectra for the Evaluation of Protein Conformation. *Biochemistry*, *8*(10), 4108–4116. https://doi.org/10.1021/bi00838a031

Hałabis, A., Zmudzińska, W., Liwo, A., Ołdziej, S., Halabist, A., Zmudzińska, W., … Oldziej, S. (2012). Conformational Dynamics of the Trp-Cage Miniprotein at Its Folding Temperature. *Journal of Physical Chemistry B*, *116*(23), 6898–6907. https://doi.org/10.1021/jp212630y

Head-Gordon, T., & Brown, S. (2003). Minimalist models for protein folding and design. *Current Opinion in Structural Biology*. https://doi.org/10.1016/S0959-440X(03)00030-7

Hellinga, H. W. (1997). Rational protein design: combining theory and experiment. *Proceedings of the National Academy of Sciences of the United States of America*, *94*(19), 10015–10017. https://doi.org/10.1073/pnas.94.19.10015

Hu, Z., Tang, Y., Wang, H., Zhang, X., & Lei, M. (2008). Dynamics and cooperativity of Trp-cage folding. *Archives of Biochemistry and Biophysics*, *475*(2), 140–147. https://doi.org/10.1016/j.abb.2008.04.024

Hudáky, P., Stráner, P., Farkas, V., Váradi, G., Tóth, G., & Perczel, A. (2008). Cooperation between a salt bridge and the hydrophobic core triggers fold stabilization in a Trp-cage miniprotein. *Biochemistry*, *47*(3), 1007–1016. https://doi.org/10.1021/bi701371x

Huyghues-Despointes, B. M. P., Klingler, T. M., & Baldwin, R. L. (1995). Measuring the Strength of Side-Chain Hydrogen Bonds in Peptide Helices: The Gln.Asp (i, i + 4) Interaction. *Biochemistry*, *34*(41), 13267–13271. https://doi.org/10.1021/bi00041a001

Huyghues□Despointes, B. M. P., Scholtz, J. M., & Baldwin, R. L. (1993). Helical peptides with three pairs of Asp□Arg and Glu□Arg residues in different orientations and spacings. *Protein Science*, *2*(1), 80–85. https://doi.org/10.1002/pro.5560020108

Hwang, T. L., & Shaka, A. J. (1995). Water Suppression That Works. Excitation Sculpting Using Arbitrary Wave-Forms and Pulsed-Field Gradients. *Journal of Magnetic Resonance - Series A*. https://doi.org/10.1006/jmra.1995.1047

Jennings, P. A., & Wright, P. E. (1993). Formation of a molten globule intermediate early in the kinetic folding pathway of apomyoglobin. *Science*, *262*, 892–896. https://doi.org/10.1126/science.8235610

Juraszek, J., & Bolhuis, P. G. (2006). Sampling the multiple folding mechanisms of Trp-cage in explicit solvent. *Proceedings of the National Academy of Sciences*, *103*(43), 15859–15864. https://doi.org/10.1073/pnas.0606692103

Kannan, S., & Zacharias, M. (2009). Folding simulations of Trp-cage mini protein in explicit solvent using biasing potential replica-exchange molecular dynamics simulations. *Proteins: Structure, Function and Bioinformatics*, *76*(2), 448–460. https://doi.org/10.1002/prot.22359

Kelly, S. M., & Price, N. C. (1997). The application of circular dichroism to studies of protein folding and unfolding. *Biochimica et Biophysica Acta*, *1338*, 161–185. https://doi.org/10.1016/S0167-4838(96)00190-2

Kier, B. L., & Andersen, N. H. (2008). Probing the lower size limit for protein-like fold stability: Ten-residue microproteins with specific, rigid structures in water. *Journal of the American Chemical Society*, *130*(44), 14675–14683. https://doi.org/10.1021/ja804656h

Kier, B. L., Anderson, J. M., & Andersen, N. H. (2014). Circular Permutation of a WW Domain: Folding Still Occurs after Excising the Turn of the Folding-Nucleating Hairpin. *Journal of American Chemical Society*, *136*, 741–749. https://doi.org/10.1021/ja410824x

Kier, B. L., Byrne, A., Scian, M., Anderson, J. M., & Andersen, N. H. (2012). Folding landscape exploration by circular permutation and capping beta structures. In G. Kokotos, V. Constantinou, & J. Matsoukas (Eds.), *Peptides 2012, Proceeding of the 32nd EPS* (pp. 70–71).

Kier, B. L., Shu, I., Eidenschink, L. A., & Andersen, N. H. (2010). Stabilizing capping motif for beta-hairpins and sheets. *Proceedings of the National Academy of Sciences of the United States of America*, *107*(23), 10466–10471. https://doi.org/10.1073/pnas.0913534107

Kim, P. S. (1990). Intermediates In The Folding Reactions Of Small Proteins. *Annual Review of Biochemistry*, *59*(1), 631–660. https://doi.org/10.1146/annurev.biochem.59.1.631

Kim, P. S., & Baldwin, R. L. (1982). Specific Intermediates in the Folding Reactions of Small Proteins and the Mechanism of Protein Folding. *Annual Review of Biochemistry*, *51*(1), 459–489. https://doi.org/10.1146/annurev.bi.51.070182.002331

Kuhlman, B., & Baker, D. (2004). Exploring folding free energy landscapes using computational protein design. *Current Opinion in Structural Biology*. https://doi.org/10.1016/j.sbi.2004.01.002

Lambert, M. P., Barlow, A. K., Chromy, B. A., Edwards, C., Freed, R., Liosatos, M., … Klein, W. L. (1998). Diffusible, nonfibrillar ligands derived from AB 1-42 are potent central nervous system neurotoxins. *Proceedings of the National Academy of Sciences*. https://doi.org/10.1073/pnas.95.11.6448

Levinthal, C. (1968). ARE THERE PATHWAYS FOR PROTEIN FOLDING ? *Extrait Du Journal de Chimie Physique*, *65*(1).

Lifson, S., & Roig, A. (1961). On the Theory of Helix—Coil Transition in Polypeptides. *The Journal of Chemical Physics*, *34*(6), 1963–1974. https://doi.org/10.1063/1.1731802

Lindorff-Larsen, K., Piana, S., Dror, R. O., & Shaw, D. E. (2011). How fast-folding proteins fold. *Science*, *334*(6055), 517–520. https://doi.org/10.1126/science.1208351

Meuzelaar, H., Marino, K. A. K., Huerta-Viga, A., Panman, M. R., Smeenk, L. E. J., Kettelarij, A. J., … Woutersen, S. (2013). Folding dynamics of the trp-cage miniprotein: Evidence for a native-like intermediate from combined time-resolved vibrational spectroscopy and molecular dynamics simulations. *Journal of Physical Chemistry B*, *117*(39), 11490–11501. https://doi.org/10.1021/jp404714c

Mok, K. H., Kuhn, L. T., Goez, M., Day, I. J., Lin, J. C., Andersen, N. H., & Hore, P. J. (2007). A pre-existing hydrophobic collapse in the unfolded state of an ultrafast folding protein. *Nature*, *447*(7140), 106–109. https://doi.org/10.1038/nature05728

Naganathan, A. N. (2012). Predictions from an ising-like statistical mechanical model on the dynamic and thermodynamic effects of protein surface electrostatics. *Journal of Chemical Theory and Computation*, *8*(11), 4646–4656. https://doi.org/10.1021/ct300676w

Nauli, S., Kuhlman, B., & Baker, D. (2001). Computer-based redesign of a protein folding pathway. *Nature Structural Biology*, *8*(7), 602–605. https://doi.org/10.1038/89638

Neidigh, J. W., Fesinmeyer, R. M., & Andersen, N. H. (2002). Designing a 20-residue protein. *Nature Structural Biology*, *9*(6), 425–430. https://doi.org/10.1038/nsb798

Neira, J. L., Davis, B., Ladurner, A. G., Buckle, A. M., de Prat Gay, G., & Fersht, A. R. (1996). Towards the complete structural characterization of a protein folding pathway. *Folding and Design*, *1*(3), 189–208. https://doi.org/10.1016/S1359-0278(96)00031-4

Olsen, K. A., Fesinmeyer, R. M., Stewart, J. M., & Andersen, N. H. (2005). Hairpin folding rates reflect mutations within and remote from the turn region. *Proceedings of the National Academy of Sciences*, *102*(43), 15483–15487. https://doi.org/10.1073/pnas.0504392102

Onuchic, J. N., Luthey-Schulten, Z., & Wolynes, P. G. (1997). THEORY OF PROTEIN FOLDING: The Energy Landscape Perspective. *Annual Review of Physical Chemistry*, *48*, 545–600. https://doi.org/0066-426X/97/1001-0545$08.00

Onuchic, J. N., & Wolynes, P. G. (2004). Theory of protein folding. *Current Opinion in Structural Biology*. 70-75. https://doi.org/10.1016/j.sbi.2004.01.009

Pande, V. S., Grosberg, A. Y., Tanaka, T., & Rokhsar, D. S. (1998). Pathways for protein folding: Is a new view needed? *Current Opinion in Structural Biology*. https://doi.org/10.1016/S0959-440X(98)80012-2

Piette, L. H., & Anderson, W. A. (1959). Potential Energy Barrier Determinations for Some Alkyl Nitrites by Nuclear Magnetic Resonance Potential Energy Barrier Determinations for Some Alkyl Nitrites by N uc1ear Magnetic Resonance. *The Journal of Chemical Physics*, *30*(4), 1878–1341. https://doi.org/10.1063/1.1742895

Plaxco, K. W., Simons, K. T., & Baker, D. (1998). Contact order, transition state placement and the refolding rates of single domain proteins. *Journal of Molecular Biology*, *277*(4), 985–994. https://doi.org/10.1006/jmbi.1998.1645

Ptitsyn, O. B., Pain, R. H., Semisotnov, G. V, Zerovnik, E., & Razgulyaev, O. I. (1990). Evidence for a molten globule state as a general intermediate in protein folding. *FEBS Letters*, *262*(1), 20–24. https://doi.org/10.1016/0014-5793(90)80143-7

Qiu, L., Pabit, S. A., Roitberg, A. E., & Hagen, S. J. (2002). Smaller and faster: The 20-residue Trp-cage protein folds in 4 μs. *Journal of the American Chemical Society*, *124*(44), 12952–12953. https://doi.org/10.1021/ja0279141

Rodriguez-Granillo, A., Annavarapu, S., Zhang, L., Koder, R. L., & Nanda, V. (2011). Computational design of thermostabilizing D-amino acid substitutions. *Journal of the American Chemical Society*, *133*(46), 18750–18759. https://doi.org/10.1021/ja205609c

Rohl, C. A., Chakrabartty, A., & Baldwin, R. L. (1996). Helix propagation and N-cap propensities of the amino acids measured in alanine-based peptides in 40 volume percent trifluoroethanol. *Protein Science*, *5*(12), 2623–2637. https://doi.org/10.1002/pro.5560051225

Rovó, P., Farkas, V., Hegyi, O., Szolomájer-Csikós, O., Tóth, G. K., & Perczel, A. (2011). Cooperativity network of Trp-cage miniproteins: Probing salt-bridges. *Journal of Peptide Science*, *17*(9), 610–619. https://doi.org/10.1002/psc.1377

Schneider, J. P., & DeGrado, W. F. (1998). The Design of Efficient α-Helical C-Capping Auxiliaries. *Journal of the American Chemical Society*, *120*(12), 2764–2767. https://doi.org/10.1021/ja9726771

Scian, M., Lin, J. C., Le Trong, I., Makhatadze, G. I., Stenkamp, R. E., & Andersen, N. H. (2012). Crystal and NMR structures of a Trp-cage mini-protein benchmark for computational fold prediction. *Proceedings of the National Academy of Sciences*, *109*(31), 12521–12525. https://doi.org/10.1073/pnas.1121421109

Scian, M., Shu, I., Olsen, K. A., Hassam, K., & Andersen, N. H. (2013). Mutational effects on the folding dynamics of a minimized hairpin. *Biochemistry*, *52*(15), 2556–2564. https://doi.org/10.1021/bi400146c

Shalongo, W., & Stellwagen, E. (1995). Incorporation of pairwise interactions into the Lifson-Roig model for helix prediction. *Protein Science*, *4*(6), 1161–1166. https://doi.org/10.1002/pro.5560040614

Simmerling, C., Strockbine, B., & Roitberg, A. E. (2002). All-atom structure prediction and folding simulations of a stable protein. *Journal of the American Chemical Society*, *124*(38), 11258–11259. https://doi.org/10.1021/ja0273851

Snow, C. D., Zagrovic, B., & Pande, V. S. (2002). The Trp cage: Folding kinetics and unfolded state topology via molecular dynamics simulations. *Journal of the American Chemical Society*, *124*(49), 14548–14549. https://doi.org/10.1021/ja028604l

Song, K., Stewart, J. M., Fesinmeyer, R. M., Andersen, N. H., & Simmerling, C. (2008). Structural insights for designed alanine-rich helices: Comparing NMR helicity measures and conformational ensembles from molecular dynamics simulation. *Biopolymers*, *89*(9), 747–760. https://doi.org/10.1002/bip.21004

Stapley, B. J., & Doig, A. J. (1997). Hydrogen bonding interactions between glutamine and asparagine in alpha-helical peptides. *Journal of Molecular Biology*, *272*(3), 465–473. https://doi.org/10.1006/jmbi.1997.1262

Stewart, J. M. (2009). *The Use of 13C Carbonyl Labeled Residues to Develop and Refine Site-Specific NMR Secondary Structure Analysis Techniques*. University of Washington.

Stewart, J. M., Lin, J. C., & Andersen, N. H. (2008). Lysine and arginine residues do not increase the helicity of alanine-rich peptide helices. *Chemical Communications*, (39), 4765–7. https://doi.org/10.1039/b807101b

Tripathi, S., Makhatadze, G. I., & Garcia, A. E. (2013). Backtracking due to residual structure in the unfolded state changes the folding of the third fibronectin type III domain from tenascin-C. *Journal of Physical Chemistry B*, *117*(3), 800–810. https://doi.org/10.1021/jp310046k

Uversky, V. N., & Fink, A. L. (2002). The chicken-egg scenario of protein folding revisited. *FEBS Letters*, *515*, 79–83. https://doi.org/10.1021/jp407074y

Williams, D. V., Barua, B., & Andersen, N. H. (2008). Hyperstable miniproteins: additive effects of d- and l-Ala mutations. *Organic & Biomolecular Chemistry*, *6*(23), 4287. https://doi.org/10.1039/b814314e

Williams, D. V., Byrne, A., Stewart, J., & Andersen, N. H. (2011). Optimal salt bridge for Trp-cage stabilization. *Biochemistry*, *50*(7), 1143–1152. https://doi.org/10.1021/bi101555y

Wolynes, P. G., Luthey-Schulten, Z. A., & Onuchic, J. N. (1996). Fast-folding experiments and the topography of protein folding energy landscapes. *Chemistry & Biology*, *3*(6), 425–32. https://doi.org/10.1016/S1074-5521(96)90090-3

Wolynes, P. G., Onuchic, J. N., & Thirumalai, D. (1995). Navigating the folding routes. *Science*. https://doi.org/10.1126/science.7886447

Wright, P. E., Dyson, H. J., & Lerner, R. A. (1988). Conformation of peptide fragments of proteins in aqueous solution: implications for initiation of protein folding. *Biochemistry*, *27*(19), 7167–7175. https://doi.org/10.1021/bi00419a001

Xia, X., Zhang, S., Huang, B., Zhou, Y., & Sun, Z. (2008). Efficient and reproducible folding simulations of the Trp-cage protein with multiscale molecular dynamics. *Chinese Science Bulletin*, *53*(11), 1699–1707. https://doi.org/10.1007/s11434-008-0186-8

Zhou, C. Y., Jiang, F., & Wu, Y. D. (2015). Folding thermodynamics and mechanism of five trp-cage variants from replica-exchange MD simulations with RSFF2 force field. *Journal of Chemical Theory and Computation*. https://doi.org/10.1021/acs.jctc.5b00581

Zhou, R. (2003). Trp-cage: folding free energy landscape in explicit water. *Proceedings of the National Academy of Sciences of the United States of America*, *100*, 13280–13285. https://doi.org/10.1073/pnas.2233312100

APPENDIX A: CHEMICAL SHIFT ASSIGNMENT TABLES

Chemical shift assignments were collected in 50 mM potassium phosphate buffer. Isolated commas indicate no data while dashes indicate not applicable.

TC15b

DAYAQWLADaGPASGRPPPS

300K pH 6.5

#	Res	HN	HA	HB	HG	HD	HE	HZ	HH
1	Asp		4.316	3.181, 3.005	-----		-----	-----	-----
2	Ala	8.987	4.284	1.516	-----	-----	-----	-----	-----
3	Tyr	8.751	4.053	3.149,	-----			-----	
4	Ala	8.308	4.112	1.592	-----	-----	-----	-----	-----
5	Gln	8.004	4.013	2.215, 2.161	2.431,	-----	,	-----	-----
6	Trp	8.083	4.216	3.147, 3.546	-----	7.003	9.672, 7.007	7.188, 7.123	7.222
7	Leu	8.438	3.341	1.844, 1.390	1.612	0.963, 0.878	-----	-----	-----
8	Ala	8.119	4.036	1.484	-----	-----	-----	-----	-----
9	Asp	7.796	4.571	2.941, 2.781	-----		-----	-----	-----
10	dAla	7.39	4.298	1.264	-----	-----	-----	-----	-----
11	Gly	8.438	0.719, 3.055	-----	-----	-----	-----	-----	-----
12	Pro	-----	4.595	2.530, 2.054	2.170,	3.761, 3.463	-----	-----	-----
13	Ala	7.409	4.336	1.402	-----	-----	-----	-----	-----
14	Ser	8.122	4.113	3.876, 3.494		-----	-----	-----	-----
15	Gly	7.815	4.268, 3.815	-----	-----	-----	-----	-----	-----
16	Arg	8.083	5.024	1.867, 1.783	1.664,	3.306, 3.247	7.588	-----	, , ,
17	Pro	-----	4.748	2.320, 1.784	1.999,	3.857, 3.663	-----	-----	-----
18	Pro	-----	2.448	1.309, 0.291	1.727, 1.626	3.488, 2.452	-----	-----	-----
19	Pro	-----	4.336	2.195, 1.972	1.814, 1.810	3.123, 2.916	-----	-----	-----
20	Ser	7.873	4.2	3.794, 3.793		-----	-----	-----	-----

TC15b

DAYAQWLADaGPASGRPPPS

300K pH 2.5

#	Res	HN	Hα	Hβ	Hγ	Hδ	Hε	Hζ	Hη
1	Asp		4.399	3.366, 3.180	-----		-----	-----	-----
2	Ala	9.045	4.277	1.52	-----	-----	-----	-----	-----
3	Tyr		4.039	3.103,	-----			-----	
4	Ala	8.118	4.103	1.584	-----	-----	-----	-----	-----
5	Gln	7.908	4.069	2.204, 2.159	2.489, 2.419	-----	,	-----	-----
6	Trp		4.203	3.168, 3.541	-----		, 7.027	7.216, 7.110	7.206
7	Leu	8.474	3.335	1.794, 1.439	1.595	0.949, 0.881	-----	-----	-----
8	Ala	8.096	4.063	1.479	-----	-----	-----	-----	-----
9	Asp	7.661	4.658	3.077, 2.906	-----		-----	-----	-----
10	dAla	7.392	4.312	1.281	-----	-----	-----	-----	-----
11	Gly		0.952, 2.958	-----	-----	-----	-----	-----	-----
12	Pro	-----	4.561	2.508, 2.044	2.144,	3.709, 3.357	-----	-----	-----
13	Ala	7.443	4.317	1.403	-----	-----	-----	-----	-----
14	Ser	8.072	4.187	3.919, 3.550		-----	-----	-----	-----
15	Gly	7.851	4.248, 3.834	-----	-----	-----	-----	-----	-----
16	Arg	8.027	4.937	1.934, 1.818	1.731, 1.677	3.271, 3.273	7.428	-----	, , ,
17	Pro	-----	4.682	2.281, 1.786	2.008, 1.978	3.856, 3.644	-----	-----	-----
18	Pro	-----	2.58	1.328, 0.458	1.742, 1.648	3.478, 2.579	-----	-----	-----
19	Pro	-----	4.372	2.228, 1.942	1.824, 1.827	3.145, 2.924	-----	-----	-----
20	Ser		4.382	3.958, 3.823		-----	-----	-----	-----

TC15b D1N D9Abu

NAYAQWLA(Abu)aGPASGRPPPS

300K pH 6.5

#	Res	HN	Hα	Hβ	Hγ	Hδ	Hε	Hζ	Hη
1	Asn		4.186	3.168, 3.058	-----	,	-----	-----	-----
2	Ala		4.254	1.483	-----	-----	-----	-----	-----
3	Tyr	8.637	4.13	3.114, 3.114	-----			-----	
4	Ala	8.221	4.118	1.545	-----	-----	-----	-----	-----
5	Gln	8.031	4.13	2.179, 2.176	2.523, 2.426	-----	,	-----	-----
6	Trp	8.044	4.284	3.194, 3.521	-----	7.067	9.647,	,	
7	Leu	8.434	3.409	1.771, 1.432	1.588	0.933, 0.851	-----	-----	-----
8	Ala	7.957	4.094	1.499	-----	-----	-----	-----	-----
9	Xaa		,	,	,	,	,	,	,
10	dAla	7.437	4.332	1.272	-----	-----	-----	-----	-----
11	Gly	8.117	3.068, 1.274	-----	-----	-----	-----	-----	-----
12	Pro	-----	4.557	2.484, 2.042	2.131,	3.701, 3.378	-----	-----	-----
13	Ala	7.539	4.317	1.403	-----	-----	-----	-----	-----
14	Ser	8.053	4.218	3.898, 3.594		-----	-----	-----	-----
15	Gly	7.893	4.198, 3.867	-----	-----	-----	-----	-----	-----
16	Arg	7.951	4.829	1.950, 1.771	1.690,	3.249, 3.247	7.354	-----	, , ,
17	Pro	-----	4.676	2.264, 1.800	1.995,	3.835, 3.622	-----	-----	-----
18	Pro	-----	2.823	1.428, 0.744	1.789, 1.696	3.515, 3.484	-----	-----	-----
19	Pro	-----	4.34	2.194, 1.954	1.850, 1.848	3.151, 2.990	-----	-----	-----
20	Ser	7.802	4.181	, 3.790		-----	-----	-----	-----

TC15b D1N D9Abu

NAYAQWLA(Abu)aGPASGRPPPS

300K pH 2.5

#	Res	HN	Hα	Hβ	Hγ	Hδ	Hε	Hζ	Hη
1	Asn		4.38	3.312, 3.161	-----	,	-----	-----	-----
2	Ala	9.01	4.281	1.48	-----	-----	-----	-----	-----
3	Tyr	8.573	4.138	3.095, 3.095	-----			-----	
4	Ala	8.194	4.118	1.535	-----	-----	-----	-----	-----
5	Gln	7.961	4.132	2.170, 2.167	2.508, 2.421	-----	,	-----	-----
6	Trp	8.026	4.295	3.190, 3.503	-----	7.077	9.677,	,	
7	Leu	8.375	3.441	1.751, 1.427	1.567	0.926, 0.844	-----	-----	-----
8	Ala	7.947	4.095	1.49	-----	-----	-----	-----	-----
9	Xaa		,	,	,	,	,	,	,
10	dAla	7.471	4.33	1.273	-----	-----	-----	-----	-----
11	Gly	8.104	3.101, 1.424	-----	-----	-----	-----	-----	-----
12	Pro	-----	4.541	2.471, 2.033	2.118,	3.689, 3.371	-----	-----	-----
13	Ala	7.582	4.311	1.397	-----	-----	-----	-----	-----
14	Ser	8.047	4.226	3.895, 3.602		-----	-----	-----	-----
15	Gly	7.909	4.179, 3.867	-----	-----	-----	-----	-----	-----
16	Arg	7.949	4.811	1.946, 1.761	1.685,	3.240, 3.239	7.276	-----	, , ,
17	Pro	-----	4.669	2.262, 1.797	1.995,	3.834, 3.618	-----	-----	-----
18	Pro	-----	2.937	1.425, 0.826	1.791, 1.713	3.529, 3.483	-----	-----	-----
19	Pro	-----	4.368	2.214, 1.930	1.849, 1.848	3.193, 3.023	-----	-----	-----
20	Ser	8.195	4.399	3.924, 3.827		-----	-----	-----	-----

TC15b D9Abu

DAYAQWLA(Abu)aGPASGRPPPS

300K pH 6.5

#	Res	HN	Hα	Hβ	Hγ	Hδ	Hε	Hζ	Hη
1	Asp		4.303	3.163, 2.997	-----		-----	-----	-----
2	Ala	8.983	4.256	1.498	-----	-----	-----	-----	-----
3	Tyr	8.667	4.092	3.151,	-----			-----	
4	Ala	8.318	4.121	1.597	-----	-----	-----	-----	-----
5	Gln	8.012	4.123	2.217, 2.181	2.551, 2.445	-----	,	-----	-----
6	Trp	8.084	4.262	3.185, 3.540	-----	7.054	9.620, 7.086	7.205, 7.086	7.205
7	Leu	8.518	3.346	1.788, 1.425	1.582	0.939, 0.852	-----	-----	-----
8	Ala	7.993	4.086	1.507	-----	-----	-----	-----	-----
9	Xaa		,	,	,	,	,	,	,
10	dAla	7.401	4.337	1.262	-----	-----	-----	-----	-----
11	Gly	8.131	1.054, 3.015	-----	-----	-----	-----	-----	-----
12	Pro	-----	4.567	2.505, 2.053	2.147,	3.718, 3.386	-----	-----	-----
13	Ala	7.496	4.319	1.404	-----	-----	-----	-----	-----
14	Ser	8.056	4.202	3.895, 3.566		-----	-----	-----	-----
15	Gly	7.883	4.209, 3.852	-----	-----	-----	-----	-----	-----
16	Arg	7.957	4.849	1.963, 1.774	1.675, 1.681	3.248,	7.32	-----	, , ,
17	Pro	-----	4.69	2.266, 1.798	1.998, 1.995	3.846, 3.631	-----	-----	-----
18	Pro	-----	2.672	1.390, 0.617	1.757, 1.672	3.485,	-----	-----	-----
19	Pro	-----	4.317	2.198, 1.949	1.832, 1.820	3.103, 2.963	-----	-----	-----
20	Ser	7.824	4.177	3.788,		-----	-----	-----	-----

TC15b D9Abu

DAYAQWLA(Abu)aGPASGRPPPS

300K pH 2.5

#	Res	HN	Hα	Hβ	Hγ	Hδ	Hε	Hζ	Hη
1	Asp		4.392	3.333, 3.169	-----		-----	-----	-----
2	Ala	9.022	4.279	1.5	-----	-----	-----	-----	-----
3	Tyr		4.094	3.104,	-----			-----	
4	Ala	8.119	4.108	1.562	-----	-----	-----	-----	-----
5	Gln	7.93	4.13	2.204, 2.165	2.524, 2.438	-----	,	-----	-----
6	Trp		4.264	3.200, 3.525	-----		, 7.100	7.216, 7.100	7.216
7	Leu	8.436	3.382	1.765, 1.424	1.568	0.935, 0.851	-----	-----	-----
8	Ala	7.953	4.086	1.499	-----	-----	-----	-----	-----
9	Xaa		,	,	,	,	,	,	,
10	dAla	7.431	4.327	1.269	-----	-----	-----	-----	-----
11	Gly	8.12	1.244, 3.059	-----	-----	-----	-----	-----	-----
12	Pro	-----	4.561	2.490, 2.047	2.136,	3.703, 3.384	-----	-----	-----
13	Ala	7.532	4.306	1.402	-----	-----	-----	-----	-----
14	Ser	8.058	4.215	3.900, 3.577		-----	-----	-----	-----
15	Gly	7.889	4.195, 3.859	-----	-----	-----	-----	-----	-----
16	Arg	7.968	4.829	1.951, 1.766	, 1.687	3.240,	7.477	-----	, , ,
17	Pro	-----	4.681	2.263, 1.793	2.002, 1.998	3.843, 3.623	-----	-----	-----
18	Pro	-----	2.795	1.389, 0.708	1.770, 1.700	3.511, 3.481	-----	-----	-----
19	Pro	-----	4.368	2.225, 1.935	1.836, 1.834	3.163, 2.985	-----	-----	-----
20	Ser	8.235	4.391	3.952, 3.824		-----	-----	-----	-----

TC15b D9S P12W

DAYAQWLASaGWASGRPPPS

300K pH 6.5

#	Res	HN	Hα	Hβ	Hγ	Hδ	Hε	Hζ	Hη
1	Asp		4.283	3.165, 2.991	-----		-----	-----	-----
2	Ala	8.983	4.233	1.489	-----	-----	-----	-----	-----
3	Tyr	8.737	3.98	3.128,	-----	7.062	6.803	-----	
4	Ala	8.355	4.104	1.607	-----	-----	-----	-----	-----
5	Gln	8.004	4.109	2.188, 2.189	2.539, 2.439	-----	7.575, 6.982	-----	-----
6	Trp	8.208	4.108	3.085, 3.469	-----	6.845	9.480, 6.817	5.967, 6.817	6.021
7	Leu	8.705	3.202	1.742, 1.450	1.528	0.935, 0.870	-----	-----	-----
8	Ala	8.155	4.078	1.486	-----	-----	-----	-----	-----
9	Ser	7.535	4.395	3.980,		-----	-----	-----	-----
10	dAla	7.31	4.352	1.249	-----	-----	-----	-----	-----
11	Gly	7.798	0.415, 2.973	-----	-----	-----	-----	-----	-----
12	Trp	8.835	4.62	3.546, 3.193	-----	7.594	10.455, 7.872	7.603, 7.212	7.33
13	Ala	7.848	4.362	1.466	-----	-----	-----	-----	-----
14	Ser	7.881	4.205	3.888, 3.543		-----	-----	-----	-----
15	Gly	7.944	4.336, 3.896	-----	-----	-----	-----	-----	-----
16	Arg	7.904	4.926	1.880, 1.630	1.705,	3.235, 3.238	7.28	-----	, , ,
17	Pro	-----	3.991	1.743, 2.267	2.036, 1.908	3.787, 3.579	-----	-----	-----
18	Pro	-----	2.136	1.149, -0.125	1.569, 1.231	3.168, 2.412	-----	-----	-----
19	Pro	-----	4.27	1.939, 2.156	1.766,	2.858, 3.057	-----	-----	-----
20	Ser	7.785	4.161	3.776,		-----	-----	-----	-----

TC15b D9S P12W

DAYAQWLASaGWASGRPPPS

300K pH 2.5

#	Res	HN	Hα	Hβ	Hγ	Hδ	Hε	Hζ	Hη
1	Asp		4.386	3.360, 3.185	-----		-----	-----	-----
2	Ala	9.046	4.256	1.497	-----	-----	-----	-----	-----
3	Tyr		3.962	3.083, 3.083	-----	7.066	6.812	-----	
4	Ala		4.096	1.589	-----	-----	-----	-----	-----
5	Gln	7.908	4.117	2.210, 2.210	2.529, 2.440	-----	,	-----	-----
6	Trp		4.109	3.080, 3.455	-----		, 6.818	5.998, 6.817	6.025
7	Leu		3.222	1.734, 1.451	1.536	0.931, 0.869	-----	-----	-----
8	Ala	8.119	4.072	1.489	-----	-----	-----	-----	-----
9	Ser	7.544	4.393	3.972,		-----	-----	-----	-----
10	dAla	7.309	4.347	1.253	-----	-----	-----	-----	-----
11	Gly	7.801	0.459, 2.973	-----	-----	-----	-----	-----	-----
12	Trp			3.543, 3.216	-----		, 7.868	7.599, 7.206	7.322
13	Ala	7.837	4.345	1.46	-----	-----	-----	-----	-----
14	Ser		4.211	3.897, 3.572		-----	-----	-----	-----
15	Gly		4.324, 3.889	-----	-----	-----	-----	-----	-----
16	Arg	7.897	4.914	1.873, 1.629	1.703,	3.231,		-----	, , ,
17	Pro	-----	3.988	1.739, 2.246	2.032, 1.907	3.777, 3.571	-----	-----	-----
18	Pro	-----	2.194	1.130, -0.111	1.572, 1.257	3.177, 2.439	-----	-----	-----
19	Pro	-----	4.32	1.919, 2.175	1.771,	2.855, 3.088	-----	-----	-----
20	Ser			,		-----	-----	-----	-----

TC15b P12W

DAYAQWLADaGWASGRPPPS

300K pH 6.5

#	Res	HN	Hα	Hβ	Hγ	Hδ	Hε	Hζ	Hη
1	Asp		4.27	3.139, 2.965	-----		-----	-----	-----
2	Ala	8.95	4.258	1.486	-----	-----	-----	-----	-----
3	Tyr	8.721	3.979	3.136, 3.082	-----	7.034	6.783	-----	
4	Ala	8.28	4.081	1.57	-----	-----	-----	-----	-----
5	Gln	8.004	3.962	2.193, 2.124	2.397,	-----	7.770, 6.926	-----	-----
6	Trp	7.964	4.121	3.040, 3.433	-----	6.787	9.537, 6.811	5.811, 6.813	5.941
7	Leu	8.331	3.259	1.814, 1.336	1.559	0.940, 0.835	-----	-----	-----
8	Ala	8.076	4.008	1.465	-----	-----	-----	-----	-----
9	Asp	7.86	4.494	2.692, 2.837	-----		-----	-----	-----
10	dAla	7.341	4.283	1.253	-----	-----	-----	-----	-----
11	Gly	8.33	0.338, 2.977	-----	-----	-----	-----	-----	-----
12	Trp	8.861	4.625	3.569, 3.176	-----	7.605	10.456, 7.927	7.630, 7.241	7.331
13	Ala	7.825	4.423	1.459	-----	-----	-----	-----	-----
14	Ser	8.279	4.02	3.921,		-----	-----	-----	-----
15	Gly	7.897	4.370, 3.847	-----	-----	-----	-----	-----	-----
16	Arg	8.115	5.09	1.745, 1.576	1.836,	3.261, 3.185	7.558	-----	, , ,
17	Pro	-----	4.207	1.767, 2.367	2.055, 1.932	3.840, 3.628	-----	-----	-----
18	Pro	-----	2.081	1.091, -0.335	1.564, 1.564	3.212, 2.397	-----	-----	-----
19	Pro	-----	4.291	1.955, 2.140	1.778, 1.731	2.841, 3.070	-----	-----	-----
20	Ser	7.78	4.155	3.768,		-----	-----	-----	-----

TC15b P12W

DAYAQWLADaGWASGRPPPS

300K pH 2.5

#	Res	HN	Hα	Hβ	Hγ	Hδ	Hε	Hζ	Hη
1	Asp		4.383	3.361, 3.174	-----		-----	-----	-----
2	Ala	9.034	4.254	1.498	-----	-----	-----	-----	-----
3	Tyr		3.952	3.073,	-----			-----	
4	Ala		4.09	1.577	-----	-----	-----	-----	-----
5	Gln		4.037	2.180, 2.132	2.457, 2.405	-----	,	-----	-----
6	Trp		4.089	3.054, 3.450	-----		, 6.823	5.932, 6.818	6.033
7	Leu		3.233	1.750, 1.414	1.532	0.932, 0.868	-----	-----	-----
8	Ala		4.053	1.461	-----	-----	-----	-----	-----
9	Asp		4.611	3.192, 2.862	-----		-----	-----	-----
10	dAla	7.342	4.307	1.265	-----	-----	-----	-----	-----
11	Gly		0.427, 2.968	-----	-----	-----	-----	-----	-----
12	Trp			3.555, 3.212	-----		,	7.609, 7.223	7.331
13	Ala		4.359	1.459	-----	-----	-----	-----	-----
14	Ser		4.199	3.914,		-----	-----	-----	-----
15	Gly		4.351, 3.887	-----	-----	-----	-----	-----	-----
16	Arg	7.95	4.969	1.735, 1.626	1.852, 1.732	3.238,		-----	, , ,
17	Pro	-----	4.006	2.258, 1.735	2.038, 1.914	3.785, 3.582	-----	-----	-----
18	Pro	-----	2.184	1.118, -0.152	1.578, 1.264	3.186, 2.440	-----	-----	-----
19	Pro	-----	4.327	1.922, 2.174	1.765, 1.768	2.846, 3.099	-----	-----	-----
20	Ser			,		-----	-----	-----	-----

TC15b P12W P19A

DAYAQWLADaGWASGRPPAS

300K pH 6.5

#	Res	HN	Hα	Hβ	Hγ	Hδ	Hε	Hζ	Hη
1	Asp		4.262	3.058, 2.954	-----		-----	-----	-----
2	Ala	8.883	4.252	1.44	-----	-----	-----	-----	-----
3	Tyr	8.439	4.239	3.090,	-----	7.063	6.791	-----	
4	Ala	8.17	4.058	1.502	-----	-----	-----	-----	-----
5	Gln	8.062	3.985	2.105, 2.135	2.378,	-----	7.751, 6.899	-----	-----
6	Trp	8.014	4.258	3.149, 3.471	-----	6.918	9.578, 7.032	6.226, 6.894	6.401
7	Leu	8.239	3.396	1.702, 1.353	1.468	0.846, 0.774	-----	-----	-----
8	Ala	7.969	4.023	1.442	-----	-----	-----	-----	-----
9	Asp	7.909	4.533	2.682, 2.775	-----		-----	-----	-----
10	dAla	7.393	4.312	1.242	-----	-----	-----	-----	-----
11	Gly	8.156	1.243, 3.029	-----	-----	-----	-----	-----	-----
12	Trp	8.429	4.696	3.467, 3.173	-----	7.498	10.364, 7.783	7.546, 7.185	7.284
13	Ala	7.867	4.306	1.386	-----	-----	-----	-----	-----
14	Ser	8.014	4.311	3.869, 3.640		-----	-----	-----	-----
15	Gly	7.861	4.246, 3.833	-----	-----	-----	-----	-----	-----
16	Arg	8.088	4.578	1.756, 1.592	1.711,	3.192,	7.304	-----	, , ,
17	Pro	-----	3.751	1.577, 1.577	1.801, 1.759	3.392, 3.293	-----	-----	-----
18	Pro	-----	3.457	1.586, 1.690	1.690, 1.365	3.133, 2.884	-----	-----	-----
19	Ala	7.687	4.236	1.321	-----	-----	-----	-----	-----
20	Ser	7.79	4.219	3.792,		-----	-----	-----	-----

TC15b P19A

DAYAQWLADaGPASGRPPAS

300K pH 2.5

#	Res	HN	HA	HB	HG	HD	HE	HZ	HH
1	Asp		4.257	3.018, 2.938	-----		-----	-----	-----
2	Ala	8.858	4.264	1.427	-----	-----	-----	-----	-----
3	Tyr	8.39	4.34	3.101,	-----	7.108	6.831	-----	
4	Ala	8.167	4.079	1.471	-----	-----	-----	-----	-----
5	Gln	8.094	4.035	2.111,	,	-----	,	-----	-----
6	Trp	8.07	4.41	3.256, 3.510	-----	7.153	9.953, 7.305	7.305, 7.131	7.208
7	Leu	8.235	3.633	1.694, 1.414	1.478	0.847, 0.801	-----	-----	-----
8	Ala	7.99	4.061	1.442	-----	-----	-----	-----	-----
9	Asp	7.928	4.554	2.774, 2.703	-----		-----	-----	-----
10	dAla	7.566	4.319	1.302	-----	-----	-----	-----	-----
11	Gly	8.229	2.137, 3.164	-----	-----	-----	-----	-----	-----
12	Pro	-----	4.491	2.372, 1.998	3.611, 3.354	2.057,	-----	-----	-----
13	Ala	7.89	4.309	1.393	-----	-----	-----	-----	-----
14	Ser	7.885	4.254	3.843,		-----	-----	-----	-----
15	Gly	8.013	4.116, 3.936	-----	-----	-----	-----	-----	-----
16	Arg	8.03	4.616	1.718, 1.572	1.795, 1.648	3.198,	7.296	-----	, , ,
17	Pro	-----	4.476	1.792, 2.103	1.947,	3.543, 3.755	-----	-----	-----
18	Pro	-----	3.741	1.685, 1.725	1.851, 1.851	3.450,	-----	-----	-----
19	Ala	7.809	4.264	1.348	-----	-----	-----	-----	-----
20	Ser	7.815	4.237	3.810,		-----	-----	-----	-----

TC15b R16Nva

DAYAQWLADaGPASG(Nva)PPAS

300K pH 6.5

#	Res	HN	Hα	Hβ	Hγ	Hδ	Hε	Hζ	Hη
1	Asp		4.304	3.169, 2.999	-----		-----	-----	-----
2	Ala	8.965	4.254	1.497	-----	-----	-----	-----	-----
3	Tyr	8.639	4.088	3.137,	-----			-----	
4	Ala	8.249	4.106	1.581	-----	-----	-----	-----	-----
5	Gln	8.048	4.017	2.186,	2.442,	-----	,	-----	-----
6	Trp	8.109	4.302	3.197, 3.524	-----	7.134	9.602, 7.218	, 7.082	7.082
7	Leu	8.426	3.347	1.784, 1.429	1.586	0.930, 0.863	-----	-----	-----
8	Ala	8.086	4.04	1.478	-----	-----	-----	-----	-----
9	Asp	7.825	4.602	2.895, 2.779	-----		-----	-----	-----
10	dAla	7.387	4.346	1.277	-----	-----	-----	-----	-----
11	Gly	8.265	1.201, 2.923	-----	-----	-----	-----	-----	-----
12	Pro	-----	4.542	2.493, 2.034	2.119,	3.665, 3.261	-----	-----	-----
13	Ala	7.477	4.306	1.408	-----	-----	-----	-----	-----
14	Ser	8.018	4.233	3.936, 3.625		-----	-----	-----	-----
15	Gly	7.83	4.204, 3.846	-----	-----	-----	-----	-----	-----
16	Xaa		,	,	,	,	,	,	,
17	Pro	-----	4.642	2.218, 1.784	1.995, 1.996	3.852, 3.667	-----	-----	-----
18	Pro	-----	2.705	1.382, 0.626	1.764, 1.676	3.504, 3.475	-----	-----	-----
19	Pro	-----	4.325	2.210, 1.931	1.821,	3.124, 2.936	-----	-----	-----
20	Ser	7.85	4.185	3.784,		-----	-----	-----	-----

TC15b R16Nva

DAYAQWLADaGPASG(Nva)PPAS

300K pH 2.5

#	Res	HN	Hα	Hβ	Hγ	Hδ	Hε	Hζ	Hη
1	Asp		4.4	3.346, 3.190	-----		-----	-----	-----
2	Ala	9.022	4.284	1.52	-----	-----	-----	-----	-----
3	Tyr		4.054	3.093,	-----			-----	
4	Ala	8.121	4.104	1.572	-----	-----	-----	-----	-----
5	Gln	7.896	4.069	2.203,	2.443,	-----	,	-----	-----
6	Trp		4.242	3.198, 3.520	-----		,	,	
7	Leu	8.471	3.342	1.766, 1.437	1.578	0.934, 0.871	-----	-----	-----
8	Ala	8.083	4.066	1.475	-----	-----	-----	-----	-----
9	Asp	7.685	4.664	3.062, 2.938	-----		-----	-----	-----
10	dAla	7.395	4.338	1.281	-----	-----	-----	-----	-----
11	Gly	8.192	1.118, 2.924	-----	-----	-----	-----	-----	-----
12	Pro	-----	4.554	2.502, 2.040	2.126,	3.673, 3.285	-----	-----	-----
13	Ala	7.454	4.305	1.406	-----	-----	-----	-----	-----
14	Ser	8.024	4.216	3.926, 3.612		-----	-----	-----	-----
15	Gly	7.83	4.212, 3.846	-----	-----	-----	-----	-----	-----
16	Xaa		,	,	,	,	,	,	,
17	Pro	-----	4.643	2.217, 1.777	2.002, 1.996	3.857, 3.663	-----	-----	-----
18	Pro	-----	2.693	1.350, 0.623	1.763, 1.690	3.513, 3.476	-----	-----	-----
19	Pro	-----	4.366	2.224, 1.917	1.815,	3.121, 2.907	-----	-----	-----
20	Ser	8.237	4.394	3.928, 3.816		-----	-----	-----	-----

TC15b Y3A

DAAAQWLADaGPASGRPPAS

300K pH 6.5

#	Res	HN	Hα	Hβ	Hγ	Hδ	Hε	Hζ	Hη
1	Asp		4.258	2.994, 2.914	-----		-----	-----	-----
2	Ala	8.826	4.282	1.456	-----	-----	-----	-----	-----
3	Ala	8.402	4.13	1.482	-----	-----	-----	-----	-----
4	Ala	8.094	4.203	1.457	-----	-----	-----	-----	-----
5	Gln	8.169	4.072	2.106,	2.370,	-----	,	-----	-----
6	Trp	8.125	4.432	3.269, 3.470	-----	7.117	9.880, 7.634	7.313, 7.632	7.187
7	Leu	8.035	3.824	1.806,	1.577	0.934,	-----	-----	-----
8	Ala	8.111	4.089	1.452	-----	-----	-----	-----	-----
9	Asp	7.96	4.559	2.801, 2.720	-----		-----	-----	-----
10	dAla	7.629	4.328	1.334	-----	-----	-----	-----	-----
11	Gly	8.374	1.997, 3.395	-----	-----	-----	-----	-----	-----
12	Pro	-----	4.503	2.413, 2.008	2.101,	3.709, 3.519	-----	-----	-----
13	Ala	7.756	4.309	1.392	-----	-----	-----	-----	-----
14	Ser	8.129	4.204	3.892, 3.650		-----	-----	-----	-----
15	Gly	7.91	4.238, 3.846	-----	-----	-----	-----	-----	-----
16	Arg	8.061	4.872	1.828, 1.664	1.829, 1.716	3.276, 3.214	7.426	-----	, , ,
17	Pro	-----	4.725	2.317, 1.809	2.000,	3.828, 3.625	-----	-----	-----
18	Pro	-----	3.352	1.487, 1.159	1.813, 1.736	3.616, 3.513	-----	-----	-----
19	Pro	-----	4.328	2.195, 1.924	1.842,	3.291, 3.188	-----	-----	-----
20	Ser	7.815	4.177	3.796,		-----	-----	-----	-----

TC15b Y3A P12W

DAAAQWLADaGWASGRPPAS

300K pH 6.5

#	Res	HN	Hα	Hβ	Hγ	Hδ	Hε	Hζ	Hη
1	Asp		4.264	3.058, 2.936	-----		-----	-----	-----
2	Ala	8.886	4.248	1.447	-----	-----	-----	-----	-----
3	Ala	8.449	4.044	1.478	-----	-----	-----	-----	-----
4	Ala	8.072	4.188	1.494	-----	-----	-----	-----	-----
5	Gln	8.166	4.006	2.157, 2.096	2.382,	-----	,	-----	-----
6	Trp	8.087	4.26	3.180, 3.435	-----	6.908	9.689, 7.487	6.144, 6.949	6.208
7	Leu	7.982	3.609	1.847, 1.574		0.940,	-----	-----	-----
8	Ala	8.132	4.054	1.466	-----	-----	-----	-----	-----
9	Asp	7.933	4.529	2.837, 2.708	-----		-----	-----	-----
10	dAla	7.462	4.302	1.294	-----	-----	-----	-----	-----
11	Gly	8.293	1.033, 3.148	-----	-----	-----	-----	-----	-----
12	Trp	8.719	4.612	3.512, 3.189	-----	7.538	10.384, 7.840	7.563, 7.206	7.295
13	Ala	7.879	4.363	1.423	-----	-----	-----	-----	-----
14	Ser	7.979	4.157	3.873, 3.552		-----	-----	-----	-----
15	Gly	7.967	4.299, 3.879	-----	-----	-----	-----	-----	-----
16	Arg	8.077	4.978	1.777,	1.588,	3.240, 3.172	7.436	-----	, , ,
17	Pro	-----	4.243	2.318, 1.762	2.024, 1.941	3.802, 3.597	-----	-----	-----
18	Pro	-----	2.671	1.156, 0.243	1.588, 1.254	3.244, 2.669	-----	-----	-----
19	Pro	-----	4.261	2.140, 1.888	1.745,	3.148, 2.995	-----	-----	-----
20	Ser	7.792	4.147	3.775,		-----	-----	-----	-----

TC15b Y3L

DALAQWLADaGPASGRPPAS

300K pH 6.5

#	Res	HN	Hα	Hβ	Hγ	Hδ	Hε	Hζ	Hη
1	Asp		4.277	3.101, 2.935	-----		-----	-----	-----
2	Ala	8.871	4.288	1.485	-----	-----	-----	-----	-----
3	Leu	8.484	4.166	1.954, 1.592	1.74	1.055, 0.974	-----	-----	-----
4	Ala	8.201	4.154	1.521	-----	-----	-----	-----	-----
5	Gln	8.015	4.031	2.226, 2.172	2.432,	-----	,	-----	-----
6	Trp	8.213	4.307	3.675, 3.311	-----	7.059	9.776,	7.208,	7.611
7	Leu	8.715	3.584	2.076, 1.479	1.98	, 1.001	-----	-----	-----
8	Ala	8.202	4.078	1.511	-----	-----	-----	-----	-----
9	Asp	7.9	4.555	2.891, 2.756	-----		-----	-----	-----
10	dAla	7.391	4.32	1.294	-----	-----	-----	-----	-----
11	Gly	8.566	0.865, 3.190	-----	-----	-----	-----	-----	-----
12	Pro	-----	4.579	2.519, 2.051	2.169,	3.795, 3.533	-----	-----	-----
13	Ala	7.429	4.332	1.405	-----	-----	-----	-----	-----
14	Ser	8.164	4.101	3.887, 3.514		-----	-----	-----	-----
15	Gly	7.805	4.264, 3.816	-----	-----	-----	-----	-----	-----
16	Arg	8.116	5.056	1.913, 1.670	1.817,	3.330, 3.243	7.663	-----	, , ,
17	Pro	-----	4.761	2.333, 1.776	1.995,	3.859, 3.664	-----	-----	-----
18	Pro	-----	2.54	1.181, 0.315	1.669, 1.580	3.516, 3.471	-----	-----	-----
19	Pro	-----	4.285	2.145, 1.902	1.722,	3.050, 2.878	-----	-----	-----
20	Ser	7.919	4.233	3.838,		-----	-----	-----	-----

TC15b Y3L P12W

DALAQWLADaGWASGRPPAS

300K pH 6.5

#	Res	HN	Hα	Hβ	Hγ	Hδ	Hε	Hζ	Hη
1	Asp		4.263	3.098, 2.928	-----		-----	-----	-----
2	Ala	8.863	4.253	1.457	-----	-----	-----	-----	-----
3	Leu	8.459	4.086	1.941, 1.553	1.705	0.980, 0.947	-----	-----	-----
4	Ala	8.151	4.131	1.519	-----	-----	-----	-----	-----
5	Gln	7.99	3.997	2.203, 2.143	2.411,	-----	,	-----	-----
6	Trp	8.119	4.197	3.198, 3.595	-----	6.861	9.635, 7.436	5.872, 6.877	5.967
7	Leu	8.642	3.481	1.949, 1.453	2.018	, 0.972	-----	-----	-----
8	Ala	8.167	4.055	1.492	-----	-----	-----	-----	-----
9	Asp	7.897	4.527	2.863, 2.730	-----		-----	-----	-----
10	dAla	7.33	4.303	1.285	-----	-----	-----	-----	-----
11	Gly	8.366	0.476, 3.036	-----	-----	-----	-----	-----	-----
12	Trp	8.871	4.603	3.561, 3.186	-----	7.597	10.443, 7.920	7.585, 7.230	7.311
13	Ala	7.815	4.403	1.462	-----	-----	-----	-----	-----
14	Ser	7.978	4.116	3.878, 3.480		-----	-----	-----	-----
15	Gly	7.898	4.365, 3.863	-----	-----	-----	-----	-----	-----
16	Arg	8.113	5.09	1.851, 1.760	1.591,	3.269, 3.192	7.569	-----	, , ,
17	Pro	-----	4.203	2.368, 1.759	2.056, 1.937	3.839, 3.626	-----	-----	-----
18	Pro	-----	2.156	0.944, -0.365	1.492, 1.130	3.192, 2.424	-----	-----	-----
19	Pro	-----	4.239	2.104, 1.881	1.668,	3.027, 2.816	-----	-----	-----
20	Ser	7.733	4.131	3.756,		-----	-----	-----	-----

TC15b Y3L P12W

DALAQWLADaGWASGRPPAS

300K pH 2.5

#	Res	HN	Hα	Hβ	Hγ	Hδ	Hε	Hζ	Hη
1	Asp		4.28	3.074, 2.847	-----		-----	-----	-----
2	Ala	8.952	4.259	1.46	-----	-----	-----	-----	-----
3	Leu	8.53	4.072	1.867, 1.542	1.708	0.959, 0.929	-----	-----	-----
4	Ala	7.951	4.147	1.512	-----	-----	-----	-----	-----
5	Gln	7.898	4.076	2.182, 2.151	2.464, 2.400	-----	,	-----	-----
6	Trp	8.107	4.188	3.192, 3.587	-----	6.923	9.612, 7.466	6.043, 6.906	6.107
7	Leu	8.704	3.503	1.938, 1.497	1.982	, 0.969	-----	-----	-----
8	Ala	8.167	4.103	1.487	-----	-----	-----	-----	-----
9	Asp	7.686	4.673	3.076, 2.893	-----		-----	-----	-----
10	dAla	7.357	4.314	1.29	-----	-----	-----	-----	-----
11	Gly	8.113	0.662, 3.027	-----	-----	-----	-----	-----	-----
12	Trp	8.755	4.593	3.521, 3.184	-----	7.577	10.415, 7.851	7.566, 7.192	7.296
13	Ala	7.851	4.344	1.444	-----	-----	-----	-----	-----
14	Ser	7.937	4.206	3.920, 3.600		-----	-----	-----	-----
15	Gly	7.973	4.334, 3.904	-----	-----	-----	-----	-----	-----
16	Arg	7.959	4.937	1.866, 1.741	1.634,	3.246, 3.237	7.365	-----	, , ,
17	Pro	-----	4.026	2.254, 1.717	2.025, 1.914	3.784, 3.581	-----	-----	-----
18	Pro	-----	2.321	0.996, -0.105	1.515, 1.201	3.176, 2.512	-----	-----	-----
19	Pro	-----	4.278	2.143, 1.858	1.731, 1.659	3.073, 2.842	-----	-----	-----
20	Ser	8.126	4.346	3.913, 3.792		-----	-----	-----	-----

trTC15b

Ac-AYAQWLADaGPASGRPPAS-NH_2

300K pH 6.5

#	Res	HN	HA	HB	HG	HD	HE	HZ	HH
2	Ala	8.556	4.228	1.477	-----	-----	-----	-----	-----
3	Tyr	9.011	4.081	3.088,	-----	7.059	6.828	-----	
4	Ala	8.379	4.112	1.523	-----	-----	-----	-----	-----
5	Gln	8.029	4.007	2.189, 2.127	2.380,	-----	7.793, 6.934	-----	-----
6	Trp	8.01	4.217	3.124, 3.539	-----	6.975	9.711, 7.201	7.168, 6.984	7.122
7	Leu	8.379	3.379	1.864, 1.373	1.628	0.981, 0.882	-----	-----	-----
8	Ala	8.073	4.028	1.481	-----	-----	-----	-----	-----
9	Asp	7.919	4.52	2.729, 2.864	-----		-----	-----	-----
10	dAla	7.396	4.295	1.26	-----	-----	-----	-----	-----
11	Gly	8.521	0.700, 3.113	-----	-----	-----	-----	-----	-----
12	Pro	-----	4.603	2.523, 2.047	2.169, 3.577	3.782, 3.508	-----	-----	-----
13	Ala	7.414	4.342	1.396	-----	-----	-----	-----	-----
14	Ser	8.139	4.096	3.862, 3.458		-----	-----	-----	-----
15	Gly	7.801	4.290, 3.808	-----	-----	-----	-----	-----	-----
16	Arg	8.108	5.068	1.894, 1.813	1.654, 1.651	3.236, 3.319	7.612	-----	7.229, , ,
17	Pro	-----	4.759	1.776, 2.336	1.999, 1.784	3.671, 3.865	-----	-----	-----
18	Pro	-----	2.456	1.265, 0.223	1.720, 1.633	3.505,	-----	-----	-----
19	Pro	-----	4.365	1.921, 2.217	1.823,	2.910, 3.176	-----	-----	-----
20	Ser	8.193	4.305	3.838, 3.779		-----	-----	-----	-----

trTC15b

Ac-AYAQWLADaGPASGRPPAS-NH_2

300K pH 2.5

#	Res	HN	HA	HB	HG	HD	HE	HZ	HH
2	Ala	8.502	4.197	1.466	-----	-----	-----	-----	-----
3	Tyr	8.926	4.093	3.092,	-----			-----	
4	Ala	8.357	4.106	1.527	-----	-----	-----	-----	-----
5	Gln	8.016	4.074	2.153,	2.415, 2.368	-----	,	-----	-----
6	Trp	8.032	4.194	3.157, 3.542	-----	7.044	9.656, 7.025	7.200, 7.103	7.2
7	Leu	8.476	3.369	1.797, 1.433	1.598	0.953, 0.882	-----	-----	-----
8	Ala	8.094	4.066	1.476	-----	-----	-----	-----	-----
9	Asp	7.709	4.667	3.075, 2.899	-----		-----	-----	-----
10	dAla	7.409	4.31	1.279	-----	-----	-----	-----	-----
11	Gly	8.242	1.006, 2.997	-----	-----	-----	-----	-----	-----
12	Pro	-----	4.567	2.500, 2.039	2.138,	3.711, 3.371	-----	-----	-----
13	Ala	7.453	4.319	1.4	-----	-----	-----	-----	-----
14	Ser	8.072	4.181	3.903, 3.577		-----	-----	-----	-----
15	Gly	7.846	4.227, 3.847	-----	-----	-----	-----	-----	-----
16	Arg	8.004	4.914	1.926, 1.816	1.727, 1.675	3.273,	7.409	-----	, , ,
17	Pro	-----	4.698	2.280, 1.785	1.997,	3.645, 3.851	-----	-----	-----
18	Pro	-----	2.632	1.324, 0.471	1.739, 1.645	3.480,	-----	-----	-----
19	Pro	-----	4.346	2.224, 1.905	1.828,	3.159, 2.930	-----	-----	-----
20	Ser	8.171	4.305	3.813,		-----	-----	-----	-----

trTC15b D9Abu

Ac-AYAQWLA(Abu)aGPASGRPPAS-NH_2

300K pH 6.5

#	Res	HN	Hα	Hβ	Hγ	Hδ	Hε	Hζ	Hη
2	Ala	8.464	4.189	1.44	-----	-----	-----	-----	-----
3	Tyr	8.823	4.146	3.095,	-----			-----	
4	Ala	8.315	4.116	1.502	-----	-----	-----	-----	-----
5	Gln	8.021	4.139	2.151,	2.462, 2.391	-----	,	-----	-----
6	Trp	8.018	4.266	3.178, 3.510	-----	7.057	9.663, 7.096	7.220, 7.096	7.22
7	Leu	8.43	3.433	1.762, 1.429	1.583	0.942, 0.861	-----	-----	-----
8	Ala	7.96	4.092	1.496	-----	-----	-----	-----	-----
9	Xaa		,	,	,	,	,	,	,
10	dAla	7.462	4.332	1.274	-----	-----	-----	-----	-----
11	Gly	8.149	1.312, 3.097	-----	-----	-----	-----	-----	-----
12	Pro	-----	4.543	2.478, 2.038	2.131,	3.707, 3.397	-----	-----	-----
13	Ala	7.56	4.317	1.399	-----	-----	-----	-----	-----
14	Ser	8.056	4.214	3.889, 3.590		-----	-----	-----	-----
15	Gly	7.902	4.188, 3.858	-----	-----	-----	-----	-----	-----
16	Arg	7.954	4.831	1.947, 1.838	1.769, 1.687	3.244,	7.297	-----	, , ,
17	Pro	-----	4.684	2.273, 1.803	1.996, 1.998	3.628, 3.840	-----	-----	-----
18	Pro	-----	2.848	1.428, 0.737	1.782, 1.701	3.525, 3.491	-----	-----	-----
19	Pro	-----	4.338	2.205, 1.953	1.845,	3.164, 3.000	-----	-----	-----
20	Ser	8.182	4.32	3.818,		-----	-----	-----	-----

trTC15b D9Abu

Ac-AYAQWLA(Abu)aGPASGRPPAS-NH_2

300K pH 2.5

#	Res	HN	Hα	Hβ	Hγ	Hδ	Hε	Hζ	Hη
2	Ala	8.485	4.189	1.442	-----	-----	-----	-----	-----
3	Tyr		4.156	3.092,	-----			-----	
4	Ala	8.341	4.106	1.503	-----	-----	-----	-----	-----
5	Gln	8.035	4.138	2.153,	2.464, 2.394	-----	,	-----	-----
6	Trp	7.997	4.264	3.191, 3.509	-----		, 7.099	7.228, 7.099	7.228
7	Leu	8.423	3.433	1.760, 1.426	1.577	0.944, 0.858	-----	-----	-----
8	Ala	7.964	4.086	1.498	-----	-----	-----	-----	-----
9	Xaa		,	,	,	,	,	,	,
10	dAla	7.472	4.331	1.277	-----	-----	-----	-----	-----
11	Gly		1.344, 3.104	-----	-----	-----	-----	-----	-----
12	Pro	-----	4.547	2.475, 2.040	2.132,	3.702, 3.399	-----	-----	-----
13	Ala	7.592	4.31	1.397	-----	-----	-----	-----	-----
14	Ser	8.057	4.209	3.889, 3.593		-----	-----	-----	-----
15	Gly	7.904	4.185, 3.855	-----	-----	-----	-----	-----	-----
16	Arg	7.97	4.84	1.952,	1.764, 1.687	3.242,	7.309	-----	, , ,
17	Pro	-----	4.665	2.269, 1.798	2.001, 1.999	3.624, 3.846	-----	-----	-----
18	Pro	-----	2.88	1.396, 0.745	1.768, 1.707	3.526, 3.493	-----	-----	-----
19	Pro	-----		2.229, 1.899	1.851,	3.197, 3.005	-----	-----	-----
20	Ser	8.203	4.309	3.806,		-----	-----	-----	-----

trTC15b D9Abu R16Cit

Ac-AYAQWLA(Abu)aGPASG(Cit)PPAS-NH_2

300K pH 6.5

#	Res	HN	Hα	Hβ	Hγ	Hδ	Hε	Hζ	Hη
2	Ala	8.459	4.202	1.435	-----	-----	-----	-----	-----
3	Tyr	8.784	4.176	3.088,	-----			-----	
4	Ala	8.318	4.119	1.493	-----	-----	-----	-----	-----
5	Gln	8.025	4.149	2.147,	2.443, 2.400	-----	,	-----	-----
6	Trp	8.006	4.306	3.191, 3.485	-----	7.108	9.686, 7.115	7.239, 7.201	7.239
7	Leu	8.401	3.466	1.749, 1.423	1.573	0.936, 0.854	-----	-----	-----
8	Ala	7.961	4.096	1.493	-----	-----	-----	-----	-----
9	Xaa		,	,	,	,	,	,	,
10	dAla	7.496	4.333	1.276	-----	-----	-----	-----	-----
11	Gly	8.167	1.447, 3.116	-----	-----	-----	-----	-----	-----
12	Pro	-----	4.535	2.466, 2.032	2.120,	3.692, 3.380	-----	-----	-----
13	Ala	7.596	4.314	1.398	-----	-----	-----	-----	-----
14	Ser	8.059	4.223	3.908, 3.598		-----	-----	-----	-----
15	Gly	7.908	4.184, 3.859	-----	-----	-----	-----	-----	-----
16	Xaa		,	,	,	,	,	,	,
17	Pro	-----	4.667	2.249, 1.795	1.998, 2.001	3.638, 3.847	-----	-----	-----
18	Pro	-----	2.949	1.407, 0.840	1.790, 1.738	3.547, 3.495	-----	-----	-----
19	Pro	-----	4.353	2.233, 1.868	1.870,	3.210, 3.005	-----	-----	-----
20	Ser	8.225	4.318	3.814,		-----	-----	-----	-----

trTC15b D9Abu R16Cit

Ac-AYAQWLA(Abu)aGPASG(Cit)PPAS-NH_2

300K pH 2.5

#	Res	HN	Hα	Hβ	Hγ	Hδ	Hε	Hζ	Hη
2	Ala	8.474	4.192	1.445	-----	-----	-----	-----	-----
3	Tyr	9.048	4.165	3.093,	-----			-----	
4	Ala	8.33	4.104	1.499	-----	-----	-----	-----	-----
5	Gln	8.023	4.144	2.151,	2.446, 2.400	-----	,	-----	-----
6	Trp	7.997	4.287	3.183, 3.497	-----	7.107	9.684, 7.097	7.226, 7.207	7.225
7	Leu	8.401	3.436	1.762, 1.420	1.574	0.941, 0.856	-----	-----	-----
8	Ala	7.953	4.085	1.495	-----	-----	-----	-----	-----
9	Xaa		,	,	,	,	,	,	,
10	dAla	7.472	4.331	1.274	-----	-----	-----	-----	-----
11	Gly	8.172	1.440, 3.099	-----	-----	-----	-----	-----	-----
12	Pro	-----	4.529	2.475, 2.031	2.125,	3.694, 3.378	-----	-----	-----
13	Ala	7.579	4.312	1.396	-----	-----	-----	-----	-----
14	Ser	8.05	4.214	3.912, 3.609		-----	-----	-----	-----
15	Gly	7.881	4.187, 3.848	-----	-----	-----	-----	-----	-----
16	Xaa		,	,	,	,	,	,	,
17	Pro	-----	4.645	2.246, 1.795	1.998, 1.997	3.635, 3.847	-----	-----	-----
18	Pro	-----	2.947	1.383, 0.788	1.782, 1.726	3.538, 3.496	-----	-----	-----
19	Pro	-----	4.351	2.227, 1.856	1.856,	3.190, 2.983	-----	-----	-----
20	Ser	8.212	4.309	3.836,		-----	-----	-----	-----

trTC15b D9Abu R16Nva

Ac-AYAQWLA(Abu)aGPASG(Nva)PPAS-NH_2

300K pH 6.5

#	Res	HN	Hα	Hβ	Hγ	Hδ	Hε	Hζ	Hη
2	Ala	8.424	4.2	1.429	-----	-----	-----	-----	-----
3	Tyr	8.738	4.188	3.085,	-----			-----	
4	Ala	8.284	4.111	1.49	-----	-----	-----	-----	-----
5	Gln	8.017	4.141	2.143,	2.436, 2.393	-----	,	-----	-----
6	Trp	7.996	4.307	3.192, 3.480	-----	7.105	9.698, 7.125	7.246, 7.197	7.246
7	Leu	8.382	3.476	1.744, 1.422	1.573	0.932, 0.848	-----	-----	-----
8	Ala	7.947	4.096	1.489	-----	-----	-----	-----	-----
9	Xaa		,	,	,	,	,	,	,
10	dAla	7.495	4.338	1.278	-----	-----	-----	-----	-----
11	Gly	8.142	1.512, 3.132	-----	-----	-----	-----	-----	-----
12	Pro	-----	4.523	2.462, 2.032	2.113,	3.685, 3.367	-----	-----	-----
13	Ala	7.588	4.311	1.396	-----	-----	-----	-----	-----
14	Ser	8.02	4.22	3.885, 3.594		-----	-----	-----	-----
15	Gly	7.891	4.170, 3.858	-----	-----	-----	-----	-----	-----
16	Xaa		,	,	,	,	,	,	,
17	Pro	-----	4.665	2.238, 1.793	2.006, 2.010	3.655, 3.849	-----	-----	-----
18	Pro	-----	3.009	1.416, 0.899	1.800, 1.755	3.570, 3.505	-----	-----	-----
19	Pro	-----	4.347	2.224, 1.849	1.851,	3.192, 2.997	-----	-----	-----
20	Ser	8.191	4.321	3.823,		-----	-----	-----	-----

trTC15b D9Abu R16Nva

Ac-AYAQWLA(Abu)aGPASG(Nva)PPAS-NH_2

300K pH 2.5

#	Res	HN	Hα	Hβ	Hγ	Hδ	Hε	Hζ	Hη
2	Ala	8.484	4.187	1.444	-----	-----	-----	-----	-----
3	Tyr		4.165	3.092,	-----			-----	
4	Ala	8.331	4.103	1.502	-----	-----	-----	-----	-----
5	Gln	8.024	4.14	2.155,	2.449, 2.400	-----	,	-----	-----
6	Trp	7.998	4.278	3.205, 3.490	-----		, 7.092	7.228, 7.207	7.228
7	Leu	8.434	3.42	1.767, 1.414	1.583	0.942, 0.850	-----	-----	-----
8	Ala	7.953	4.103	1.5	-----	-----	-----	-----	-----
9	Xaa		,	,	,	,	,	,	,
10	dAla	7.462	4.335	1.272	-----	-----	-----	-----	-----
11	Gly		1.334, 3.084	-----	-----	-----	-----	-----	-----
12	Pro	-----	4.528	2.482, 2.036	2.124,	3.695, 3.367	-----	-----	-----
13	Ala	7.556	4.315	1.396	-----	-----	-----	-----	-----
14	Ser	8.016	4.204	3.874, 3.599		-----	-----	-----	-----
15	Gly	7.865	4.184, 3.840	-----	-----	-----	-----	-----	-----
16	Xaa		,	,	,	,	,	,	,
17	Pro	-----		2.237, 1.789	2.007, 2.006	3.657, 3.858	-----	-----	-----
18	Pro	-----	2.881	1.383, 0.786	1.782, 1.734	3.552, 3.496	-----	-----	-----
19	Pro	-----	4.349	2.219, 1.882	1.834,	3.157, 2.959	-----	-----	-----
20	Ser	8.211	4.304	3.800,		-----	-----	-----	-----

trTC15b P12W

Ac-AYAQWLADaGWASGRPPAS-NH_2

300K pH 6.5

#	Res	HN	Hα	Hβ	Hγ	Hδ	Hε	Hζ	Hη
2	Ala	8.514	4.198	1.452	-----	-----	-----	-----	-----
3	Tyr	8.968	4.004	3.057,	-----			-----	
4	Ala	8.332	4.072	1.509	-----	-----	-----	-----	-----
5	Gln	7.983	3.971	2.164, 2.098	2.357,	-----	,	-----	-----
6	Trp	7.921	4.117	3.025, 3.431	-----	6.791	9.556, 6.790	5.849, 6.790	5.942
7	Leu	8.307	3.275	1.808, 1.342	1.563	0.953, 0.846	-----	-----	-----
8	Ala	8.021	4.002	1.462	-----	-----	-----	-----	-----
9	Asp	7.897	4.489	2.829, 2.693	-----		-----	-----	-----
10	dAla	7.343	4.281	1.254	-----	-----	-----	-----	-----
11	Gly	8.307	0.385, 2.982	-----	-----	-----	-----	-----	-----
12	Trp	8.815	4.617	3.565, 3.180	-----		10.441, 7.924	7.606, 7.237	7.329
13	Ala	7.822	4.405	1.457	-----	-----	-----	-----	-----
14	Ser	7.943	4.111	3.859, 3.439		-----	-----	-----	-----
15	Gly	7.888	4.356, 3.857	-----	-----	-----	-----	-----	-----
16	Arg	8.093	5.072	1.829, 1.764	1.777, 1.577	3.261, 3.188	7.501	-----	, , ,
17	Pro	-----	4.208	2.368, 1.767	2.060, 1.937	3.838, 3.625	-----	-----	-----
18	Pro	-----	2.129	1.057, -0.326	1.566, 1.226	2.428, 3.222	-----	-----	-----
19	Pro	-----	4.311	2.171, 1.901	1.769,	3.107, 2.828	-----	-----	-----
20	Ser	8.146	4.288	3.801,		-----	-----	-----	-----

trTC15b P12W

Ac-AYAQWLADaGWASGRPPAS-NH_2

300K pH 2.5

#	Res	HN	Hα	Hβ	Hγ	Hδ	Hε	Hζ	Hη
2	Ala	8.52	4.175	1.45	-----	-----	-----	-----	-----
3	Tyr	8.974	4.002	3.068,	-----			-----	
4	Ala	8.377	4.081	1.521	-----	-----	-----	-----	-----
5	Gln	7.99	4.045	2.129,	2.393, 2.346	-----	,	-----	-----
6	Trp	7.969	4.083	3.042, 3.442	-----	6.832	9.522, 6.806	5.929, 6.806	6.024
7	Leu	8.459	3.256	1.753, 1.406	1.544	0.943, 0.871	-----	-----	-----
8	Ala	8.087	4.043	1.46	-----	-----	-----	-----	-----
9	Asp	7.681	4.623	3.064, 2.867	-----		-----	-----	-----
10	dAla	7.355	4.315	1.262	-----	-----	-----	-----	-----
11	Gly	8.084	0.423, 2.976	-----	-----	-----	-----	-----	-----
12	Trp	8.812	4.611	3.552, 3.188	-----		10.455, 7.885	7.609, 7.217	7.332
13	Ala	7.856	4.367	1.458	-----	-----	-----	-----	-----
14	Ser	7.917	4.193	3.896, 3.539		-----	-----	-----	-----
15	Gly	7.941	4.339, 3.895	-----	-----	-----	-----	-----	-----
16	Arg	7.957	4.957	1.857, 1.738	1.741, 1.623	3.241, 3.238	7.379	-----	, , ,
17	Pro	-----	4.034	2.273, 1.739	2.041, 1.921	3.793, 3.591	-----	-----	-----
18	Pro	-----	2.193	1.102, -0.166	1.569, 1.256	2.449, 3.191	-----	-----	-----
19	Pro	-----	4.305	2.182, 1.883	1.774,	3.102, 2.841	-----	-----	-----
20	Ser	8.171	4.285	3.800,		-----	-----	-----	-----

trTC15b P12W R16Cit

Ac-AYAQWLADaGWASG(Cit)PPAS-NH_2

300K pH 6.5

#	Res	HN	Hα	Hβ	Hγ	Hδ	Hε	Hζ	Hη
2	Ala	8.459	4.201	1.436	-----	-----	-----	-----	-----
3	Tyr	8.819	4.05	3.050,	-----			-----	
4	Ala	8.282	4.072	1.489	-----	-----	-----	-----	-----
5	Gln	7.957	3.991	2.130, 2.127	2.367,	-----	,	-----	-----
6	Trp	7.96	4.216	3.071, 3.396	-----	6.921	9.511, 6.867	6.014, 6.799	6.096
7	Leu	8.32	3.308	1.743, 1.383	1.536	0.924, 0.851	-----	-----	-----
8	Ala	7.972	4.008	1.458	-----	-----	-----	-----	-----
9	Asp	7.913	4.513	2.774, 2.690	-----		-----	-----	-----
10	dAla	7.337	4.312	1.249	-----	-----	-----	-----	-----
11	Gly	8.196	0.705, 2.999	-----	-----	-----	-----	-----	-----
12	Trp	8.626	4.631	3.525, 3.181	-----	7.555	10.399, 7.861	7.589, 7.211	7.317
13	Ala	7.856	4.346	1.433	-----	-----	-----	-----	-----
14	Ser	7.89	4.217	3.925, 3.548		-----	-----	-----	-----
15	Gly	7.914	4.310, 3.880	-----	-----	-----	-----	-----	-----
16	Xaa		,	,	,	,	,	,	,
17	Pro	-----	4.091	2.199, 1.733	2.006, 1.917	3.749, 3.586	-----	-----	-----
18	Pro	-----	2.411	1.158, 0.093	1.614, 1.320	2.625, 3.228	-----	-----	-----
19	Pro	-----	4.309	2.202, 1.861	1.778,	3.157, 2.876	-----	-----	-----
20	Ser	8.179	4.288	3.797,		-----	-----	-----	-----

trTC15b P12W R16Cit

Ac-AYAQWLADaGWASG(Cit)PPAS-NH_2

300K pH 2.5

#	Res	HN	Hα	Hβ	Hγ	Hδ	Hε	Hζ	Hη
2	Ala	8.48	4.183	1.447	-----	-----	-----	-----	-----
3	Tyr	8.902	4.014	3.059,	-----			-----	
4	Ala	8.326	4.077	1.514	-----	-----	-----	-----	-----
5	Gln	7.961	4.039	2.135, 2.133	2.367,	-----	,	-----	-----
6	Trp	7.978	4.127	3.064, 3.424	-----	6.888	9.497, 6.820	6.005, 6.820	6.005
7	Leu	8.441	3.263	1.739, 1.405	1.544	0.932, 0.863	-----	-----	-----
8	Ala	8.061	4.041	1.456	-----	-----	-----	-----	-----
9	Asp	7.694	4.616	3.064, 2.911	-----		-----	-----	-----
10	dAla	7.349	4.307	1.256	-----	-----	-----	-----	-----
11	Gly	8.078	0.523, 2.968	-----	-----	-----	-----	-----	-----
12	Trp	8.689	4.623	3.541, 3.183	-----	7.58	10.422, 7.882	7.609, 7.219	7.325
13	Ala	7.838	4.354	1.443	-----	-----	-----	-----	-----
14	Ser	7.899	4.205	3.923, 3.545		-----	-----	-----	-----
15	Gly	7.901	4.331, 3.882	-----	-----	-----	-----	-----	-----
16	Xaa		,	,	,	,	,	,	,
17	Pro	-----	4.068	2.200, 1.728	2.014, 1.914	3.754, 3.590	-----	-----	-----
18	Pro	-----	2.285	1.126, -0.026	1.599, 1.293	2.557, 3.214	-----	-----	-----
19	Pro	-----	4.303	2.190, 1.867	1.785,	3.111, 2.839	-----	-----	-----
20	Ser	8.159	4.286	3.803,		-----	-----	-----	-----

trTC15b P12W R16Nva

Ac-AYAQWLADaGWASG(Nva)PPAS-NH_2

300K pH 6.5

#	Res	HN	Hα	Hβ	Hγ	Hδ	Hε	Hζ	Hη
2	Ala	8.485	4.2	1.433	-----	-----	-----	-----	-----
3	Tyr	8.837	4.047	3.048,	-----			-----	
4	Ala	8.308	4.076	1.491	-----	-----	-----	-----	-----
5	Gln	7.971	3.987	2.135,	2.375,	-----	6.868, 7.816	-----	-----
6	Trp	7.979	4.223	3.079, 3.401	-----	6.936	9.502, 6.865	6.135, 6.784	5.992
7	Leu	8.332	3.295	1.732, 1.396	1.532	0.921, 0.856	-----	-----	-----
8	Ala	7.982	4.002	1.461	-----	-----	-----	-----	-----
9	Asp	7.927	4.525	2.674, 2.773	-----		-----	-----	-----
10	dAla	7.321	4.338	1.242	-----	-----	-----	-----	-----
11	Gly	8.165	0.736, 2.986	-----	-----	-----	-----	-----	-----
12	Trp	8.592	4.639	3.518, 3.184	-----	7.533	10.389, 7.851	7.582, 7.206	7.31
13	Ala	7.86	4.327	1.429	-----	-----	-----	-----	-----
14	Ser	7.851	4.252	3.916, 3.576		-----	-----	-----	-----
15	Gly	7.825	4.165, 3.772	-----	-----	-----	-----	-----	-----
16	Arg			,	,	,		-----	, , ,
17	Pro	-----	4.079	1.721, 2.141	1.989, 1.919	3.597, 3.744	-----	-----	-----
18	Pro	-----	2.461	1.176, 0.142	1.621, 1.342	3.240, 2.678	-----	-----	-----
19	Pro	-----	4.316	1.855, 2.201	1.801,	2.880, 3.166	-----	-----	-----
20	Ser	8.199	4.288	3.821, 3.793		-----	-----	-----	-----

trTC15b P12W R16Nva

Ac-AYAQWLADaGWASG(Nva)PPAS-NH_2

300K pH 2.5

#	Res	HN	Hα	Hβ	Hγ	Hδ	Hε	Hζ	Hη
2	Ala	8.477	4.171	1.442	-----	-----	-----	-----	-----
3	Tyr	8.888	4.021	3.058,	-----			-----	
4	Ala	8.32	4.073	1.512	-----	-----	-----	-----	-----
5	Gln	7.961	4.042	2.134,	2.366,	-----	,	-----	-----
6	Trp	7.979	4.128	3.066, 3.416	-----	6.905	9.503, 6.818	6.066, 6.817	5.94
7	Leu	8.443	3.258	1.720, 1.421	1.537	0.925, 0.861	-----	-----	-----
8	Ala	8.058	4.037	1.455	-----	-----	-----	-----	-----
9	Asp	7.696	4.615	3.046, 2.912	-----		-----	-----	-----
10	dAla	7.335	4.319	1.25	-----	-----	-----	-----	-----
11	Gly	8.03	0.577, 2.963	-----	-----	-----	-----	-----	-----
12	Trp	8.634	4.639	3.531, 3.187	-----	7.564	10.404, 7.873	7.594, 7.218	7.317
13	Ala	7.833	4.332	1.436	-----	-----	-----	-----	-----
14	Ser	7.845	4.224	3.904, 3.566		-----	-----	-----	-----
15	Gly	7.893	4.311, 3.878	-----	-----	-----	-----	-----	-----
16	Arg			,	,	,		-----	, , ,
17	Pro	-----	4.088	2.151, 1.720	1.998, 1.921	3.599, 3.743	-----	-----	-----
18	Pro	-----	2.37	1.149, 0.048	1.612, 1.323	3.233, 2.645	-----	-----	-----
19	Pro	-----	4.3	2.184, 1.863	1.771,	2.840, 3.112	-----	-----	-----
20	Ser	8.154	4.285	3.801,		-----	-----	-----	-----

trTC15b R16A

Ac-AYAQWLADaGPASGAPPAS-NH_2

300K pH 6.5

#	Res	HN	Hα	Hβ	Hγ	Hδ	Hε	Hζ	Hη
2	Ala	8.395	4.228	1.416	-----	-----	-----	-----	-----
3	Tyr	8.596	4.25	3.074,	-----			-----	
4	Ala	8.225	4.125	1.447	-----	-----	-----	-----	-----
5	Gln	8.031	4.069	2.115,	2.373,	-----	,	-----	-----
6	Trp	8.03	4.43	3.213, 3.470	-----	7.209	9.784, 7.308	7.308, 7.120	7.229
7	Leu	8.254	3.636	1.727, 1.452	1.554	0.924, 0.860	-----	-----	-----
8	Ala	7.999	4.073	1.463	-----	-----	-----	-----	-----
9	Asp	7.981	4.572	2.778, 2.721	-----		-----	-----	-----
10	dAla	7.575	4.359	1.325	-----	-----	-----	-----	-----
11	Gly	8.252	2.097, 3.170	-----	-----	-----	-----	-----	-----
12	Pro	-----	4.501	2.413, 2.007	2.074,	3.637, 3.311	-----	-----	-----
13	Ala	7.737	4.317	1.405	-----	-----	-----	-----	-----
14	Ser	8.089	4.323	3.961, 3.713		-----	-----	-----	-----
15	Gly	7.978	4.170, 3.883	-----	-----	-----	-----	-----	-----
16	Ala	7.998	4.753	1.419	-----	-----	-----	-----	-----
17	Pro	-----	4.606	2.190, 1.807	2.004,	3.814, 3.645	-----	-----	-----
18	Pro	-----	3.44	1.551, 1.257	1.859, 1.801	3.595, 3.500	-----	-----	-----
19	Pro	-----	4.383	2.258, 1.903	1.905,	3.368, 3.169	-----	-----	-----
20	Ser	8.215	4.343	3.842, 3.842		-----	-----	-----	-----

trTC15b R16A

Ac-AYAQWLADaGPASGAPPAS-NH_2

300K pH 2.5

#	Res	HN	Hα	Hβ	Hγ	Hδ	Hε	Hζ	Hη
2	Ala	8.43	4.197	1.438	-----	-----	-----	-----	-----
3	Tyr	8.738	4.161	3.077,	-----			-----	
4	Ala	8.273	4.098	1.489	-----	-----	-----	-----	-----
5	Gln	7.996	4.074	2.133,	2.379,	-----	,	-----	-----
6	Trp	8.021	4.298	3.186, 3.502	-----	7.166	9.701, 7.251	7.251, 7.116	7.214
7	Leu	8.384	3.464	1.738, 1.446	1.568	0.921, 0.859	-----	-----	-----
8	Ala	8.039	4.074	1.462	-----	-----	-----	-----	-----
9	Asp	7.776	4.669	3.057, 2.944	-----		-----	-----	-----
10	dAla	7.464	4.334	1.299	-----	-----	-----	-----	-----
11	Gly	8.156	1.607, 2.988	-----	-----	-----	-----	-----	-----
12	Pro	-----	4.51	2.441, 2.010	2.076,	3.625, 3.245	-----	-----	-----
13	Ala	7.564	4.299	1.395	-----	-----	-----	-----	-----
14	Ser	8.056	4.28	3.950, 3.669		-----	-----	-----	-----
15	Gly	7.886	4.210, 3.845	-----	-----	-----	-----	-----	-----
16	Ala	7.989	4.791	1.418	-----	-----	-----	-----	-----
17	Pro	-----	4.541	2.126, 1.770	1.976,	3.798, 3.633	-----	-----	-----
18	Pro	-----	3.15	1.460, 1.015	1.804, 1.730	3.519, 3.447	-----	-----	-----
19	Pro	-----	4.344	2.229, 1.864	1.863,	3.252, 3.050	-----	-----	-----
20	Ser	8.169	4.313	3.840, 3.805		-----	-----	-----	-----

trTC15b R16Cit

Ac-AYAQWLADaGPASG(Cit)PPAS-NH_2

300K pH 6.5

#	Res	HN	Hα	Hβ	Hγ	Hδ	Hε	Hζ	Hη
2	Ala	8.454	4.222	1.441	-----	-----	-----	-----	-----
3	Tyr	8.771	4.154	3.075,	-----	7.061	6.826	-----	
4	Ala	8.282	4.104	1.482	-----	-----	-----	-----	-----
5	Gln	8.005	4.026	2.189, 2.138	2.379,	-----	7.751, 6.867	-----	-----
6	Trp	8.028	4.344	3.480, 3.181	-----	7.122	9.683, 7.100	7.192, 7.233	7.233
7	Leu	8.337	3.47	1.771, 1.418	1.576	0.936, 0.865	-----	-----	-----
8	Ala	8.005	4.04	1.466	-----	-----	-----	-----	-----
9	Asp	7.935	4.555	2.724, 2.804	-----		-----	-----	-----
10	dAla	7.448	4.327	1.284	-----	-----	-----	-----	-----
11	Gly	8.332	1.421, 3.055	-----	-----	-----	-----	-----	-----
12	Pro	-----	4.53	2.462, 2.018	2.109,	3.680, 3.346	-----	-----	-----
13	Ala	7.563	4.315	1.399	-----	-----	-----	-----	-----
14	Ser	8.068	4.218	3.940, 3.615		-----	-----	-----	-----
15	Gly	7.869	4.193, 3.850	-----	-----	-----	-----	-----	-----
16	Xaa	8.108	,	1.894, 1.813	1.654,	3.236, 3.319	,	,	,
17	Pro	-----	4.667	2.251, 1.790	1.995,	3.838, 3.650	-----	-----	-----
18	Pro	-----	2.889	1.386, 0.733	1.775, 1.699	3.524, 3.491	-----	-----	-----
19	Pro	-----	4.355	2.245, 2.217	1.878,	3.239, 2.997	-----	-----	-----
20	Ser	8.21	4.312	3.813, 3.779		-----	-----	-----	-----

trTC15b R16Cit

Ac-AYAQWLADaGPASG(Cit)PPAS-NH_2

300K pH 2.5

#	Res	HN	Hα	Hβ	Hγ	Hδ	Hε	Hζ	Hη
2	Ala	8.488	4.202	1.463	-----	-----	-----	-----	-----
3	Tyr	8.889	4.108	3.088,	-----	7.064	6.83	-----	
4	Ala	8.338	4.104	1.521	-----	-----	-----	-----	-----
5	Gln	8.001	4.075	2.157,	2.388,	-----	7.549, 7.082	-----	-----
6	Trp	8.043	4.249	3.176, 3.519	-----	7.098	9.638, 7.035	7.096, 7.203	7.2
7	Leu	8.473	3.378	1.787, 1.432	1.596	0.949, 0.881	-----	-----	-----
8	Ala	8.08	4.066	1.472	-----	-----	-----	-----	-----
9	Asp	7.735	4.655	3.089, 2.950	-----		-----	-----	-----
10	dAla	7.417	4.319	1.282	-----	-----	-----	-----	-----
11	Gly	8.253	1.093, 2.978	-----	-----	-----	-----	-----	-----
12	Pro	-----	4.548	2.495, 2.032	2.126,	3.696, 3.333	-----	-----	-----
13	Ala	7.458	4.315	1.4	-----	-----	-----	-----	-----
14	Ser	8.063	4.193	3.938, 3.595		-----	-----	-----	-----
15	Gly	7.83	4.227, 3.837	-----	-----	-----	-----	-----	-----
16	Xaa		,	,	,	,	,	,	,
17	Pro	-----	4.676	2.252, 1.779	1.997,	3.654, 3.850	-----	-----	-----
18	Pro	-----	2.669	1.332, 0.560	1.752, 1.672	3.489,	-----	-----	-----
19	Pro	-----	4.348	2.231, 1.881	1.829,	3.148, 2.907	-----	-----	-----
20	Ser	8.186	4.305	3.813,		-----	-----	-----	-----

trTC15b R16Nva

Ac-AYAQWLADaGPASG(Nva)PPAS-NH_2

300K pH 6.5

#	Res	HN	Hα	Hβ	Hγ	Hδ	Hε	Hζ	Hη
2	Ala	8.476	4.219	1.438	-----	-----	-----	-----	-----
3	Tyr	8.786	4.148	3.074,	-----	7.06	6.826	-----	
4	Ala	8.308	4.107	1.483	-----	-----	-----	-----	-----
5	Gln	8.015	4.028	2.140,	2.389,	-----	7.805, 6.882	-----	-----
6	Trp	8.038	4.352	3.191, 3.485	-----	7.139	9.662, 7.244	7.189, 7.089	7.089
7	Leu	8.343	3.454	1.759, 1.430	1.572	0.933, 0.864	-----	-----	-----
8	Ala	8.015	4.034	1.467	-----	-----	-----	-----	-----
9	Asp	7.95	4.554	2.700, 2.788	-----		-----	-----	-----
10	dAla	7.44	4.353	1.283	-----	-----	-----	-----	-----
11	Gly	8.287	1.498, 3.013	-----	-----	-----	-----	-----	-----
12	Pro	-----	4.529	2.460, 2.014	2.099,	3.659, 3.288	-----	-----	-----
13	Ala	7.574	4.304	1.401	-----	-----	-----	-----	-----
14	Ser	8.031	4.254	3.932, 3.641		-----	-----	-----	-----
15	Gly	7.866	4.188, 3.851	-----	-----	-----	-----	-----	-----
16		-----	-----	-----	-----	-----	-----	-----	-----
17	Pro	-----	4.648	1.785, 2.221	1.999, 1.998	3.661, 3.856	-----	-----	-----
18	Pro	-----	2.928	1.394, 0.777	1.781, 1.704	3.530, 3.493	-----	-----	-----
19	Pro	-----	4.361	2.242, 2.219	1.867, 1.832	2.991, 3.231	-----	-----	-----
20	Ser	8.227	4.315	3.841, 3.795		-----	-----	-----	-----

trTC15b R16Nva

Ac-AYAQWLADaGPASG(Nva)PPAS-NH_2

300K pH 2.5

#	Res	HN	Hα	Hβ	Hγ	Hδ	Hε	Hζ	Hη
2	Ala	8.481	4.198	1.456	-----	-----	-----	-----	-----
3	Tyr	8.867	4.111	3.088,	-----	7.06	6.826	-----	
4	Ala	8.332	4.107	1.518	-----	-----	-----	-----	-----
5	Gln	8.001	4.076	2.150,	2.391,	-----	,	-----	-----
6	Trp	8.043	4.247	3.174, 3.512	-----	7.113	9.640, 7.230	7.199,	7.101
7	Leu	8.469	3.384	1.769, 1.445	1.59	0.939, 0.872	-----	-----	-----
8	Ala	8.078	4.069	1.47	-----	-----	-----	-----	-----
9	Asp	7.733	4.658	3.055, 2.940	-----		-----	-----	-----
10	dAla	7.414	4.337	1.279	-----	-----	-----	-----	-----
11	Gly	8.195	1.189, 2.961	-----	-----	-----	-----	-----	-----
12	Pro	-----	4.545	2.486, 2.027	2.113,	3.678, 3.290	-----	-----	-----
13	Ala	7.47	4.31	1.4	-----	-----	-----	-----	-----
14	Ser	8.012	4.22	3.914, 3.616		-----	-----	-----	-----
15	Gly	7.828	4.214, 3.840	-----	-----	-----	-----	-----	-----
16		-----	-----	-----	-----	-----	-----	-----	-----
17	Pro	-----	4.658	1.774, 2.216	2.000, 1.997	3.667, 3.857	-----	-----	-----
18	Pro	-----	2.755	1.350, 0.637	1.761, 1.685	3.501, 3.502	-----	-----	-----
19	Pro	-----	4.352	2.224,	1.863, 1.819	2.917, 3.150	-----	-----	-----
20	Ser	8.181	4.309	3.809,		-----	-----	-----	-----

trTC15b Y3A

Ac-AAAQWLADaGPASGRPPAS-NH_2

300K pH 6.5

#	Res	HN	Hα	Hβ	Hγ	Hδ	Hε	Hζ	Hη
2	Ala	8.301	4.226	1.389	-----	-----	-----	-----	-----
3	Ala	8.431	4.207	1.422	-----	-----	-----	-----	-----
4	Ala	8.099	4.192	1.364	-----	-----	-----	-----	-----
5	Gln	8.151	4.128	2.025,	2.302,	-----	7.604, 6.839	-----	-----
6	Trp	8.026	4.545	3.244, 3.409	-----	7.166	9.977, 7.612	7.375, 7.168	7.233
7	Leu	8.022	3.993	1.699, 1.543	1.628	0.907, 0.872	-----	-----	-----
8	Ala	8.033	4.11	1.413	-----	-----	-----	-----	-----
9	Asp	8.005	4.555	2.733, 2.721	-----		-----	-----	-----
10	dAla	7.789	4.349	1.362	-----	-----	-----	-----	-----
11	Gly	8.271	2.811, 3.602	-----	-----	-----	-----	-----	-----
12	Pro	-----	4.445	2.338, 1.981	2.054,	3.662, 3.519	-----	-----	-----
13	Ala	7.991	4.299	1.382	-----	-----	-----	-----	-----
14	Ser	8.102	4.277	3.901, 3.739		-----	-----	-----	-----
15	Gly	8.085	4.059, 3.913	-----	-----	-----	-----	-----	-----
16	Arg	8.02	4.764	1.828, 1.763	1.662, 1.663	3.232, 3.195	7.276	-----	, , ,
17	Pro	-----	4.699	1.832, 2.315	2.003,	3.605, 3.816	-----	-----	-----
18	Pro	-----	3.895	1.633, 1.633	1.871, 1.876	3.675, 3.549	-----	-----	-----
19	Pro	-----	4.372	, 2.249	1.919,	3.495, 3.352	-----	-----	-----
20	Ser	8.197	4.349	3.847,		-----	-----	-----	-----

trTC15b Y3A

Ac-AAAQWLADaGPASGRPPAS-NH_2

300K pH 2.5

#	Res	HN	Hα	Hβ	Hγ	Hδ	Hε	Hζ	Hη
2	Ala	8.292	4.216	1.387	-----	-----	-----	-----	-----
3	Ala	8.411	4.206	1.413	-----	-----	-----	-----	-----
4	Ala	8.092	4.185	1.367	-----	-----	-----	-----	-----
5	Gln	8.146	4.153	2.027, 2.030	2.302,	-----	,	-----	-----
6	Trp	7.985	4.531	3.268, 3.410	-----	7.195	10.007, 7.612	7.399, 7.170	7.231
7	Leu	8.039	3.991	1.689, 1.552	1.597	0.903, 0.868	-----	-----	-----
8	Ala	8.044	4.135	1.41	-----	-----	-----	-----	-----
9	Asp	7.989	4.688	2.996, 2.918	-----		-----	-----	-----
10	dAla	7.799	4.347	1.376	-----	-----	-----	-----	-----
11	Gly	8.091	2.973, 3.547	-----	-----	-----	-----	-----	-----
12	Pro	-----	4.384	2.262, 1.942	1.942,	3.524, 3.393	-----	-----	-----
13	Ala	8.034	4.288	1.379	-----	-----	-----	-----	-----
14	Ser	8.084	4.321	3.909, 3.789		-----	-----	-----	-----
15	Gly	8.131	4.034, 3.930	-----	-----	-----	-----	-----	-----
16	Arg	7.994	4.687	1.859, 1.860	1.724, 1.657	3.209, 3.209	7.22	-----	, , ,
17	Pro	-----	4.667	1.835, 2.292	2.000,	3.591, 3.804	-----	-----	-----
18	Pro	-----	4.055	1.694, 1.795	1.899, 1.891	3.683, 3.546	-----	-----	-----
19	Pro	-----	4.422	, 2.307	2.026, 1.965	3.620, 3.442	-----	-----	-----
20	Ser	8.209	4.355	3.853, 3.851		-----	-----	-----	-----

trTC15b Y3Abu

Ac-A(Abu)AQWLADaGPASGRPPAS-NH_2

300K pH 6.5

#	Res	HN	Hα	Hβ	Hγ	Hδ	Hε	Hζ	Hη
2	Ala	8.396	4.238	1.414	-----	-----	-----	-----	-----
3	Xaa		,	,	,	,	,	,	,
4	Ala	8.188	4.185	1.401	-----	-----	-----	-----	-----
5	Gln	8.133	4.098	2.080,	2.344,	-----	7.697, 6.906	-----	-----
6	Trp	8.067	4.459	3.264, 3.520	-----	7.129	9.903, 7.626	7.318, 7.182	7.233
7	Leu	8.337	3.824	1.795, 1.511		0.938, 0.900	-----	-----	-----
8	Ala	8.096	4.094	1.45	-----	-----	-----	-----	-----
9	Asp	7.981	4.552	2.798, 2.737	-----		-----	-----	-----
10	dAla	7.663	4.341	1.337	-----	-----	-----	-----	-----
11	Gly	8.405	2.115, 3.441	-----	-----	-----	-----	-----	-----
12	Pro	-----	4.504	2.405, 2.008	2.096,	3.709, 3.509	-----	-----	-----
13	Ala	7.808	4.312	1.393	-----	-----	-----	-----	-----
14	Ser	8.132	4.223	3.901, 3.667		-----	-----	-----	-----
15	Gly	8.006	4.138, 3.878	-----	-----	-----	-----	-----	-----
16	Arg	8.07	4.86	1.828, 1.822	1.711, 1.666	3.273, 3.217	7.401	-----	, , ,
17	Pro	-----	4.718	1.806, 2.319	2.002,	3.628, 3.836	-----	-----	-----
18	Pro	-----	3.402	1.469, 1.191	1.814, 1.773	3.627, 3.521	-----	-----	-----
19	Pro	-----	4.341	, 2.231	1.861,	3.336, 3.170	-----	-----	-----
20	Ser	8.213	4.32	3.821,		-----	-----	-----	-----

trTC15b Y3Abu

Ac-A(Abu)AQWLADaGPASGRPPAS-NH_2

300K pH 2.5

#	Res	HN	Hα	Hβ	Hγ	Hδ	Hε	Hζ	Hη
2	Ala	8.317	4.227	1.4	-----	-----	-----	-----	-----
3	Xaa		,	,	,	,	,	,	,
4	Ala	8.146	4.178	1.381	-----	-----	-----	-----	-----
5	Gln	8.117	4.139	2.063,	2.334,	-----	,	-----	-----
6	Trp	7.999	4.483	3.280, 3.487	-----	7.178	9.935, 7.628	7.234, 7.372	7.174
7	Leu	8.278	3.868	1.749, 1.525	1.709	0.914, 0.866	-----	-----	-----
8	Ala	8.064	4.122	1.435	-----	-----	-----	-----	-----
9	Asp	7.915	4.696	3.022, 2.926	-----		-----	-----	-----
10	dAla	7.709	4.349	1.359	-----	-----	-----	-----	-----
11	Gly	8.15	2.570, 3.434	-----	-----	-----	-----	-----	-----
12	Pro	-----	4.452	2.352, 1.984	2.048,	3.634, 3.407	-----	-----	-----
13	Ala	7.908	4.291	1.386	-----	-----	-----	-----	-----
14	Ser	8.077	4.296	3.914, 3.757		-----	-----	-----	-----
15	Gly	8.07	4.076, 3.915	-----	-----	-----	-----	-----	-----
16	Arg	7.993	4.726	1.880,	1.747, 1.668	3.224,	7.255	-----	, , ,
17	Pro	-----	4.667	1.819, 2.279	1.995,	3.596, 3.813	-----	-----	-----
18	Pro	-----	3.747	1.585, 1.538	1.861, 1.821	3.637, 3.518	-----	-----	-----
19	Pro	-----	4.361	, 2.241	1.895,	3.268, 3.416	-----	-----	-----
20	Ser	8.182	4.337	3.840,		-----	-----	-----	-----

trTC15b Y3L

Ac-ALAQWLADaGPASGRPPAS-NH_2

300K pH 6.5

#	Res	HN	Hα	Hβ	Hγ	Hδ	Hε	Hζ	Hη
2	Ala	8.43	4.224	1.434	-----	-----	-----	-----	-----
3	Leu	8.626	4.204	1.850, 1.583	1.732	1.023, 0.943	-----	-----	-----
4	Ala	8.184	4.14	1.458	-----	-----	-----	-----	-----
5	Gln	8.031	4.05	2.174, 2.131	2.390, 2.386	-----	,	-----	-----
6	Trp	8.085	4.325	3.288, 3.649	-----	7.073	9.819,	,	
7	Leu	8.621	3.638	1.930, 1.484	2.001	0.981, 0.982	-----	-----	-----
8	Ala	8.127	4.078	1.492	-----	-----	-----	-----	-----
9	Asp	7.926	4.552	2.857, 2.746	-----		-----	-----	-----
10	dAla	7.435	4.321	1.3	-----	-----	-----	-----	-----
11	Gly	8.495	1.158, 3.227	-----	-----	-----	-----	-----	-----
12	Pro	-----	4.557	2.487, 2.036	2.147,	3.769, 3.512	-----	-----	-----
13	Ala	7.501	4.321	1.399	-----	-----	-----	-----	-----
14	Ser	8.13	4.132	3.891, 3.551		-----	-----	-----	-----
15	Gly	7.83	4.225, 3.830	-----	-----	-----	-----	-----	-----
16	Arg	8.078	5.001	1.858, 1.773	1.672, 1.668	3.317, 3.243	7.517	-----	, , ,
17	Pro	-----	4.745	2.324, 1.780	1.998, 2.001	3.656, 3.855	-----	-----	-----
18	Pro	-----	2.753	1.205, 0.455	1.689, 1.607	3.532, 3.483	-----	-----	-----
19	Pro	-----	4.311	2.184, 1.848	1.752,	3.163, 2.941	-----	-----	-----
20	Ser	8.106	4.284	3.800,		-----	-----	-----	-----

trTC15b Y3L

Ac-ALAQWLADaGPASGRPPAS-NH_2

300K pH 2.5

#	Res	HN	Hα	Hβ	Hγ	Hδ	Hε	Hζ	Hη
2	Ala	8.409	4.202	1.429	-----	-----	-----	-----	-----
3	Leu	8.582	4.205	1.839, 1.600	1.724	1.006, 0.934	-----	-----	-----
4	Ala	8.173	4.144	1.463	-----	-----	-----	-----	-----
5	Gln	8.035	4.107	2.147,	2.419, 2.369	-----	,	-----	-----
6	Trp	8.09	4.317	3.303, 3.641	-----	7.134	9.787,	,	
7	Leu	8.676	3.647	1.919, 1.508	1.964	0.966, 0.972	-----	-----	-----
8	Ala	8.138	4.119	1.485	-----	-----	-----	-----	-----
9	Asp	7.767	4.697	3.076, 2.925	-----		-----	-----	-----
10	dAla	7.462	4.328	1.319	-----	-----	-----	-----	-----
11	Gly	8.254	1.458, 3.122	-----	-----	-----	-----	-----	-----
12	Pro	-----	4.524	2.459, 2.024	2.112,	3.700, 3.387	-----	-----	-----
13	Ala	7.562	4.302	1.401	-----	-----	-----	-----	-----
14	Ser	8.078	4.209	3.918, 3.653		-----	-----	-----	-----
15	Gly	7.9	4.190, 3.864	-----	-----	-----	-----	-----	-----
16	Arg	7.996	4.859	1.926, 1.804	1.695, 1.695	3.265,	7.37	-----	, , ,
17	Pro	-----	4.692	2.274, 1.785	1.993, 1.996	3.630, 3.841	-----	-----	-----
18	Pro	-----	2.943	1.283, 0.711	1.713, 1.631	3.520, 3.468	-----	-----	-----
19	Pro	-----	4.314	2.195, 1.836	1.772,	3.169, 2.983	-----	-----	-----
20	Ser	8.112	4.292	3.800,		-----	-----	-----	-----

trTC15b Y3V

Ac-AVAQWLADaGPASGRPPAS-NH_2

300K pH 6.5

#	Res	HN	Hα	Hβ	Hγ	Hδ	Hε	Hζ	Hη
2	Ala	8.345	4.266	1.411	-----	-----	-----	-----	-----
3	Val	8.337	3.856	2.086	1.003, 0.973	-----	-----	-----	-----
4	Ala	8.215	4.175	1.388	-----	-----	-----	-----	-----
5	Gln	8.105	4.094	2.081, 2.081	2.347,	-----	,	-----	-----
6	Trp	7.999	4.458	3.265, 3.523	-----	7.131	9.877, 7.616	7.316, 7.180	7.237
7	Leu	8.406	3.81	1.798, 1.480	1.798	0.931, 0.882	-----	-----	-----
8	Ala	8.076	4.092	1.448	-----	-----	-----	-----	-----
9	Asp	7.941	4.55	2.797, 2.734	-----		-----	-----	-----
10	dAla	7.636	4.339	1.334	-----	-----	-----	-----	-----
11	Gly	8.392	2.111, 3.437	-----	-----	-----	-----	-----	-----
12	Pro	-----	4.498	2.404, 2.005	2.093,	3.703, 3.482	-----	-----	-----
13	Ala	7.777	4.313	1.392	-----	-----	-----	-----	-----
14	Ser	8.105	4.224	3.902, 3.672		-----	-----	-----	-----
15	Gly	7.981	4.136, 3.873	-----	-----	-----	-----	-----	-----
16	Arg	8.049	4.857	1.826, 1.826	1.712, 1.666	3.272, 3.220	7.382	-----	, , ,
17	Pro	-----	4.712	2.310, 1.806	1.998, 2.001	3.834, 3.625	-----	-----	-----
18	Pro	-----	3.382	1.465, 1.187	1.819, 1.764	3.619, 3.515	-----	-----	-----
19	Pro	-----	4.337	2.226, 1.842	1.846,	3.326, 3.119	-----	-----	-----
20	Ser	8.136	4.31	3.821,		-----	-----	-----	-----

trTC15b Y3V

Ac-AVAQWLADaGPASGRPPAS-NH_2

300K pH 2.5

#	Res	HN	Hα	Hβ	Hγ	Hδ	Hε	Hζ	Hη
2	Ala	8.339	4.251	1.408	-----	-----	-----	-----	-----
3	Val	8.316	3.864	2.085	1.004, 0.973	-----	-----	-----	-----
4	Ala	8.216	4.169	1.387	-----	-----	-----	-----	-----
5	Gln	8.115	4.128	2.085,	2.360, 2.351	-----	,	-----	-----
6	Trp	7.984	4.453	3.287, 3.530	-----	7.174	9.885, 7.636	7.237, 7.181	7.335
7	Leu	8.431	3.791	1.780, 1.496	1.496	0.925, 0.868	-----	-----	-----
8	Ala	8.09	4.122	1.448	-----	-----	-----	-----	-----
9	Asp	7.864	4.7	3.037, 2.930	-----		-----	-----	-----
10	dAla	7.649	4.351	1.35	-----	-----	-----	-----	-----
11	Gly	8.194	2.298, 3.357	-----	-----	-----	-----	-----	-----
12	Pro	-----	4.474	2.382, 1.995	2.063,	3.650, 3.378	-----	-----	-----
13	Ala	7.815	4.299	1.392	-----	-----	-----	-----	-----
14	Ser	8.07	4.279	3.920, 3.735		-----	-----	-----	-----
15	Gly	8.025	4.120, 3.900	-----	-----	-----	-----	-----	-----
16	Arg	7.995	4.752	1.893, 1.761	1.675, 1.676	3.236,	7.282	-----	, , ,
17	Pro	-----	4.666	2.277, 1.809	1.991, 1.995	3.603, 3.817	-----	-----	-----
18	Pro	-----	3.505	1.518, 1.352	1.830, 1.777	3.602, 3.503	-----	-----	-----
19	Pro	-----	4.342	2.230, 1.858	,	3.340, 3.159	-----	-----	-----
20	Ser	8.145	4.316	3.816,		-----	-----	-----	-----

Ac-cp TC4e

Ac-RPPPSDAALYAQWLADaGPAS

300K pH 6.5

#	Res	HN	Hα	Hβ	Hγ	Hδ	Hε	Hζ	Hη
1	Arg	8.307	4.361	1.783, 1.654	1.653, 1.533	3.194,	7.192	-----	, , ,
2	Pro	-----	4.681	2.266, 1.795	1.951, 1.957	3.736, 3.396	-----	-----	-----
3	Pro	-----	3.761	1.582, 1.512	1.893, 1.897	3.680, 3.531	-----	-----	-----
4	Pro	-----	4.163	2.147, 1.793	1.811, 1.790	3.278, 3.114	-----	-----	-----
5	Ser	8.065	4.213	3.913, 3.798		-----	-----	-----	-----
6	Asp	7.807	4.631	2.748, 2.658	-----		-----	-----	-----
7	Ala	8.465	4.109	1.485	-----	-----	-----	-----	-----
8	Ala	8.424	4.298	1.496	-----	-----	-----	-----	-----
9	Leu	8.071	4.267	1.764, 1.557	1.716	0.979, 0.891	-----	-----	-----
10	Tyr	8.687	4.158	3.104, 3.039	-----			-----	
11	Ala	8.143	4.091	1.542	-----	-----	-----	-----	-----
12	Gln	7.805	4.047	2.448, 2.410	2.168,	-----	,	-----	-----
13	Trp	8.146	4.364	3.529, 3.247	-----	7.177	10.021, 7.250	7.365, 7.088	7.214
14	Leu	8.364	3.649	1.673, 1.463		0.845, 0.843	-----	-----	-----
15	Ala	7.848	4.061	1.461	-----	-----	-----	-----	-----
16	Asp	7.922	4.568	2.763, 2.685	-----		-----	-----	-----
17	dAla	7.517	4.296	1.294	-----	-----	-----	-----	-----
18	Gly	8.009	2.486, 2.740	-----	-----	-----	-----	-----	-----
19	Pro	-----	4.44	2.301, 2.026	,	3.461, 3.185	-----	-----	-----
20	Ala	8.072	4.396	1.418	-----	-----	-----	-----	-----
21	Ser	7.812	4.225	3.853, 3.793		-----	-----	-----	-----

Ac-cp TC4e

Ac-RPPPSDAALYAQWLADaGPAS

300K pH 2.5

#	Res	HN	Hα	Hβ	Hγ	Hδ	Hε	Hζ	Hη
1	Arg	8.149	3.97	1.615, 1.517	1.440, 1.218	3.107,	7.134	-----	, , ,
2	Pro	-----	4.47	2.119, 1.974	1.824,	3.728, 3.572	-----	-----	-----
3	Pro	-----	3.977	1.764, 1.921	1.921,	3.594, 3.515	-----	-----	-----
4	Pro	-----	4.654	2.251, 1.896	1.785,	3.591, 3.138	-----	-----	-----
5	Ser	8.046	4.46	3.837, 3.837		-----	-----	-----	-----
6	Asp	7.811	4.666	3.010, 2.911	-----		-----	-----	-----
7	Ala	8.107	4.088	1.495	-----	-----	-----	-----	-----
8	Ala	8.485	4.268	1.488	-----	-----	-----	-----	-----
9	Leu	7.707	4.25	1.751, 1.602	1.7	0.983, 0.916	-----	-----	-----
10	Tyr	8.496	4.073	2.952,	-----			-----	
11	Ala	8.183	4.044	1.54	-----	-----	-----	-----	-----
12	Gln	7.8	4.07	2.473, 2.395	2.208,	-----	,	-----	-----
13	Trp	8.152	4.245	3.446, 3.209	-----	7.057	10.162, 7.198	7.316, 7.066	7.189
14	Leu	8.349	3.575	1.666, 1.402	1.451	, 0.803	-----	-----	-----
15	Ala	7.921	4.072	1.454	-----	-----	-----	-----	-----
16	Asp	8.132	4.862	3.053, 2.923	-----		-----	-----	-----
17	dAla	7.535	4.267	1.286	-----	-----	-----	-----	-----
18	Gly	7.901	2.308, 2.775	-----	-----	-----	-----	-----	-----
19	Pro	-----	4.367	2.266, 1.985	1.981,	3.389, 3.067	-----	-----	-----
20	Ala	7.981	4.38	1.407	-----	-----	-----	-----	-----
21	Ser	7.873	4.226	3.974, 3.841		-----	-----	-----	-----

Ac-cp TC4e D22

Ac-RPPPSDAALYAQWLADaGPASD

300K pH 6.5

#	Res	HN	Hα	Hβ	Hγ	Hδ	Hε	Hζ	Hη
1	Arg	8.286	4.316	1.764, 1.638	, 1.496	3.185,	7.205	-----	, , ,
2	Pro	-----	4.677	2.265, 1.790	1.943, 1.946	3.711, 3.356	-----	-----	-----
3	Pro	-----	3.839	1.574, 1.575	1.897, 1.899	3.685, 3.534	-----	-----	-----
4	Pro	-----	4.128	2.118, 1.772	1.825, 1.825	3.284, 3.127	-----	-----	-----
5	Ser	8.139	4.447	3.871, 3.820		-----	-----	-----	-----
6	Asp	7.807	4.64	2.758, 2.647	-----		-----	-----	-----
7	Ala		4.109	1.487	-----	-----	-----	-----	-----
8	Ala	8.434	4.299	1.497	-----	-----	-----	-----	-----
9	Leu	8.065	4.262	1.766, 1.553	1.722	0.980, 0.895	-----	-----	-----
10	Tyr	8.711	4.167	3.106, 3.028	-----			-----	
11	Ala	8.141	4.09	1.544	-----	-----	-----	-----	-----
12	Gln	7.798	4.041	2.456, 2.172	2.172,	-----	,	-----	-----
13	Trp	8.153	4.364	3.534, 3.252	-----	7.225	10.149, 7.256	7.371, 7.091	7.207
14	Leu	8.348	3.654	1.674, 1.456		0.841, 0.838	-----	-----	-----
15	Ala	7.847	4.057	1.461	-----	-----	-----	-----	-----
16	Asp	7.923	4.567	2.755, 2.670	-----		-----	-----	-----
17	dAla	7.516	4.302	1.292	-----	-----	-----	-----	-----
18	Gly	7.99	2.509, 2.701	-----	-----	-----	-----	-----	-----
19	Pro	-----	4.423	2.294, 2.006	1.943, 1.946	3.467, 3.187	-----	-----	-----
20	Ala	8.101	4.385	1.419	-----	-----	-----	-----	-----
21	Ser	8.027	4.204	3.912, 3.795		-----	-----	-----	-----
22	Asp	8.024	4.438	2.706, 2.608	-----		-----	-----	-----

Ac-cp TC4e D22

Ac-RPPPSDAALYAQWLADaGPASD

300K pH 2.5

#	Res	HN	Hα	Hβ	Hγ	Hδ	Hε	Hζ	Hη
1	Arg	8.25	4.575	1.801, 1.676	,	3.190,	7.182	-----	, , ,
2	Pro	-----	4.686	2.280, 1.785	1.945, 1.948	3.722, 3.327	-----	-----	-----
3	Pro	-----	4.002	1.775, 1.962	1.928, 1.928	3.613, 3.527	-----	-----	-----
4	Pro	-----	4.65	1.891, 2.247	1.788,	3.589, 3.147	-----	-----	-----
5	Ser	8.031	4.423	3.860, 3.860		-----	-----	-----	-----
6	Asp	7.811	4.672	3.023, 2.913	-----		-----	-----	-----
7	Ala	8.11	4.087	1.494	-----	-----	-----	-----	-----
8	Ala	8.471	4.266	1.492	-----	-----	-----	-----	-----
9	Leu	7.727	4.241	1.768, 1.605	1.708	0.982, 0.916	-----	-----	-----
10	Tyr	8.492	4.042	2.939,	-----			-----	
11	Ala	8.167	4.032	1.541	-----	-----	-----	-----	-----
12	Gln	7.804	4.067	2.474, 2.391	2.207,	-----	,	-----	-----
13	Trp	8.142	4.247	3.442, 3.204	-----	7.208	10.121, 7.312	7.312, 7.066	7.179
14	Leu	8.351	3.553	1.667, 1.393	1.45	, 0.797	-----	-----	-----
15	Ala	7.919	4.072	1.456	-----	-----	-----	-----	-----
16	Asp	7.811	4.672	3.017, 2.915	-----		-----	-----	-----
17	dAla	7.517	4.278	1.288	-----	-----	-----	-----	-----
18	Gly	7.915	2.300, 2.737	-----	-----	-----	-----	-----	-----
19	Pro	-----	4.457	2.336, 2.056	1.962,	3.507, 3.242	-----	-----	-----
20	Ala	7.894	4.34	1.396	-----	-----	-----	-----	-----
21	Ser	7.896	4.239	3.987, 3.851		-----	-----	-----	-----
22	Asp	8.241	4.769	2.967, 2.967	-----		-----	-----	-----

Ac-cp TC4e P19W

Ac-RPPPSDAALYAQWLADaGWAS

300K pH 6.5

#	Res	HN	Hα	Hβ	Hγ	Hδ	Hε	Hζ	Hη
1	Arg		4.5	1.779, 1.636	1.539,	3.046, 3.050	7.054	-----	, , ,
2	Pro	-----	4.37	1.766, 2.273	1.988, 1.950	3.831, 3.487	-----	-----	-----
3	Pro	-----	3.263	1.333, 0.796	1.788, 1.655	3.402, 3.366	-----	-----	-----
4	Pro	-----	4.256	1.776, 2.229	1.773,	3.093, 2.834	-----	-----	-----
5	Ser	8.132	4.302	3.881, 3.787		-----	-----	-----	-----
6	Asp	7.953	4.542	2.757, 2.662	-----		-----	-----	-----
7	Ala	8.638	4.095	1.486	-----	-----	-----	-----	-----
8	Ala	8.426	4.304	1.507	-----	-----	-----	-----	-----
9	Leu	8.132	4.293	1.800, 1.587	1.794	1.008, 0.912	-----	-----	-----
10	Tyr	8.829	4.039	3.090, 3.016	-----			-----	
11	Ala	8.131	4.069	1.568	-----	-----	-----	-----	-----
12	Gln	7.704	4.017	2.186,	2.469, 2.424	-----	,	-----	-----
13	Trp	8.144	4.127	3.044, 3.457	-----	6.706	9.200,	,	
14	Leu	8.462	3.476	1.633, 1.455		, 0.856	-----	-----	-----
15	Ala	7.771	4.026	1.461	-----	-----	-----	-----	-----
16	Asp	7.683	4.587	2.683, 2.687	-----		-----	-----	-----
17	dAla	7.32	4.222	1.145	-----	-----	-----	-----	-----
18	Gly	7.87	1.662, 2.732	-----	-----	-----	-----	-----	-----
19	Trp	7.787	4.747	3.383, 3.225	-----	7.407	10.222, 7.691	7.486, 7.189	7.265
20	Ala	8.012	4.413	1.341	-----	-----	-----	-----	-----
21	Ser	7.722	4.2	3.848, 3.742		-----	-----	-----	-----

Ac-cp TC4e P19W

Ac-RPPPSDAALYAQWLADaGWAS

300K pH 2.5

#	Res	HN	Hα	Hβ	Hγ	Hδ	Hε	Hζ	Hη
1	Arg			1.571, 1.448	1.347, 1.073	2.999, 2.958	7.03	-----	, , ,
2	Pro	-----	4.488	1.754, 2.234	,	,	-----	-----	-----
3	Pro	-----	3.946	1.708, 1.445	1.914, 1.816	3.414, 3.295	-----	-----	-----
4	Pro	-----	4.481	1.753, 2.236	1.894,	3.599, 3.118	-----	-----	-----
5	Ser	7.967	4.4	3.952, 3.815		-----	-----	-----	-----
6	Asp	7.975		3.014, 2.926	-----		-----	-----	-----
7	Ala		4.086	1.503	-----	-----	-----	-----	-----
8	Ala	8.507	4.274	1.489	-----	-----	-----	-----	-----
9	Leu	7.669	4.295	1.720, 1.606	1.72	0.987, 0.912	-----	-----	-----
10	Tyr	8.618	4.064	3.046, 2.999	-----			-----	
11	Ala	8.247	4.065	1.557	-----	-----	-----	-----	-----
12	Gln	7.743	4.069	2.213,	2.484, 2.394	-----	,	-----	-----
13	Trp	8.169	4.084	3.078, 3.413	-----	6.804	9.686,	,	
14	Leu	8.425	3.508	1.641, 1.442		, 0.829	-----	-----	-----
15	Ala	7.884	4.061	1.45	-----	-----	-----	-----	-----
16	Asp	7.806	4.655	3.001, 2.874	-----		-----	-----	-----
17	dAla	7.377	4.193	1.138	-----	-----	-----	-----	-----
18	Gly	7.803	1.871, 2.727	-----	-----	-----	-----	-----	-----
19	Trp	7.609	4.666	3.332, 3.214	-----	7.342	10.195, 7.664	7.490, 7.175	7.258
20	Ala	7.898	4.372	1.307	-----	-----	-----	-----	-----
21	Ser	7.834	4.165	3.937, 3.809		-----	-----	-----	-----

cp TC4e

RPPPSDAALYAQWLADaGPAS

300K pH 6.5

#	Res	HN	HA	HB	HG	HD	HE	HZ	HH
1	Arg		4.341	1.954, 1.656	1.819,	3.244,	7.394	-----	, , ,
2	Pro	-----	4.782	2.357, 1.790	1.981,	3.696, 3.460	-----	-----	-----
3	Pro	-----	3.218	1.441, 1.019	1.851, 1.790	3.630, 3.521	-----	-----	-----
4	Pro	-----	4.256	2.208,	1.821,	3.191, 2.972	-----	-----	-----
5	Ser	8.179	4.21	3.892, 3.797		-----	-----	-----	-----
6	Asp	7.641	4.62	2.727, 2.659	-----		-----	-----	-----
7	Ala	8.643	4.093	1.486	-----	-----	-----	-----	-----
8	Ala	8.486	4.307	1.503	-----	-----	-----	-----	-----
9	Leu	8.081	4.351	1.794, 1.615	1.726	0.996, 0.895	-----	-----	-----
10	Tyr	8.638	4.097	3.098,	-----			-----	
11	Ala	8.296	4.111	1.564	-----	-----	-----	-----	-----
12	Gln	7.873	4.028	2.431, 2.181	2.140,	-----	,	-----	-----
13	Trp	8.075	4.301	3.180, 3.571	-----	7.121	9.837, 7.327	7.325, 7.083	7.223
14	Leu	8.413	3.495	1.718, 1.445	1.51	0.876,	-----	-----	-----
15	Ala	7.863	4.04	1.471	-----	-----	-----	-----	-----
16	Asp	7.919	4.549	2.794, 2.686	-----		-----	-----	-----
17	dAla	7.428	4.293	1.28	-----	-----	-----	-----	-----
18	Gly	8.131	1.884, 2.724	-----	-----	-----	-----	-----	-----
19	Pro	-----	4.481	2.369,	2.038,	3.493, 3.170	-----	-----	-----
20	Ala	7.831	4.431	1.404	-----	-----	-----	-----	-----
21	Ser	7.72	4.149	3.874, 3.683		-----	-----	-----	-----

cp TC4e

RPPPSDAALYAQWLADaGPAS

300K pH 2.5

#	Res	HN	HA	HB	HG	HD	HE	HZ	HH
1	Arg		4.085	1.840, 1.456	1.681, 1.651	3.158, 3.120	7.208	-----	, , ,
2	Pro	-----	4.447	2.091, 1.832	1.984,	3.756, 3.582	-----	-----	-----
3	Pro	-----	4.113	1.929, 1.818	2.049,	3.593, 3.496	-----	-----	-----
4	Pro	-----	4.358	2.245, 1.970	1.916,	3.371, 3.031	-----	-----	-----
5	Ser	8.037	4.459	3.965, 3.840		-----	-----	-----	-----
6	Asp	7.812	4.675	3.011, 2.906	-----		-----	-----	-----
7	Ala	8.237	4.109	1.485	-----	-----	-----	-----	-----
8	Ala	8.387	4.261	1.488	-----	-----	-----	-----	-----
9	Leu	7.763	4.243	1.768, 1.599	1.689	0.976, 0.911	-----	-----	-----
10	Tyr	8.414		2.916,	-----			-----	
11	Ala	8.154	4.039	1.528	-----	-----	-----	-----	-----
12	Gln	7.831	4.069	2.472, 2.385	2.200,	-----	,	-----	-----
13	Trp	8.142	4.249	3.196, 3.440	-----	7.056	10.140, 7.330	7.331, 7.074	7.183
14	Leu	8.354	3.566	1.653, 1.419		0.797,	-----	-----	-----
15	Ala	7.918	4.075	1.454	-----	-----	-----	-----	-----
16	Asp	8.205	4.791	3.028, 2.929	-----		-----	-----	-----
17	dAla	7.539	4.281	1.296	-----	-----	-----	-----	-----
18	Gly	7.929	2.322, 2.800	-----	-----	-----	-----	-----	-----
19	Pro	-----	4.76	2.345, 1.815	1.951,	3.560, 3.242	-----	-----	-----
20	Ala	7.962	4.38	1.405	-----	-----	-----	-----	-----
21	Ser	8.018	4.267	3.987, 3.859		-----	-----	-----	-----

cp TC4e –GGGGGGGG- D22

RPPPGGGGGGGGYAQWLADaGPASD

300K pH 6.5

#	Res	HN	HA	HB	HG	HD	HE	HZ	HH
1	Arg		4.367	1.949,	1.754, 1.700	3.216,	7.268	-----	, , ,
2	Pro	-----	4.753	1.840, 2.362	1.991,	3.732, 3.546	-----	-----	-----
3	Pro	-----	4.471	1.817, 2.109	1.960,	3.743, 3.549	-----	-----	-----
4	Pro	-----	4.382	2.240, 2.246	1.992,	3.686, 3.542	-----	-----	-----
5	Gly		,	-----	-----	-----	-----	-----	-----
6	Gly		,	-----	-----	-----	-----	-----	-----
7	Gly		,	-----	-----	-----	-----	-----	-----
8	Gly		,	-----	-----	-----	-----	-----	-----
9	Gly		,	-----	-----	-----	-----	-----	-----
10	Gly		,	-----	-----	-----	-----	-----	-----
11	Gly		,	-----	-----	-----	-----	-----	-----
12	Gly		,	-----	-----	-----	-----	-----	-----
13	Tyr	8.172	4.395	3.004,	-----			-----	
14	Ala	8.545	4.375	1.417	-----	-----	-----	-----	-----
15	Gln	8.05	4.105	1.991, 1.991	2.282,	-----	,	-----	-----
16	Trp	7.959	4.518	3.386, 3.214	-----	7.194	10.126, 7.579	, 7.139	7.234
17	Leu	8.108	3.944	1.574, 1.450		0.822, 0.821	-----	-----	-----
18	Ala	7.948	4.107	1.393	-----	-----	-----	-----	-----
19	Asp	8.016	4.591	2.772, 2.769	-----		-----	-----	-----
20	dAla	7.841	4.325	1.355	-----	-----	-----	-----	-----
21	Gly	8.075	3.224, 3.447	-----	-----	-----	-----	-----	-----
22	Pro	-----	4.399	1.946, 2.241	1.992,	3.520, 3.383	-----	-----	-----
23	Ala	8.16	4.331	1.374	-----	-----	-----	-----	-----
24	Ser	8.131	4.417	3.874, 3.810		-----	-----	-----	-----
25	Asp	8.078	4.496	2.787, 2.734	-----		-----	-----	-----

cp TC4e –SGUDA- Y10A

RPPPSGUDAAAQWLADaGPAS

300K pH 6.5

#	Res	HN	Hα	Hβ	Hγ	Hδ	Hε	Hζ	Hη
1	Arg		4.377	1.951,	1.751, 1.710	3.217,	7.216	-----	, , ,
2	Pro	-----	4.773	1.873, 2.391	2.027, 2.005	3.749, 3.566	-----	-----	-----
3	Pro	-----	4.548	1.856, 2.246	2.016,	3.791, 3.595	-----	-----	-----
4	Pro	-----	4.432	1.872, 2.250	1.965,	3.661, 3.527	-----	-----	-----
5	Ser	8.366	4.44	3.893, 3.841		-----	-----	-----	-----
6	Gly	8.454	3.963, 3.896	-----	-----	-----	-----	-----	-----
7	Aib		-----	,	-----	-----	-----	-----	-----
8	Asp	8.226	4.571	2.821, 2.731	-----		-----	-----	-----
9	Ala	8.035	4.189	1.417	-----	-----	-----	-----	-----
10	Ala	8.009	4.164	1.404	-----	-----	-----	-----	-----
11	Ala				-----	-----	-----	-----	-----
12	Gln	8.12	4.166	1.983,	2.279,	-----	,	-----	-----
13	Trp	7.993	4.629	3.368, 3.266	-----	7.236	10.140, 7.606	7.457, 7.152	7.23
14	Leu	8.001	4.162	1.651, 1.548		0.889, 0.851	-----	-----	-----
15	Ala				-----	-----	-----	-----	-----
16	Asp	8.07	4.639	2.845,	-----		-----	-----	-----
17	dAla	7.939	4.192	1.393	-----	-----	-----	-----	-----
18	Gly	8.054	3.657,	-----	-----	-----	-----	-----	-----
19	Pro	-----	4.359	2.212,	1.975,	3.526, 3.442	-----	-----	-----
20	Ala	8.273	4.315	1.37	-----	-----	-----	-----	-----
21	Ser	7.887	4.282	3.854,		-----	-----	-----	-----

cp TC4e –SGUDA- Y10L

RPPPSGUDALAQWLADaGPAS

300K pH 6.5

#	Res	HN	Hα	Hβ	Hγ	Hδ	Hε	Hζ	Hη
1	Arg		4.399	1.991, 1.808	1.724,	3.241,	7.297	-----	, , ,
2	Pro	-----	4.748	2.351, 1.817	1.997, 2.001	3.733, 3.558	-----	-----	-----
3	Pro	-----	3.804	1.575, 1.575	1.877, 1.873	3.677, 3.514	-----	-----	-----
4	Pro	-----	4.4	2.187,	1.834, 1.779	3.231, 3.104	-----	-----	-----
5	Ser	7.774	4.204	3.856, 3.778		-----	-----	-----	-----
6	Gly	8.262	3.999, 3.869	-----	-----	-----	-----	-----	-----
7	Aib		-----	,	-----	-----	-----	-----	-----
8	Asp	8.305	4.474	2.732, 2.654	-----		-----	-----	-----
9	Ala	7.955	4.235	1.419	-----	-----	-----	-----	-----
10	Leu	8.107	4.19	1.849, 1.588	1.674	0.957, 0.893	-----	-----	-----
11	Ala	7.875	4.168	1.492	-----	-----	-----	-----	-----
12	Gln	8.072	4.096	2.111, 2.111	2.385, 2.383	-----	,	-----	-----
13	Trp	8.076	4.473	3.300, 3.571	-----	7.216	10.044, 7.622	7.397, 7.150	7.214
14	Leu	8.493	3.922	1.847, 1.521		0.935,	-----	-----	-----
15	Ala	7.958	4.115	1.461	-----	-----	-----	-----	-----
16	Asp	7.978	4.576	2.752, 2.703	-----		-----	-----	-----
17	dAla	7.651	4.315	1.341	-----	-----	-----	-----	-----
18	Gly	8.119	2.752, 3.110	-----	-----	-----	-----	-----	-----
19	Pro	-----	4.414	2.296, 2.015	2.015,	3.488, 3.285	-----	-----	-----
20	Ala	8.088	4.371	1.401	-----	-----	-----	-----	-----
21	Ser	8.285	4.385	3.852, 3.812		-----	-----	-----	-----

cp TC4e –SGUDA- Y10L

RPPPSGUDALAQWLADaGPAS

300K pH 2.5

#	Res	HN	Hα	Hβ	Hγ	Hδ	Hε	Hζ	Hη
1	Arg		4.377	1.969, 1.774	1.719,	3.236,	7.237	-----	, , ,
2	Pro	-----	4.722	2.358, 1.838	2.004, 2.009	3.741, 3.549	-----	-----	-----
3	Pro	-----	4.238	1.716, 1.949	1.948,	3.719, 3.531	-----	-----	-----
4	Pro	-----	4.407	2.240,	1.903, 1.837	3.447, 3.294	-----	-----	-----
5	Ser	8.06	4.446	3.979, 3.848		-----	-----	-----	-----
6	Gly		3.969, 3.870	-----	-----	-----	-----	-----	-----
7	Aib		-----	,	-----	-----	-----	-----	-----
8	Asp		4.599	2.947, 2.885	-----		-----	-----	-----
9	Ala		4.196	1.425	-----	-----	-----	-----	-----
10	Leu		4.215	1.811, 1.586	1.653	0.934, 0.872	-----	-----	-----
11	Ala		4.128	1.457	-----	-----	-----	-----	-----
12	Gln	8.084	4.105	2.097, 2.095	2.404, 2.354	-----	,	-----	-----
13	Trp		4.446	3.338, 3.532	-----		, 7.568	7.392, 7.108	7.189
14	Leu	8.475	3.941	1.823, 1.514		0.911,	-----	-----	-----
15	Ala		4.128	1.457	-----	-----	-----	-----	-----
16	Asp	7.905	4.695	2.982, 2.919	-----		-----	-----	-----
17	dAla		4.29	1.349	-----	-----	-----	-----	-----
18	Gly		2.850, 3.220	-----	-----	-----	-----	-----	-----
19	Pro	-----	4.374	2.248, 1.974	1.978,	3.459, 3.245	-----	-----	-----
20	Ala		4.326	1.387	-----	-----	-----	-----	-----
21	Ser	8.259	4.403	3.896, 3.833		-----	-----	-----	-----

cp TC4e –SGUNA- Y10L

RPPPSGUNALAQWLADaGPAS

300K pH 6.5

#	Res	HN	Hα	Hβ	Hγ	Hδ	Hε	Hζ	Hη
1	Arg		4.383	1.978, 1.788	1.718, 1.718	3.233,	7.276	-----	, , ,
2	Pro	-----	4.742	2.350, 1.828	2.001, 2.002	3.735, 3.555	-----	-----	-----
3	Pro	-----	4.004	1.639, 1.747	1.901,	3.692, 3.525	-----	-----	-----
4	Pro	-----	4.401	2.203, 1.877	1.829, 1.828	3.333, 3.201	-----	-----	-----
5	Ser	7.785	4.211	3.854, 3.795		-----	-----	-----	-----
6	Gly	8.291	3.999, 3.879	-----	-----	-----	-----	-----	-----
7	Aib		-----	,	-----	-----	-----	-----	-----
8	Asn	8.34	4.609	2.869, 2.791	-----	,	-----	-----	-----
9	Ala	7.979	4.238	1.413	-----	-----	-----	-----	-----
10	Leu	8.109	4.215	1.789, 1.596	1.661	0.947, 0.884	-----	-----	-----
11	Ala	7.928	4.162	1.438	-----	-----	-----	-----	-----
12	Gln	8.098	4.107	2.082, 2.082	2.386, 2.345	-----	,	-----	-----
13	Trp	8.062	4.513	3.287, 3.526	-----	7.224	10.076, 7.614	7.410, 7.145	7.214
14	Leu	8.394	3.982	1.788, 1.514		0.913,	-----	-----	-----
15	Ala	7.964	4.12	1.439	-----	-----	-----	-----	-----
16	Asp	7.995	4.576	2.711, 2.711	-----		-----	-----	-----
17	dAla	7.726	4.321	1.353	-----	-----	-----	-----	-----
18	Gly	8.119	2.986, 3.238	-----	-----	-----	-----	-----	-----
19	Pro	-----	4.405	2.275, 2.006	2.005,	3.497, 3.321	-----	-----	-----
20	Ala	8.142	4.358	1.394	-----	-----	-----	-----	-----
21	Ser	8.269	4.389	3.858, 3.816		-----	-----	-----	-----

cp TC4e –SGUNA- Y10L

RPPPSGUNALAQWLADaGPAS

300K pH 2.5

#	Res	HN	Hα	Hβ	Hγ	Hδ	Hε	Hζ	Hη
1	Arg		4.376	1.963, 1.775	1.717,	3.235,	7.237	-----	, , ,
2	Pro	-----	4.728	2.352, 1.833	2.001, 2.004	3.737, 3.545	-----	-----	-----
3	Pro	-----	4.2	1.701, 1.935	1.933,	3.712, 3.523	-----	-----	-----
4	Pro	-----	4.401	2.237,	1.896, 1.833	3.415, 3.265	-----	-----	-----
5	Ser	8.06	4.446	3.980, 3.847		-----	-----	-----	-----
6	Gly		3.978, 3.886	-----	-----	-----	-----	-----	-----
7	Aib		-----	,	-----	-----	-----	-----	-----
8	Asn		4.606	2.857, 2.801	-----	,	-----	-----	-----
9	Ala		4.197	1.423	-----	-----	-----	-----	-----
10	Leu		4.211	1.806, 1.581	1.65	0.940, 0.876	-----	-----	-----
11	Ala		4.131	1.459	-----	-----	-----	-----	-----
12	Gln		4.108	2.097, 2.095	2.406, 2.353	-----	,	-----	-----
13	Trp		4.453	3.335, 3.539	-----		, 7.573	7.397, 7.117	7.195
14	Leu	8.471	3.943	1.825, 1.518		0.918,	-----	-----	-----
15	Ala		4.131	1.459	-----	-----	-----	-----	-----
16	Asp	7.909	4.689	2.981, 2.934	-----		-----	-----	-----
17	dAla		4.291	1.349	-----	-----	-----	-----	-----
18	Gly		2.849, 3.209	-----	-----	-----	-----	-----	-----
19	Pro	-----	4.371	2.253, 1.976	1.979,	3.465, 3.266	-----	-----	-----
20	Ala		4.327	1.388	-----	-----	-----	-----	-----
21	Ser	8.282	4.397	3.891, 3.828		-----	-----	-----	-----

cp TC4e A15G P19W D22

RPPPSDAALYAQWLGDaGWASD

300K pH 6.5

#	Res	HN	Hα	Hβ	Hγ	Hδ	Hε	Hζ	Hη
1	Arg		4.483	1.991,	1.849, 1.619	3.248, 3.190	7.573	-----	, , ,
2	Pro	-----	4.246	1.751, 2.403	2.058, 1.984	3.776, 3.525	-----	-----	-----
3	Pro	-----	2.563	1.174, 0.209	1.682, 1.443	3.263, 2.704	-----	-----	-----
4	Pro	-----	4.352	1.914, 2.226	1.797,	3.148, 2.821	-----	-----	-----
5	Ser	8.279	4.216	3.882, 3.803		-----	-----	-----	-----
6	Asp	8.216	4.432	2.753, 2.612	-----		-----	-----	-----
7	Ala	8.735	4.048	1.442	-----	-----	-----	-----	-----
8	Ala	8.497	4.287	1.483	-----	-----	-----	-----	-----
9	Leu	8.023	4.414	1.755, 1.657		0.985, 0.871	-----	-----	-----
10	Tyr	8.422	4.03	3.101,	-----			-----	
11	Ala	8.39	4.12	1.544	-----	-----	-----	-----	-----
12	Gln	7.943	4.035	2.139,	2.422, 2.350	-----	,	-----	-----
13	Trp	7.969	4.158	3.043, 3.468	-----	6.818	9.490,	6.296, 6.909	6.447
14	Leu	8.484	3.378	1.693, 1.417	1.5	0.908, 0.843	-----	-----	-----
15	Gly	7.982	3.869, 3.782	-----	-----	-----	-----	-----	-----
16	Asp	7.758	4.616	2.824, 2.680	-----		-----	-----	-----
17	dAla	7.377	4.257	1.209	-----	-----	-----	-----	-----
18	Gly	8.026	1.104, 2.947	-----	-----	-----	-----	-----	-----
19	Trp	8.389	4.609	3.463, 3.175	-----	7.48	10.314, 7.799	7.538, 7.231	7.306
20	Ala	7.822	4.452	1.368	-----	-----	-----	-----	-----
21	Ser	7.636	4.228	3.895, 3.591		-----	-----	-----	-----
22	Asp	7.953	4.639	2.770, 2.653	-----		-----	-----	-----

cp TC4e A15G P19W D22

RPPPSDAALYAQWLGDaGWASD

300K pH 2.5

#	Res	HN	Hα	Hβ	Hγ	Hδ	Hε	Hζ	Hη
1	Arg			1.858, 1.767	1.679, 1.519	3.104, 3.065	7.181	-----	, , ,
2	Pro	-----	4.639	1.815, 2.355	1.977,	3.643, 3.367	-----	-----	-----
3	Pro	-----	4.16	1.702, 1.902	1.792,	3.559, 3.508	-----	-----	-----
4	Pro	-----	4.209	1.861, 2.106	1.802,	3.468, 3.317	-----	-----	-----
5	Ser	7.901	4.348	3.825, 3.827		-----	-----	-----	-----
6	Asp	8.147	4.726	2.913,	-----		-----	-----	-----
7	Ala	8.319	4.101	1.448	-----	-----	-----	-----	-----
8	Ala	8.258	4.237	1.446	-----	-----	-----	-----	-----
9	Leu	7.762	4.237	1.677, 1.524	1.599	0.921, 0.837	-----	-----	-----
10	Tyr	8.252	4.172	3.011, 2.945	-----			-----	
11	Ala	8.13	4.078	1.466	-----	-----	-----	-----	-----
12	Gln	7.912	4.084	2.115,	2.391, 2.287	-----	,	-----	-----
13	Trp	8.065	4.288	3.142, 3.377	-----	6.982	9.747,	6.957, 7.155	6.901
14	Leu	8.376	3.677	1.572, 1.433		0.804, 0.802	-----	-----	-----
15	Gly		,	-----	-----	-----	-----	-----	-----
16	Asp	7.824	4.736	2.958, 2.869	-----		-----	-----	-----
17	dAla	7.668	4.217	1.189	-----	-----	-----	-----	-----
18	Gly	7.915	2.535, 3.101	-----	-----	-----	-----	-----	-----
19	Trp	7.739	4.578	3.278, 3.190	-----	7.281	10.137, 7.624	7.465, 7.157	7.229
20	Ala	7.845	4.292	1.254	-----	-----	-----	-----	-----
21	Ser	8.119	4.266	3.960, 3.846		-----	-----	-----	-----
22	Asp			,	-----		-----	-----	-----

cp TC4e D6N P19W

RPPPSNAALYAQWLADaGWAS

300K pH 6.5

#	Res	HN	Hα	Hβ	Hγ	Hδ	Hε	Hζ	Hη
1	Arg		4.477	1.961, 1.961	1.798, 1.683	3.200,	7.309	-----	, , ,
2	Pro	-----	4.065	1.719, 2.381	2.081, 2.009	3.788, 3.517	-----	-----	-----
3	Pro	-----	2.495	1.159, 0.206	1.646, 1.429	3.215, 2.680	-----	-----	-----
4	Pro	-----	4.318	1.769, 2.208	1.891,	3.085, 2.771	-----	-----	-----
5	Ser	8.303	4.205	3.892, 3.819		-----	-----	-----	-----
6	Asn	7.959	4.494	2.773, 2.699	-----	,	-----	-----	-----
7	Ala	8.883	4.048	1.446	-----	-----	-----	-----	-----
8	Ala	8.237	4.288	1.482	-----	-----	-----	-----	-----
9	Leu	7.887	4.471	1.715, 1.625	1.715	0.986, 0.874	-----	-----	-----
10	Tyr	8.271	3.99	3.114,	-----			-----	
11	Ala	8.519	4.1	1.554	-----	-----	-----	-----	-----
12	Gln	7.976	3.979	2.171, 2.096	2.417,	-----	,	-----	-----
13	Trp	7.913	4.157	3.018, 3.497	-----	6.812	9.234, 6.891	6.606, 6.891	6.251
14	Leu	8.356	3.271	1.698, 1.434	1.509	0.901, 0.843	-----	-----	-----
15	Ala	7.865	4.002	1.462	-----	-----	-----	-----	-----
16	Asp	7.593	4.686	2.863, 2.776	-----		-----	-----	-----
17	dAla	7.282	4.302	1.2	-----	-----	-----	-----	-----
18	Gly	8.075	0.999, 2.803	-----	-----	-----	-----	-----	-----
19	Trp	8.415	4.614	3.457, 3.177	-----	7.503	10.378, 7.774	7.546, 7.215	7.317
20	Ala	7.78	4.452	1.373	-----	-----	-----	-----	-----
21	Ser	7.502	4.083	3.856, 3.530		-----	-----	-----	-----

cp TC4e D6N P19W

RPPPSNAALYAQWLADaGWAS

300K pH 2.5

#	Res	HN	Hα	Hβ	Hγ	Hδ	Hε	Hζ	Hη
1	Arg		4.332	1.909, 1.870	1.718, 1.614	3.126, 3.072	7.181	-----	, , ,
2	Pro	-----	4.515	1.809, 2.354	2.009, 2.005	3.718, 3.466	-----	-----	-----
3	Pro	-----		1.493, 1.228	1.826, 1.723	3.402, 3.366	-----	-----	-----
4	Pro	-----	4.296	1.792, 2.179	,	3.257, 3.029	-----	-----	-----
5	Ser	8.202	4.25	3.959, 3.845		-----	-----	-----	-----
6	Asn	7.998	4.652	2.883, 2.784	-----	,	-----	-----	-----
7	Ala	8.626	4.107	1.466	-----	-----	-----	-----	-----
8	Ala	8.218	4.272	1.5	-----	-----	-----	-----	-----
9	Leu	7.987	4.287	1.790, 1.616	1.687	0.958, 0.866	-----	-----	-----
10	Tyr	8.507	4.021	2.995,	-----			-----	
11	Ala	8.193	4.039	1.549	-----	-----	-----	-----	-----
12	Gln	7.78	4.052	2.194, 2.195	2.474, 2.388	-----	,	-----	-----
13	Trp	8.132	4.074	3.054, 3.440	-----	6.751	9.366,	,	
14	Leu	8.471	3.462	1.622, 1.431	1.432	0.839, 0.803	-----	-----	-----
15	Ala	7.861	4.056	1.453	-----	-----	-----	-----	-----
16	Asp	7.804	4.648	3.010, 2.875	-----		-----	-----	-----
17	dAla	7.34	4.197	1.119	-----	-----	-----	-----	-----
18	Gly	7.88	1.734, 2.734	-----	-----	-----	-----	-----	-----
19	Trp		4.596	3.308, 3.199	-----	7.339	10.186, 7.679	7.473, 7.183	7.248
20	Ala	7.779	4.362	1.284	-----	-----	-----	-----	-----
21	Ser	7.872	4.368	3.943, 3.780		-----	-----	-----	-----

cp TC4e D9Abu P19W

RPPPSDAALYAQWLA(Abu)aGWAS

300K pH 6.5

#	Res	HN	Hα	Hβ	Hγ	Hδ	Hε	Hζ	Hη
1	Arg			1.912,	,	3.152, 3.094		-----	, , ,
2	Pro	-----	4.241	2.371, 1.756	2.051, 2.003	3.746, 3.490	-----	-----	-----
3	Pro	-----	2.925	1.259, 0.515	1.713, 1.546	3.308, 3.004	-----	-----	-----
4	Pro	-----	4.292	2.226,	1.832, 1.772	3.073, 2.798	-----	-----	-----
5	Ser	8.201	4.19	3.881, 3.803		-----	-----	-----	-----
6	Asp	7.566	4.599	2.668,	-----		-----	-----	-----
7	Ala	8.682	4.068	1.474	-----	-----	-----	-----	-----
8	Ala	8.471	4.297	1.493	-----	-----	-----	-----	-----
9	Leu	8.032	4.372	1.777, 1.646	1.717	0.990, 0.884	-----	-----	-----
10	Tyr	8.563	4.029	3.094,	-----			-----	
11	Ala	8.28	4.104	1.576	-----	-----	-----	-----	-----
12	Gln	7.823	4.121	2.184,	2.510, 2.410	-----	,	-----	-----
13	Trp	8.071	4.081	3.481, 3.044	-----	6.729	9.138, 6.944	6.589, 6.874	6.783
14	Leu	8.483	3.375	1.627, 1.482	1.482	, 0.869	-----	-----	-----
15	Ala	7.753	4.056	1.481	-----	-----	-----	-----	-----
16	Xaa		,	,	,	,	,	,	,
17	dAla	7.282	4.241	1.149	-----	-----	-----	-----	-----
18	Gly	7.832	1.388, 2.896	-----	-----	-----	-----	-----	-----
19	Trp	8.097	4.631	3.200, 3.434	-----	7.451	10.275, 7.732	7.519, 7.201	7.304
20	Ala	7.853	4.427	1.365	-----	-----	-----	-----	-----
21	Ser	7.595	4.157	3.834, 3.637		-----	-----	-----	-----

cp TC4e D9S P19W

RPPPSDAALYAQWLASaGWAS

300K pH 6.5

#	Res	HN	Hα	Hβ	Hγ	Hδ	Hε	Hζ	Hη
1	Arg		4.42	1.931, 1.928	1.750, 1.674	3.179, 3.131	7.178	-----	, , ,
2	Pro	-----	4.165	1.738, 2.364	2.064, 2.002	3.765, 3.498	-----	-----	-----
3	Pro	-----	2.741	1.223, 0.370	1.683, 1.481	3.271, 2.887	-----	-----	-----
4	Pro	-----	4.297	2.227, 1.850	1.778, 1.781	3.080, 2.786	-----	-----	-----
5	Ser	8.248	4.188	3.886, 3.806		-----	-----	-----	-----
6	Asp	7.554	4.606	2.700, 2.650	-----		-----	-----	-----
7	Ala	8.756	4.062	1.468	-----	-----	-----	-----	-----
8	Ala	8.507	4.301	1.502	-----	-----	-----	-----	-----
9	Leu	8.039	4.4	1.788, 1.674	1.789	0.992, 0.882	-----	-----	-----
10	Tyr	8.536	4.004	3.099,	-----			-----	
11	Ala	8.42	4.113	1.594	-----	-----	-----	-----	-----
12	Gln	7.951	4.129	2.188, 2.189	2.517, 2.432	-----	,	-----	-----
13	Trp	8.225	4.05	3.054, 3.519	-----	6.762	9.146, 6.749	6.500, 6.909	6.5
14	Leu	8.648	3.308	1.621, 1.496	1.508	0.881, 0.881	-----	-----	-----
15	Ala	7.923	4.087	1.483	-----	-----	-----	-----	-----
16	Ser	7.61	4.401	3.981, 3.923		-----	-----	-----	-----
17	dAla	7.251	4.286	1.152	-----	-----	-----	-----	-----
18	Gly	7.781	1.249, 2.783	-----	-----	-----	-----	-----	-----
19	Trp	8.153	4.625	3.420, 3.206	-----	7.448	10.314, 7.729	7.526, 7.199	7.304
20	Ala	7.79	4.421	1.352	-----	-----	-----	-----	-----
21	Ser	7.555	4.144	3.837, 3.631		-----	-----	-----	-----

cp TC4e D9S P19W

RPPPSDAALYAQWLASaGWAS

300K pH 2.5

#	Res	HN	Hα	Hβ	Hγ	Hδ	Hε	Hζ	Hη
1	Arg			1.842, 1.726	1.654, 1.481	3.083, 3.024	7.139	-----	, , ,
2	Pro	-----	4.597	1.803, 2.340	1.975, 1.975	3.623, 3.334	-----	-----	-----
3	Pro	-----	4.04	, 1.651	,	3.490, 3.541	-----	-----	-----
4	Pro	-----		,	,	,	-----	-----	-----
5	Ser	8.084	4.249	3.991, 3.862		-----	-----	-----	-----
6	Asp	8.133	4.74	2.957, 2.915	-----		-----	-----	-----
7	Ala	8.37	4.092	1.47	-----	-----	-----	-----	-----
8	Ala	8.301	4.255	1.495	-----	-----	-----	-----	-----
9	Leu	7.8	4.28	1.788, 1.628	1.69	0.951, 0.869	-----	-----	-----
10	Tyr	8.413	4.042	2.977, 2.888	-----			-----	
11	Ala	8.25	4.036	1.551	-----	-----	-----	-----	-----
12	Gln	7.901	4.121	2.232, 2.234	2.523, 2.421	-----	,	-----	-----
13	Trp	8.267	4.035	3.093, 3.427	-----		,	,	
14	Leu	8.553	3.468	1.611, 1.420		, 0.794	-----	-----	-----
15	Ala	7.894	4.088	1.47	-----	-----	-----	-----	-----
16	Ser	7.617	4.398	3.978, 3.916		-----	-----	-----	-----
17	dAla	7.361	4.209	1.084	-----	-----	-----	-----	-----
18	Gly	7.721	2.041, 2.771	-----	-----	-----	-----	-----	-----
19	Trp		4.578	3.262, 3.206	-----	7.268	10.148, 7.618	7.457, 7.149	7.227
20	Ala	7.783	4.35	1.264	-----	-----	-----	-----	-----
21	Ser	7.92	4.396	3.950, 3.812		-----	-----	-----	-----

cp TC4e D22

RPPPSDAALYAQWLADaGPASD

300K pH 6.5

#	Res	HN	Hα	Hβ	Hγ	Hδ	Hε	Hζ	Hη
1	Arg		4.521	2.042,	2.401,	3.216,		-----	, , ,
2	Pro	-----	4.764	2.361, 1.773	1.974,	3.705, 3.459	-----	-----	-----
3	Pro	-----	3.051	1.399, 0.850	1.833, 1.768	3.606, 3.522	-----	-----	-----
4	Pro	-----	4.283	2.200, 1.866	1.810,	3.214, 2.958	-----	-----	-----
5	Ser	8.193	4.213	3.894, 3.806		-----	-----	-----	-----
6	Asp	7.616	4.641	2.809, 2.704	-----		-----	-----	-----
7	Ala	8.675	4.097	1.486	-----	-----	-----	-----	-----
8	Ala	8.498	4.311	1.503	-----	-----	-----	-----	-----
9	Leu	8.072	4.374	1.734, 1.630	1.801	0.998, 0.896	-----	-----	-----
10	Tyr	8.639	4.069	3.107,	-----	7.061	6.806	-----	
11	Ala	8.354	4.122	1.576	-----	-----	-----	-----	-----
12	Gln	7.885	4.036	2.191, 2.134	2.423,	-----	6.902, 7.698	-----	-----
13	Trp	8.054	4.259	3.151, 3.567	-----	7.09	9.869, 7.283	7.278, 7.081	7.212
14	Leu	8.445	3.431	1.759, 1.538	1.423	0.915, 0.864	-----	-----	-----
15	Ala	7.88	4.038	1.473	-----	-----	-----	-----	-----
16	Asp	7.92	4.573	2.816, 2.720	-----		-----	-----	-----
17	dAla	7.402	4.284	1.269	-----	-----	-----	-----	-----
18	Gly	8.2	1.442, 2.780	-----	-----	-----	-----	-----	-----
19	Pro	-----	4.417	2.266, 1.981	1.992,	3.751, 3.581	-----	-----	-----
20	Ala	7.667	4.426	1.387	-----	-----	-----	-----	-----
21	Ser	7.881	4.281	3.921, 3.666		-----	-----	-----	-----
22	Asp	8.06	4.471	2.764, 2.692	-----		-----	-----	-----

cp TC4e D22

RPPPSDAALYAQWLADaGPASD

300K pH 2.5

#	Res	HN	Hα	Hβ	Hγ	Hδ	Hε	Hζ	Hη
1	Arg		4.386	1.957,	1.733,	3.229,	7.237	-----	, , ,
2	Pro	-----	4.789	2.407, 2.030	1.873,	3.768, 3.578	-----	-----	-----
3	Pro	-----	4.086	1.804, 2.026	1.925, 1.925	3.572, 3.476	-----	-----	-----
4	Pro	-----	4.353	2.264,	1.953,	3.403, 3.028	-----	-----	-----
5	Ser	8.026	4.421	3.864,		-----	-----	-----	-----
6	Asp	7.812	4.681	3.016, 2.906	-----		-----	-----	-----
7	Ala	8.238	4.11	1.486	-----	-----	-----	-----	-----
8	Ala	8.407	4.264	1.486	-----	-----	-----	-----	-----
9	Leu	7.743	4.247	1.679, 1.587	1.753	0.974, 0.905	-----	-----	-----
10	Tyr		4.156	3.034,	-----			-----	
11	Ala	8.155	4.051	1.532	-----	-----	-----	-----	-----
12	Gln	7.83	4.073	2.472, 2.380	2.189,	-----	,	-----	-----
13	Trp	8.131	4.272	3.453, 3.219	-----	7.131	10.112, 7.337	7.337, 7.079	7.189
14	Leu	8.363	3.562	1.662, 1.419	1.452	0.808,	-----	-----	-----
15	Ala	7.915	4.079	1.454	-----	-----	-----	-----	-----
16	Asp	8.252	4.762	2.962,	-----		-----	-----	-----
17	dAla	7.53	4.285	1.296	-----	-----	-----	-----	-----
18	Gly	7.942	2.332, 2.806	-----	-----	-----	-----	-----	-----
19	Pro	-----	4.756	2.341, 1.806	1.944,	3.546, 3.212	-----	-----	-----
20	Ala	7.895	4.344	1.393	-----	-----	-----	-----	-----
21	Ser		4.167	4.050, 3.996		-----	-----	-----	-----
22	Asp	8.317	4.735	,	-----		-----	-----	-----

cp TC4e P4A P19W D22

RPPASDAALYAQWLADaGWASD

300K pH 6.5

#	Res	HN	Hα	Hβ	Hγ	Hδ	Hε	Hζ	Hη
1	Arg		3.959	1.727, 1.533	1.287,	3.026, 2.973	7.155	-----	, , ,
2	Pro	-----	4.613	2.240,	1.883, 1.760	3.427,	-----	-----	-----
3	Pro	-----	4.304	1.898, 2.141	1.941, 1.941	3.626, 3.510	-----	-----	-----
4	Ala	8.227	3.86	1.175	-----	-----	-----	-----	-----
5	Ser	7.949	4.201	3.963, 3.815		-----	-----	-----	-----
6	Asp	7.455	4.565	3.256,	-----		-----	-----	-----
7	Ala	8.414	4.262	1.489	-----	-----	-----	-----	-----
8	Ala	8.13	4.101	1.483	-----	-----	-----	-----	-----
9	Leu	7.871	4.228	1.752, 1.579	1.692	0.950, 0.886	-----	-----	-----
10	Tyr	8.456	4.111	3.003, 2.954	-----			-----	
11	Ala	8.121	4.041	1.523	-----	-----	-----	-----	-----
12	Gln	7.823	4.047	2.205,	2.463, 2.391	-----	,	-----	-----
13	Trp	8.134	4.188	3.118, 3.403	-----	6.958	9.988, 7.088	6.866, 7.043	6.866
14	Leu	8.31	3.534	1.657, 1.373	1.436	0.779,	-----	-----	-----
15	Ala	7.871	4.053	1.451	-----	-----	-----	-----	-----
16	Asp	7.878	4.623	2.892, 2.789	-----		-----	-----	-----
17	dAla	7.415	4.198	1.118	-----	-----	-----	-----	-----
18	Gly	7.85	2.414, 2.607	-----	-----	-----	-----	-----	-----
19	Trp	7.953	4.747	2.915, 2.686	-----	7.236	10.164, 7.593	7.456, 7.147	7.226
20	Ala	7.835	4.302	1.238	-----	-----	-----	-----	-----
21	Ser	7.91	4.384	3.875, 3.816		-----	-----	-----	-----
22	Asp	8.039	4.528	2.829, 2.777	-----		-----	-----	-----

cp TC4e P19W

RPPPSDAALYAQWLADaGWAS

300K pH 6.5

#	Res	HN	Hα	Hβ	Hγ	Hδ	Hε	Hζ	Hη
1	Arg		4.516	1.981, 1.954	1.810, 1.687	3.207,	7.335	-----	, , ,
2	Pro	-----	4.051	2.386, 1.718	2.087, 2.009	3.803, 3.536	-----	-----	-----
3	Pro	-----	2.373	1.108, 0.025	1.638, 1.397	3.214, 2.623	-----	-----	-----
4	Pro	-----	4.341	2.243, 1.902	1.785, 1.759	3.078, 2.727	-----	-----	-----
5	Ser	8.29	4.19	3.869, 3.798		-----	-----	-----	-----
6	Asp	7.61	4.61	2.688, 2.621	-----		-----	-----	-----
7	Ala	8.807	4.031	1.445	-----	-----	-----	-----	-----
8	Ala	8.544	4.292	1.493	-----	-----	-----	-----	-----
9	Leu	8.011	4.446	1.775, 1.690		0.992, 0.877	-----	-----	-----
10	Tyr	8.404	3.976	3.113,	-----			-----	
11	Ala	8.46	4.105	1.567	-----	-----	-----	-----	-----
12	Gln	7.948	3.976	2.174, 2.099	2.416,	-----	,	-----	-----
13	Trp	7.939	4.134	3.509, 3.007	-----	6.788	9.188, 6.879	6.204, 6.879	6.582
14	Leu	8.383	3.258	1.701, 1.440	1.506	0.911, 0.856	-----	-----	-----
15	Ala	7.843	4	1.463	-----	-----	-----	-----	-----
16	Asp	7.958	4.489	2.783, 2.701	-----		-----	-----	-----
17	dAla	7.255	4.301	1.194	-----	-----	-----	-----	-----
18	Gly	8.075	0.894, 2.791	-----	-----	-----	-----	-----	-----
19	Trp	8.442	4.62	3.178, 3.470	-----	7.515	10.358, 7.789	7.551, 7.228	7.322
20	Ala	7.771	4.457	1.378	-----	-----	-----	-----	-----
21	Ser	7.491	4.077	3.856, 3.517		-----	-----	-----	-----

cp TC4e P19W

RPPPSDAALYAQWLADaGWAS

300K pH 2.5

#	Res	HN	Hα	Hβ	Hγ	Hδ	Hε	Hζ	Hη
1	Arg		4.2	1.850, 1.747	1.661, 1.494	3.083, 3.018	7.148	-----	, , ,
2	Pro	-----	4.581	2.352, 2.350	1.979, 1.807	3.641, 3.354	-----	-----	-----
3	Pro	-----	4.007	1.625, 1.625	1.868, 1.825	3.482, 3.482	-----	-----	-----
4	Pro	-----	4.192	2.084,	,	,	-----	-----	-----
5	Ser	8.097	4.248	3.992, 3.862		-----	-----	-----	-----
6	Asp	7.626	4.591	3.281, 3.201	-----		-----	-----	-----
7	Ala	8.403	4.099	1.47	-----	-----	-----	-----	-----
8	Ala	8.285	4.254	1.489	-----	-----	-----	-----	-----
9	Leu	7.805	4.274	1.794, 1.614	1.68	0.941, 0.854	-----	-----	-----
10	Tyr	8.41	4.035	2.971,	-----			-----	
11	Ala	8.225	4.028	1.54	-----	-----	-----	-----	-----
12	Gln	7.826	4.057	2.203,	2.476, 2.390	-----	,	-----	-----
13	Trp	8.12	4.091	3.080, 3.422	-----	6.822	9.543,	,	
14	Leu	8.427	3.473	1.629, 1.611	1.418	0.818, 0.786	-----	-----	-----
15	Ala	7.885	4.057	1.453	-----	-----	-----	-----	-----
16	Asp	7.805	4.66	3.005, 2.877	-----		-----	-----	-----
17	dAla	7.359	4.192	1.109	-----	-----	-----	-----	-----
18	Gly	7.851	1.885, 2.700	-----	-----	-----	-----	-----	-----
19	Trp			,	-----	7.299	10.164,	,	
20	Ala	7.776	4.354	1.267	-----	-----	-----	-----	-----
21	Ser	7.883	4.38	3.948, 3.808		-----	-----	-----	-----

cp TC4e P19W D22

RPPPSDAALYAQWLADaGWASD

300K pH 6.5

#	Res	HN	Hα	Hβ	Hγ	Hδ	Hε	Hζ	Hη
1	Arg	7.637	4.517	2.014, 1.970	1.871, 1.622	3.273, 3.200		-----	, , ,
2	Pro	-----	4.189	1.736, 2.401	1.983, 2.069	3.545, 3.795	-----	-----	-----
3	Pro	-----	2.309	1.086, -0.055	1.636, 1.369	3.216, 2.562	-----	-----	-----
4	Pro	-----	4.364	1.926, 2.232	1.777,	2.740, 3.095	-----	-----	-----
5	Ser	8.287	4.205	3.876, 3.798		-----	-----	-----	-----
6	Asp	7.911	4.512	2.835, 2.706	-----		-----	-----	-----
7	Ala	8.811	4.042	1.451	-----	-----	-----	-----	-----
8	Ala	8.534	4.296	1.494	-----	-----	-----	-----	-----
9	Leu	8.04	4.448	1.784, 1.687	1.691	0.996, 0.881	-----	-----	-----
10	Tyr	8.456	3.969	3.099,	-----	7.014	6.76	-----	
11	Ala	8.457	4.105	1.567	-----	-----	-----	-----	-----
12	Gln	7.929	3.986	2.175, 2.091	2.410,	-----	,	-----	-----
13	Trp	7.915	4.108	3.493, 2.987	-----	6.767	9.410, 6.815	6.126, 6.856	6.335
14	Leu	8.388	3.281	1.746, 1.511	1.399	0.923, 0.851	-----	-----	-----
15	Ala	7.845	4.017	1.462	-----	-----	-----	-----	-----
16	Asp	8.019	4.453	2.729, 2.653	-----		-----	-----	-----
17	dAla	7.276	4.252	1.188	-----	-----	-----	-----	-----
18	Gly	8.098	0.720, 2.832	-----	-----	-----	-----	-----	-----
19	Trp	8.463	4.609	3.492, 3.159	-----	7.513	10.349, 7.834	7.547, 7.240	7.316
20	Ala	7.795	4.48	1.381	-----	-----	-----	-----	-----
21	Ser	7.58	4.201	3.899, 3.556		-----	-----	-----	-----
22	Asp	8.249	4.445	2.770, 2.617	-----		-----	-----	-----

cp TC4e P19W D22

RPPPSDAALYAQWLADaGWASD

300K pH 2.5

#	Res	HN	Hα	Hβ	Hγ	Hδ	Hε	Hζ	Hη
1	Arg		4.178	1.833, 1.723	1.662, 1.460	3.075, 3.010	7.18	-----	, , ,
2	Pro	-----	4.571	1.979, 2.351	1.800,	3.627, 3.324	-----	-----	-----
3	Pro	-----		, 1.790	1.859,	3.451,	-----	-----	-----
4	Pro	-----	4.16	, 2.067	, 1.788	,	-----	-----	-----
5	Ser	8.072	4.227	3.967, 3.843		-----	-----	-----	-----
6	Asp	8.286	4.76	2.955,	-----		-----	-----	-----
7	Ala	8.434	4.096	1.475	-----	-----	-----	-----	-----
8	Ala	8.313	4.262	1.486	-----	-----	-----	-----	-----
9	Leu	7.769	4.292	1.769, 1.618	1.671	0.947, 0.860	-----	-----	-----
10	Tyr	8.441	4.051	3.005,	-----			-----	
11	Ala	8.27	4.044	1.544	-----	-----	-----	-----	-----
12	Gln	7.821	4.059	2.188,	2.466, 2.383	-----	,	-----	-----
13	Trp	8.106	4.105	3.428, 3.082	-----	6.84	9.537,	,	
14	Leu	8.435	3.458	1.638,	1.425	, 0.819	-----	-----	-----
15	Ala	7.883	4.06	1.451	-----	-----	-----	-----	-----
16	Asp	7.794	4.658	3.008, 2.870	-----		-----	-----	-----
17	dAla	7.361	4.202	1.125	-----	-----	-----	-----	-----
18	Gly	7.851	2.730, 1.800	-----	-----	-----	-----	-----	-----
19	Trp		4.571	3.298, 3.198	-----	7.323	10.180, 7.660	7.473, 7.175	7.242
20	Ala	7.785	4.32	1.277	-----	-----	-----	-----	-----
21	Ser	7.839	4.361	3.856, 3.796		-----	-----	-----	-----
22	Asp			,	-----		-----	-----	-----

cp TC4e P19W S21-NH_2

RPPPSDAALYAQWLADaGWAS-NH_2

300K pH 6.5

#	Res	HN	Hα	Hβ	Hγ	Hδ	Hε	Hζ	Hη
1	Arg		4.433	1.948,	1.791, 1.639	3.207, 3.166	7.397	-----	, , ,
2	Pro	-----	4.283	1.768, 2.383	2.053, 1.980	3.764, 3.526	-----	-----	-----
3	Pro	-----	2.756	1.222, 0.361	1.710, 1.482	3.299, 2.878	-----	-----	-----
4	Pro	-----	4.333	1.795, 2.243	1.871,	3.164, 2.841	-----	-----	-----
5	Ser	8.248	4.21	3.882, 3.805		-----	-----	-----	-----
6	Asp	7.907	4.526	2.757, 2.662	-----		-----	-----	-----
7	Ala	8.73	4.068	1.461	-----	-----	-----	-----	-----
8	Ala	8.473	4.293	1.498	-----	-----	-----	-----	-----
9	Leu	8.088	4.366	1.795, 1.630	1.734	0.989, 0.884	-----	-----	-----
10	Tyr	8.602	4.008	3.077, 3.076	-----			-----	
11	Ala	8.312	4.081	1.563	-----	-----	-----	-----	-----
12	Gln	7.84	4.007	2.173, 2.125	2.420,	-----	,	-----	-----
13	Trp	8.013	4.141	3.030, 3.490	-----	6.826	9.335, 6.522	6.373, 6.908	6.535
14	Leu	8.428	3.357	1.693, 1.422	1.477	, 0.867	-----	-----	-----
15	Ala	7.832	4.02	1.463	-----	-----	-----	-----	-----
16	Asp	7.592	4.589	2.672, 2.672	-----		-----	-----	-----
17	dAla	7.317	4.269	1.183	-----	-----	-----	-----	-----
18	Gly	8.001	1.168, 2.800	-----	-----	-----	-----	-----	-----
19	Trp	8.273	4.589	3.429, 3.186	-----	7.486	10.346, 7.775	7.534, 7.223	7.303
20	Ala	7.813	4.382	1.348	-----	-----	-----	-----	-----
21	Ser	7.686	4.237	3.853, 3.661		-----	-----	-----	-----

cp TC4e P19W S21-NH_2

RPPPSDAALYAQWLADaGWAS-NH_2

300K pH 2.5

#	Res	HN	Hα	Hβ	Hγ	Hδ	Hε	Hζ	Hη
1	Arg			1.841, 1.721	1.655, 1.469	3.091, 3.009	7.156	-----	, , ,
2	Pro	-----	4.627	1.814, 2.348	1.974, 1.975	3.624, 3.334	-----	-----	-----
3	Pro	-----		1.661, 1.842	1.842,	3.537, 3.486	-----	-----	-----
4	Pro	-----	4.39	, 2.234	1.904,	,	-----	-----	-----
5	Ser	7.804	4.297	3.856, 3.787		-----	-----	-----	-----
6	Asp			,	-----		-----	-----	-----
7	Ala	8.378	4.102	1.472	-----	-----	-----	-----	-----
8	Ala	8.316	4.257	1.489	-----	-----	-----	-----	-----
9	Leu		4.268	1.787, 1.615	1.683	0.951, 0.871	-----	-----	-----
10	Tyr	8.28	4.029	2.971, 2.976	-----			-----	
11	Ala	8.212	4.026	1.539	-----	-----	-----	-----	-----
12	Gln	7.812	4.057	2.201, 2.200	2.476, 2.385	-----	,	-----	-----
13	Trp	8.13	4.096	3.086, 3.415	-----		,	,	
14	Leu	8.436	3.474	1.637, 1.415	1.415	, 0.802	-----	-----	-----
15	Ala	7.875	4.062	1.449	-----	-----	-----	-----	-----
16	Asp	7.805	4.662	3.008, 2.878	-----		-----	-----	-----
17	dAla	7.364	4.195	1.109	-----	-----	-----	-----	-----
18	Gly	7.851	1.965, 2.685	-----	-----	-----	-----	-----	-----
19	Trp		4.572	3.264, 3.209	-----	7.312	10.193, 7.651	7.477, 7.179	7.241
20	Ala	7.773	4.293	1.241	-----	-----	-----	-----	-----
21	Ser	8.074	4.246	3.981, 3.853		-----	-----	-----	-----

cp TC4e R1Δ

PPPSDAALYAQWLADaGPAS

300K pH 6.5

#	Res	HN	Hα	Hβ	Hγ	Hδ	Hε	Hζ	Hη
2	Pro	-----	4.375	2.250, 2.033	,	3.380, 3.190	-----	-----	-----
3	Pro	-----	3.81	1.571, 1.636	1.919, 1.844	3.598, 3.416	-----	-----	-----
4	Pro	-----	4.335	2.318, 1.823	1.923, 1.880	3.238, 3.066	-----	-----	-----
5	Ser	8.283	4.244	3.902, 3.803		-----	-----	-----	-----
6	Asp	7.901	4.55	2.682,	-----		-----	-----	-----
7	Ala	8.588	4.14	1.474	-----	-----	-----	-----	-----
8	Ala	8.339	4.288	1.491	-----	-----	-----	-----	-----
9	Leu	8.13	4.248	1.771, 1.539	1.703	0.972, 0.884	-----	-----	-----
10	Tyr	8.597	4.232	3.100, 3.045	-----			-----	
11	Ala	8.083	4.078	1.514	-----	-----	-----	-----	-----
12	Gln	7.835	4.051	2.416, 2.149	2.149,	-----	,	-----	-----
13	Trp	8.163	4.417	3.540, 3.276	-----	7.23	10.147, 7.337	7.337, 7.117	7.204
14	Leu	8.321	3.736	1.642, 1.443		0.821, 0.825	-----	-----	-----
15	Ala	7.838	4.063	1.454	-----	-----	-----	-----	-----
16	Asp	7.945	4.576	2.747, 2.669	-----		-----	-----	-----
17	dAla	7.594	4.285	1.31	-----	-----	-----	-----	-----
18	Gly	7.99	2.751, 2.751	-----	-----	-----	-----	-----	-----
19	Pro	-----	4.578	2.491, 1.938	2.051, 2.003	3.382,	-----	-----	-----
20	Ala	8.229	4.398	1.427	-----	-----	-----	-----	-----
21	Ser	7.846	4.243	3.840, 3.840		-----	-----	-----	-----

cp TC4e R1Δ

PPPSDAALYAQWLADaGPAS

300K pH 2.5

#	Res	HN	Hα	Hβ	Hγ	Hδ	Hε	Hζ	Hη
2	Pro	-----	4.391	2.279, 1.877	1.974,	3.631, 3.475	-----	-----	-----
3	Pro	-----	4.5	1.815, 2.207	1.992, 1.992	3.674, 3.504	-----	-----	-----
4	Pro	-----	4.323	2.205, 1.867	1.938,	3.333, 2.972	-----	-----	-----
5	Ser	8.037	4.467	3.970, 3.850		-----	-----	-----	-----
6	Asp	7.836	4.676	3.028, 2.918	-----		-----	-----	-----
7	Ala	8.389	4.141	1.462	-----	-----	-----	-----	-----
8	Ala	8.209	4.249	1.49	-----	-----	-----	-----	-----
9	Leu	7.89	4.222	1.816, 1.618	1.687	0.973, 0.907	-----	-----	-----
10	Tyr	8.404	4.701	2.956,	-----			-----	
11	Ala	8.058	3.997	1.498	-----	-----	-----	-----	-----
12	Gln	7.88	4.069	2.458, 2.381	2.196,	-----	,	-----	-----
13	Trp	8.142	4.242	3.416, 3.180	-----	7.212	10.127, 7.313	7.215, 7.078	7.167
14	Leu	8.33	3.587	1.615, 1.398		0.773, 0.774	-----	-----	-----
15	Ala	7.905	4.075	1.448	-----	-----	-----	-----	-----
16	Asp	7.836	4.676	3.028, 2.918	-----		-----	-----	-----
17	dAla	7.56	4.286	1.302	-----	-----	-----	-----	-----
18	Gly	7.945	2.435, 2.825	-----	-----	-----	-----	-----	-----
19	Pro	-----	4.598	2.519, 1.997	2.051, 1.999	3.382,	-----	-----	-----
20	Ala	8.417	4.378	1.402	-----	-----	-----	-----	-----
21	Ser	8.339	4.331	4.012, 3.889		-----	-----	-----	-----

cp TC4e R1Δ D22

PPPSDAALYAQWLADaGPASD

300K pH 6.5

#	Res	HN	Hα	Hβ	Hγ	Hδ	Hε	Hζ	Hη
2	Pro	-----	4.361	2.270, 1.974	,	3.363, 3.083	-----	-----	-----
3	Pro	-----	3.616	1.536, 1.537	1.904, 1.826	3.585, 3.404	-----	-----	-----
4	Pro	-----	4.323	2.324, 1.834	1.891, 1.811	3.160, 3.008	-----	-----	-----
5	Ser	8.29	4.224	3.889, 3.798		-----	-----	-----	-----
6	Asp	7.827	4.561	, 2.682	-----		-----	-----	-----
7	Ala	8.644	4.14	1.482	-----	-----	-----	-----	-----
8	Ala	8.368	4.3	1.497	-----	-----	-----	-----	-----
9	Leu	8.143	4.273	1.786, 1.562	1.718	0.982, 0.890	-----	-----	-----
10	Tyr	8.637	4.205	3.124, 3.054	-----			-----	
11	Ala	8.127	4.077	1.532	-----	-----	-----	-----	-----
12	Gln	7.837	4.037	2.417, 2.159	2.159,	-----	,	-----	-----
13	Trp	8.178	4.394	3.549, 3.276	-----	7.231	10.153, 7.281	7.316, 7.117	7.205
14	Leu	8.371	3.657	1.645, 1.449		0.837, 0.824	-----	-----	-----
15	Ala	7.835	4.053	1.461	-----	-----	-----	-----	-----
16	Asp	7.935	4.574	2.763, 2.668	-----		-----	-----	-----
17	dAla	7.531	4.291	1.302	-----	-----	-----	-----	-----
18	Gly	8.009	2.527, 2.646	-----	-----	-----	-----	-----	-----
19	Pro	-----	4.587	2.482, 1.918	2.049, 1.991	3.379,	-----	-----	-----
20	Ala	8.044	4.382	1.426	-----	-----	-----	-----	-----
21	Ser	8.132	4.474	3.881, 3.825		-----	-----	-----	-----
22	Asp	8.17	4.461	2.730, 2.622	-----		-----	-----	-----

cp TC4e R1Δ D22

PPPSDAALYAQWLADaGPASD

300K pH 2.5

#	Res	HN	Hα	Hβ	Hγ	Hδ	Hε	Hζ	Hη
2	Pro	-----	4.389	2.277, 1.874	1.971,	3.614, 3.464	-----	-----	-----
3	Pro	-----	4.483	1.809, 2.190	1.984,	3.672, 3.501	-----	-----	-----
4	Pro	-----	4.314	2.216, 1.863	1.930,	3.362, 2.947	-----	-----	-----
5	Ser	8.333	4.325	4.011, 3.887		-----	-----	-----	-----
6	Asp	7.835	4.681	3.036, 2.922	-----		-----	-----	-----
7	Ala	8.401	4.145	1.463	-----	-----	-----	-----	-----
8	Ala	8.212	4.25	1.49	-----	-----	-----	-----	-----
9	Leu	7.894	4.225	1.811, 1.613	1.686	0.970, 0.904	-----	-----	-----
10	Tyr			,	-----			-----	
11	Ala	8.073	4.001	1.503	-----	-----	-----	-----	-----
12	Gln	7.885	4.068	2.458, 2.378	2.191,	-----	,	-----	-----
13	Trp	8.124	4.259	3.420, 3.183	-----	7.21	10.122, 7.311	7.205, 7.078	7.168
14	Leu	8.331	3.577	1.618, 1.401		0.777, 0.776	-----	-----	-----
15	Ala	7.903	4.071	1.449	-----	-----	-----	-----	-----
16	Asp	7.835	4.681	3.036, 2.922	-----		-----	-----	-----
17	dAla	7.543	4.292	1.302	-----	-----	-----	-----	-----
18	Gly	7.964	2.441, 2.798	-----	-----	-----	-----	-----	-----
19	Pro	-----	4.597	2.516, 1.999	2.052, 2.052	3.376,	-----	-----	-----
20	Ala	7.895	4.333	1.387	-----	-----	-----	-----	-----
21	Ser	8.025	4.423	3.860, 3.858		-----	-----	-----	-----
22	Asp	8.231	4.765	2.963, 2.963	-----		-----	-----	-----

cp TC4e R1A

APPPSDAALYAQWLADaGPAS

300K pH 6.5

#	Res	HN	Hα	Hβ	Hγ	Hδ	Hε	Hζ	Hη
1	Ala		4.344	1.505	-----	-----	-----	-----	-----
2	Pro	-----	4.725	2.320, 1.945	1.783,	3.527, 3.293	-----	-----	-----
3	Pro	-----	3.914	1.640, 1.912	1.912,	3.684, 3.534	-----	-----	-----
4	Pro	-----	4.13	2.115, 1.791	1.839,	3.338, 3.194	-----	-----	-----
5	Ser	8.05	4.211	3.928, 3.811		-----	-----	-----	-----
6	Asp	7.865	4.619	2.889, 2.788	-----		-----	-----	-----
7	Ala	8.396	4.103	1.485	-----	-----	-----	-----	-----
8	Ala	8.422	4.288	1.495	-----	-----	-----	-----	-----
9	Leu	7.995	4.258	1.766, 1.565	1.703	0.974, 0.894	-----	-----	-----
10	Tyr	8.624	4.145	3.069, 3.007	-----			-----	
11	Ala	8.163	4.083	1.546	-----	-----	-----	-----	-----
12	Gln	7.819	4.053	2.461, 2.399	2.177,	-----	,	-----	-----
13	Trp	8.157	4.331	3.510, 3.238	-----	7.189	10.079, 7.209	7.364, 7.087	7.23
14	Leu	8.399	3.605	1.664, 1.452		0.830, 0.830	-----	-----	-----
15	Ala	7.878	4.066	1.462	-----	-----	-----	-----	-----
16	Asp	7.883	4.659	2.802, 2.699	-----		-----	-----	-----
17	dAla	7.516	4.286	1.299	-----	-----	-----	-----	-----
18	Gly	7.974	2.401, 2.693	-----	-----	-----	-----	-----	-----
19	Pro	-----	4.396	2.280, 1.970	2.006, 2.010	3.393, 3.088	-----	-----	-----
20	Ala	8.034	4.405	1.417	-----	-----	-----	-----	-----
21	Ser	7.814	4.246	3.872, 3.804		-----	-----	-----	-----

cp TC4e R1A

APPPSDAALYAQWLADaGPAS

300K pH 2.5

#	Res	HN	Hα	Hβ	Hγ	Hδ	Hε	Hζ	Hη
1	Ala		4.343	1.506	-----	-----	-----	-----	-----
2	Pro	-----		2.330, 1.929	1.789,	3.455, 3.178	-----	-----	-----
3	Pro	-----	4.077	1.801, 2.028	1.924,	3.609, 3.511	-----	-----	-----
4	Pro	-----		,	,	,	-----	-----	-----
5	Ser		4.459	3.988, 3.844		-----	-----	-----	-----
6	Asp		4.797	3.038, 2.920	-----		-----	-----	-----
7	Ala		4.093	1.488	-----	-----	-----	-----	-----
8	Ala		4.248	1.49	-----	-----	-----	-----	-----
9	Leu		4.238	1.781, 1.607	1.699	0.977, 0.912	-----	-----	-----
10	Tyr			,	-----			-----	
11	Ala		4.015	1.529	-----	-----	-----	-----	-----
12	Gln		4.06	2.476, 2.391	2.209,	-----	,	-----	-----
13	Trp		4.228	3.194, 3.441	-----		, 7.177	7.325, 7.070	7.188
14	Leu		3.547	1.649, 1.389		0.781, 0.786	-----	-----	-----
15	Ala		4.063	1.454	-----	-----	-----	-----	-----
16	Asp		4.671	3.008, 2.887	-----		-----	-----	-----
17	dAla		4.273	1.295	-----	-----	-----	-----	-----
18	Gly		2.294, 2.733	-----	-----	-----	-----	-----	-----
19	Pro	-----	4.357	2.251, 1.921	1.967,	3.369, 3.012	-----	-----	-----
20	Ala		4.379	1.409	-----	-----	-----	-----	-----
21	Ser		4.362	3.840, 3.840		-----	-----	-----	-----

cp TC4e R1Cit P19W D22

(Cit)PPPSDAALYAQWLADaGWASD

300K pH 6.5

#	Res	HN	Hα	Hβ	Hγ	Hδ	Hε	Hζ	Hη
1	Xaa		,	,	,	,	,	,	,
2	Pro	-----	4.402	2.353, 1.753	2.018, 1.968	3.708, 3.458	-----	-----	-----
3	Pro	-----	2.932	1.283, 0.609	1.763, 1.573	3.362, 3.124	-----	-----	-----
4	Pro	-----	4.268	2.243, 1.816	1.770,	3.158, 2.851	-----	-----	-----
5	Ser	8.189	4.179	3.873, 3.790		-----	-----	-----	-----
6	Asp	8.705	4.038	3.112, 3.055	-----		-----	-----	-----
7	Ala	8.229	4.088	1.569	-----	-----	-----	-----	-----
8	Ala	8.472	4.307	1.507	-----	-----	-----	-----	-----
9	Leu	8.1	4.343	1.795, 1.743	1.635	1.003, 0.898	-----	-----	-----
10	Tyr	7.631	4.594	2.682,	-----	6.762	7.029	-----	
11	Ala	8.684	4.094	1.487	-----	-----	-----	-----	-----
12	Gln	7.783	4.004	2.166,	2.441,	-----	,	-----	-----
13	Trp	8.108	4.176	3.487, 3.082	-----	6.932	9.465, 6.951	6.678, 6.884	6.607
14	Leu	8.455	3.41	1.663, 1.468	1.663	0.877,	-----	-----	-----
15	Ala	7.81	4.02	1.466	-----	-----	-----	-----	-----
16	Asp	7.943	4.537	2.778, 2.643	-----		-----	-----	-----
17	dAla	7.285	4.247	1.145	-----	-----	-----	-----	-----
18	Gly	7.905	1.519, 2.675	-----	-----	-----	-----	-----	-----
19	Trp	7.85	4.627	3.394, 3.218	-----	7.395	10.325, 7.745	7.535, 7.221	7.303
20	Ala	7.885	4.399	1.329	-----	-----	-----	-----	-----
21	Ser	7.764	4.357	3.872, 3.732		-----	-----	-----	-----
22	Asp	8.102	4.437	2.728, 2.594	-----		-----	-----	-----

cp TC4e R1Nva P19W D22

(Nva)PPPSDAALYAQWLADaGWASD

300K pH 6.5

#	Res	HN	Hα	Hβ	Hγ	Hδ	Hε	Hζ	Hη
1	Xaa		,	,	,	,	,	,	,
2	Pro	-----	4.448	2.334, 1.752	1.976,	3.666, 3.429	-----	-----	-----
3	Pro	-----	3.17	1.350, 0.821	1.788, 1.626	3.378, 3.241	-----	-----	-----
4	Pro	-----	4.224	2.205, 1.791	1.786,	3.197, 2.901	-----	-----	-----
5	Ser	8.14	4.175	3.878, 3.788		-----	-----	-----	-----
6	Asp	8.705	4.054	3.110, 3.036	-----		-----	-----	-----
7	Ala	8.202	4.082	1.565	-----	-----	-----	-----	-----
8	Ala	8.46	4.302	1.504	-----	-----	-----	-----	-----
9	Leu	8.086	4.325	1.786, 1.741	1.614	0.998, 0.899	-----	-----	-----
10	Tyr	7.671	4.593	2.715, 2.664	-----	6.763	7.023	-----	
11	Ala	8.613	4.088	1.484	-----	-----	-----	-----	-----
12	Gln	7.783	4.016	2.185,	2.465, 2.431	-----	,	-----	-----
13	Trp	8.136	4.176	3.098, 3.481	-----	6.949	9.531, 6.981	6.801, 6.877	6.7
14	Leu	8.438	3.455	1.464,	1.657	0.862,	-----	-----	-----
15	Ala	7.815	4.025	1.465	-----	-----	-----	-----	-----
16	Asp	7.942	4.546	2.780, 2.654	-----		-----	-----	-----
17	dAla	7.309	4.245	1.145	-----	-----	-----	-----	-----
18	Gly	7.871	1.716, 2.636	-----	-----	-----	-----	-----	-----
19	Trp	7.71	4.619	3.361, 3.223	-----	7.358	10.295, 7.713	7.515, 7.207	7.292
20	Ala	7.907	4.38	1.321	-----	-----	-----	-----	-----
21	Ser	7.821	4.372	3.860, 3.763		-----	-----	-----	-----
22	Asp	8.076	4.449	2.735, 2.625	-----		-----	-----	-----

cp TC4e R1Nva P19W D22

(Nva)PPPSDAALYAQWLADaGWASD

300K pH 2.5

#	Res	HN	Hα	Hβ	Hγ	Hδ	Hε	Hζ	Hη
1	Xaa		,	,	,	,	,	,	,
2	Pro	-----		1.806, 2.339	1.931,	3.501, 3.244	-----	-----	-----
3	Pro	-----	4.081	1.919, 1.796	2.022,	3.625, 3.505	-----	-----	-----
4	Pro	-----	4.344	, 2.248	1.961,	3.354, 3.010	-----	-----	-----
5	Ser		4.366	3.834,		-----	-----	-----	-----
6	Asp			,	-----		-----	-----	-----
7	Ala		4.004	1.527	-----	-----	-----	-----	-----
8	Ala		4.249	1.494	-----	-----	-----	-----	-----
9	Leu		4.25	,		0.988, 0.922	-----	-----	-----
10	Tyr			,	-----			-----	
11	Ala		4.086	1.485	-----	-----	-----	-----	-----
12	Gln		4.056	2.213,	2.479, 2.391	-----	,	-----	-----
13	Trp		4.216	3.204, 3.438	-----		, 7.341	7.215, 7.085	7.196
14	Leu		3.586	1.651, 1.403	1.65	0.774, 0.780	-----	-----	-----
15	Ala		4.066	1.453	-----	-----	-----	-----	-----
16	Asp		4.675	2.995, 2.899	-----		-----	-----	-----
17	dAla		4.261	1.301	-----	-----	-----	-----	-----
18	Gly		,	-----	-----	-----	-----	-----	-----
19	Trp			,	-----		,	,	
20	Ala		4.374	1.407	-----	-----	-----	-----	-----
21	Ser		4.457	3.987, 3.845		-----	-----	-----	-----
22	Asp			,	-----		-----	-----	-----

cp TC4e R1Nva

(Nva)PPPSDAALYAQWLADaGPAS

300K pH 6.5

#	Res	HN	Hα	Hβ	Hγ	Hδ	Hε	Hζ	Hη
1	Xaa		,	,	,	,	,	,	,
2	Pro	-----	4.733	2.323, 1.951	1.783,	3.588, 3.359	-----	-----	-----
3	Pro	-----	3.761	1.588, 1.520	1.889,	3.672, 3.521	-----	-----	-----
4	Pro	-----	4.154	2.148, 1.789	1.822, 1.824	3.321, 3.121	-----	-----	-----
5	Ser	8.063	4.205	3.909, 3.796		-----	-----	-----	-----
6	Asp	7.821	4.635	2.752, 2.656	-----		-----	-----	-----
7	Ala	8.447	4.106	1.487	-----	-----	-----	-----	-----
8	Ala	8.425	4.297	1.498	-----	-----	-----	-----	-----
9	Leu	8.06	4.268	1.771, 1.560	1.723	0.976, 0.895	-----	-----	-----
10	Tyr	8.682	4.156	3.100, 3.028	-----			-----	
11	Ala	8.145	4.091	1.545	-----	-----	-----	-----	-----
12	Gln	7.812	4.04	2.448, 2.410	2.171, 2.170	-----	,	-----	-----
13	Trp	8.147	4.359	3.526, 3.251	-----	7.182	10.046, 7.250	7.397, 7.098	7.264
14	Leu	8.358	3.644	1.674, 1.460		0.835, 0.833	-----	-----	-----
15	Ala	7.862	4.059	1.463	-----	-----	-----	-----	-----
16	Asp	7.922	4.583	2.779, 2.688	-----		-----	-----	-----
17	dAla	7.527	4.289	1.304	-----	-----	-----	-----	-----
18	Gly	7.984	2.520, 2.674	-----	-----	-----	-----	-----	-----
19	Pro	-----	4.406	2.294, 2.020	2.022, 2.018	3.411, 3.109	-----	-----	-----
20	Ala	8.062	4.405	1.419	-----	-----	-----	-----	-----
21	Ser	7.836	4.237	3.840, 3.840		-----	-----	-----	-----

cp TC4e R1Nva

(Nva)PPPSDAALYAQWLADaGPAS

300K pH 2.5

#	Res	HN	Hα	Hβ	Hγ	Hδ	Hε	Hζ	Hη
1	Xaa		,	,	,	,	,	,	,
2	Pro	-----		1.803, 2.340	1.931,	3.502, 3.243	-----	-----	-----
3	Pro	-----	4.084	1.802, 2.022	1.919,	3.625, 3.499	-----	-----	-----
4	Pro	-----		2.249,	1.965, 1.916	3.355, 3.010	-----	-----	-----
5	Ser		4.261	4.015, 3.868		-----	-----	-----	-----
6	Asp		4.8	3.042, 2.934	-----		-----	-----	-----
7	Ala		4.082	1.479	-----	-----	-----	-----	-----
8	Ala		4.249	1.493	-----	-----	-----	-----	-----
9	Leu		4.25	1.787, 1.620	1.718	0.986, 0.922	-----	-----	-----
10	Tyr		4.004	, 2.923	-----			-----	
11	Ala		4.004	1.527	-----	-----	-----	-----	-----
12	Gln		4.056	2.478, 2.393	2.214,	-----	,	-----	-----
13	Trp		4.216	3.438, 3.204	-----		, 7.215	7.341, 7.085	7.195
14	Leu		3.586	1.651, 1.404	1.581	0.778,	-----	-----	-----
15	Ala		4.066	1.453	-----	-----	-----	-----	-----
16	Asp		4.671	2.994, 2.903	-----		-----	-----	-----
17	dAla		4.261	1.301	-----	-----	-----	-----	-----
18	Gly		2.280, 2.748	-----	-----	-----	-----	-----	-----
19	Pro	-----		2.318,	, 2.028	,	-----	-----	-----
20	Ala		4.374	1.407	-----	-----	-----	-----	-----
21	Ser		4.365	3.834, 3.834		-----	-----	-----	-----

cp TC4e Y10A D22

RPPPSDAALAAQWLADaGPASD

300K pH 6.5

#	Res	HN	Hα	Hβ	Hγ	Hδ	Hε	Hζ	Hη
1	Arg		4.373	1.786, 1.701	1.966,	3.230, 3.236	7.339	-----	, , ,
2	Pro	-----	4.776	2.385, 1.847	2.007,	3.737, 3.553	-----	-----	-----
3	Pro	-----	4.064	1.696, 1.856	1.935, 1.935	3.735, 3.566	-----	-----	-----
4	Pro	-----	4.374	2.255,	1.895, 1.902	3.463, 3.325	-----	-----	-----
5	Ser	8.322	4.306	3.937, 3.849		-----	-----	-----	-----
6	Asp	7.978	4.581	2.701, 2.646	-----		-----	-----	-----
7	Ala	8.448	4.139	1.427	-----	-----	-----	-----	-----
8	Ala	8.552	4.38	1.416	-----	-----	-----	-----	-----
9	Leu	7.983	4.275	1.697, 1.579	1.635	0.946, 0.869	-----	-----	-----
10	Ala	8.132	4.107	1.446	-----	-----	-----	-----	-----
11	Ala	8.297	4.238	1.442	-----	-----	-----	-----	-----
12	Gln	8.019	4.133	2.072, 2.073	2.338,	-----	,	-----	-----
13	Trp	8.048	4.564	3.274, 3.437	-----	7.214	10.044, 7.645	7.421, 7.168	7.232
14	Leu	8.084	4.02	1.721, 1.585	1.637	0.883,	-----	-----	-----
15	Ala	8.042	4.21	1.415	-----	-----	-----	-----	-----
16	Asp	8.049	4.572	2.760, 2.708	-----		-----	-----	-----
17	dAla	7.832	4.333	1.375	-----	-----	-----	-----	-----
18	Gly	8.178	3.130, 3.481	-----	-----	-----	-----	-----	-----
19	Pro	-----	4.396	2.250, 1.981	1.971,	3.518, 3.349	-----	-----	-----
20	Ala	8.116	4.354	1.387	-----	-----	-----	-----	-----
21	Ser	8.107	4.408	3.888, 3.786		-----	-----	-----	-----
22	Asp	8.063	4.413	2.706, 2.594	-----		-----	-----	-----

cp TC4e Y10A P19W D22

RPPPSDAALAAQWLADaGWASD

300K pH 6.5

#	Res	HN	Hα	Hβ	Hγ	Hδ	Hε	Hζ	Hη
1	Arg		4.445	1.967, 1.967	1.806, 1.668	3.199, 3.183	7.399	-----	, , ,
2	Pro	-----	4.399	2.382, 1.777	2.011, 2.014	3.762, 3.546	-----	-----	-----
3	Pro	-----	3.244	1.337, 0.956	1.743, 1.583	3.348, 3.081	-----	-----	-----
4	Pro	-----	4.345	2.219, 1.868	1.788, 1.583	3.238, 2.986	-----	-----	-----
5	Ser	8.311	4.227	3.902, 3.822		-----	-----	-----	-----
6	Asp	7.711	4.587	2.692, 2.626	-----		-----	-----	-----
7	Ala	8.583	4.096	1.446	-----	-----	-----	-----	-----
8	Ala	8.393	4.243	1.454	-----	-----	-----	-----	-----
9	Leu	7.964	4.36	1.710, 1.628		0.958, 0.865	-----	-----	-----
10	Ala	8.12	4.05	1.471	-----	-----	-----	-----	-----
11	Ala	8.146	4.204	1.461	-----	-----	-----	-----	-----
12	Gln	7.999	4.069	2.099, 2.074	2.374,	-----	,	-----	-----
13	Trp	7.958	4.365	3.159, 3.474	-----	6.952	9.674, 7.557	6.786, 7.034	6.711
14	Leu	8.193	3.74	1.777, 1.606	1.706	0.914, 0.875	-----	-----	-----
15	Ala	7.947	4.085	1.45	-----	-----	-----	-----	-----
16	Asp	7.974	4.558	2.793, 2.711	-----		-----	-----	-----
17	dAla	7.566	4.284	1.26	-----	-----	-----	-----	-----
18	Gly	8.138	2.014, 3.186	-----	-----	-----	-----	-----	-----
19	Trp	8.136	4.629	3.376, 3.180	-----	7.382	10.274, 7.694	7.505, 7.181	7.273
20	Ala	7.899	4.386	1.331	-----	-----	-----	-----	-----
21	Ser	7.746	4.301	3.872, 3.689		-----	-----	-----	-----
22	Asp	8.151	4.43	2.726, 2.606	-----		-----	-----	-----

cp TC4e Y10L D22

RPPPSDAALLAQWLADaGPASD

300K pH 6.5

#	Res	HN	Hα	Hβ	Hγ	Hδ	Hε	Hζ	Hη
1	Arg		4.39	2.010, 2.006	1.868, 1.686	3.310, 3.265	7.578	-----	, , ,
2	Pro	-----	4.779	2.372, 1.764	1.982,	3.708, 3.524	-----	-----	-----
3	Pro	-----	3.051	1.308, 0.941	1.787, 1.752	3.629, 3.499	-----	-----	-----
4	Pro	-----	4.314	2.243, 1.862	1.778, 1.743	2.891, 3.072	-----	-----	-----
5	Ser	8.237	4.25	3.897, 3.809		-----	-----	-----	-----
6	Asp	7.557	4.616	2.712, 2.618	-----		-----	-----	-----
7	Ala	8.698	4.032	1.488	-----	-----	-----	-----	-----
8	Ala	8.495	4.255	1.474	-----	-----	-----	-----	-----
9	Leu	7.964	4.413	1.766, 1.659		0.989, 0.882	-----	-----	-----
10	Leu	8.094	4.098	1.843, 1.650	1.71	0.996, 0.921	-----	-----	-----
11	Ala	8.304	4.167	1.503	-----	-----	-----	-----	-----
12	Gln	8.033	4.059	2.182, 2.127	2.427,	-----	,	-----	-----
13	Trp	8.041	4.385	3.280, 3.665	-----	7.108	9.889, 7.630	7.318, 7.630	7.176
14	Leu	8.701	3.692	1.936, 1.515	1.98	1.002, 0.971	-----	-----	-----
15	Ala	8.001	4.091	1.494	-----	-----	-----	-----	-----
16	Asp	7.931	4.584	2.848, 2.760	-----		-----	-----	-----
17	dAla	7.481	4.306	1.305	-----	-----	-----	-----	-----
18	Gly	8.274	1.725, 2.997	-----	-----	-----	-----	-----	-----
19	Pro	-----	4.502	2.384,	2.040, 2.006	3.571, 3.278	-----	-----	-----
20	Ala	7.742	4.411	1.392	-----	-----	-----	-----	-----
21	Ser	7.897	4.299	3.926, 3.689		-----	-----	-----	-----
22	Asp	8.168	4.434	2.747, 2.621	-----		-----	-----	-----

cp TC4e Y10L P19W D22

RPPPSDAALLAQWLADaGWASD

300K pH 6.5

#	Res	HN	Hα	Hβ	Hγ	Hδ	Hε	Hζ	Hη
1	Arg		4.531	2.031, 1.976	1.883, 1.651	3.281, 3.202	7.636	-----	, , ,
2	Pro	-----	4.187	2.409, 1.726	2.070, 1.990	3.801, 3.559	-----	-----	-----
3	Pro	-----	2.314	0.940, -0.070	1.571, 1.317	3.206, 2.586	-----	-----	-----
4	Pro	-----	4.311	2.208, 1.887	1.726, 1.628	2.988, 2.658	-----	-----	-----
5	Ser	8.26	4.185	3.866, 3.792		-----	-----	-----	-----
6	Asp	7.384	4.602	2.699, 2.583	-----		-----	-----	-----
7	Ala	8.795	4.009	1.487	-----	-----	-----	-----	-----
8	Ala	8.571	4.246	1.468	-----	-----	-----	-----	-----
9	Leu	7.923	4.5	1.742, 1.702	1.633	0.985, 0.871	-----	-----	-----
10	Leu	7.909	4.023	1.832, 1.669	1.68	0.943, 0.880	-----	-----	-----
11	Ala	8.438	4.15	1.499	-----	-----	-----	-----	-----
12	Gln	8.084	4.006	2.183, 2.091	2.420,	-----	,	-----	-----
13	Trp	7.88	4.225	3.119, 3.627	-----	6.805	9.498, 7.502	6.208, 6.957	6.403
14	Leu	8.705	3.493	1.943, 1.494		, 0.948	-----	-----	-----
15	Ala	7.999	4.053	1.49	-----	-----	-----	-----	-----
16	Asp	7.944	4.529	2.845, 2.746	-----		-----	-----	-----
17	dAla	7.332	4.275	1.227	-----	-----	-----	-----	-----
18	Gly	8.18	0.892, 2.924	-----	-----	-----	-----	-----	-----
19	Trp	8.482	4.617	3.495, 3.169	-----	7.577	10.504, 7.246	7.538, 7.833	7.316
20	Ala	7.824	4.477	1.394	-----	-----	-----	-----	-----
21	Ser	7.578	4.225	3.919, 3.588		-----	-----	-----	-----
22	Asp	8.267	4.422	2.737, 2.575	-----		-----	-----	-----

Cyclized cp TC4e P19W

RPPPSDAALYAQWLADaGWASG

300K pH 6.5

#	Res	HN	Hα	Hβ	Hγ	Hδ	Hε	Hζ	Hη
1	Arg	8.01	5.068	1.800, 1.801	1.599,	3.299, 3.213	7.555	-----	, , ,
2	Pro	-----	4.186	1.758, 2.367	2.073, 1.915	3.850, 3.629	-----	-----	-----
3	Pro	-----	2.017	1.024, -0.260	1.682, 1.307	3.239, 2.423	-----	-----	-----
4	Pro	-----	4.422	2.270, 1.915	1.808, 1.740	3.191, 2.759	-----	-----	-----
5	Ser	8.3	4.214	3.851, 3.786		-----	-----	-----	-----
6	Asp	7.456	4.563	2.672, 2.631	-----		-----	-----	-----
7	Ala	8.868	4.072	1.468	-----	-----	-----	-----	-----
8	Ala	8.492	4.313	1.507	-----	-----	-----	-----	-----
9	Leu	8.176	4.382	1.806, 1.614	1.753	0.994, 0.876	-----	-----	-----
10	Tyr	8.753	3.953	3.117, 3.070	-----			-----	
11	Ala	8.31	4.115	1.583	-----	-----	-----	-----	-----
12	Gln	7.758	3.979	2.174, 2.100	2.404,	-----	,	-----	-----
13	Trp	7.97	4.102	2.961, 3.479	-----	6.814	9.574, 6.728	5.862, 6.796	5.963
14	Leu	8.422	3.281	1.798, 1.378	1.51	0.957, 0.871	-----	-----	-----
15	Ala	7.988	4.11	1.31	-----	-----	-----	-----	-----
16	Asp	7.879	4.505	2.834, 2.684	-----		-----	-----	-----
17	dAla	7.298	4.307	1.256	-----	-----	-----	-----	-----
18	Gly	8.293	0.307, 2.954	-----	-----	-----	-----	-----	-----
19	Trp	8.817	4.559	3.558, 3.179	-----	7.584	10.443, 7.917	7.604, 7.226	7.332
20	Ala	7.792	4.364	1.449	-----	-----	-----	-----	-----
21	Ser	7.958	4.113	3.894, 3.460		-----	-----	-----	-----
22	Gly	7.878	4.354, 3.884	-----	-----	-----	-----	-----	-----

Cyclized cp TC4e P19W

RPPPSDAALYAQWLADaGWASG

300K pH 2.5

#	Res	HN	Hα	Hβ	Hγ	Hδ	Hε	Hζ	Hη
1	Arg	7.876	4.974	1.878, 1.732	1.621,	3.254, 3.256	7.38	-----	, , ,
2	Pro	-----	4.031	1.739, 2.336	2.072, 1.906	3.839, 3.593	-----	-----	-----
3	Pro	-----	2.011	1.055, -0.089	1.637, 1.237	3.193, 2.425	-----	-----	-----
4	Pro	-----	4.357	2.271, 1.885	1.800, 1.749	3.138, 2.751	-----	-----	-----
5	Ser	8.32	4.201	3.868, 3.809		-----	-----	-----	-----
6	Asp	7.566	4.698	2.933, 2.819	-----		-----	-----	-----
7	Ala	9.013	4.076	1.464	-----	-----	-----	-----	-----
8	Ala	8.144	4.289	1.483	-----	-----	-----	-----	-----
9	Leu	7.718	4.458	1.731, 1.682	1.643	0.989, 0.870	-----	-----	-----
10	Tyr	8.475	3.967	3.133, 3.120	-----			-----	
11	Ala	8.505	4.107	1.578	-----	-----	-----	-----	-----
12	Gln	7.796	4.042	2.144, 2.141	2.449, 2.361	-----	,	-----	-----
13	Trp	7.948	4.066	3.005, 3.467	-----	6.854	9.498, 6.765	5.939, 6.810	6.034
14	Leu	8.553	3.259	1.720, 1.478	1.451	0.939, 0.901	-----	-----	-----
15	Ala	7.935	4.059	1.467	-----	-----	-----	-----	-----
16	Asp	7.654	4.641	3.063, 2.857	-----		-----	-----	-----
17	dAla	7.302	4.309	1.261	-----	-----	-----	-----	-----
18	Gly	8.077	0.352, 2.942	-----	-----	-----	-----	-----	-----
19	Trp	8.793	4.547	3.534, 3.182	-----	7.594	10.396, 7.862	7.589, 7.194	7.315
20	Ala	7.832	4.337	1.451	-----	-----	-----	-----	-----
21	Ser	7.913	4.191	3.928, 3.557		-----	-----	-----	-----
22	Gly	7.946	4.333, 3.908	-----	-----	-----	-----	-----	-----

VITA

Education

Doctor of Philosophy, Chemistry, 2018
University of Washington
Seattle, WA

Masters of Science, Chemistry, 2016
University of Washington
Seattle, WA

Bachelor of Science, Biochemistry, 2006
Western Washington University
Bellingham, WA